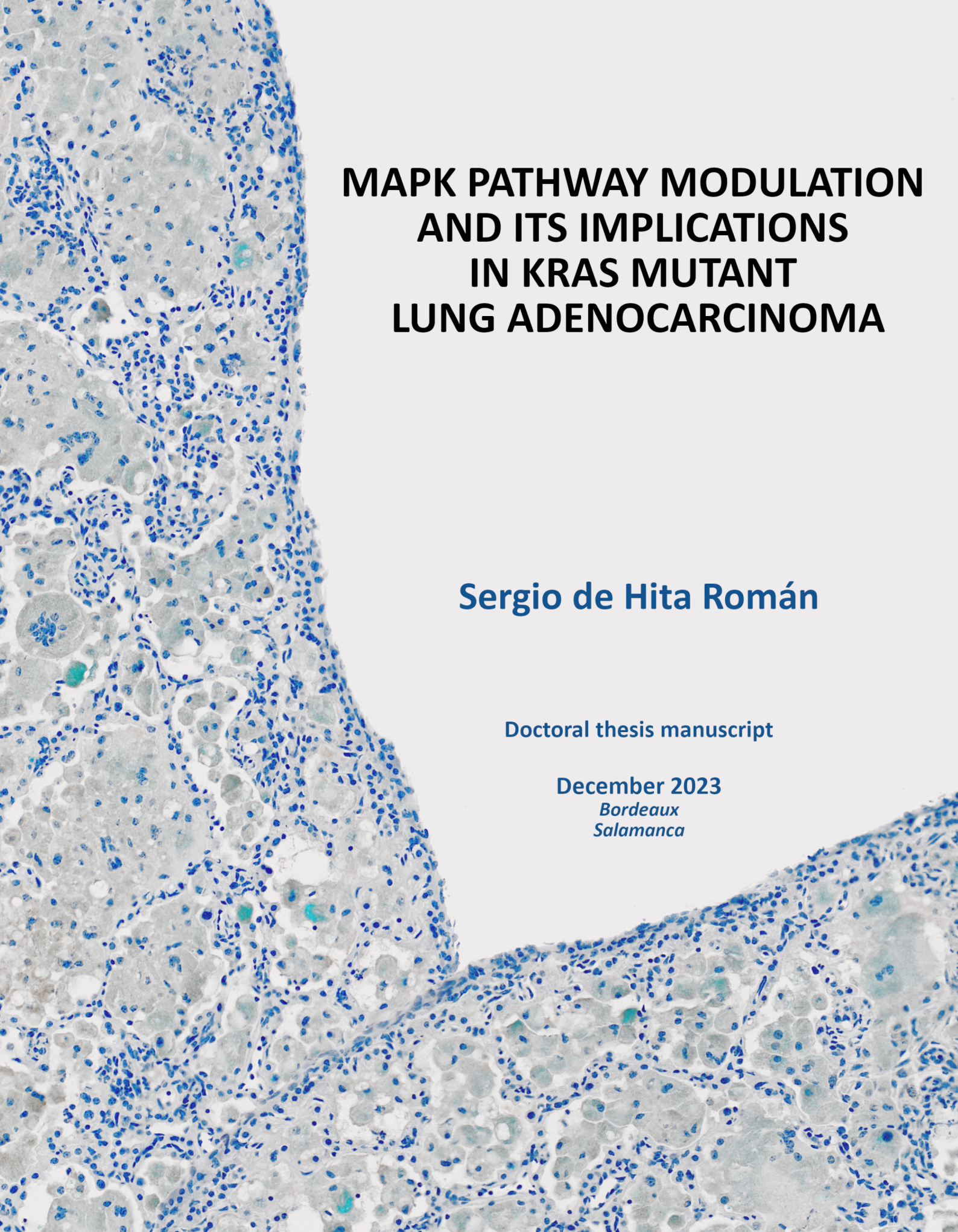

MAPK PATHWAY MODULATION AND ITS IMPLICATIONS IN KRAS MUTANT LUNG ADENOCARCINOMA

Sergio de Hita Román

Doctoral thesis manuscript

December 2023

Bordeaux

Salamanca

université de BORDEAUX

VNiVERSiDAD D SALAMANCA

THÈSE EN COTUTELLE PRÉSENTÉE
POUR OBTENIR LE GRADE DE

DOCTEUR

DE

L'UNIVERSITÉ DE BORDEAUX

École doctorale Sciences de la Vie et de la Santé
Spécialité Génétique

ET DE

L'UNIVERSITÉ DE SALAMANCA

École doctorale *Studii Salamantini*
Spécialité Biosciences, Biologie et Clinique du Cancer et Médecine Translationnelle

PAR

SERGIO DE HITA ROMÁN

INTITULÉE

LA RÉGULATION DE LA VOIE MAPK ET SES CONSÉQUENCES DANS L'ADÉNOCARCINOME DE POUMON KRAS MUTÉ

Sous la direction de
David Santamaría Velilla
et de
David Cappellen

Soutenue le 7 décembre 2023

Membres du jury :

M. TEICHMANN Martin, Professeur à l'Université de Bordeaux	Président
Mme. SÁNCHEZ-CÉSPEDES Montserrat, Directrice de Recherche au IJC Barcelone	Rapporteur
M. PRIOR Ian, Professeur à l'Université de Liverpool	Rapporteur
Mme. CASTELLANO Esther, Directrice de Recherche au CIC-IBMCC Salamanca	Examinateur

Escuela de Doctorado *Studii Salamantini*
Ecole Doctorale *Sciences de la Vie et de la Santé*

MAPK PATHWAY MODULATION AND ITS IMPLICATIONS IN KRAS MUTANT LUNG ADENOCARCINOMA

Tesis doctoral

Sergio de Hita Román

Dirigida por
David Santamaría Velilla
y David Cappellen

7 de diciembre de 2023
Bordeaux
Salamanca

Dr. David Santamaría, Principal Investigator at the Institute of Molecular and Cellular Biology of Cancer (IBMCC-CIC) in Salamanca,

and

Dr. David Cappellen, *Maître de Conférences* at the Biotherapies, Genetics & Oncology laboratory of the Bordeaux Institute of Oncology (BRIC-U1312 INSERM), *Praticien Hospitalier* at the Tumor Biology service of the Bordeaux University Hospital (CHU),

hereby certify that the Doctoral Thesis:

MAPK pathway modulation and its implications in KRAS mutant lung adenocarcinoma

submitted by Sergio de Hita Román for the degree of Doctor of Philosophy and carried out under the supervision of the undersigned in both the University of Bordeaux and the University of Salamanca, duly meets the requirements laid out by the Spanish RD99/2011, the French Arrêté du 26 août 2022, and the regulation of both Universities.

Having reviewed the present work, we consider that it meets all the necessary merits for its presentation and defense, in order to qualify for the degree of doctor through the program "Biociences: Biology and Clinical Cancer and Translational Medicine" at the University of Salamanca and the program of "Genetics" at the University of Bordeaux.

Dr. David Santamaría Velilla

Dr. David Cappellen

Dr David CAPPELLEN,
Maitre de Conférences-Praticien Hospitalier
Service de Biologie des Tumeurs, CHU de Bordeaux,
& Équipe "*Biotherapy, Genetics & Oncology*",
U1312 Inserm, *Bordeaux Institute of Oncology (BRIC)*
Université de Bordeaux

English

Title

MAPK Pathway Modulation and its implications in KRAS mutant Lung Adenocarcinoma

Abstract

This thesis delves into the intricate regulation of the RAS-MAPK pathway in lung adenocarcinoma, where genetic alterations drive tumor progression by upregulating MAPK activity. Nonetheless, the tumor must keep a tight balance between positive and negative regulators within this pathway as excessive signaling levels are detrimental.

In this study, we present a robust transcriptional signature reflecting MAPK activity in KRAS lung adenocarcinoma patient data to demonstrate that high MAPK levels are associated with impaired tumor progression, whereas moderate MAPK activation correlates with greater malignancy and poor prognosis.

Genomic analysis of these tumors revealed that DUSP4, considered a negative regulator of the pathway, exhibits complex behavior, as copy number variations differ between low and high MAPK patient groups, particularly remarking a high frequency of DUSP4 copy losses in high MAPK patients.

In this manuscript we show that deletion of DUSP4 is selected in early lesions by synergizing with KRAS activation and granting an initial proliferative advantage. However, advanced tumor progression is hindered in the absence of DUSP4, as MAPK hypersignaling generates toxic effects .

To further unravel MAPK modulation, this study identifies potential novel pathway regulators, including additional genes and phosphatases, that may play a potential role in mediating responses of KRAS mutant tumors.

In summary, this research highlights the significance of MAPK regulation in KRAS driven lung oncogenesis, offering possible insights into patient outcomes, and postulating that MAPK activation levels are determinant for future therapeutic strategies.

Keywords

Cancer, LUAD, Mice, MAPK, CRISPR, KRAS, DUSP4, Phosphatases, Bioinformatics

---

Research units

U1312 BRIC Bordeaux Institute of Oncology, France
IBMCC-CIC, Centro de Investigación del Cáncer de Salamanca, Espagne

Français

Titre

La régulation de la voie MAPK et ses conséquences dans l'adénocarcinome de poumon KRAS muté

Résumé

Cette thèse explore la régulation de la voie RAS-MAPK dans l'adénocarcinome pulmonaire, où des altérations génétiques favorisent la progression tumorale en augmentant l'activité de la MAPK. Cependant, la tumeur doit maintenir un équilibre entre les régulateurs positifs et négatifs au sein de cette voie, car des niveaux de signalisation excessifs sont toxiques.

Dans cette étude, nous présentons une signature transcriptionnelle reflétant l'activité de la MAPK dans les données des patients atteints d'adénocarcinome pulmonaire KRAS muté, pour démontrer que des niveaux élevés de MAPK sont associés à une progression tumorale altérée, tandis qu'une activation modérée de la MAPK est corrélée à une malignité accrue et à un pronostic défavorable.

L'analyse génomique de ces tumeurs a révélé que DUSP4, considéré comme un régulateur négatif de la voie, présente un comportement complexe, car les variations du nombre de copies diffèrent entre les groupes de patients à faible et à forte MAPK, avec une fréquence élevée de pertes de copies de DUSP4 chez les patients à forte MAPK.

Dans ce manuscrit, nous montrons que la suppression de DUSP4 est sélectionnée dans les lésions précoces en agissant en synergie avec l'activation de KRAS et en conférant un avantage prolifératif initial. Cependant, la progression tumorale avancée est entravée en l'absence de DUSP4, car une signalisation excessive génère des effets toxiques.

Pour mieux comprendre la modulation de la MAPK, cette étude identifie de potentiels nouveaux régulateurs de la voie, y compris des gènes et des phosphatases supplémentaires, qui pourraient jouer un rôle dans la médiation des réponses des tumeurs KRAS mutés.

En résumé, ces travaux mettent en lumière l'importance de la régulation de la MAPK dans l'oncogenèse pulmonaire induite par KRAS, offrant des perspectives possibles sur les résultats des patients et postulant que les niveaux d'activation de la MAPK sont déterminants pour les futures stratégies thérapeutiques.

Mots clés

Cancer, Poumon, Souris, MAPK, CRISPR, KRAS, DUSP4, Phosphatases, Bioinformatics

---

Unités de recherche

U1312 BRIC Bordeaux Institute of Oncology, France
IBMCC-CIC, Centro de Investigación del Cáncer de Salamanca, Espagne

Español

Título

La regulación de la vía MAPK y sus consecuencias en el desarrollo del adenocarcinoma de pulmón KRAS mutado

Resumen

Esta tesis explora la compleja regulación de la vía RAS-MAPK en el adenocarcinoma de pulmón, donde las alteraciones genéticas impulsan la progresión tumoral al aumentar la actividad de MAPK. Sin embargo, el tumor debe mantener un equilibrio preciso entre los reguladores positivos y negativos dentro de esta vía, ya que niveles excesivos de señalización son perjudiciales.

En este estudio, presentamos una firma transcripcional que refleja la actividad de MAPK en datos de pacientes con adenocarcinoma de pulmón KRAS mutado para demostrar que niveles elevados de MAPK se asocian con una progresión tumoral deteriorada, mientras que una activación moderada de MAPK se correlaciona con una mayor malignidad y un mal pronóstico.

El análisis genómico de estos tumores reveló que DUSP4, considerado un regulador negativo de la vía, presenta un comportamiento complejo, ya que las variaciones en el número de copias del gen (CNVs) difieren entre los grupos de pacientes con niveles bajos y altos de MAPK, destacando en particular una alta frecuencia de pérdida de copias de DUSP4 en pacientes con altos niveles de MAPK.

En este manuscrito, mostramos que la eliminación de DUSP4 se selecciona en lesiones tempranas al colaborar con la activación de KRAS y proporcionar una ventaja proliferativa inicial. Sin embargo, la progresión tumoral avanzada se ve obstaculizada en ausencia de DUSP4, ya que la hiperseñalización de MAPK genera efectos tóxicos.

Para profundizar en la modulación de MAPK, este estudio identifica posibles nuevos reguladores de la vía, incluyendo genes y fosfatasas adicionales, que pueden desempeñar un papel en la mediación de las respuestas de los tumores con mutación de KRAS.

En resumen, esta investigación destaca la importancia de la regulación de MAPK en la oncogénesis mediada por KRAS en el pulmón, ofreciendo posibles perspectivas sobre los resultados de los pacientes y postulando que los niveles de activación de MAPK son determinantes para las futuras estrategias terapéuticas.

Palabras clave

Cáncer, LUAD, Ratones, MAPK, CRISPR, KRAS, DUSP4, Fosfatasas, Bioinformática

---

Centros de Investigación

U1312 BRIC Bordeaux Institute of Oncology
IBMCC-CIC Centro de Investigación del Cáncer de Salamanca

The present work has been funded with the following public and mixed trusts :

I would like to acknowledge and thank all the donors, patients and funds that made this work possible and contributed to these research initiatives.

Every day, these efforts help building a better world

I would like to acknowledge the French and Spanish academic communities involved :

“The nitrogen in our DNA, the calcium in our teeth, the iron in our blood, the carbon in our apple pies were made in the interiors of collapsing stars. We are made of starstuff.”
— Carl Sagan, **Cosmos**


References
Conclusions
Discussion
Results
Mat&Met
Objectives
Introduction

Index

List of figures

44. DUSP4 does not contribute to RAS-mediated transformation process
45. DUSP4 inducible knock-out generates increased MAPK levels.
46. DUSP4 deletion induces cellular increase of ROS and oxidative stress levels
47. Abrupt deletion of DUSP4 in formed tumors increases genomic instability and apoptotic rate
48. An inducible KRAS tumor formation model reveals that DUSP4 loss initially grants a selective advantage
49. pSECC model allows for direct DUSP4 genome editing combined with Cre activity
50. Experimental plan for the pSECC experiments
51. DUSP4 loss increases the proliferative rate of early lesions
52. Limited tumor frequency in DUSP4 knockout tumors
53. Tumoral burden is reduced in KRAS-driven lesions affected by DUSP4 deletion
54. Knockout of DUSP4 in a panel of LUAD KRAS mutant cell lines
55. DUSP4 deletion results in an increased resistance to MEK inhibitor trametinib in a panel of LUAD cell lines
56. DUSP4 knockout cell lines have increased MAPK levels, presenting increased trametinib resistance
57. Overexpression of DUSP4 leads to reduced levels of MAPK activity
58. DUSP4 overexpression sensitizes LUAD cell lines to MAPK inhibitors
59. MAPK induction by the combined action of tamoxifen activatable KRAS and BRAF D594A
60. Activation of KRAS in presence of BRAF kinase dead results in a MAPK dependent cell death
61. KRAS and BRAF activation leads to apoptosis in ATII cells
62. Triggered MAPK activity generates oncogenic stress
63. Inducible and precise doxycycline BRAF activation cooperates with KRAS induction and triggers mild toxicities
64. Combined induction of KRAS and BRAF induces MAPK levels and generates MAPK dependent genomic stress
65. MAPK hypersignaling obtained from KRAS and BRAF induction generates MEK dependent apoptosis
66. Excessive MAPK activity impairs cellular growth and limits colony formation without significantly affecting cell cycle
67. MAPK induction by BRAF kinase dead inducible expression
68. The transcriptional signature recapitulates how BRAF kinase dead mutant is able to activate MAPK levels
69. Overexpression of BRAF D594A results toxic in a KRAS mutant context
70. BRAF kinase dead activity conveys MAPK output
71. Exploiting the toxic effect of over-driving MAPK activity with CRISPR/Cas9
72. Cas9 editing function in ATII cell line
73. CRISPR screening strategy for identifying MAPK putative regulators in ATII cell line
74. Screening results depict distinct gRNA enrichment patterns
75. CRISPR screening KB enrichment analysis
76. CRISPR screening KB depletion analysis
77. GPCRs effect on KRAS mutant LUAD patient prognosis are independent of MAPK signature effect
78. TTC1 roundly shapes KRAS mutant LUAD patient prognosis
79. TTC1 deletion in ATII KB cell line
80. TTC1 depletion does not modify the effect of MAPK dependent toxicities
81. Inconsistent depletion of TTC1 by both gRNAs and shRNAs on LUAD cell lines
82. TTC1 inhibition by inducible shRNA is toxic in a panel of KRAS mutant LUAD cell lines
83. CSK deletion sensitizes cells to KRAS and BRAF activation
84. Knockout of CSK significantly enhances and overdrives MAPK signature levels
85. CSK ablation in a KRAS mutant context
86. Elimination of CSK activity results in a decreased sensitivity to RAS/MAPK inhibitors
87. CSK-SRC interplay with MAPK pathway in a KRAS mutant LUAD cell line
88. RAS-MAPK increased resistance in absence of CSK is not altered by PP2 inhibitors

Abbreviations

A

A.U.	Arbitrary units
ANOVA	Analysis of Variance
ATP	Adenosine triphosphate
ATII	Alveolar type II

B

BSA	Bovine Serum Albumin
BRCA	Breast Cancer

C

CNV	Copy Number Variant
CRISPR	Clustered Regularly Interspaced Short Palindromic Repeats
CRC	Colorectal Cancer
ccRCC	Clear Cell Renal Carcinoma

D

Da, kDa	Dalton, Kilodalton
DAPI	diamidino-2-phenylindole (6')
DDR	DNA damage response
DMEM	Dulbecco's Modified Eagle Medium
DNA	Deoxyribonucleic acid
cDNA	Complementary DNA
gDNA	Genomic DNA
DSB	Double Strand Break
DTT	Dithithreitol-1,4

E

ECL	Enhanced chemiluminescence
EDTA	Ethylenediamine tetra-acetic acid
EMEM	Eagle's Minimum Essential Medium

F

FACS	Fluorescence activated cell sorting
FBS	Fetal bovine serum
FITC	Fluorescein Isothiocyanate
FPs	
YFP	Yellow fluorescent protein
GFP	Green fluorescent protein

G

GDP	Guanosine Diphosphate
GTP	Guanosine Triphosphate

H

HBSS	Hank's Balanced Solution
HDR	Homology directed repair
HEPES	Hydroxyethylpiperazine-N-2-ethane sulfonic acid
HRP	Horseradish peroxidase

I

i	Inhibitors (as in MAPKi, KRASi, MEKi, etc)

L

LUAD	Lung adenocarcinoma

M

MAPK	Mitogen associated protein kinase
MEFs	Mouse embryonic fibroblasts
MOI	Multiplicity of Infection
mol, M	moles, Molar
MSS	Microsatellite Stable
MSI	Microsatellite Instable

N

n	Number of individuals Samples of the study group
NAC	N-acetylcysteine
NS	Non Significant
NGS	Next generation sequencing
NHEJ	Non-homologous end joining
NLS	Nuclear Localization Signal
NSCLC	Non-small cell lung cancer

O

ORF	Open reading frame

P

PAGE	Polyacrylamide gel electrophoresis
PAM	Protospacer Adjacent Motif
pb, kb	Base pairs, kilobases
PBS	Phosphate Buffered Saline
PCR	Polymerase chain reaction
PE	Phycoerythrin fluorochrome
PFA	Paraformaldehyde
PS	Penicillin Streptomycin

R

RNA	Ribonucleic acid
mRNA	Messenger Ribonucleic acid
gRNA	Guide Ribonucleic acid
shRNA	Short hairpin Ribonucleic acid
crRNA	CRISPR associated RNA
tracrRNA	Transactivating CRISPR RNA
sgRNA	Single Guide Ribonucleic acid
RNP	Ribonucleoprotein
RPMI	Roswell Park Memorial Institute Medium
RT	Reverse transcription or Room Temperature

S

SD	Standard deviation
SDS	Sodium dodecyl sulfate
SNP	Single Nucleotide Polymorphisms
SV40	Simian virus 40

T

TBS	Tris buffered saline
TBHP	Tert-Butyl-hydroperoxide

U

UTR	Untranslated region

W

WT	Wild type

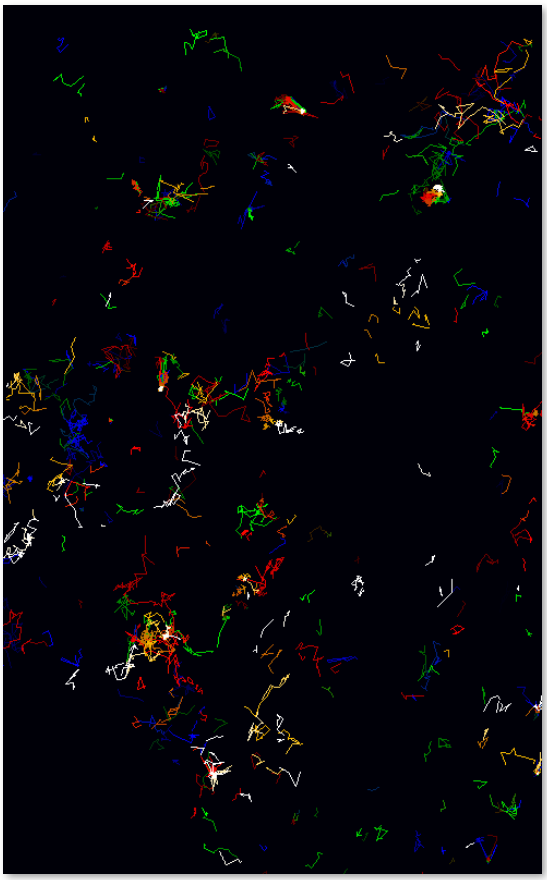

Picture I. Single particle tracking of KRAS molecules visualized on SPT-PALM microscopy thanks to a Halo-tag system.
Credit: Tra-Ly Nguyen, BRIC, Université de Bordeaux

Introduction

"A lung cancer is not simply a cancer. It doesn't simply have a certain kind of appearance under the microscope or a certain behavior, but it also has a set of changes in the genes or in the molecules that modify gene behavior that allows us to categorize cancers in ways that is very useful in thinking about new ways to control cancer by prevention and treatment."

Harold E. Varmus

1 MALIGNANT TUMORS AND LUNG CANCER

1.1 LUNG CANCER : THE LEADING CAUSE OF CANCER DEATH

During the year 2020, the International Agency for Research on Cancer calculated that 18 million new cases of cancer were diagnosticated all over the world (Sung et al., 2021). According to recent predictions, these numbers will keep going up and even double, reaching 40 million cases per year in 2070 (Soerjomataram & Bray, 2021).

In Europe, cancer is the second leading cause of mortality after cardiovascular diseases. The European commission warned that every year, up to 2 million people die every year from the disease (OECD & European-Union, s.d.). Considering that Europe accounts for a quarter of all cancer cases in the globe and less than 10% of the world's population, it is evident that cancer is an emerging threat to our society.

Leading the number of deaths, lung cancer is estimated to be the most lethal type of cancer in the world. Each year, more people die of lung cancer than of breast, pancreas and prostate cancers combined (**Figure 1**).

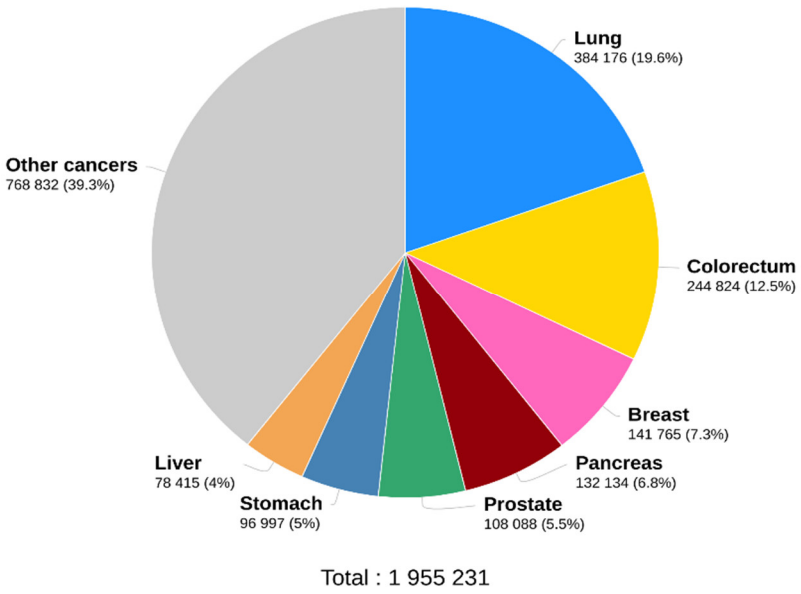

Figure 1. ***Death estimations from 2020 GLOBOCAN study (World Health Organization) in the EU****. Lung accounts for the majority of cancer-associated deaths in Europe, but also at global level. Adapted figure from WHO.*

Overall, the current chance that a man will develop lung cancer in his lifetime is about 1 in 15; for a woman, the risk is about 1 in 17 (American-Cancer-Society, 2022). Lung tumors have very aggressive features, and the prognosis of the diagnosed patients is noticeably short, with less than 30% of patients reaching the 5-Year Relative Survival (National-Cancer-Institute & DCCPS, 2021).

If identified at early stages, surgical resection of localized tumors grants almost 90% of 5-year survival. However, this is infrequent and only 16% percent of patients benefit from an early detection (National-Cancer-Institute & DCCPS, 2021), generally because they do not present any particular symptoms until more advanced stages. This results in 56% of the patients being diagnosed with distant stage IV lung cancer (National-Cancer-Institute & DCCPS, 2021). These figures indicate that, without better early detection methods, we may be battling a disease that has already progressed to an advanced stage, requiring the use of intricate therapeutic approaches.

Classification of these tumors is determinant when estimating survival and treatment options. Around 80% of lung cancers are classified as non-small cell lung cancers (NSCLCs), these include squamous cell carcinoma (SCC), large cell lung carcinoma (LCLC) and lung adenocarcinomas (LUAD), this last one being the most common one. Small cell lung carcinoma (SCLC) is the least frequent type of lung cancer, accounting for 15% of the cases. This type of cancer behaves very differently from the rest and is characterized for deriving from a neuroendocrine origin and being molecularly driven by p53/Rb loss (George et al., 2015). In this manuscript, we will address our efforts working on the most common subtype, LUAD.

1.2 HALLMARKS OF LUAD TUMOR CELLS

Lung adenocarcinomas (LUAD) are tumors that develop from secreting epithelial cells, generally lining the peripheral alveolar region of the lung (Xu et al., 2012). These regions are particularly exposed to environmental factors such as tobacco smoke or air contaminants that could potentially generate the inflammatory environment responsible for the disease.

Smoking individuals have an increased risk of developing lung cancer, about 30 times higher than normal (Vineis et al., 2004). In fact, the estimation is that almost 80% of lung cancer deaths can be directly prevented by smoke cessation (P. Zhang et al., 2022).

There exist various other risk factors that are directly correlated with lung cancer incidence and oncogenic events. Somatic genetic predisposition, for example, has been widely studied through gene association studies, revealing at least 20 genes strongly associated with lung cancer susceptibility (J. Wang et al., 2017). Ancestry has also been linked to lung tumor susceptibility. For example, Native American ancestry correlates with somatic driver alterations frequency in EGFR and KRAS genes that have a latter impact on lung cancer incidence (Carrot-Zhang et al., 2021).

Exposure to environmental pollutants such as radon gas has been historically, although controversially, linked to lung cancer incidence and severity (S. M. Lim et al., 2019). More recent findings show that particulate matter (PM) from air pollution, very fine carcinogenic particles present in areas housing 99% of the world population, are shown to promote EGFR and KRAS driven lung cancers, probably by generating macrophage activation fueling tumorigenesis (Hill et al., 2023).

Although carcinogenic exposure promotes tumor induction, recent studies have shown that, indeed, these agents barely increase mutational burden and rather encourage tumor-favorable microenvironments through genomic landscaping and inflammation (Riva et al., 2020). This is not the case for tobacco, as the carcinogens present in smoke do generate particular and very defined mutational signatures (Alexandrov et al., 2016), including the preference for particular mutations such as KRAS G12C (Dogan et al., 2012 ; X. Wang et al., 2021). However, although these multiple risk factors have been clearly implicated in the pathogenesis of lung cancer, about 20% of lung cancer cases worldwide are not attributable to tobacco smoking and no other clear-cut dominant factor (S. Sun, Schiller, & Gazdar, 2007).

While the precise mechanism of oncogenesis in lung cancer remains incompletely understood, a general model posits that the disease arises through the accumulation of genetic alterations that

confer a tumoral phenotype after transformation (Herbst, Heymach, & Lippman, 2008), a set of fundamental biological capabilities that define the malignant characteristics of cancer, the hallmarks of cancer (Hanahan & Weinberg, 2000). These hallmarks provide a framework for understanding the underlying biology of cancer and developing novel strategies against it.

In the lung, the central hallmark of tumor progression is overriding the mechanisms governing cellular proliferation. Mutations of genes behind these functions are the main drivers of the tumor and include mutations in several genes such as KRAS.

How these mutations occur is not clearly understood. Most probably, these mutations are random events occurring in the cell during lifetime. A second event, for example as previously mentioned the exposure to a carcinogen, changes the selective constraints in the somatic tissue and causes changes in the microenvironment, promoting inflammation and tumor-promoting conditions. A cell with a preexisting mutation on these proto-oncogenes has a selective advantage in these conditions, leading to clonal expansion and cancer (Lopez-Bigas & Gonzalez-Perez, 2020) (**Figure 2**).

These mutations constitute the root of the malignancy, inside all of the tumor heterogeneity, and allow for individual specific properties. For this reason, these are called driver mutations. Understanding the unique identity of these tumors, driven by their distinctive genetic universe, has revolutionized cancer treatment strategies and clinical outcomes.

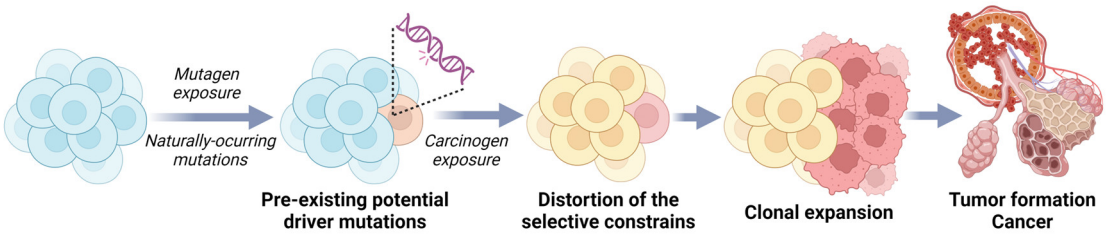

*Figure 2. C**arcinogenesis model**. During a lifetime, mutations accumulate in cells. These pre-existing mutations can become driver events when the selective constraints of the individual cells are modified. At that point, cells harboring these driver mutations expand and become what we know as cancer.*

2 KRAS DRIVEN LUAD: ALL THE PATHS LEAD TO MAPK

2.1 RAS FAMILY

In 1984, the team of Eugenio Santos & Mariano Barbacid identified the presence of a mutated KRAS oncogene in a biopsy of a lung tumor that was not present in the rest of the cells of the patient (Santos et al., 1984). This was one of the first pieces of evidence of RAS oncogenes being present in naturally occurring lung cancers. By then, the concept of oncogene, defined as a gene capable of inducing malignant transformation in cells, was still in debate (Malumbres & Barbacid, 2003).

The RAS superfamily is a set of at least 154 highly conserved human G proteins, small proteins that are able to cycle between active and inactive states thanks to the action of GTP (Wennerberg, Rossman, & Der, 2005). From this superfamily, there exists a subfamily of 36 genes closely related to the RAS functions historically described, including three particular main suspects for cancer biology, HRAS, KRAS and NRAS.

Interestingly, more than a third of all human cancers, including pancreatic, lung and colorectal, are driven by mutation in these three main RAS genes.

2.1.1 RAS GTPase

RAS was initially described to have guanine nucleotide binding capabilities by Edward Scolnick's group, suggesting that they could function as proteins having intrinsic GTP hydrolysis capacities, shuttling between active to inactive states (Shih, Papageorge, Stokes, Weeks, & Scolnick, 1980). Today, we have more insights on how these proteins work, most importantly on how the oncogenic variants modify the GTPase nature of the proteins. RAS functions as a binary GTP-switch, transiting between a GTP-bound active form and a GDP-bound inactive form (**Figure 3**).

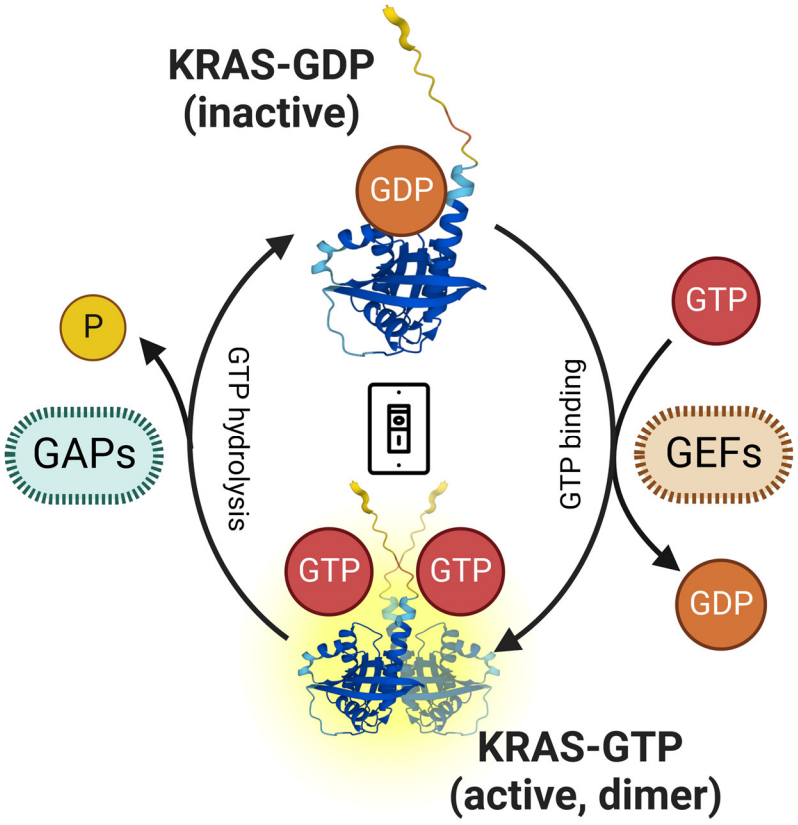

Figure 3. ***The RAS GTPase binary switch transitions between GTP active and GPD inactive states****. This process is facilitated by GAPs and GEFs, that actuate GTP/GPD molecules for making the transitioning of RAS states possible. Recent studies have shown that RAS is able to dimerize, or to form clusters, in its active form in the presence of GTP.*

This is only possible thanks to the action of regulatory proteins that put in motion the nucleotide molecules: the guanine nucleotide exchange factors (GEFs) and the GTPase activating proteins (GAPs). GAPs are essential for proper GTP hydrolysis, as the actual reaction is very inefficient by itself and needs to be accompanied by the cleavage step of the GTP that is granted by GAPs at the position Q61 of RAS (Scheffzek et al., 1997). On the other hand, GEFs allow to accelerate the GDP exchange process, modifying the affinity for GDP of the nucleotide-binding site and liberating the nucleotide from RAS (Vetter & Wittinghofer, 2001). This release is then followed by the loading of a new GTP molecule to be hydrolyzed, so the cycle can start again. In turn, the switching cycle is able to structurally modify two primary domains of RAS proteins, the switch I and switch II regions, that will become ready for interaction with downstream effectors (Milburn et al., 1990).

2.1.2 RAS coordinates upstream signals in the membrane

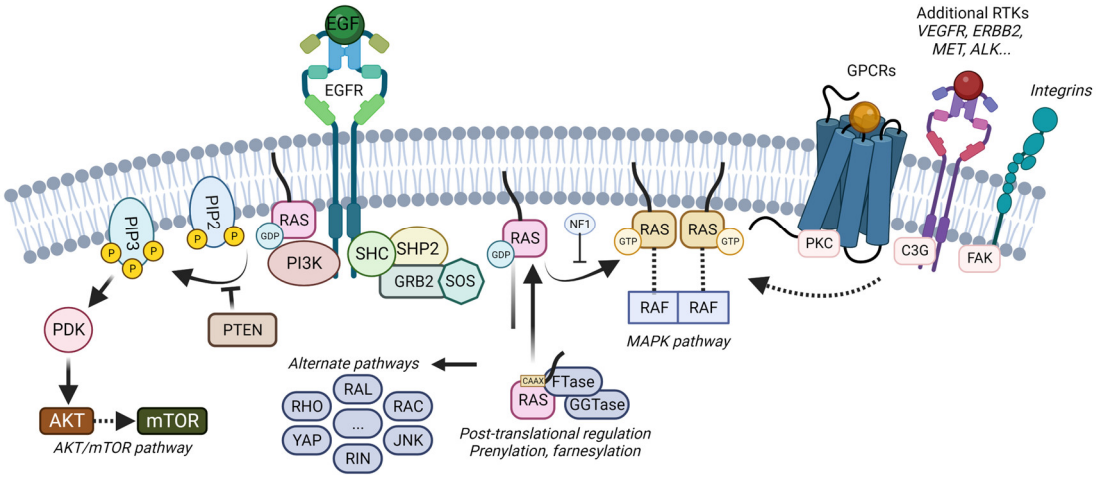

Figure 4. ***RAS pathway activation and signaling networks****. Visual representation of the complex web of RAS pathway activation, illustrating the interconnected molecular events activating the MAPK, AKT/mTOR and additional pathways.*

The GTP switch is only active in the presence of signals coming from upstream tyrosine kinase receptors (RTKs), such as the epidermal growth factor receptor (EGFR), bound to receptor-specific ligands. Ligand-induced dimerization on the RTK releases the initial auto-inhibitory conformation and allows trans-phosphorylation events of tyrosine residues (X. Zhang, Gureasko, Shen, Cole, & Kuriyan, 2006). This results in the recruitment of docking proteins, such as SHC, that acts as an assembly platform for recruiting additional molecules, such as adaptor proteins (Pelicci et al., 1992). RTK autophosphorylation generates SH2 binding sites that directly recruit the adaptor protein GRB2 (Lowenstein et al., 1992), although GRB2 can also be recruited indirectly via SHC binding (Liao et al., 2003). GRB2 is bound, by its SH3 domains, to a protein called SOS in pre-formed complexes in the cytoplasm (Egan et al., 1993 ; N. Li et al., 1993). SOS, as the main GEF activating RAS (Chardin et al., 1993), is activated when brought to the membrane by the SHC-GRB2-SOS ternary complex to facilitate the exchange of GDP for GTP on RAS proteins (Buday & Downward, 1993). The phosphatase scaffold SHP2 is able to promote GRB2/SOS recruitment to RTKs docking sites (Liao et al., 2003) and enhance RAS activity by dephosphorylating the inhibitory Y32 (Liotti et al., 2021). At this point, RAS becomes active and is able to form dimer/cluster structures that promote signal transduction by recruiting additional downstream effectors (Mysore et al., 2021). Recent work has proposed that nucleotide free RAS is also important

for signal regulation (Khan et al., 2022). This is only part of the complex signaling platform that is established in order to ensure RAS is specifically activated upon mitogen stimulation (**Figure 4**). These regulatory mechanisms can be hijacked by tumors in order to trigger oncogenic activation of RAS signaling.

2.1.3 MAPK proteins are downstream effectors of RAS

When switching to the GTP-bound status, RAS is able to relay signals to an incredible number of downstream effectors, involved in many cellular pathways. The most studied associate of RAS is the serine/threonine kinase family of RAF, linking RAS signaling with mitogen associated protein kinases (MAPK) pathway (Moodie, Willumsen, Weber, & Wolfman, 1993) (**Figure 5**).

The GTP bound form of RAS is able to bind both the three forms: RAF1 (also called CRAF), ARAF and BRAF kinases (Aelst, Barr, Marcus, Polverino, & Wigler, 1993 ; Vojtek, Hollenberg, & Cooper, 1993 ; X.-F. Zhang et al., 1993). However, upon GTP loading, RAS will only recruit CRAF to the membrane, as the switch I domain of RAS interacts with the RAS-binding domain (RBD) of RAF1 (Herrmann, Martin, & Wittinghofer, 1995). This interaction will displace 14-3-3 scaffold protein, liberating CRAF from its autoinhibited state and targeting the protein to the plasma membrane (Roy et al., 1998 ; Simanshu & Morrison, 2022).

In this conformation, CRAF forms heterodimers with BRAF, that trigger the phosphorylation of activatory RAF residues S338 and Y341 (Hu et al., 2013 ; Marais, Light, Paterson, & Marshall, 1995) that are essential for signal transduction (Rushworth, Hindley, O'Neill, & Kolch, 2006 ; Weber, Slupsky, Kalmes, & Rapp, 2001). ARAF is also able to form heterodimers with BRAF in this manner (Mooz et al., 2014). Together with active RAF heterodimers, the scaffolding protein KSR is able to increase the presence of local MEK kinase (Brennan et al., 2011 ; Rajakulendran, Sahmi, Lefrançois, Sicheri, & Therrien, 2009).

This process facilitates the following BRAF phosphorylation of MEK1 residues S218/S222 and MEK2 residues S222/T226 (Alessi et al., 1994 ; Gardner, Vaillancourt, Lange-Carter, & Johnson, 1994 ; Zheng & Guan, 1994). In turn, MEK will phosphorylate ERK simply on its activatory

residues. These phosphorylation events trigger a conformational change, stimulating ERK dimerization in the cytoplasm (Herrero et al., 2015 ; Khokhlatchev et al., 1998), followed by translocation of ERK to the nucleus (Payne et al., 1991).

The exact mechanisms governing ERK translocation are unclear but definitively unconventional, as ERK does not have any nuclear localization signal (NLS). Some studies point to a possible importin-driven transport thanks to a putative nuclear translocation signal (NTS) dependent on ERK2 activation by MEK (Chuderland, Konson, & Seger, 2008), while other studies suggest that ERK2 translocation is independent from carrier-driven mechanisms and directly involves the nuclear pore (Whitehurst et al., 2002).

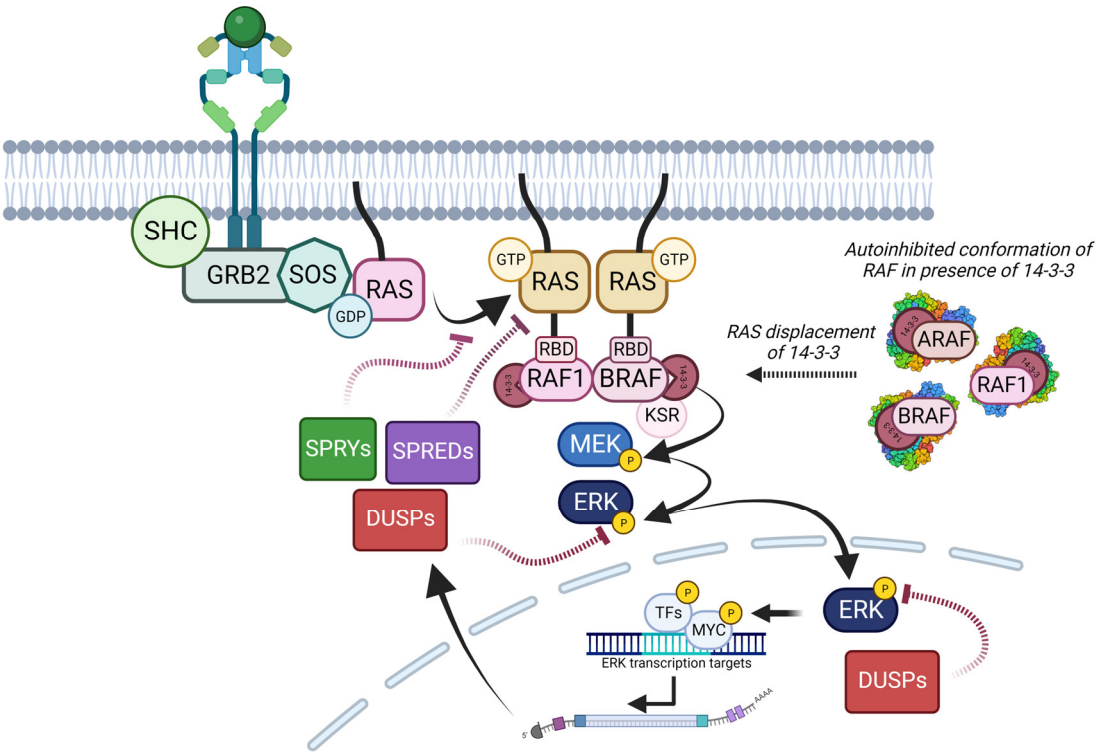

Figure 5. ***RAS model of activation of RAF and the MAPK pathway.*** *GTP active RAS recruits RAF by displacing 14-3-3, allowing for activation of RAF heterodimers and MEK phosphorylation. When ERK is phosphorylated by MEK, it is translocated to the nucleus where transcription factors are engaged in order to trigger the MAPK transcriptional program, including the expression of negative regulator genes such as SPRYs, SPREDs and DUSPs. Based on the model described by Dhirendra Simanshu (Simanshu & Morrison, 2022)*

2.1.4 Alternative downstream outlets for RAS

Current knowledge would suggest that MAPK remains the primary passageway for RAS signaling, as only RAF/MEK/ERK components are able to rescue RAS-less cells viability (Drosten et al., 2010). However, the functionalities of parallel signaling pathways seem to drive multiple tumor processes also driven by RAS activity. Upon RTK stimulation, RAS is able to recruit to the membrane the functional subunit p110α of PI3K in order to functionally activate the kinase together with p85 subunit (Rodriguez-Viciana et al., 1994 ; Rodriguez-Viciana, Warne, Vanhaesebroeck, Waterfield, & Downward, 1996). PI3K has lipid-modifying capabilities, transforming phosphatidylinositol (4,5)-bisphosphate (PIP_2) into phosphatidylinositol (3,4,5)-trisphosphate (PIP_3). PIP_3 will recruit AKT kinase, one of the main effectors of the pathway that will, in turn, phosphorylate mTOR substrates through TSC1/2 dimer investment (J. Huang, Dibble, Matsuzaki, & Manning, 2008). Activation of mTOR targets such as S6 kinase regulates multiple key process including cell cycle and cytoskeleton control (García, Kumar, Marqués, Cortés, & Carrera, 2006 ; Rodriguez-Viciana et al., 1997). The action of PI3K is antagonized by a tumor suppressor phosphatase, PTEN, that is capable of removing activating phosphate groups from PIP_3 lipids (Maehama & Dixon, 1998).

PI3K signaling has proven to be essential in many RAS-mediated oncogenesis processes, notably in tumor maintenance (Castellano et al., 2013 ; Gupta et al., 2007). Still, the PI3K/Akt pathway also presents tumor promoting capabilities on its own and has been seen affected in many cancer types (Samuels et al., 2004). Most relevant, there exist a complex pathway crosstalk between MAPK and PI3K signaling cascades, compensation mechanisms and synergies between the two, all deeply engaged in RAS-driven tumor progression (Castellano & Downward, 2011 ; Mendoza, Er, & Blenis, 2011).

Certainly, RAS proteins are well known for having various other downstream effectors in the cell. The list of effectors keeps growing as novel molecules specifically interacting with RAS are discovered, mediating multiple processes that contribute to the fine-tuned physiological balance (Malumbres & Barbacid, 2003 ; Schubbert, Shannon, & Bollag, 2007).

2.1.5 KRAS sweet spot in cancer

The K-RAS gene seems to be unique among its family members due to its unprecedented high mutation frequency, 10% of cancers present alterations in this gene. KRAS is frequently seen altered in lung, pancreatic and colorectal cancer (**Figure 6**).

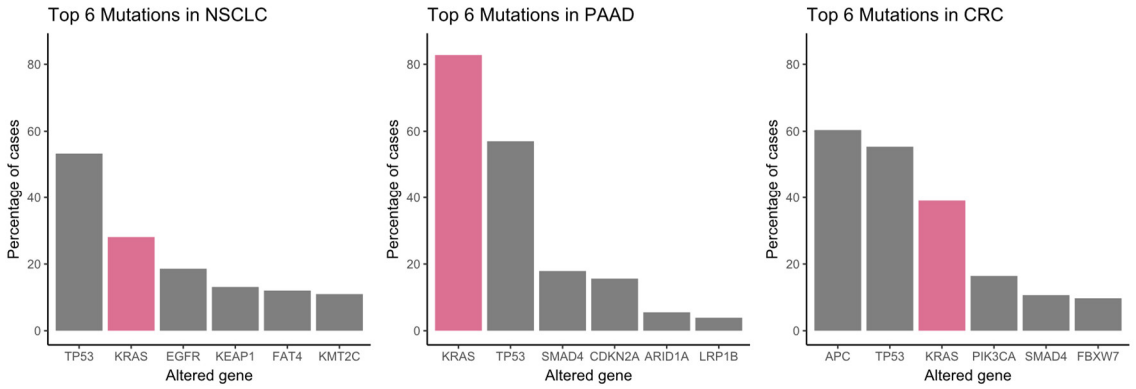

Figure 6. ***KRAS is frequently mutated in NSCLC, PAAD and CRC.*** *Histogram depicting the percentage of cases mutated in each tumor type (NSCLC, non-small cell lung cancer, PAAD, pancreatic adenocarcinoma, CRC, colorectal cancer) for the top 6 mutated genes in each category. KRAS is highlighted in pink. Data was obtained and adapted from INTEGO database (Martínez-Jiménez et al., 2020)*

The oncogenic mutations of KRAS observed in these tumors function differently, both structurally and functionally. Tumorigenic variants often show impaired GTPase activity that allow to maintain what historically was considered a constantly active state (Sweet et al., 1984). This activation is achieved thanks to the conformational modifications granted by substitutions in various residues, including G12, G13 (Clark, Wong, Arnheim, Nitecki, & McCormick, 1985) and Q61 (Der, Finkel, & Cooper, 1986). Indeed, these substitutions result in slower kinetics of return to the guanosine diphosphate-bound status, but GTP switching still needs from upstream stimulants and effectors to be activated, meaning that KRAS oncogenic mutants are not constantly active (H. Huang et al., 2014).

The main mutations, found at residues G12, G13, Q61, and others, are not equal. They have different intrinsic transforming "potencies", due to structural and functional dissimilarities, and they are selected across multiple cancer types depending on their specific transforming thresholds (Haigis, 2017 ; Prior, Lewis, & Mattos, 2012). Although this mechanistic selection is not yet clearly understood, each mutation has distinct affinities for RAF and other effectors (Hunter et al., 2015 ;

Zhou et al., 2020), allowing for precise molecular properties that develop distinct cellular consequences (Zafra et al., 2020). In this context, a particular mutation that grants a determined oncogenic signaling intensity, combined with appropriate timing, generates a tumor favorable environment for the cell. As such, there exists a narrow window where RAS signaling is able to conduce to tumor formation. This is the so-called "sweet spot", where too much RAS signaling conduces to stress processes, and little signaling fails to promote proliferation. Tumoral cells undergo a selective process for RAS mutations that fit the ideal level of signaling in specific cells of origin (S. Li, Balmain, & Counter, 2018).

In consequence, KRAS is also selected, rather than HRAS or NRAS, in these specific tumor types due to their different oncogenic potential. Protein dosage could also be important to explain isoform-specific frequencies. KRAS is the most abundant isoform in the cell and, contrarily to HRAS or NRAS, few dosage modifications result highly influential when reaching the "sweet spot" (Hood, Sahraoui, Jenkins, & Prior, 2023).

Simultaneously, the presence of the wild-type (WT) allele must be accounted for. Most KRAS mutations come in heterozygosity. The wild-type KRAS molecule is able to function as a tumor-suppressor factor facing its oncogenic counterpart, explaining why the WT allele is frequently lost in LOH advanced tumor stages (Burgess et al., 2017 ; Z. Zhang et al., 2001).

The recent understanding of KRAS dimerization has brought light to these LOH events. The ability of KRAS to form multimer complexes, generally known as nanoclusters, is now more evident thanks to computational characterization of KRAS dimerization interfaces and the putative structures that they form to recruit effectors to the membrane (Mysore et al., 2021 ; Sarkar-Banerjee et al., 2017). In a complex manner, receptor signaling controls the spatial distribution of these oligomers, which travel across lipid rafts in the plasma membrane. Upon stimulation, RAS molecules immobilize and form stable nanoclusters that are able to recruit downstream effectors (Goswami et al., 2020 ; Plowman, Muncke, Parton, & Hancock, 2005). Nanoclustering has proven to play a critical role in regulating RAS activity and the activation of MAPK effectors (Nan et al., 2015 ; Tian et al., 2007). With all the increasing evidence, it is understood that wild type protomers

disrupt oncogenic function of KRAS mutants, modulating their ability to signal (Ambrogio et al., 2018). Now that the emerging KRAS nanoclustering field has started to shed light onto previously unanswered questions, it is necessary to better understand how the signalosome assembly occurs. KRAS nanoclustering occurs only, upon stimulation, in the presence of a particular set of proteins, including scaffolds such as galectin-3 (Shalom-Feuerstein et al., 2008). The role of these scaffolds in cluster stabilization is still poorly understood, and there is a high probability that many other unknown scaffolding proteins engage in the structure of the signalosome.

2.2 THE ARRIVAL OF TARGETED THERAPIES

2.2.1 Precision therapies for MAPK pathway

Despite KRAS being one of the earliest known and most common oncogenic drivers in NSCLC, effective targeting has been challenging due to the complex mechanistic regulation intrinsic to the multiple effectors and pathways that are behind its signal transduction.

As virtually all the mutations found in NSCLC are directly related to RAS/MAPK pathway, the principal therapeutic strategy that has been conducted since the development of small molecule inhibitors has been the direct targeting of its main effectors.

One of the first pharmacological approaches used to block the MAPK pathway in tumors was the multi-tyrosine kinase inhibitor sorafenib, the first of its name to be orally active and approved by the FDA (Wilhelm et al., 2006). This compound was able to target multiple kinases in the pathway, specially CRAF, BRAF and many RTKs (L. Liu et al., 2006). This compound presented many clinical benefits in patients with hepatic, thyroid and renal cancer and it is still recommended and used to this day in well-established contexts (Liao et al., 2003). However, in KRAS mutant lung cancer the clinical benefit was very limited (E. S. Kim et al., 2011), and presented higher toxicity levels than the FDA standards (Y. Li, Gao, & Qu, 2015).

Contrarily to KRAS-mutant NSCLCs, EGFR-mutant tumors may benefit from several rounds of receptor tyrosine kinase inhibitor treatments (RTKi) (Goulart, Larkins, Beaver, & Singh, 2023).

KRAS mutant tumors certainly did not respond to RTK inhibition alone as upstream signaling blockade spared the actual driver signaling (Karapetis-Christos et al., 2008 ; Lièvre et al., 2006). For this reason, research efforts have been centered in inhibitors focusing on downstream effectors of KRAS, such as RAF, MEK and ERK, that may prove useful in these cases.

As no selective CRAF inhibitor has ever been developed, the focus turned onto BRAF targeting. Multiple BRAF kinase inhibitors have been developed during the years in a combined effort to treat melanoma, characterized by a prevalence of nearly 60% of cases involving a BRAF mutation (Colombino et al., 2012). Initial drug development efforts were focused on inhibitors with high specificity against V600E oncogenic mutant of BRAF. The compounds vemurafenib, dabrafenib or encorafenib, presented high success responses in melanoma patients, but when enrolled for NSCLC treatment, all of them failed to show benefits in KRAS-driven tumors. These BRAF inhibitors were found to inhibit ERK in V600E cell lines but paradoxically activated ERK in RAS-mutant cell lines with wild-type BRAF (Kaplan, Shao, Mayberry, & Aplin, 2011). This rewiring of the MAPK pathway was the consequence of paradoxical transactivation of CRAF protomers by negative cooperativity, aggravated by the presence of active RAS (Hatzivassiliou et al., 2010 ; Poulikakos, Zhang, Bollag, Shokat, & Rosen, 2010). Actually, some of the patients treated with vemurafenib spontaneously developed secondary skin squamous carcinomas with RAS mutations, consequence of paradoxical MAPK activation in pre-neoplastic lesions harboring these mutations (Su et al., 2012). In order to overcome this issue, some pan-RAF inhibitors are being developed, and have to prove adequate when evaluating their high toxicity (Hong et al., 2017 ; Martinez-Garcia et al., 2012). The challenge for developing paradox-breaking RAF inhibitors is still ongoing, as one of the main goals for the new generation of inhibitors will be to block RAF dimerization and prevent paradoxical ERK activation (Tutuka et al., 2017 ; C. Zhang et al., 2015). The question still remains unanswered regarding the suitability of these inhibitors for KRAS-driven NSCLC and the method of their implementation.

Inhibiting MEK has demonstrated remarkable efficacy treating RAS/MAPK driven cancers, most particularly in melanoma (Flaherty et al., 2012). As MEK is a converging effector, MEK inhibition

has the potential to inhibit all the MAPK driven tumors. Despite its good candidacy, inhibiting MEK seems to be an inefficient way to blockade MAPK output in KRAS mutant NSCLC. Because of the importance of the RAF-MEK interaction in the mechanism of action of these compounds, initial MEK inhibitors such as cobimetinib, refametinib, selumetinib or mirdametinib, present one-hundred-fold weaker potency against KRAS-mutant than BRAF-mutant cells (Hatzivassiliou et al., 2013). Newer MEK inhibitors such as trametinib or avutometinib showed improved results against KRAS mutant cells, but prompt reactivation of CRAF may prevent full ERK inhibition in these cases (Lito et al., 2014). In consequence, trametinib shows superior results in combination with dabrafenib, a RAF inhibitor, but only in BRAF mutant tumors (Bollag et al., 2010 ; Long et al., 2017). Selective MEK inhibitors, even in combination with BRAF inhibitors, demonstrate insufficient phosphorylated ERK depletion and, in result, have marginal effects on NSCLC patients whose tumors harbor KRAS mutations (Blumenschein et al., 2015 ; Jänne et al., 2017).

Pharmacological targeting of all these multiple substrates is challenging. Henceforth, the most logical, and potentially the ultimate target in the MAPK pathway, would be downstream ERK kinases. Plus, direct inhibition of ERK could have the potential to overcome the limitations observed with RAF and MEK inhibitors, seen the persistence of ERK signaling during the presence of the inhibitors. The currently developing ERK inhibitors, such as ulixertinib, seem to be remarkably effective against RAF and MEK inhibitor resistant tumors (Hatzivassiliou et al., 2012). These have entered clinical trials, still ongoing, but missed the opportunity to include KRAS-mutant patients (Sullivan et al., 2017). One of the main concerns for the use of this strategy is the inactivation of negative feedback mechanisms that could originate from ERK inhibition, such as the downregulation of DUSP6 (Germann et al., 2017). Because of the negative feedback inactivation, and the problematic toxicity triggered by vertical inhibition of the pathway, ERK inhibitors remain a challenging piece of the puzzle that may not be relevant in the KRAS mutant field.

In essence, it is difficult to target individual MAPK components, as it may result in compensatory mechanisms that are able to adapt pathway responses. MEK inhibition through trametinib itself is

able to activate feedback mechanisms that phosphorylate tyrosine kinase receptors such as IGF1R and ERBB3, leading to adaptative resistance (Kitai et al., 2016 ; Yohe et al., 2018). A similar process occurs in BRAF mutant cancers through reactivation of EGFR (Corcoran et al., 2012 ; Prahallad et al., 2012). In turn, monotherapy with these MAPK inhibitors seems to be associated with little clinical improvement, probably because of cytostatic effects that hamper tumor regression and even promote resistances (Corcoran et al., 2013).

In contrast, combinatorial strategies are promising increased efficiencies by exploiting the whole MAPK arsenal that we currently have on the shelf, while it keeps growing (**Table 7**).

RTK inhibitors					
EGFR	Erlotinib	Osimertinib	Neratinib	Gefitinib	Cetuximab
Other	Afatinib	Neratinib	Pazopanib	Panitumumab	Lenvatinib
RAS processing					
SOS	BAY-293	BI-3406		BI-1701963	
SHP2	Vociprotafib	JAB-3068	Batoprotafib	RLY-1971	BBP-398
Ras PTM	Tipifarnib	Cysmethynil	UCM-1336	Deltarasin	NHTD
MAPK components					
RAF	Belvarafenib	Lifirafenib	Sorafenib	Vemurafenib	Dabrafenib
	Encorafenib	LXH254	PLX8394	LY3009120	AZ-628
MEK	Pimasertib	Cobimetinib	Binimetinib	Selumetinib	Mirdametinib
	Trametinib	Refametinib	Avutometinib	TAK-733	GDC-0623
ERK	Ulixertinib	MK-8353	Ravoxertinib	Temuterkib	Rineterkib
Multikinase	Ruxolitinib	Sunitinib	Regorafenib	Nintedanib	Cabozantinib
PI3K components					
P110	Alpelisib	Copanlisib	Duvelisib	Idelalisib	Taselisib
AKT	Capivasertib	Ipatasertib	Miransertib	Afuresertib	MK-2206
mTOR	RMC-5552	Everolimus	Sirolimus	Temsirolimus	
Immune therapy					
PD1/PD-L1	Pembrolizumab	Nivolumab	Cemiplimab	Atezolizumab	Dostarlimab
CTLA4	Ipilimumab		Tremelimumab		
Other					
CDK4/6	Palbociclib	Ribociclib		Abemaciclib	
PARP	Niraparib	Olaparib	Talazoparib	Rucaparib	
Proteasome	Bortezomib	Ixazomib		Carfilzomib	

*Table 7. **List of currently available drugs commonly used in NSCLC targeted therapies**. FDA approved drugs (for NSCLC and/or in solid tumors treatment) are in blue, while those in active clinical trials are in green. Drug names in purple refer to pre-clinical and/or investigational treatments currently unavailable to NSCLC patients.*

Co-targeting KRAS downstream effectors MEK and AKT may appear an interesting approach to exhaust RAS signaling and target pathway compensatory crosstalk mechanisms (Molina-Arcas et al., 2019 ; Turke et al., 2012). Nevertheless, these combinations, despite having favorable efficiency compared to the individual treatments, present a considerable challenge respecting the overlapping toxicities (Shimizu et al., 2012 ; Tolcher et al., 2015). To circumvent these toxicities, multiple low dose approaches are being proposed. Recent work has proven the efficiency of using a combination

of three or four MAPK inhibitors at very low doses (EGFRi + RAFi + MEKi + ERKi) to treat EGFR mutant NSCLC *in vitro* models (Neto et al., 2020). These strategies are capable of limiting the toxic effects while delaying resistance mechanisms derived from the combination, but still need to prove useful in a KRAS mutant context. Drugging the undruggable: the G12C breakthrough

Mutant KRAS has long been referred to as an undruggable target because of its unusual shape. Compared to other proteins in the cell, RAS has a relatively smooth protein surface, meaning that designing inhibitors to bind surface grooves, and to be specific for mutant variants, is challenging. On top of that, RAS has an exceptionally high affinity for GTP, in the picomolar range, needing more potent inhibitors than traditional TKIs (John et al., 1990). For these reasons, drug development of KRAS inhibitors has been stalled for 40 years, leaving behind hundreds of small molecule binders that either inefficiently inhibited RAS activity or had unacceptable toxic effects (Riely et al., 2011).

Recent technological advances in compound screening allowed better understanding of the structural openings that were generated by oncogenic mutants such as $KRAS^{G12C}$. In 2013, it was revealed that G12C mutation induced the expansion of the switch II pocket by displacing residue Q61, revealing a novel potential binding site (Ostrem, Peters, Sos, Wells, & Shokat, 2013). This discovery established the foundation for the development of two G12C specific inhibitors suitable for clinical testing, Amgen's AMG-510 (Sotorasib) (Canon et al., 2019) and Mirati's MRTX849 (Adagrasib) (Hallin et al., 2020). These molecules were the result of years of chemical refinement of the original compounds and were theoretically specific to the oncogenic variant, as the wild-type molecule did not present this particular pocket. These inhibitors were denominated RAS (OFF) molecules because they were able to block KRAS signaling by covalently binding cysteine 12, only in the GDP-bound state of the molecule, blocking reactivation through nucleotide exchange, and reducing the pool of GTP-bound forms (Lito, Solomon, Li, Hansen, & Rosen, 2016). Since, many more inhibitors have been developed and are currently under development, exploiting this market opening.

Name	Developer	Pharma ID	Type	Current state
Sotorasib	AMGEN	AMG-510	KRAS-G12C	FDA, EMA, approved (NSCLC)
Adagrasib	Mirati	MRTX849	KRAS-G12C	FDA approved, EMA pending
Garsorasib	Inventis Bio	D-1533	KRAS-G12C	Phase II
Opnurasib	Novartis	JDQ433	KRAS-G12C	Phase II
-	GenFleet	IBI351(GFH925)	KRAS-G12C	Phase II/I
Divarasib	Genentech/Roche	GDC-6036 (RG6330)	KRAS-G12C	Phase I
-	Johnson & Johnson	NJ-74699157 (ARS-3248)	KRAS-G12C	Phase I
-	Lilly-Loxo	LY3537982	KRAS-G12C	Phase I
-	Genhouse	GH35	KRAS-G12C	Phase I
-	Huayabio	HBI-2438	KRAS-G12C	Phase I
-	GenEros	GEC255	KRAS-G12C	Phase I
-	Jacobio	JAB-21822	KRAS-G12C	Phase I
-	Betta	BPI-421286	KRAS-G12C	Phase I
-	Merck	MK-1084	KRAS-G12C	Phase I
-	D3Bio	D3S-001	KRAS-G12C	Phase I
-	Jiangsu	HRS-4642	KRAS-G12D	Phase I
-	US NCI	Anti-KRAS G12V	mTCR PBLs	Phase I
-	Astellas	ASP3082	KRAS-G12D Degrader	Phase I
-	RasCal	RSC-1255	Pan-RAS (WT/MUT)	Phase I
-	Erasca	ERAS-3490	KRAS-G12C	Pre-clinical trials
-	Bridge Bio	BBO-8520	KRAS-G12C	Pre-clinical trials
Salirasib	Concordia	162520-00-5	Pan-Ras	Phase II Failed
-	Boehringer	BI-1823911	KRAS-G12C	Phase I
-	Boehringer	BI-1701963	SOS1::Pan-KRAS	Phase I
-	Revolution Medicines	RMC-6236	Pan-RAS (ON)	Phase I
-	Revolution Medicines	RMC-6291	KRAS-G12C (ON)	Phase I
-	Revolution Medicines	RMC-9805	KRAS-G12D (ON)	Phase I
-	Revolution Medicines	RMC-8839	KRAS-G13C (ON)	Pre-clinical trials
-	Revolution Medicines	RMC-0708	KRAS-Q61H (ON)	Pre-clinical trials
-	Revolution Medicines	RMC-5127	KRAS-G12V (ON)	Pre-clinical trials

Table 8. ***Compendium of RAS targeted therapies currently available.*** *The market of RAS-targeting drugs exploded since the discovery of the G12C pocket. Sotorasib and adagrasib remain the most used for the moment.*

In the clinic, these inhibitors seemed to be highly efficient only to a small fraction of patients and obtained poor results in progression-free survival, being barely more efficient than routine chemotherapy in NSCLC. This lack of efficiency was confirmed in a basket trial including melanoma, colorectal cancer, and further solid tumors (Hong et al., 2020). Sotorasib, which was the first one to be tested as monotherapy for advanced pre-treated solid tumors with G12C mutation, had a 32.2% response rate in NSCLC in phase 1 clinical trials, and 37.1% in the phase 2 study (Hong et al., 2020 ; Skoulidis et al., 2021). Adagrasib outperformed these results by increasing the response rate up to 42.9% (Jänne et al., 2022). Neither of them was able to reach 7 months of median progression-free survival. A recent phase 3 study in NSCLC has confirmed that sotorasib only increased median progression-free survival up to 5.6 months, versus 4.5 months for the docetaxel chemotherapy group (Langen et al., 2023). No significant differences were observed in the overall survival between these two groups. Furthermore, sotorasib showed incompatibility with immunotherapy agents, such as checkpoint inhibitors, as the combination therapy recurrently induces hepatic failure (Begum, Goldin, Possamai, & Popat, 2021), a secondary effect that has rarely been observed in mono-treated patients (Kinahan, 2022).

This poor performance of the inhibitors in the clinic pointed to a short-lasting activity of these agents. The RAS(OFF) mode of action was soon questioned by the prompt emergence of diverse resistances, through both primary and acquired mechanisms.

2.2.2 Resistance to RAS inhibition is mediated by reactivation of MAPK

Primary mechanisms of resistance prevent, to some extent, a good response of the tumor to the inhibitor, since early timepoints of the treatment. Specific alterations co-occurring with G12C mutation, comprised inside the tumor heterogeneity, are behind the different levels of response to therapy. For G12C inhibitors, the refractory mechanisms that were identified through long-term sotoRASib clinical trials included the existence of co-mutations in genes such as KEAP1, SMARCA4, CDKN2A and STK11 (Dy et al., 2023 ; Negrao et al., 2023). The pre-existence of secondary KRAS mutations that could redirect inhibitor binding is very rare in NSCLC. Less than 3% of the tumors present more than one RAS mutation at the initial time of treatment (Cannataro

et al., 2018 ; Zhao et al., 2021). For these reasons, alternative horizontal re-activatory mechanisms may be more important for primary resistance.

Another partner in crime for resistance is the wild-type allele. Adaptative pathway activation can be mediated through wild-type RAS expression, as G12C inhibition deploys compensatory mechanisms that activate the rest of RAS isoforms, that are insensitive to inhibitors (Ryan et al., 2020). This phenomenon, which was also observed in MEK inhibitor resistance (Burgess et al., 2017), is poorly understood. Although the exact role of the wild-type allele in acquired resistance has not been elucidated yet, it is very possible that it relies on its dimerization capabilities with the mutant KRAS (Ambrogio et al., 2018).

At the same time, multiple acquired resistance mechanisms have been reported over these years, being very heterogeneous and diverse. The first cases to be reported, and the most evident, were the emergence of secondary events that counteracted the original G12C mutation. These accounted for half of the resistant tumors and included secondary KRAS oncogenic mutations, amplifications of the G12C locus and additional genomic rearrangements involving the RAS-MAPK pathway members (Awad et al., 2021 ; Zhao et al., 2021).

Intrinsic resistance is inevitable. The term adaptative resistance refers to the rapid reactivation of the RAS-MAPK pathway through rebalancing of signaling networks. As previously mentioned for MAPK inhibitors, feedback activation mechanisms have also been observed in G12C inhibition, through RTKs such as ERBB2/3, FGFR1 and AXL (Solanki et al., 2021). Adaptative resistance sems to also rely in prompt G12C reactivation upon inhibition, possibly through transcriptional rewiring, which allows quick synthesis of new molecules that undergo nucleotide exchange and rapidly transition to the drug-insensitive state, bypassing inhibitor binding (Xue et al., 2020).

In spite of having uncovered some resistance mechanisms, most allosteric inhibitor resistance cases remain a mystery, the vast majority going through very complex processes of idiosyncratic enrichment of clonal populations that escape our comprehension (Tsai et al., 2022). In all the cases,

we cannot exclude the importance of KRAS-independent mechanisms, including the roles of tumor microenvironment and immune escape, among others.

A possible answer to the lack of functional response of the inhibitors and the rising of resistances could be in the combined inhibition of positive feedback. Vertical inhibition of SHP2 could contribute to the enrichment of the GDP-bound pool and increase the efficiency of G12C inhibitors (Fedele et al., 2020 ; C. Liu et al., 2021). SHP2 inhibition in combination with PI3K inhibitors could be an efficient way to overcome sotorasib resistance driven through AKT and ERK reactivation (Adachi et al., 2020). Plus, EGFR has emerged as an early lead with G12C inhibitor or SHP2 inhibitor combinations as RTKi may have the ability to directly increase the residency of KRAS in its inactive state (Amodio et al., 2020 ; Lito et al., 2016 ; Patricelli et al., 2016).

On the other hand, SOS1 has already shown in vitro synergy with MAPK inhibitors such as trametinib (Lake, Correa, & Ler, 2016) and has been identified as a potential vulnerability for G12C cell lines (Lou et al., 2019). Recent studies combining adagrasib with SOS1-KRAS interaction inhibitors suggest that this approach could enhance tumor response and even delay the emergence of acquired resistance (Thatikonda et al., 2023). Yet, possible compensatory effects may be observed by SOS2 action or additional GEFs.

At present, mutant selective inhibitors could be outcompeted by a recent wave of compounds that try to circumvent these resistances by adopting a RAS (ON) mode of action, able to target the active form of KRAS (Schulze et al., 2023).

2.2.3 Pan-KRAS inhibitors are already here

In the meantime, while KRAS mutant-specific inhibitors are being developed and tested in imaginative combinatorial treatments, the pharmacological race to find the ultimate inhibitor has already struck some very interesting competitors, the Pan-KRAS inhibitors.

Although KRAS full inhibition was initially supposed to present toxicity, it is possible to develop therapeutic strategies to totally deprive the organism of KRAS activity. Indeed, there is no evidence that could support an essential role of KRAS in adult tissues (Johnson et al., 1997), and its inhibition

through complete body ablation is totally viable, since mice fully lacking KRAS do not present any kind of toxicity (Dhawahir, 2009).

The most recent and striking evidence of the use of these inhibitors was the one developed by Piro Lito's team (D. Kim et al., 2023). This non-covalent inhibitor, called BI-2865, was refined from previous selective inhibitor structures that failed to advance to later stages, and proved to be KRAS specific, not HRAS nor NRAS. KRAS inhibition was achieved independently of the mutational status with clear suppression of downstream signaling and cancer growth in vivo. The results of reduced tumor growth were accompanied with no effect in animal weight and did not report further toxicities.

Still, future studies will have to confirm clinical tolerance of pan-KRAS inhibitors as some studies report that KRAS is potentially involved in maintenance of human thrombopoietin biosynthesis, an essential process to deliver hematopoietic stem cells in the adult bone marrow (Damnernsawad et al., 2016).

Although very promising, these inhibitors will also have to address the concerns on rising resistances, as the preclinical studies that are presented by Kim et al. do show small but existent resilience of the tumors at the end of the treatment. Although pan-KRAS inhibitors will probably show increased efficiency for targeting cancer cells, it is very probable that they will also favor the appearance of resistance mechanisms through spatio-temporal rewiring of the RAS-MAPK effector network.

2.2.4 Degraders, toxins, vaccines and more

Creative solutions have been emerging through recent years in order to solve the un-druggable puzzle presented by KRAS.

Among the strategies that try to overcome the limitations driven by the intrinsic properties of small molecule inhibitors that, in general, covalently bind KRAS, emerged the possibility of directly removing the protein by degradation. The so-called RAS degraders are able to force the removal of the protein from the cell through proteolysis-targeted chimeRAS (PROTACs). These are bivalent

small molecules that are able to sequester the protein of interest and bring it to an E3 ubiquitin ligase that will mediate its degradation. This strategy has already been implemented for targeting KRAS by exploiting previously developed and efficient warheads, such as antibody-mimetics designed ankyrin repeat proteins (DARPins) (Bery, Miller, & Rabbitts, 2020). Many degraders have recycled unsuccessful small molecule warheads that bind oncogenic mutants with high affinity, but did not present good inhibitory material, to create very efficient PROTACs (Bond, Chu, Nalawansha, Li, & Crews, 2020 ; S. Lim et al., 2021). These degraders have shown very high efficiency and paint a very promising future for cancer therapeutics. However, the important size and complex molecular structure of these degraders is a major challenge to be addressed to achieve future clinical goals.

An alternative approach to targeting RAS degradation directly is the use of toxins, such as bacterial endopeptidases. A recent example is the use of a RAS/RAP1-specific endopeptidase fused to a fragment of the diphtheria toxin. This chimera is able to enter the cell through EGF-mediated endocytosis and cleaves switch I region of RAS, inhibiting MAPK signalling and resulting in tumor regression without resistance (Vidimar et al., 2022). Despite the current efforts to improve pharmacological stability, increase uptake selectivity and reduce their toxicity, these compounds could be interesting competitors to PROTACs in the future.

Other therapeutic approaches count on profiting from the immune system naturally present in the patients and developing individualized solutions. Adaptive cell therapy is able to use in vitro expanded tumor infiltrating lymphocytes to target tumor cells expressing precise and unique MHCs that were described to be specific of KRAS-driven tumors (Rosenberg et al., 2011). This personalized medicine approach has already been successfully tested in both melanoma and metastatic lung cancer (Bear et al., 2021 ; Tran et al., 2016). Nonetheless, immune evasion was an inevitable event when the selected MHC was lost by the tumor and no longer available. To counterbalance the immune evasion effect on MHCs, cancer vaccines strategies ought to target KRAS directly. These are composed of peptides including the mutant KRAS amino acids and an

immune stimulant that are able to induce cytotoxic T cell activity against solid tumors in clinical trials (Pant et al., 2022).

It is officially time to say that KRAS has lost its “undruggable” title. All these novel approaches have filled with optimism the cancer therapy field and will open a broad spectrum of possibilities that will eventually succeed and colonize the clinic. Granting all the effects and clinical responses described previously, the durability of response to targeted therapies seems to always be curbed by incomplete cell death and/or the development of resistance. Thus, it will be crucial to develop better understanding of RAS biology and keep scrutinizing the MAPK pathway regulation in order to evolve the ultimate therapeutic strategies to suppress KRAS-driven tumors.

3 THE ENDLESS MAPK REGULATION PARADIGM

3.1 MAPK EFFECTORS ARE SUBMITTED TO TIGHT MECHANISMS OF CONTROL

As the main effector under RAS signaling, the MAPK pathway is an intricate signaling cascade interconnected at many levels with multiple partners. As we have previously discussed, a large number of alterations confer severe MAPK signaling modifications that result in pathological and event malignant consequences.

One of the main questions submerged in the field has been how KRAS addiction is maintained in mutant cancers. Tumor cells grow and evolve with a broken KRAS switch, hyperactivating the pathways underneath to obtain malignant hallmarks. But this hijacking of a fundamental cellular control mechanism never comes without a price. In 1983, two different teams found out that RAS was insufficient to promote transformation in primary rodent cells (Land, Parada, & Weinberg, 1983 ; Ruley, 1983). Further oncogenic partners, in this case oncogenes MYC and E1A, were needed to inactivate cellular responses that normally would be required for RAS-mediated inhibition of cell proliferation and, in turn, could convert RAS into a growth-promoting gene (Franza, Maruyama, Garrels, & Ruley, 1986). This was the first evidence that oncogenic mutations required cooperation of additional events, that could support the tumorigenic state. Failure to accompany RAS with the presence of these factors would result in cellular toxicities such as replicative stress and induced senescence (Serrano, Lin, McCurrach, Beach, & Lowe, 1997). This phenomenon not only applies to RAS, but extends to many other oncogenes that, unless implemented properly in a naïve cell, will induce immediate cytotoxicities (Evan et al., 1992 ; Rao et al., 1992).

Although these experiments may rise hypothesis from gross overexpression settings, the consequences of this particular feature are very observable in the clinic. EGFR activating mutations do not occur at the same time as KRAS mutations (Kosaka et al., 2004). The co-occurrence of these two oncogenic entities over-activates MAPK signaling, resulting in deleterious consequences for

the cell (Unni, Lockwood, Zejnullahu, Lee-Lin, & Varmus, 2015). EGFR and KRAS mutations are mutually exclusive, not because they are redundant, but because combined potencies lead to an oncogenic conflict that derives in irreversible toxicity (Ambrogio, Barbacid, & Santamaría, 2017).

Similarly, compound RAS and BRAF mutations are extremely rare (Seth et al., 2009) and when found in the same tumor they can be traced to independent original single-cell clones, each with an individual mutation (Sensi et al., 2006). Coexistence of these two mutations induces prompt senescence, driven by an overactivation of the MAPK system (Petti et al., 2006). In a BRAF V600E setting, the expression of a concomitant oncogenic KRAS G12V destabilizes cell cycling and metabolism and reduces viability when compared to a KRAS WT (Monticone et al., 2008). Naturally, BRAF V600E individual cells that obtain parallel KRAS G12D mutations, or vice versa, are outcompeted by single-mutant cells that do not enter p16-mediated senescence (Cisowski, Sayin, Liu, Karlsson, & Bergo, 2016). High intracellular MAPK activity tends to activate senescence mechanisms driven by p38 MAPK and p53/p21 upregulation, a phenomenon that can be accompanied by high reactive oxygen species (ROS) (P. Sun et al., 2007).

Mutual exclusivity is also observed therapeutically. Intermittent use of BRAF and MEK inhibitors, a method commonly known as “drug holiday”, has shown that increased cytotoxicity can be generated upon release of the treatment, as MAPK levels rebound and generate growth stop upon inhibitor withdrawal (Moriceau et al., 2015 ; Seghers, Wilgenhof, Lebbé, & Neyns, 2012). All this data suggests that, in the tumor, there exists a constant pressure for activating oncogenic signaling while, at the same time, limiting excessive, out of reach, signaling levels. Disproportionate RAS/MAPK signaling, that may initially favor the nature of malignancy in initiating cells, categorically fails to promote long-term tumor phenotypes (Nieto et al., 2017).

MAPK hyperactivation is also pathological outside the cancer realm. RAS proteins, as well as other GTPases and MAPK effectors, have also been associated with rare pathologies such as Noonan-syndrome. Noonan is the most frequent manifestation of the so-called RASopathies, which are perfect examples of how genetic alterations of the MAPK pathway directly produced by point mutations, in this case in the germinal line, generate pathological excessive MAPK signals (Cuevas-

Navarro et al., 2023). These not-so-rare syndromes, affecting 1 in 1,000 individuals, also benefit from MAPK inhibitor treatment to halt the development of the disease (Rauen, 2012).

The intrinsic nature of MAPK helps in the task of limiting itself, through complex adaptability mechanisms naturally evolved. While abrupt modifications may not present selective advantages, rewiring of the MAPK machinery happens constantly to keep physiological levels upon sudden stimuli. This is achieved thanks to an extensive network of pathway modulators. Most importantly, activated MAPK exploits its own negative regulation systems to inactivate itself and buffer uncompensated signals from the extracellular compartment. Under non-stimulated conditions, negative feedback regulation mechanisms are kept silenced until needed. The capicua (CIC) transcriptional repressor is one example of how this mechanism actuates, as it blocks the expression of negative regulators such as DUSP6 until CIC gets phosphorylated by p90RSK MAPK effector and exits the nucleus (Ren et al., 2020 ; Weissmann et al., 2018).

During targeted treatment, MAPK responses rebalance, and the only manner to reactivate pathway signaling after drug inhibition, without additional pathway alterations, is by enhancing negative and positive feedback loops. MAPK modulation, primarily thanks to feedback interactions, transforms input signals into non-uniform ERK activity pulses of constant amplitude and duration (Hiratsuka et al., 2015). The nature of these pulses shapes proliferative activity, relying more in their frequency than amplitude or intensity, although both are necessary to maintain MAPK-driven phenotypes (Albeck, Mills, & Brugge, 2013). Organically, spatiotemporal regulation of ERK pulses is fundamental to coordinate cell fate and tissue homeostasis (Ender et al., 2022 ; Ryu et al., 2015). Very much as the “sweet spot” model, ERK frequencies shape cellular fates, as medium-frequency pulses orient cells to survival and proliferation and disruption of the average ERK rhythm can direct the cells into apoptosis (Aoki et al., 2013).

3.2 PHOSPHATASE ACTION AND DUSPS

Reversible phosphorylation is one of the simplest, yet complex, ways by which the MAPK orchestrates a fine balance. While kinases phosphorylate residues in MAPK proteins and effectors, phosphatases are able to remove these markings.

Yet, all phosphorylation events are not activatory. Many of the MAPK proteins residues phosphorylation inhibit kinase activity. One example are RAF proteins, as they can be submitted to inhibitory phosphorylation by many effectors, including itself, that can be dangerously relieved during inhibitor treatment (Holderfield et al., 2013 ; Zimmermann & Moelling, 1999).

In consequence, the action of phosphatases can be cryptic in some cases as they can have multiple roles at different residues for one particular substrate. The most common phosphatases in the cell, phospho-protein phosphatases (PPPs) PP1 and PP2, have this multifaceted activity (Seshacharyulu, Pandey, Datta, & Batra, 2013). When dealing with CRAF, PP1/PP2 de-phosphorylation can resuscitate inhibited accumulated CRAF molecules in the membrane, facilitating 14-3-3 displacement and RAS-dependent activation (Jaumot & Hancock, 2001). These are very pleiotropic phosphatases involved in many cellular processes, so in order to obtain substrate specificity they form macromolecular complexes with an army of regulatory subunits (Shi, 2009). For instance, PP1 complies with MRAS and SHOC2 to obtain substrate specificity towards RAF inhibitory residues (Young et al., 2018). Ultimately, these phosphatases can be implicated in modulation of MAPK signals that shape the response of tumoral cells to targeted inhibitors. PP2A deregulation drives MEK inhibitor resistance by increasing signaling in a KRAS mutant context (Kauko et al., 2018). PP6 negatively regulates MAPK and mitigates inhibitor sensitivity through direct de-phosphorylation of MEK (Cho, Lou, Kuruvilla, Calderwood, & Turk, 2021).

In parallel, members of the protein tyrosine phosphatase (PTP) superfamily catalyze the dephosphorylation reaction of phosphotyrosine residues and present an important role in modulating various sources of signaling, including oncogenic stimuli (Bollu, Mazumdar, Savage, & Brown, 2017 ; Hendriks et al., 2013). Furthermore, many PTP members are able to dephosphorylate phosphoserine and phosphothreonine, proteins called dual-specificity

phosphatases (DUSPs). Contrarily to the rest of PTPs, no germline DUSP alterations have ever been associated with any kind of hereditary pathology nor with increased cancer incidence (Hendriks et al., 2013 ; Pulido & Huijsduijnen, 2008). However, DUSPs are deeply integrated in MAPK signaling regulation as they control, primarily, ERK activation by undoing activatory phosphorylation (C.-Y. Huang & Tan, 2012).

DUSP genes take direct part in the negative feedback loop of MAPK, as they are directly controlled by ERK activity (Brondello, Brunet, Pouysségur, & McKenzie, 1997a), particularly thanks to the activation of MAPK dependent transcription factors such as CREB, CTCF, FOXA1, KLF4, SRF and STAT3 (Blüthgen et al., 2009 ; Patel, Xi, Seo, McGaughey, & Segre, 2006 ; Varela, Conceição, Laizé, & Cancela, 2021). Upon expression, typical DUSPs separate into two localizations, nuclear and cytoplasmic, in order to cover the ground and follow ERK wherever it goes (**Table 9**).

Despite this differential localization, the functional roles of the various DUSPs are similar but somehow different, as they are not redundant (Lawan et al., 2011). Cytoplasmic DUSP6 is capable of targeting multiple ERK proteins before they reach the nuclear pore, including ERK1/2 and ERK5 (Karlsson, Mathers, Dickinson, Mandl, & Keyse, 2004 ; Moncho-Amor et al., 2019), while nuclear DUSP2 or DUSP4 exclusively de-phosphorylate ERK1/2 (Chu, Solski, Khosravi-Far, Der, & Kelly, 1996). Nuclear DUSP5 is expressed by and able to directly control ERK activity (Kidger et al., 2017) but, in parallel, its expression is induced upon p53-driven DNA damage (Ueda, Arakawa, & Nakamura, 2003), suggesting that these phosphatases are also nodes for pathway crosstalk and stress control. Their expression is also sensitive to HDAC, and their inhibitors, showing that the negative feedback system is highly flexible to different regulatory demands (Ferguson et al., 2013).

Because of their function as negative regulators of ERK, DUSPs have traditionally been associated with tumor suppressive functions (Moncho-Amor et al., 2019). However, DUSPs have proven to have more complex roles and, depending on the tumor, can even assume tumor promoting functions (Liao et al., 2003 ; Messina et al., 2011). Negative feedback driven by DUSP4 was identified as a potential super-enhancer of trametinib response in RAS-driven rhabdomyosarcoma (Yohe et al.,

2018), suggesting that, indeed, these phosphatases assume different roles depending on specific MAPK/tumor-dependent context.

	Gene Symbol	Alias	Localization	MAPK substrates
Typical DUSPs (KIM domain)	DUSP1	MKP1, CL100, VH1, PTPN10	Nuclear	JNK > p38 > ERK
	DUSP4	MKP2, VH2, HVH2, TYP	Nuclear	ERK > JNK > p38
	DUSP6	MKP3, PYST1	Cytoplasmic	ERK
	DUSP7	PYST2, MKPX	Cytoplasmic	ERK
	DUSP9	MKP4	Cytoplasmic	ERK > p38
	DUSP10	MKP5	Cytoplasmic, Nuclear	JNK, p38
	DUSP16	MKP7	Cytoplasmic, Nuclear	JNK (p38?)
	DUSP2	PAC1	Nuclear	ERK, JNK, p38
	DUSP5	VH3, HVH3	Nuclear	ERK
	DUSP8	HB5, VH5, HVH-5, HVH8, (Mouse: M3/6)	Cytoplasmic, Nuclear	JNK (p38?)
Atypical DUSPs	DUSP3	VHR	Cytoplasmic	-
	DUSP11	PIR1	Nuclear	-
	DUSP12	YVH1	Cytoplasmic, Nuclear	-
	DUSP13	BEDP, MDSP, SKRP4, TMDP	Cytoplasmic	-
	DUSP15	VHY	Cytoplasmic	-
	DUSP18	DUSP20, LMW-DSP20	Cytoplasmic, Nuclear, Mitochondrion IM	-
	DUSP19	DUSP17, LMW-DSP3, SKRP1	Cytoplasmic	-
	DUSP21	LMW-DSP21	Cytoplasmic, Nuclear	-
	DUSP22	JKAP, JSP1, VHX, LMW-DSP2, MKPX	Cytoplasmic	JNK
	DUSP23	DUSP25, VHZ, LDP-3, MOSP	Cytoplasmic, Nuclear	-
	DUSP24	STYXL1, MK-STYX	Mitochondrion Matrix	-
	DUSP27	DUSP29, DUPD1	Cytoplasmic, Nuclear	-
	DUSP28	VHP, DUSP26	Cytoplasmic, Nuclear	-
	DUSP14	MKP6, MKP-L	Cytoplasmic, Nuclear	JNK > ERK > p38
	DUSP26	MKP8, LDP-4, NATA1, SKRP3, NEAP, DUSP24	Cytoplasmic, Nuclear, Golgi	p38 (ERK?)

Table 9. ***DUSP family proteins in the human genome.*** *DUSPs can be classified as typical and atypical DUSPs depending if they present a KIM (kinase interacting motif) domain that allows for MAPK interaction. Adapted from (C.-Y. Huang & Tan, 2012)*

It is fundamental for the tumoral cells to sustain fitness by maintaining control of ERK phosphorylation on both localizations. Otherwise, the "sweet spot" is deregulated either by toxic hyperactivation or insufficient MAPK signaling. While DUSP5 or DUSP6 loss increases KRAS driven tumorigenicity, combined deletion of both no longer synergizes with oncogenic activity

(Kidger et al., 2017). DUSP4 and DUSP6 have been identified as a digenic dependence of MAPK driven cancers (Ito et al., 2021), implying that the tumor would not be able to afford losing this dual limiting system of MAPK. DUSP1 and DUSP6 deletion is toxic by triggering rapid MAPK signaling and cell death in chronic lymphocytic leukemia (Ecker et al., 2023). Furthermore, DUSP4 and DUSP5 have been identified as top genetic dependencies to ERK2 overexpressing melanoma cells (Chang et al., 2023), reiterating that MAPK negative feedback through DUSPs action is absolutely necessary for avoiding hypersignaling.

3.3 MAPK FEEDBACK EXTENDS FURTHER THAN PHOSPHORYLATION

Negative feedback, as it happens, does not always come from phosphatase activity. The family of sprouty (Spry) is able to inhibit signaling by antagonizing RTKs at GRB2/SOS level (Hanafusa, Torii, Yasunaga, & Nishida, 2002). SPRYs are able to counteract RTK signaling during a precise timing, until they are deactivated by SHP2 proteins, liberating GRB2 to the adaptor protein FRS2 to activate RAS (Hanafusa, Torii, Yasunaga, Matsumoto, & Nishida, 2004 ; R.-Y. Zhang et al., 2020).

SPREDs are a close relative of SPRYs, that also collaborate in negative feedback loops, in turn de-activating RAF by mediating its interaction with RAS (Wakioka et al., 2001). These proteins are involved in MAPK rewiring during inhibitor response and can, in turn, mediate resistance mechanisms to MEK inhibitors (Ablain, Liu, Moriceau, Lo, & Zon, 2020).

Positive feedback loops do exist too. RAS/MAPK signals are able to allosterically enhance and phosphorylate SOS to increase its activity (Boykevisch et al., 2006 ; Douville & Downward, 1997). A mechanism that will allow to amplify sparse signals from the vicinity of the receptor and generate rapid spatial spreading of RAS activation (Kochańczyk et al., 2017). These positive feedback loops are indispensable for producing the ERK oscillatory pattern that maintains MAPK homeostasis in the cell and in the organism (Shin et al., 2009).

This multifaceted network of regulations, comprising a myriad of feedback loops, crosstalk mechanisms, and fine-tuned modulations, serves to tightly control the initiation, propagation, and

termination of signals within the MAPK pathway, thereby orchestrating a precise and context-dependent functionality in various physiological and pathological contexts. The complexity of this regulatory framework emphasizes the importance of maintaining the "sweet spot" (**Figure 10**), ensuring that the MAPK pathway can effectively contribute to vital processes while preventing aberrant outcomes that could lead to diseases like cancer, but also neurodegenerative, cardiac, immune, and developmental disorders.

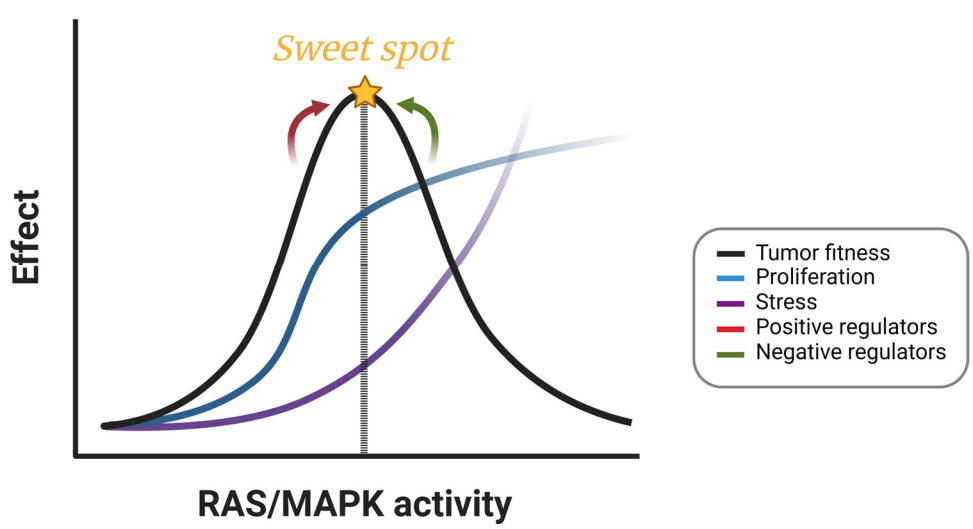

Figure 10. ***The sweet spot model****. Adaptation inspired from Chris Counter RAS sweet spot model (S. Li et al., 2018).*

3.4 RECAPITULATING RAS-MAPK ACTIVITY THROUGH TRANSCRIPTIONAL SIGNATURES

Phosphorylated ERK signal has traditionally been a marker of pathway activity both for in vitro and clinical samples. Indeed, ERK1/2 activation has been associated with advanced and aggressive solid tumors, especially for NSCLCs (Hoshino et al., 1999 ; Vicent et al., 2004). Immune techniques, such as SDS-PAGE and immunohistochemistry of tumoral tissues, rely on the use of antibodies to specifically detect the phospho-residues characteristically found in the active form of ERK (Yao et al., 2000). These techniques have proven to lack consistency in quantitatively measuring phospho-form distributions (Prabakaran et al., 2011). In addition to this lack of precision, the nature of ERK phosphorylation is very heterogeneous, and in some cases, it does not reflect the mutational status of the pathway (Houben et al., 2008). Globally, highly phosphorylated ERK does not convey a significant prognostic effect for computed overall survival in advanced NSCLC in the presence of other prognostic factors (Reissig et al., 2020).

Thus, phosphorylated ERK seems to no longer represent a good reporter mechanism for MAPK activity. This has been increasingly evident through the past years as the scientific community has been passionately developing better and more direct reporters to monitor MAPK status.

One of the first methods of in vitro detection of MAPK-dependent transcription was the use of serum response elements (SREs). Currently, there exist commercial transfection and lentiviral vectors that follow MAPK activity by using these SREs located in ectopically expressed luciferase gene promoters. These have been carefully derived from c-Fos promoter domains that correspond to Ets binding sites the that are sensitive to MAPK activation (Janknecht, Ernst, Pingoud, & Nordheim, 1993). The main concern when using these systems is that they rely on ERK1/2 phosphorylation of tertiary complex factors (TCFs), such as Elk-1, and binding of the serum response factor (SRF) to promote transcription. Plus, endogenous c-Fos transcription is only part of a second wave of genes activated by RAS-MAPK activity, being principally dependent on RSK activation (Cesare, Jacquot, Hanauer, & Sassone-Corsi, 1998) . On top of that, c-Fos expression may not be specifically linked to MAPK as other TCF-containing factors, such as SAP1 and SAP2, also bind these particular Ets-binding sites and can be associated with other pathways, as well as with other RAS-unrelated MAPKs like JNK and p38 (Y. Wang & Prywes, 2000). In order to battle the lack of specificity of gene reporter systems, ERK biosensors started to appear and have been constantly being updated through the years. These are a battery of fluorescent reporters that monitor ERK translocation to the nucleus. These have been very popular because of the importance of MAPK/ERK in development and cardiac biology (Nakamura, Goto, Kondo, & Aoki, 2021).

Despite their usefulness in the laboratory, these systems may not, at least for now, find their way into the clinic. Currently, there is no direct method to clinically measure MAPK activity directly. However, recent technological advances in genomic sequencing have facilitated the obtention of transcriptional data coming from these tumors, generating increasing amounts of information that may be key to understand how RAS/MAPK drive the different stages of oncogenesis.

For addressing this transcriptional approach, all the individual genes and transcriptional programs dependent on MAPK activity must be integrated. In the literature, several approaches have been

used to try to consolidate the pathway's outputs and compute scores that could account for MAPK activity (**Table 11**).

Reference	*Name*	*Size*	*Genes*	*Study*
(Dry et al., 2010)	*lung MEK signature*	18 13	*ZFP106, PROS1, LZTS1, ANKRD15, TRIB2, DUSP4, ETV4, ETV5, DUSP6, PHLDA1, SPRY2, ELF1, LGALS3, FXYD5, S100A6, SERPINB1, SLCO4A1, MAP2K3*	MEK functional output in response to MEK inhibitors in pan cancer cell lines
(Pratilas et al., 2009)	*MEK signature*	52	-	BRAF mutant MEK inhibition expression pattern
(Brant et al., 2017)	-	6	*DUSP4, DUSP6, ETV4, ETV5, PHLDA1, SPRY2*	Clinically viable gene expression refinement of Dry signature
(Vallejo et al., 2017)	*iKRAS*	19	*ADAM19, AOX1, AREG, CLU, DLK1, DOCK4, DUSP4, DUSP6, FOSL1, GRLX, HDAC9, LAMB3, LAMC2, NAV3, PHLDA1, SPRY2, SPRY4, STC1, MT1*	Interspecies KRAS signature, genes consistently regulated by KRAS in mouse and human experimental systems
(Creighton, 2007)	-	812	-	AKT/mTOR signature for BRCA
(Loboda et al., 2010)	-	147	-	RAS dependence upon PI3K/MAPKi in lung and breast tumors
(Wagle et al., 2018)	*MPAS*	10	*PHLDA1, SPRY2, SPRY4, DUSP4, DUSP6, CCND1, EPHA2, EPHA4, ETV4, ETV5*	BRAF mutant melanoma, other solid tumors and response to vemurafenib
(Chesnokov, Yadav, & Chefetz, 2022)	*COMS*	3	*PHLDA1, DUSP4, EPHA2*	Ovarian cancer and platinum resistance
(Paulitschke et al., 2019)	-	15	*ALDH1A1, ALDH1A3, FAM129A, IGFBP7, KYNU, NAMPT, NID1, OXCT1, PCOLCE, PDLIM1, PRDX2, PTRF, SERPINB6, THBS2, UCHL1*	Proteomic analysis of MAPKi resistant melanoma BRAF mutant cells
(Singh et al., 2009)	*RAS addiction*	380	-	Upregulated genes in KRAS mutant "addict" LUAD/PDAC cellular models
(Sweet-Cordero et al., 2005)	*KRASLA*	89	-	Upregulated KRAS genes in mouse LUAD tumor models
(Liberzon et al., 2011)	*MSigDB*	200	-	Hallmark KRAS Signaling Up meta-signature from MSigDB
(Shirasawa, Furuse, Yokoyama, & Sasazuki, 1993)	*G13D*	134	-	G13D mutant gene expression in colon tumoral cell lines
(Feng et al., 2019)	-	1000	-	MAPK-driven "mesenchymal-like" transcriptional program in BRAF mutant melanoma PDXs resistant to MAPKi
(East et al., 2022)	*RAS84*	84	-	Machine-learning integaration of RAS dependent signatures and stratify LUAD and solid tumor patients

Table 11. ***Compendium of RAS/MAPK signatures described in the literature for NSCLC, melanoma, and solid tumors.***

One of the first approaches to identify genes that were driven by MAPK activity, was the use of 52 genes that were altered upon MEK inhibition in a BRAF mutant melanoma context (Pratilas et al., 2009). This work included genes from the negative feedback regulation and direct effectors of RAS driven transformation.

A similar approach was taken in melanoma, where 18 genes were discovered to be specially altered in inhibitor-sensitive tumors (Dry et al., 2010). They confirmed these results in a panel of solid tumor cell lines by RTqPCR and Affymetrix microarray, both fast and clinic-compatible techniques.

Both in these works, the genes DUSP4, DUSP6, SPRY2 and PHLDA1, all transcriptional targets of ERK (Brondello, Brunet, Pouysségur, & McKenzie, 1997b ; Ekerot et al., 2008 ; Oberst et al., 2008 ; Ozaki et al., 2001), were contained in the final signatures. However, these signatures, containing a large number of genes, were highly specific of BRAF driven tumors.

Later on, in silico optimizations integrated these genes and more RAS-enabled targets into a KRAS mutant specific signature (Brant et al., 2017). This signature, composed of 6 genes: DUSP4, DUSP6, ETV4, ETV5, PHLDA1 and SPRY2; was successful in finding patient populations differently sensitive to MEK inhibitors when compared to a simple KRAS mutation testing. However, the predictive power of this signature was not computed in further NSCLC patient data.

Considering all these precedents and paradigms, it becomes evident that deeper research is an imperative necessity in order to effectively confront the challenges posed by the RAS/MAPK oncogenesis. The complexities previously mentioned, that are inherent to this molecular cascade, demand innovative and comprehensive approaches. One of the most important challenges will be to develop advanced and refined strategies for quantifying and characterizing MAPK activity, in order to associate precise output levels with clinically relevant phenotypes. Such advancements in precision oncology will ultimately lead to enhanced and more informed care of patients affected by KRAS mutant LUAD.

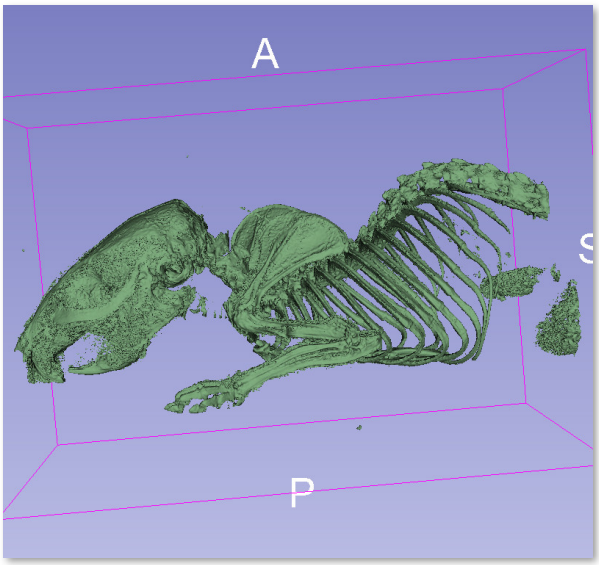

Picture II. 3D reconstruction of a mouse squelettal system. High contrast images obtained by micro-computer tomography (CT) were used to assemble the osseus profile .

Objectives

High-quality basic research is essential for subsequent development, as it will yield unforeseeable results.

Margarita Salas

Objectives

Tumoral progression is an intricate process requiring a series of hallmarks that synergize towards a common goal. Every process and every alteration selected in the tumor has been carefully dosed and grants given advantages to the malignant cells. RAS-MAPK regulation is an important hallmark that is systematically altered in LUAD. However, we now understand that driving signaling not only requires activatory processes but also compensatory mechanisms that maintain balance. For this reason, the hallmark of MAPK pathway modulation, thus the alterations that could involve known and unknown regulators, must have clinical consequences.

For this purpose, we decided to functionally study clinical data of KRAS mutant LUAD cases and evaluate how MAPK signaling levels affect clinical outcome. From these analyses, we have built the foundations for studying how precise alterations for given, and novel, regulators could affect tumor progression. This approach not only enables the establishment of direct causal relationship between MAPK activity and tumor fitness in the clinic, but also gain further mechanistic insights into how different regulatory contexts in a KRAS setting could determine treatment response and putative resistances.

The global objectives of this mission were the following:

1. Studying the MAPK component from clinical, publicly available, databases to better understand how regulation of the pathway affects KRAS mutant LUAD patient fate, and the molecular mechanisms that could underlie their prognosis.
2. Develop KRAS-driven LUAD models that recapitulate clinical settings, for determining how excessive MAPK levels are toxic to the tumor.
3. Dissection of molecular changes affecting MAPK regulators, such as the DUSP4 alterations retrieved in patients. Understand its putative role in the MAPK specific response, trying to comprehend how DUSP4 status shapes tumor fate by controlling MAPK signaling balance.
4. Identifying and characterizing novel RAS-MAPK regulators that could contribute to a better interpretation of the pathway in the molecular oncology environment.

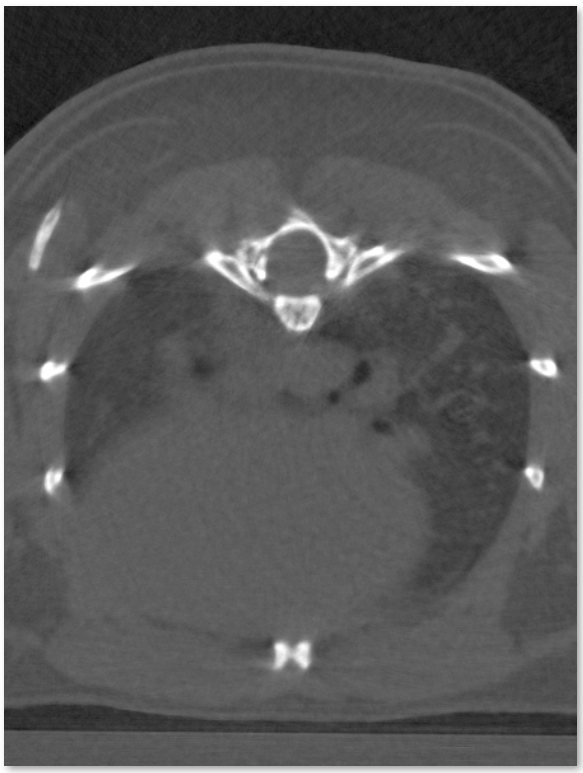

Picture III. Micro-computer tomography (CT) of mouse thoracic cavity, including the lungs.

Materials & Methods

Those who enjoy marching in ranks to music: it must be by mistake that they have received a brain, a spinal cord would suffice them

Albert Einstein

All the experimental protocols in the present manuscript have been performed at the European Institute of Chemistry and Biology and the University of Bordeaux and at the Cancer Research Center and the University of Salamanca. Safety precautions were constantly taken to avoid biological, chemical, and physical hazards to both the personnel, the facilities, and the environment.

1. ANIMAL MODELS

1.1 ANIMAL WELFARE

Following European directive 2010/63/EU, all the animal housing, care and handling happened inside of controlled facilities. Both the animal departments of the University of Bordeaux and the University of Salamanca are certified for research purposes.

- The Service Commun des Animaleries de l'Université de Bordeaux (SCA) is certified according to the Décret nº2013-118 du 1er février 2013 relatif à la protection des animaux utilisés à des fins scientifiques French regulation. The University of Bordeaux Comité d'éthique approved the experimental plan.
- The *Servicio de Experimentación Animal de la Universidad de Salamanca* (SEA) is certified according to the *Real Decreto 53/2013* Spanish regulation. The University of Salamanca through the *Comité de Ética de la Investigación* approved the experimental plan under the reference nº736.

All the practices carried out in each of the animal facilities were conducted in accordance with the current national legislation. All scientific personnel involved were certified according to Art.23 of 2010/63/EU directive, including myself, after having received appropriate education and training.

Mice were housed in environment-controlled, specific pathogen free facilities, grouped in ventilated cages. Day-night cycles were routinely implemented. Mice were fed *ad libidum* standard diet (2018 Teklad Global 18% Protein diet, irradiated, Inotiv-Envigo Cat# TD.2918). Mouse models were genotyped by PCR amplification and electrophoresis agarose gel analysis.

Vital and experimental measurements were blindly performed. Simple randomization was used for assigning groups of treatment. Mice were sacrificed by cervical dislocation. All possible efforts were conducted to reduce the number of mice used for each experiment, avoid any kind of animal suffering, and improve overall animal welfare.

1.2 INDUCIBLE KRAS MODEL

K-Ras$^{+/LSLG12Vgeo}$ mouse strain, with C57BL6/6J background, was developed in Mariano Barbacid's laboratory (Guerra et al., 2003), following Tyler Jacks & David Tuveson's *K-Ras* models (Jackson et al., 2001; Johnson et al., 2001). This system allows the expression of the oncogenic mutant in a temporally and spatially controlled manner. The mutant allele is secured with a *loxP-Stop-loxP* cassette that impedes proper transcription of KRAS G12V protein thanks to the transcriptional termination *Stop* element. Upon Cre recombinase exposure, the *lox* sites and the DNA in between are excised and removed from the chromosome, leaving a *pseudo-loxP* scar. Following removal of the *Stop* cassette, oncogenic KRAS is expressed and can become an oncogenic driver leading to malignant transformation of targeted cells. These mice carried in parallel a reporter construct in the Rosa26 locus that enables fluorescent follow-up of Cre activity in the genome with a *loxP-Stop-loxP-YFP* (yellow fluorescent protein gene) either in heterozygous or homozygous state (**Figure 12**).

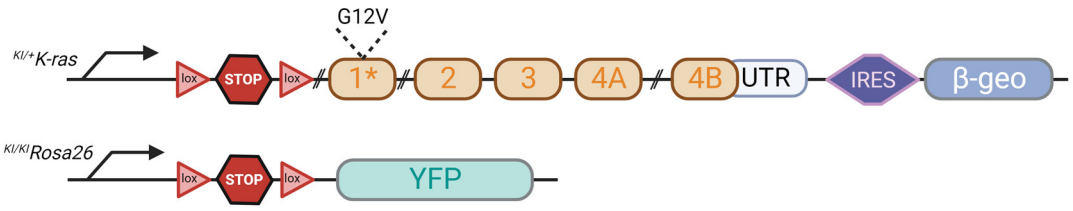

Figure 12. ***Mouse model for oncogenic KRAS activation****. The model was established in a C57BL6/6J mice background, carrying both the oncogenic KRAS*$^{lox\text{-}STOP\text{-}lox\text{-}G12V.Bgeo}$ *construct and the Rosa26*$^{lox\text{-}STOP\text{-}lox\text{-}YFP}$

1.3 INTRANASAL INFECTION OF LENTIVIRAL PSECC PARTICLES

In our model, we used an intranasal infection of lentiviral particles that could locally target the lung tissue after instillation. In order to couple *Cre* activity with gene-targeting technology, we took

advantage of the pSECC lentiviral plasmid from the Tyler Jack's laboratory [*Addgene #60820*] (Sanchez-Rivera et al., 2014).

This vector uses CRISPR/Cas9 technology, a very powerful gene-targeting strategy that uses bacterial machinery to target the genome of interest. The CRISPR/Cas9 system exists through its main component, the *S. pyogenes* Cas9 endonuclease, capable of generating target DNA breaks, only thanks to the directions of the guide RNAs (gRNAs) that are complementary to the region of interest. Together, the DNA breaks are punctually generated in the genome and the repairing mechanism will determine the fate of that locus. Unless a homologous DNA sequence is found, the break will be repaired by non-homologous end joining (NHEJ), an error-prone mechanism leading to non-specific insertions and deletions that will repair the locus altering its native sequence. If the region of interest is in between a particular gene, this will often result in a knock-out derived from the open reading frame shift. We will exploit this editing system to perform point knockouts in genes of interest.

In vivo, using the pSECC will allow for parallel co-expression of a sgRNA of interest, the Cas9 protein and the Cre recombinase. This technique has proven to be useful to generate models of *Kras* activation combined with individual knockouts of a gene. In this work, we generated plasmids that allowed CRISPR/Cas9 targeting of DUSP4 gene. In parallel, non-targeting control vectors were generated, for example using gRNAs specific to a non-human protein such as turboGFP (Evdokimov et al., 2006).

In order to deliver the system to the lung tissue in the animals, we generated lentiviral particles carrying the pSECC machinery and inoculated them through the aerial tract. Lentiviral supernatants were prepared in 293T cells, filtered, and concentrated by ultracentrifugation at the Vect'UB (TBM core) Vectorology Unit at the University of Bordeaux. The viral pellet was resuspended in OptiMEM and titered by qPCR. Lentiviral supernatants were diluted in Hanks' Balanced Salt Solution (HBSS) prior to mice infection. Tumors were induced with a single intra-nasal instillation

of $5x10^5$ viral particles ($1x10^6$ particles for 1-year timepoints) of pSECC lentivirus during anesthesia, as reported in (DuPage et al., 2009).

1.4 TAIL-VEIN INJECTION

For this procedure, either athymic nude (Crl:NU(NCr)-*Foxn1*^{nu}) or NSG® (JAX® NOD.Cg-Prkdc^{scid} Il2rg^{tm1WjI}/SzJ) immunodeficient mice bred in a Charles River facility were used. Invasive cell lines were trypsinized, centrifugated and prepared in a 100 µL PBS suspension (a volume of up to 1% of the animal's body weight is recommended) at different concentrations, depending on the malignancy of the cell line, between 50,000 and 2 million cells per injection. Cells were kept on ice prior to injection. Mice were restrained in a pillory and heated with a warming bulb in order to expose the left and right lateral veins. The cells were carefully inserted in the syringes (BD Plastipak™ 1mL Test, 0,40mm x 10mm 27G, Cat# 305502) without forming any bubbles, injected, and beveled up towards the front, dispensed individually without any aspiration. The needle was removed, and gentle compression was applied to the tail with some antibiotic solution. Injected mice were returned to their cage and observed for a few minutes to ensure there was no health problem derived from the procedure (watching for further bleeding or air bubble-derived embolism). Following the injection, the mice were supervised weekly and evaluated for tumor formation by luciferase monitoring.

1.5 ORTHOTOPIC LUNG INJECTION

For this procedure, either athymic nude (Crl:NU(NCr)-*Foxn1*^{nu}) or NSG® (JAX® NOD.Cg-Prkdc^{scid} Il2rg^{tm1WjI}/SzJ) immunodeficient mice from the Charles River laboratory were used. Mice were anesthetized with 2% isoflurane (Vetflurane® 1000mg/g per mL, Virbac) by inhalation in 100% oxygen at a rate of 1000cc/min, prior to and during the procedure. One mouse was elongated on his right lateral and their abdomen was shaved, still under anesthesia. In this case, the resuspended cells were prepared in a 10% Matrigel solution and around 100.000 to 1 million cells were used, depending on the cell line. The insulin syringe (BD Insulin syringes 6mm x 31G UltraFine® Veo™, US.Cat.#324909) was loaded with a single preparation of the cells and injected

in the thoracic cavity, in-between the ribs. The needle was inserted perpendicularly to the mouse and left inside for a couple of seconds after injection before removing in order to maintain air pressure inside the diaphragm. Injected mice were returned to their cage and observed for a few minutes to ensure there was no health problem derived from the procedure (watching for bleeding and breathing problems).

1.6 LUCIFERASE MONITORING

The mice that were subject of luciferase monitoring were tested daily or weekly depending on the experimental protocol. A cage of mice was prepared to the imaging by intraperitoneal injection of an appropriate dose of a 30mg/mL luciferin-PBS solution (5 µL per gram per mice, around 100 µL for a 20g mouse) prepared from powder (Gold-Bio Cat# LUCK-1g). Mice were anesthetized with 2% isoflurane by inhalation in 100% oxygen at a rate of 1000cc/min, prior to and during the whole imaging process. We performed a kinetic assay, and a 10-minutes incubation time was established to be the most efficient timepoint to detect luciferase activity in our system. Consequently, the mice were placed facing upwards in the imaging tray and analyzed 10 minutes after the injection. Variable exposure times were used depending on the experimental demands, being increased in low-signal conditions. However, all the acquisitions were photon normalized to ensure that the comparison was possible across the conditions and timepoints. The imaging system was an IVIS®Lumina X5 (Perkin Elmer) coupled to an anesthesia flux system.

1.7 TREATMENTS

1.7.1 Tamoxifen diet

For tamoxifen administration, we employed a diet-based delivery method. One week before starting tamoxifen diet, the animals were fed a transition diet reducing natural estrogens (2016 Teklad Global 16% Protein diet, without soybean, limiting isoflavones, irradiated, Inotiv Envigo Cat# TD.2916) that are present in the standard diet and could compete with tamoxifen. Once the transition protocol was complete, mice were fed a tamoxifen citrate diet (Citrate TAM400/CreER

diet, irradiated, Inotiv Envigo EU. Cat# TD.55125). This form of tamoxifen allows the hydroxylation of the tamoxifen on the mouse liver, forming an active metabolite (4-hydroxytamoxifen, 4-OHT).

1.7.2 Doxycycline

For doxycycline treatment, we implemented a drinking water-based delivery. Doxycycline hydrochloride was purchased (97% purity, Thermo Fisher Cat# 446061000) as powder and resuspended in autoclaved tap water as a 10X solution of 10mg/mL supplemented with sucrose (30%). Every three days during the treatment period, the drinking water bottle was replaced with the diluted solution of doxycycline, reaching a final concentration of 1mg/mL.

1.8 Micro X-ray computer tomography scan (micro-CT)

Image studies were conducted at the Radioprotection and Radioisotope detection laboratory of the Nucleus USAL department. Mice were anesthetized by inhalation of 5% isoflurane in 100% oxygen at a rate of 1000cc/min prior to and during the imaging process. The imaging was acquired in a SuperArgus eXplore Vista-CT scanner with PET compartment (GE Healthcare, Suinsa Medical System). The thoracic area was selected, and the following parameters were selected: intensity of the power supply of 400mA and 45kV for a standard resolution of 38 μm, 360º rotation in 720 projections, with 8 shots per projection in a single bed position. This acquisition would result in a 0.6 Gy radiation dose for the mouse. Processing and analysis were performed with the SedecaACQ software with a FDK algorithm adapted for micro-CT reconstruction. The volume of the tumor was manually calculated by volumetric segmentation using the 3DSlicer software.

1.9 Mouse embryonary fibroblasts (MEFs) generation

Starting from a pregnant female, sacrifice was performed at 13.5 days *post-coitum* (dpc). The uterus was extracted, and the embryos were collected in sterile PBS. Dissection of the embryos with scissors allowed to discard cranial, liver, and hematopoietic tissue. The head is conserved for genotyping. The remaining parts were dissociated and incubated in 0.05% trypsin-EDTA, for homogenization, at 37ºC for 10 minutes. This procedure was repeated at least three times until the

tissue was completely dissociated. The cell suspension was transferred to 150mm plates with 20mL of complete DMEM. Freshly extracted cells were incubated in tissue culture incubators and allowed to grow to confluency, after 3 to 4 days, until they were frozen down or maintained *in vitro*. Immortalization was performed by lentiviral infection of SV40 large T antigen particles .

1.10 TISSUE DISSOCIATION

The following protocol was used to dissociate lung (or other organ) tissue, from tumoral or organic origin, extracted from mouse models. These samples were processed in order to separate individual cells for subsequent protocols, so the cells could be sorted by flow cytometry and/or be cultured in tissue culture dishes.

For this protocol, we used Miltenyi Biotec gentleMACS Tumor Dissociation kits. Tissue samples were diced with a surgical blade and were collected in 5mL of DMEM supplemented with H+R+A enzyme mix following manufacturers recommendations. The solution was then transferred to a gentleMACS C tube and inserted upside down into the gentleMACS dissociator. We first used the m_impTumor_01 program, that lasted over 1 minute. Once finished, the tubes were then transferred into an incubator at 37ºC in order to digest the samples for 40 minutes, under rotation. After incubation, the C tubes were again placed into the gentleMACS dissociator and the program m_impTumor_03 was started.

The cellular suspension was then filtered with a 100 μm nylon strainer and washed with additional DMEM. The cells were centrifuged at 400g for 5 minutes in order to form a pellet. The supernatant was discarded. The pellet was resuspended and analyzed according to the following protocol.

2 TISSUE CULTURE

2.1 LIST OF CELL LINES USED

The following cell lines were ATCC® certified cell lines maintained in the lab:

Cell line name	ATCC ID	Cellosaurus ID	Origin	Sex	Growth conditions	Mutational state	Other
HEK-293T	CRL-3216	CVCL_0063	Human embryonic kidney	F	DMEM + 10% FBS + PS	Unknown, polyploid	Transformed by SV40 T antigen, NeoR
NCI-H1792	CRL-5895	CVCL_1495	Lung adenocarcinoma	M	RPMI + 10% FBS + PS	CDKN2A (G125R), KRAS (G12C), TP53 (null)	MSS
NCI-H23	CRL-5800	CVCL_1547	Lung adenocarcinoma	M	RPMI + 10% FBS + PS	ATM (G1919P), KRAS (G12C), STK11 (W332Ter), TP53 (M246I)	MSS
NCI-H358	CRL-5807	CVCL_1550	Lung adenocarcinoma	M	RPMI + 10% FBS + PS	TP53 (DEL), KRAS (G12C)	MSS
NCI-H2122	CRL-5985	CVCL_1531	Lung adenocarcinoma	M	RPMI + 10% FBS + PS	KRAS (G12C), TP53 (G16L, C176F)	MSS
NCI-H2030	CRL-5914	CVCL_1517	Lung adenocarcinoma	M	RPMI + 10% FBS + PS	KRAS (G12C), TP53 (G262V)	MSS
HBEC-3-KT	CRL-4051	CVCL_1292	Human bronchial epithelium	F	EMEM + 10% FBS + PS	None	Telomerase immortalized
A549	CCL-185	CVCL_0023	Lung adenocarcinoma	M	DMEM + 10% FBS + PS	KRAS (G12C), TP53 (+/-), STK11 (Q37Ter)	MSS
NCI-H460	HTB-177	CVCL_0459	Lung large cell carcinoma	M	RPMI + 10% FBS + PS	KRAS (G61H), PI3KCA (E545K), STK11(Q37Ter), TP53 (null)	MSS
HCC364	CRL-2868	CVCL_5134	Lung adenocarcinoma	F	DMEM + 10% FBS + PS	BRAF (V600E), TP54 (E180K)	
HCC4006	CRL-2871	CVCL_1574	Lung squamous carcinoma	M	DMEM + 10% FBS + PS	EGFR (Deletion: L747-E749), TP53 (Y205H)	
PC9	-	CVCL_B260	Lung adenocarcinoma	M	DMEM + 10% FBS + PS	EGFR (Exon 19 deletion: E746-A750), TP53 (R248Q)	

Table 13. ***Table of external cell lines used for the experiments***

These cell lines were properly certified when arrived at the lab and have periodically been submitted for certification.

The following cell lines were either generated in the lab or were obtained externally from another institution:

Cell line name	Origin	Growth conditions	Mutational state	Other	Ref
ChA 14.6	CNIO	DMEM + 10% FBS + PS	Kras (G12V/?), TP53 (+/+)	-	-
ChA 14.9	CNIO	DMEM + 10% FBS + PS	Kras (G12V/?), TP53 (+/+)	-	-
DU 315.6.1	DS Lab	DMEM + 10% FBS + PS	HRas(-/-) NRas(-/-) KRas(lox/lox) RERT(Ki/Ki)	Upon tamoxifen treatment, the cells become Rasless	(Drosten et al., 2010)
ATII pneumocytes	Julian Downward	RPMI + 10% FBS + PS	None	inf. Kras(G12V-ER), inf. Tet-BRAF(D594A)	(Kemp et al., 2008)
DSA MEFs (2.1.1)	DS Lab	DMEM + 10% FBS + PS	Kras(+/LSLG12Vgeo) B-Raf(+/+) UbCreERT2(+/T)	-	-
DSD MEFs	DS Lab	DMEM + 10% FBS + PS	Kras(+/Lox) UbCre-ERT2(+/T)	-	-
DSB MEFs	DS Lab	DMEM + 10% FBS + PS	Kras(+/LSLG12Vgeo) UbCre ERT2(+/T)	-	-

Table 14. ***Table of cell lines generated in the laboratory for the experimental procedures***

2.2 REAGENTS

Dulbecco's Modified Eagle's Medium (DMEM, high glucose, pyruvate, Gibco Cat# 41966029) and Roswell Park Memorial Institute (RPMI 1640, Gibco Cat# 21875034) were completed with 10% Fetal Bovine Serum (FBS, Brazil origin, Gibco Cat# A5256701). For cell lines harboring doxycycline-inducible constructs, 10% FBS without tetracycline (FBS Premium, South America origin, tetracycline free, 0.2 µm sterile filtered, Pan Biotech, Cat# P30-3601) was used in order to avoid promoter leakiness derived from tetracycline present in the standard serum. The FBS lot number was maintained across batches in order to maintain low differences of growth factor. Media were also completed with antibiotics, 1% penicillin (final 100 units/mL) streptomycin (final 100 µg/mL) cocktail (Gibco Cat# 15070-063). For detaching the cells from the solid substrate, we used 0.05% trypsin-EDTA (Gibco Cat# 25300096).

For cryopreservation of the cell lines, cells were trypsinized, resuspended in 500 µL of complete medium and transferred into a cryovial. Then, 500 µL of a 2X freezing solution (DMEM, 40% serum and 20% DMSO) were added and the vial was homogenized. Cells were always frozen down at slow rates thanks to Corning® CoolCell® containers that were introduced in the -80ºC freezer. Once the cells had reached that temperature, the cryovials were stored in liquid nitrogen (-195ºC) for long-term storage purposes.

The following antibiotics were used for mammalian selection, generally at the following use concentrations depending on the cell line: blasticidin 10 µg/mL, puromycin 1 µg/mL (Fisher Cat#

BP2956), zeocyn 100 µg/mL, G418-geneticin 500 µg/mL (Invivogen Cat# Ant-Gn-1), hygromycin B 50 µg/mL (Thermo Scientific Cat# J60681).

The cells were maintained in mammalian specific incubators, temperature was constant at 37ºC, and 5% CO_2 was used to buffer the pH of the cultures. All the plastic labware used for cell culturing was purchased from Falcon® or Corning®.

All cell lines have been regularly tested for mycoplasma contamination by PCR and/or MycoStrip™ detection kit. Positive detections were rare and immediately discarded, avoiding further contamination. PCR standard conditions were used (See PCR section) and several couples of primers were used at a time (See Primers section).

2.3 DRUG TREATMENT AND INHIBITORS

Drugs were received in powder and resuspended according to manufacturer recommendations, generally in DMSO. Consequently, drugs were administered in vitro, directly on cellular growth media, in parallel to a vehicle control. Exposure time to the particular reagent is indicated in each individual protocol.

Small molecule inhibitors were purchased from different providers, ensuring that the CAS number and purity was constant across batches. KRAS G12C inhibitors used were adagrasib (MedChem Express, Cat# HY-130149) and sotorasib (TargetMol, Cat# T8684), BRAF kinase inhibitor used was dabrafenib mesylate (AbMole Cat# M1855), MEK1/2 kinase inhibitor used was trametinib (Sellekchem Cat# S2673). SRC family kinase inhibitor was PP2 (AbMole Cat# M2331). Doxycycline hydrochloride was purchased (97% purity, ThermoFisher Cat# 446061000) as powder and resuspended in PBS.

All the molecular compounds were submitted to IC50 calculation prior to further experimental protocols.

2.4 TRANSFECTION AND LENTIVIRAL PRODUCTION

Transfection was performed to transiently introduce DNA into mammalian cells, in order to achieve temporal expression of the introduced genes. The following protocol refers to a classic transfection in a 100mm plate. The plasmid DNA (up to 10 µg) was mixed with 40 µL of 1 mg/mL linear polyethyleneimine (PEI, Polysciences Cat# NC1014320) and 500 µL of DMEM. The mixture was vortexed for 5 seconds and incubated at room temperature for 15 minutes. The complexes were distributed dropwise on the well and the plate was rocked before returning to the incubator.

When transfections were performed in other cell lines, jetOptimus® (Polyplus Cat# 101000051) lipid-based transfection reagent was used, following manufacturer's recommendations.

Lentiviral supernatants were produced in HEK 293T cells, at a 70-80% confluence on the transfection day. Third generation packaging plasmids pLP1 (1.9 µg), pLP2 (1.3 µg) and pLP/VSVG (1.64 µg) (ViraPower™ plasmids, Invitrogen Cat# K497500) were mixed with the lentiviral construct of interest (5 µg), together with the transfection mixture of PEI and DMEM described before. The next day, the medium was replaced. At 48h post transfection, the media was collected and filtered with 0.45 µm pore size filters.

For infection, cells were trypsinized and counted. A suspension of cells (around 200,000) was mixed with the lentiviral supernatants and supplemented with polybrene up to 8 µg/mL. Cells were incubated for 48 hours with the supernatants, then the medium was replaced, or cells were trypsinized, with antibiotic selection if necessary.

2.5 PHENOTYPING ASSAYS

2.5.1 MTT

For evaluating cellular density and estimating a relative cell number, we used a colorimetric MTT assay. Cells were seeded on 96-well plates at different concentrations depending on the cell line. The next day, these cultures were treated with the drugs of interest, replacing the media, during a period of time established in the corresponding experiment. For establishing an IC50, cells were

treated with increasing concentrations of the compound for a duration of 72h. At the end timepoint, media was removed from the plate and replaced with 100 µL MTT1 solution (final 1mg/mL 3-(4,5-dimethylthazolk-2-yl)-2,5-diphenyl tetrazolium bromide, Sigma, M2128) diluted in growth medium for 3 hours and placed back in the incubator. During this stage, dehydrogenases in active mitochondria of living cells will process the tetrazolium ring of the MTT and generate purple formazan granules that precipitate inside the cell. After the incubation, 100 µL of MTT2 solution (10% SDS + 10mM HCl) were used to lyse the cells and liberate the purple coloration to the media overnight in the incubator. The next day, absorbance of the plate was read at 590nm. Quantification was performed relative to the untreated control, ranging from 0 to 100%.

2.5.2 Isolation of individual colonies: subcloning

For generating individual clones of cells derived from an asynchronous population without using FACS, we performed manual clone isolation. Cells were seeded at low density (around 1,000 cells) in 100mm plates and let grow for 1-2 weeks. Clusters of cells could be observed and individually harvested using small glass cylinders (Sigma Cat# C1059) that were attached to the plate with silicone grease (high vacuum grease, Dow-Corning™ Cat# 044224.KT). 50 µL of 0.05% trypsin-EDTA were used to detach the cells. After incubation, 150 µL of complete medium were used to stop the reaction and was transferred to a 96-well plate. Single cell subclones were expanded until they reached enough confluency to be frozen or used as a conventional cell line.

2.5.3 Clonogenic assay in soft agar

In order to evaluate cellular transformation and clonogenic capabilities in 3D, we performed soft agar cultures. For this protocol, we used a low melting agarose (Agarose LM3, Euromedex, Cat# 1670B) to form the different layers in a 6-well plate. First, a bottom layer of 0.6% agarose is prepared with culture media. After this first layer was solidified, a cellular suspension of around 100,000 cells (depending on the cell line) was diluted in a 0.3% agarose solution with the corresponding growth medium. The top layer was placed on top of the basal layer and replenished with medium to avoid desiccation. These agarose mixtures are prepared at 42ºC in order to avoid

heat-shock derived cell death. After several days or weeks, agarose beds can be stained with crystal violet to visualize colonies, although they are generally visible without any staining. Colonies were observed at an inverted phase contrast microscope.

2.5.4 Crystal violet

Clonogenic capability in 2D culture was assessed by clone visualization under crystal violet coloration. Cells were seeded at low densities (around 5,000 cells, depending on the cell line) in 6-well plates under treatment and the individual experimental conditions. After 1-3 weeks, the cells were washed with PBS and fixed in formalin (4% formaldehyde) for 10 minutes. Formalin was rinsed and the gentian violet staining (hexamethyl p-rosaniline chloride in 20% methanol, Prolab, Cat# PL.7002) was added to the cells for 10 minutes. The plates were rinsed with tap water and let dry before imaging at a ChemiDoc™ XRS+ System (Biorad). Quantification was performed by cellular lysis adding 0.5-1% SDS to the plates, allowing the liberation and dissolution of the crystals. Volume was then transferred to a 96-well plate for reading absorbance at 590nm.

2.5.5 Cell cycle analysis

Cells in culture were trypsinized and resuspended in PBS. At least 250,000 were taken for the cell cycle preparation. Cells were centrifuged and washed with cold PBS. The pellet was resuspended in 300 µL of cold PBS and 700 µL of ice cold 100% ethanol were added under constant agitation, dropwise. Cells were then transferred to -20ºC for at least 1 hour. This fixing stage maintains cell integrity with the intact nucleus for the following. Cells were then centrifuged, washed in PBS and resuspended in a 50 µg/mL propidium iodide (PI, Sigma Cat# 81845) solution containing 50 µg/mL RNAse A (Sigma, Cat# R6148). The suspension was vortexed and incubated at room temperature, in the dark, for 30 minutes. The abundance of cells in the different cell cycle peaks (G1/S/G2) were analyzed by flow cytometry.

2.5.6 Apoptosis assay

The fraction of dying cells in a cell culture population was estimated with an apoptotic staining such as Annexin V coupled to 7-AAD. Annexin V allows to track phosphatidylserine residues

present in the lipid cell membrane during apoptosis. In normal cells, these residues are limited to the inner layer of the membrane. The apoptotic process renders the membrane unstable, losing its asymmetry and exposing the phosphatidyl residues to the outer layer, where they can be bound to Annexin V. At the same time, 7-AAD is a membrane impermeant dye that is excluded from viable cells. When cells lose membrane integrity, upon late apoptosis or necrosis, 7-AAD can enter the cell and bind to DNA.

For this protocol, cells in culture were trypsinized and resuspended in PBS. Two additional washes are necessary before resuspending the cells in 100 µL of the diluted Annexin Buffer (prepared as 10X, filtered 0.1M Hepes (pH 7.4), 1.4M NaCl, 25mM $CaCl_2$, in water). Then, 3 µL of Annexin V (Immunostep, Cat# ANXVPE) and 3 µL of 7-AAD (from Apoptosis Detection Kit I, BD, Cat# 559763) were added to the cell suspension. For multiple conditions, a mix was prepared. Cells were vortexed and incubated with the reagents for 15 minutes at room temperature in the dark. Then, 400 µL of the Annexin Buffer were added and the cells were passed through the cytometer. The bi-color staining allowed to correlate population percentages with apoptosis fraction estimates (Annexin V^- / 7-AAD^- cells were viable cells, Annexin V^+ / 7-AAD^- were early apoptotic cells, Annexin V^+ / 7-AAD^+ were late apoptotic cells and Annexin V^- / 7-AAD^+ were necrotic cells).

2.5.7 Oxidative stress monitoring

In order to study the presence of reactive oxygen species (ROS) in cultured cells, we used the CellROX® reagent kit (Green fluorescence, Thermo Scientific Cat# C10492) to monitor the oxidative state by the integration of a fluorescent probe that only emits signal upon oxidation. This fluorescent oxidative state is only present when ROS and other oxidative species are present in the cells and is compatible with detection by cytometry. Cells are trypsinized and prepared in complete media at a concentration of 500,000 cells per mL. To stain the cells, 2 µL of 250 µM CellRox probe are used per tube, preparing a mix. Cells are incubated for 30 minutes at 37ºC and washed with PBS. Cells are then analyzed by flow cytometry, in this case calculating the percentage of positive cells and the mean intensity of the fluorescence derived from the green probe. Positive and negative

controls for the presence of ROS are prepared for this experiment by adding 200 μM tert-Butyl hydroperoxide (TBHP) and 500 μM N-acetylcysteine (NAC), respectively, to the media for 1 hour previous to the cytometry.

2.5.8 Cytokinesis block micronucleus assay (CBMN)

For evaluating genomic instability, Cytokinesis Block Micronucleus (CBMN) Assay was performed. Cells were grown in glass coverslips and treated with cytochalasin B (Sigma or MCE, CAS nº14930-96-2) at 1 μg/mL working concentration for 24h. Cells were fixed and counterstained with 1 μg/mL Hoechst 33258 (Sigma, CAS nº 23491-45-4) and 5nM phalloidin (1/10,000 from Alexa Fluor™ Plus 647 Phalloidin, Invitrogen). Cells were imaged on an epifluorescence microscope Leica DM4 with Thunder Imaging System located in CIC-IBMCC facilities. Images were processed on ImageJ FIJI software to evaluate number of micronuclei per cell. The CBMN score, or nuclear division index (NDI) was established with the following formula, as described here (Fenech, 2007): NDI = (1xM1 + 2xM2 + 3xM3 + 4xM4)/N, where M1–M4 represent the number of cells with 1–4 nuclei and N is the total number of viable cells scored (excluding necrotic and apoptotic cells).

3 MOLECULAR BIOLOGY

3.1 NUCLEIC ACID EXTRACTION

DNA extraction by salt lysis. Harvested cells and tissue were incubated overnight at 55ºC with 500 µL TNES lysis buffer (20mM Tris HCl pH8, 100mM NaCl, 0.,5% SDS, 10mM EDTA) supplemented with 10 µL proteinase K (20 mg/mL). Saturated NaCl salt was added to the mixture and centrifugated to eliminate cellular debris. DNA strands were precipitated with isopropanol and cleaned with several ethanol washes. Dried DNA pellets were resuspended in molecular-grade water or TE and quantified at 260nm in a Nanodrop system. This protocol is inspired by (Aljanabi & Martinez, 1997).

For finer purposes, such as the CRISPR screening, genomic DNA was extracted by column purification, Monarch® DNA kit (Cat# T1020 New England Biolabs) or Quick-DNA Midiprep kit (Cat# D4075 Zymo Research) in this case using the latter.

RNA extraction. Commercial kits were used to perform RNA extraction by column purification: NZY Total RNA Isolation kit (Cat# MB13402 NzyTech) or Quick-RNA Miniprep Kit (Cat# R1055 Zymo Research). RNA was resuspended in molecular-grade water and quantified at 260nm in a Nanodrop system.

3.2 PCR AND GEL ELECTROPHORESIS

Polymerase chain reaction (PCR) amplification was used for cloning, genotyping, and sequencing of DNA fragments of interest. Primers pairs were designed to flank the selected region at different amplicon sizes. The reaction was optimized according to manufacturer protocol of the Taq DNA polymerase. Commercial polymerases used were FirePol® (Cat# 01-01-02000 Solis Biodyne), NzyTaqII (Cat# MB35403 NzyTech) and Q5® High Fidelity (Cat# M0491 New England Biolabs). Template DNA quantities vary, around 5 to 10ng of gDNA and less than 1ng of plasmid DNA. Primers were used at 0.4 µM each and 200 µM of dNTPs in a final reaction volume of 20 µL

(although volumes may be increased up to 100 µL depending on the experiment conditions). PCR conditions were drawn by the manufacturer, with variations on the number of cycles depending on the amplicon and on the annealing temperature depending on the primers used to perform the amplification, being 60ºC the standard annealing temperature.

Fragments were separated on agarose gels of different concentrations by electrophoresis. Agarose gels were prepared with SYBR® Safe DNA stain (Cat# S33102 Invitrogen) to visualize DNA under ultraviolet light in a ChemiDoc™ XRS+ System (Biorad). Gel bands could be cut and purified using column purification kits (NZYGelpure™, NZYtech).

The list of primers used for PCR, genotyping and sequencing were the following:

ID	Name	Sequence
1	Kras G12V F	CGTCCAGCGTGTCCTAGACTTTA
2	Kras G12V R	ACTATTTCATACTGGGTCTGCCTT
9	Cre F	CCCGCAGAACCTGAAGATGT
10	Cre R	GTTCGAACGCTAGAGCCTGTTT
11	RosaLSLYFP KI	AAGACCGCGAAGAGTTTGTC
12	RosaLSLYFP common	AAAGTCGCTCTGAGTTGTTAT
13	RosaLSLYFP wild type	GGAGCGGGAGAAATGGATATG
14	Kras lox F	CCACAGGGTATAGCGTACTATGCAG
15	Kras lox R	CTCAGTCATTTTCAGCAGGC
26	CMV Fw	CGCAAATGGGCGGTAGGCGTG
114	hU6-F sequencing primer	GAGGGCCTATTTCCCATGATT
115	LKO.1 5' sequencing primer	GACTATCATATGCTTACCGT
190	U6-pLKO-Fbis	CGATACAAGGCTGTTAGAGAGAT
191	pLKO-Rbis	CGACTCGGTGCCACTTTTTCA
289	pTRIP TRE Fw	ACAGTGCAGGGGAAAGAATAGTA
290	Topires Rev 1 (PTRIP-TRE)	GCTTCCAGAGGAACTGCTTCCTTCA
366	U6 seq gRNA Fw	CAAGGCTGTTAGAGAGATAATTGGA
377	BRAF internal Fwd	TATCGTTAGAGTCTTCCTGC
384	hPGK promoter reverse	CAGGGCTGCCTTGGAAAAG
456	EF1a Fw	TCAAGCCTCAGACAGTGGTTC
504	DUSP6 human seq primer 5' A	CAGGGTTCCAGCACAGCAGC
505	DUSP6 human seq primer 3' A	GAGAAACTGCTGAAGGGCCA
552	DUSP6 human F	TGACATGGCTGCAGATCACAG
553	DUSP6 human R	TGCCCTACTATGCCTACAAGTC
616	DUSP6 human 2 F	GCTGTTAATCGTTCTTGCTGC
617	DUSP6 human 2 R	CCCTTCTTCACAATCAAATGCA
564	H1 sequencing primer	TCGCTATGTGTTCTGGGAAA
567	T7 sequencing primer	TAATACGACTCACTATAGGG
570	P2A R	CTTCGACATCTCCGGCTTGT

Table 15. ***Table of primers used for PCR, genotyping, and sequencing***

3.3 CRISPR SCREENING LIBRARY PREPARATION

We performed a CRISPR knock-out screening, a high-throughput experimental technique used to systematically disrupt the complete set of individual genes in the genome with CRISPR/Cas9 gene editing technology (Joung et al., 2017). The process involves introducing a library of gRNAs in a

Cas9-expressing cell population, ensuring that one gRNA is distributed in each cell. For this purpose, we selected the optimized sgRNA Brunello library (Doench et al., 2016; Sanson et al., 2018). The Brunello library contains 1,000 non-targeting control gRNAs, 76,441 functional gRNAs and is able to target a total of 19,114 human genes with the SpCas9 in the plentiCRISPRv2 plasmid format. This library has significantly reduced off-target activity and an increased number of statistically significant genes compared to previous existing GeCKO (Sanjana et al., 2014) and Wang (Wang et al., 2014) libraries.

The Brunello library was ordered from Addgene (#73179) and amplified following the Broad Institute recommendations, in STBL3 bacteria. NGS was performed to verify the plasmid pool representation and distribution. Lentivirus supernatants were produced as mentioned previously in 293T cells and concentrated by ultracentrifugation. The initial titering was performed by qPCR on infected 293T cells, but during the optimization process an actual physical titer was performed in the cells of interest. The preparation of the library and the viral production processes were done in collaboration with the CRISP'edit and the VectUB platforms (TBM Core) in the University of Bordeaux.

3.4 NESTED PCR FOR ENRICHMENT OF CRISPR SCREENING LIBRARIES

The CRISPR screening requires identifying the individual gRNAs present at the end of the treatment phase. This is achieved by mass-sequencing of the gRNA insertion locus, decrypting the sequences of the totality of the gRNAs of the Brunello library. To this end, we optimized a two-step nested PCR protocol for Illumina library preparation, allowing the amplification of the gRNA locus combined to an Illumina adapter insertion. The polymerase used for the nested PCR protocol was the Kapa HiFi HotStart PCR Kit (with Fidelity buffer) (Roche, Cat# KR0369).

The PCR conditions were optimized with controls in order to ensure that there was a proper enrichment of the gRNA sequences (**Figure 16**). The first PCR (of 462bp) amplifying the gRNA from the lentiviral locus in the genome was performed with the whole extract of gDNA, corresponding to 40 million cells per condition. A total of 30-50 tubes per condition were used,

depending on gDNA concentrations, in 100 µL reactions with 4 µg of template gDNA per reaction. This PCR1 step ensured that representativity of the Brunello library was maintained through the whole process up until the sequencing step. The resulting material was pooled in a single tube. A dilution of 1/10 of this PCR1 was used as the template to perform PCR2 (nested PCR). At this time, representativity was abundantly guaranteed so a single 50 µL PCR per condition was sufficient to amplify the library, obtaining around 2 µg of final product. The PCR2 fragments were used as template in the Illumina sequencing reaction.

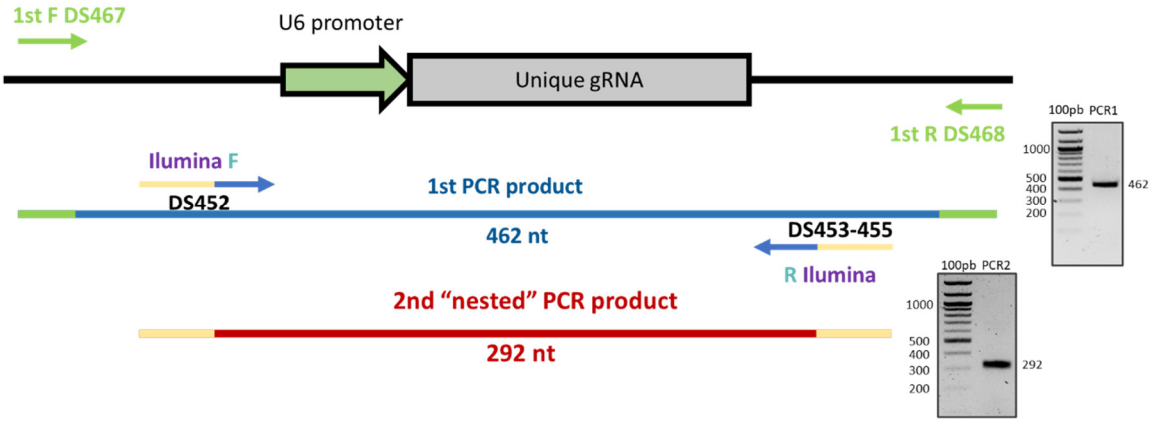

Figure 16. ***Nested PCR approach for generating the CRISPR screening sequencing library****. The 1st PCR was performed directly on the gDNA in order to amplify the Brunello plentigRNA construct region of the gRNA, including the U6 promoter. This first amplicon was then used as a template in a 2nd PCR that used extended primers in order to amplify the gNRA sequencing while inserting Illumina sequencing ends and barcodes specific to the screening condition. Both PCRs were gel purified and PCR2 quality and size was evaluated by TapeStation™ analysis.*

The primers used for these two steps were:

PCR1	
F1.od_64.48	ACAAAGATATTAGTACAAAATACGTGACGTAGA
R1.od_64.59	TGGATCTCTGCTGTCCCTGTA
PCR2 (nested)	Adaptor (ID) + Complementary
P5-F2.od	AATGATACGGCGACCACCGAGATCTACACGGACTATCATATGCTTACCGTAACTTGA
P7-pLGuide-R2.od.Idx01	CAAGCAGAAGACGGCATACGAGATCGTGATGTGACTGGAGTTCAGACGTGTGCTCTTCCGATCTCAAGATCTAGTTACGCCAAGC
P7-pLGuide-R2.od.Idx03	CAAGCAGAAGACGGCATACGAGATGCCTAAGTGACTGGAGTTCAGACGTGTGCTCTTCCGATCTCAAGATCTAGTTACGCCAAGC
P7-pLGuide-R2.od.Idx09	CAAGCAGAAGACGGCATACGAGATTCAAGTGTGACTGGAGTTCAGACGTGTGCTCTTCCGATCTCAAGATCTAGTTACGCCAAGC

Table 17. ***Table or primers used for CRISPR screening library generation.*** *PCR1 was common for the three conditions, while PCR2 used different barcodes for PRE (Idx01), K (Idx03), KB (Idx09).*

3.5 RT-qPCR

RNA extracts were used to synthesize cDNA in vitro. A total of 500 ng of RNA were added to the reverse transcription (RT) reaction using a viral reverse transcriptase (OneScript® Plus cDNA Synthesis Kit, ABM Cat# G236). The product was used as template for qPCR diluted 1/10 with molecular-grade water.

For the amplification step, we performed real-time fluorescence-based PCR. Amplification products containing the cDNA were mixed in triplicate reactions with fluorescent SYBR Green® (SsoAdvanced Universal, Biorad Cat# 1725270 or NZYSupreme ROX plus, NzyTech Cat# MB44001). The reaction was completed with pairs of primers (500nM each) specific of cDNA sequences for the genes of interest. The systems used for this step were the CFX984 (BioRad) from the OneCell TBM platform in Bordeaux and the QuantStudio™ 3 at the CIC Salamanca.

Two controls were used for every qPCR experiment, water (to verify primer-dimer formation of the qPCR primers and check for contaminants) and a sample without the RT step (to verify off-target amplifications coming from the residual gDNA).

The primers used for cDNA amplification were:

ID	Name	Sequence	ID	Name	Sequence
1	Dusp4-1F (M)	CGTGCGCTGCAATACCATC	106	18S R (H)	GATCACACGTTCCACCTCATC
2	Dusp4-1R (M)	CTCATAGCCACCTTTAAGCAGG	121	EGFR (M) F (M)	GCCATCTGGGCCAAAGATACC
3	Dusp4-2F (M)	GTACATCGACGCAGTAAAGGAC	122	EGFR (M) R (M)	GTCTTCGCATGAATAGGCCAAT
4	Dusp4-2R (M)	GCTTGACGAACTCAAAAGCCTC	123	B-Actin F (H)	CTCGACACCAGGGCGTTATG
5	Dusp6-1F (M)	ATAGATACGCTCAGACCCGTG	124	B-Actin R (H)	CCACTCCATGCTCGATAGGAT
6	Dusp6-1R (M)	ATCAGCAGAAGCCGTTCGTT	129	PPEF1 F (H)	ACCGAGGTTACAAAGCTCGAC
7	Dusp6-2F (M)	CGAGTCGTCACACATCGAATC	130	PPEF1 R (H)	TCAGCATATTCGATGGACTGGAA
8	Dusp6-2R (M)	GCTATTCTCGTCGTACAGCAC	131	PPP2R1B F (H)	CTTGTGTCAGTATTGCCCAGT
9	Spry2-1F (M)	TCCAAGAGATGCCCTTACCCA	132	PPP2R1B R (H)	TGCTGCTTGTCGAAGTGTAGG
10	Spry2-1R (M)	GCAGACCGTGGAGTCTTTCA	133	CTDSP2 F (H)	ACATCTTCAAGGCCCTTTTCTG
11	Spry2-2F (M)	AATCCGAGTGCAGCCTAAATC	134	CTDSP2 R (H)	TTCCTCCTTATACGCAGCGAG
12	Spry2-2R (M)	CGCAGTCCTCACACCTGTA	135	MTMR8 F (H)	AACGTGAAATTGGTGGATCGT
13	Spry4-1F (M)	GCAGCGTCCCTGTGAATCC	136	MTMR8 R (H)	GGCAATGTGATGGAGTGCAATC
14	Spry4-1R (M)	TCTGGTCAATGGGTAAGATGGT	137	PPP1R14C F (H)	CTGGGTCAGCTCTACGGCT
15	Spry4-2F (M)	CCCGCTGTGACCAGGATATTA	138	PPP1R14C R (H)	CATGCCTCTTATCCGAGAAAGC
16	Spry4-2R (M)	GCCATGTGATCTAGGAGCCTC	159	GAPDH F (H)	GCACAAGAGGAAGAGAGAGACC
17	GAPDH-F (M)	AGGTTGTCTCCTGCGACTTCA	160	GAPDH R (H)	AGGGGAGATTCAGTGTGGT
18	GAPDH-R (M)	GGTGGTCCAGGGTTTCTTACTC	161	B2M F (H)	ACTCTCTCTTTCTGGCCTGG
19	TBP-F (M)	TGTACCGCAGCTTCAAAATATTGTAT	162	B2M R (H)	GACAAGTCTGAATGCTCCACT
20	TBP-R (M)	AAATCAACGCAGTTGTCCGTG	163	EEF1A1 F (H)	AGCAAAAATGACCCACCAA
21	βactin-F (M)	ACCAACTGGGACGATATGGAGAAGA	164	EEF1A1 R (H)	GGCCTGGATGGTTCAGGATA
22	βactin-R (M)	TACGACCAGAGGCATACAGGGACAA	165	PPP1R1B p.2 F (H)	GAGCCTCAGCTGGAGATCCG
49	KRas WT F (M)	CCACAGGGTATAGCGTACTATGCAG	166	PPP1R1B p.2 R (H)	TTTCAGCGAAGGTGGTGTGT
50	KRas WT R (M)	CTCAGTCATTTTCAGCAGGC	167	PPP1R14C p.2 F(H)	TCTACGGCTGCGAGGAAGAA
51	KRas KI F (M)	TAGTGCCTTGACTAGAGATCA	168	PPP1R14C p.2 R(H)	TCTGGGAGAGTTTCACCCTGT
52	KRas KI R (M)	CTCAGTCATTTTCAGCAGGC	169	PPP2R2C p. 2 F (H)	CGACCTCGAAGTTTCCGAAGA
53	PHLDA1 F (M)	GGGCTACTGCTCATACCGC	170	PPP2R2C p. 2 R (H)	GGGCGCATTTTTACTCTCTGGT
54	PHLDA1 R (M)	AAAAGTGCAATTCCTTCAGCTTG	171	PIK3CA F (H)	CCACGACCATCATCAGGTGAA
55	Spry2 F (M)	TCCAAGAGATGCCCTTACCCA	172	PIK3CA R (H)	CCTCACGGAGGCATTCTAAAGT
56	Spry2 R (M)	GCAGACCGTGGAGTCTTTCA	173	INSM1 F (H)	GTCCACGCCCGTTTCCTAC
57	Dusp6 F (M)	GCGTCGGAAATGGCGATCT	174	INSM1 R (H)	CCAGGTTGAAGCTGCGTTC
58	Dusp6 R (M)	ATGTGTGACGACTCGTACAGC	175	PPAPDC1A F (H)	CTGGCCATTGAGATCGGGG
59	Dusp4 F (M)	CGTGCGCTGCAATACCATC	176	PPAPDC1A R (H)	TCAGTCTTGTCTGTTCGCCG
60	Dusp4 R (M)	CTCATAGCCACCTTTAAGCAGG	177	MTMR12 F (H)	ACGACAAAGAGGAGGTTCCTG
61	Etv4 F (M)	CGGAGGATGAAAGGCGGATAC	178	MTMR12 R (H)	CCACACGGTGAGCAGATTCA
62	Etv4 R (M)	TCTTGGAAGTGACTGAGGTCC	179	PTPRE F (H)	TAGCTTTTCCCGGCTCACCTG
63	Etv5 F (M)	TCAGTCTGATAACTTGGTGCTTC	180	PTPRE R (H)	TGTCCAGATGGCAATGAGTTGAA
64	Etv5 R (M)	GGCTTCCTATCGTAGGCACAA	181	PHACTR3 F (H)	CCGCCCGAGATCCTGC
77	DUSP4 F (H)	GGCGGCTATGAGAGGTTTTCC	182	PHACTR3 R (H)	CTTCTCCAGCGCTGACGTT
78	DUSP4 R (H)	TGGTCGTGTAGTGGGGTCC	183	EYA1 F (H)	AGCATTGTCGTTCTCAGCCA
79	DUSP16 F (H)	GCCCATGAGATGATTGGAACTC	184	EYA1 R (H)	TGCATTTCCATAGACCTGCAAC
80	DUSP16 R (H)	CGGCTATCAATTAGCAGCACTTT	185	EYA2 F (H)	AGCTTGAACCATTCCCCTGG
81	DUSP22 F (H)	AGCAGCGGATTCACCATCTC	186	EYA2 R (H)	TAGAACCCTGTTGTGCCGTG
82	DUSP22 R (H)	TGATGTATGCGATCACCAGTGT	187	PLPPR1 F (H)	GCACCTCCGCCCCAC
83	PPAPDC1B F (H)	TGGAGGCGGAGTATTTCCC	188	PLPPR1 R (H)	TGTCCAGGCTCCCGCA
84	PPAPDC1B R (H)	TGTGTTGGTAAAGACGCCATT	189	PTPRN F (H)	CCTCCAGTGAAGTCCAGCAG
85	PPP2R2C F (H)	CACTCCTGTCCACCAACGATA	190	PTPRN R (H)	CTGGTCCCACCACATTCTGA
86	PPP2R2C R (H)	CATTGGCAAAGATCCTCCGAG	191	CDKN3 F (H)	AGCCGCCCAGTTCAATACAA
87	PPP1R1B F (H)	CAAGTCGAAGAGACCCAACCC	192	CDKN3 R (H)	ACTCGTGACAAAGATAGCCATGA
88	PPP1R1B R (H)	GCCTGGTTCTCATTCAAATTGCT	193	PTPRZ1 F (H)	AGTGCAGAGCTGTACTGTTGA
89	PTPN13 F (H)	GAGTTTCTGTTCGGACTGTGC	194	PTPRZ1 R (H)	TTTGGTCTGTTGTAGCCATCA
90	PTPN13 R (H)	TGTTACAGGAAAGCTGATCTGTC	223	NRF2 F (H)	TCCAGTCAGAAACCAGTGGAT
91	HDHD1A F (H)	ACCTGCGGAAACATGGCAT	224	NRF2 R (H)	GAATGTCTGCGCCAAAAGCTG
92	HDHD1A R (H)	GGCTTGTCTTCATATCGAACGA	225	KEAP1 F (H)	CAACTTCGCTGAGCAGATTGGC
93	MTMR3 F (H)	GACTGAACAACGCAATCCGAC	226	KEAP1 R (H)	TGATGAGGGTCACCAGTTGGCA
94	MTMR3 R (H)	CCTTGAAGTTACATGCTCCCC	239	GFP F	AAGGGCATCGACTTCAAGG
95	PPP2R3A F (H)	CTGTCCTCTCTATTGGAAAGCCC	240	GFP R	TGCTTGTCGGCCATGATATAG
96	PPP2R3A R (H)	TGAATGACTGTGCTGTCACAAAT	241	CSK F (H)	AGGACCCCAACTGGTACAAAG
97	PTPRG F (H)	TGGAACCGTGTTGGTGGATTT	242	CSK R (H)	CGTGGAACCAAGGCATGAG
98	PTPRG R (H)	CAACGTAGCCTTCTGTCAACG	243	c-SRC F (H)	GAGCGGCTCCAGATTGTCAA
99	PPM1B F (H)	TGGGAATGGTTTACGTTATGGC	244	c-SRC R (H)	CTGGGGATGTAGCCTGTCTGT
100	PPM1B R (H)	GCCGTGAGGAATACCTACAACAG	245	PAG1 F (H)	TTCCTGTGCTCTAGTTGTGACA
101	18S F (H)	TGCCATCACTGCCATTAAG	246	PAG1 R (H)	CACGTTCATCAGGTTCTCATGG
102	18S R (H)	TGCTTTCCTCAACACCACATG	247	TTC1 F (H)	GAGCGGACAAGGTTGAGAACA
103	HPRT F (H)	TGACACTGGCAAAACAATGCA	248	TTC1 R (H)	CTCCTCCTTTAGTCTAGTGCTCT
104	HPRT R (H)	GGTCCTTTTCACCAGCAAGCT	249	PPP4C F (H)	AAGGTTCGCTATCCTGATCGC
105	18S F (H)	GCGGCGGAAAATAGCCTTTG	250	PPP4C R (H)	AGCCATAGACCTGCGTGATCT

Table 18. ***Table of primers used for cDNA amplification by RTqPCR***

3.6 SANGER SEQUENCING

Fragments of DNA to be sequenced were purified from agarose gel bands and resuspended in molecular grade water, at low concentrations depending on the size of the region of interest. For plasmid DNA, 200ng of DNA were sequenced, while PCR products needed between 1-10 ng of DNA depending on the size of fragment. Primer quantity was established at 3.2 pmol per 8 µL reaction.

Sanger reaction and analysis was performed internally in a 3100 Genetic Analyzer (Applied Biosystems) at the IBMCC-CIC Genomics Facilities and/or at Nucleus Sequencing Department (USAL).

3.7 CONSTRUCTS

3.7.1 Enzymatic reactions

Restriction analysis was used to prepare inserts and vectors and to verify the integrity of the whole constructs. All the restriction enzymes used in the laboratory come from New England Biolabs and we follow the recommended protocol for their use. Once the digestion reaction is over, digested products are analyzed by electrophoresis. The product can also be purified through a column (GenElute™, Sigma Cat# NA1111). When enzyme combinations were not possible, digestions were done sequentially, gel purifying the intermediates.

Prior to ligation, digested plasmids were dephosphorylated with an alkaline phosphatase (Antarctic, NEB Cat# M0289) for 1 hour at 37ºC, in order to avoid self-ligating empty vectors, most importantly with blunt digestions.

We used non-phosphorylated primers for amplifying PCR-generated DNA fragments used for ligation into vectors, so we phosphorylated them with a T4 polynucleotide kinase (NEB, Cat# M0201) in presence of 1mM ATP from the T4 ligase buffer for 37ºC for 30 minutes.

For blunting DNA ends from inserts or vectors, we used a T4 DNA polymerase with 3’ exonuclease activity (NEB, Cat# M0203). The reaction was supplemented with 100 µM dNTP and incubated in

a lukewarm water glass with ice, at 12ºC, for 15 minutes, then heat inactivated at 75ºC for 20 minutes.

Ligation reaction between inserts and vectors was performed by a T4 ligase (Thermo Scientific, Cat# EL0016). The reaction was normally prepared with a vector-insert ratio of 1:5, calculating the proportions using around 50 ng of digested plasmid. The reaction was completed in a 10 µL volume and incubated for 20 minutes at room temperature (at 16ºC overnight if necessary). The whole ligation reaction was directly inoculated to the bacterial preparation for transformation.

3.7.2 Bacterial culture

E. coli bacteria cultures were transformed directly with ligation products in order to perform plasmid amplification. Different bacterial strains were used according to plasmid demands, STBL3 (Genotype: *F−mcrB mrr hsdS20 (rB−, mB−) recA13 supE44 ara14 galK2 lacY1 proA2 rpsL20 (StrR) xyl5 λ−leu mtl1* – Invivogen) strain was used for lentiviral and recombination-susceptible plasmids (because of their recA defective mutations), while DH10β (Genotype: *F−mcrA Δ(mrr-hsdRMS-mcrBC) ϕ80dlacZΔM15 ΔlacX74 endA1 recA1 deoR Δ(ara, leu)7,697 araD139 galU galK nupG rpsL λ* – Invivogen) bacteria were used for the rest of plasmids.

These competent strains were prepared at the lab from an established stock with the following protocol. A starter culture of DH10β/STBL3 was inoculated in a 400mL LB culture with no antibiotics for approximately 1h at 37ºC, until reaching an OD-595nm of 0.49 units, avoiding overgrowth. The culture was stopped on ice for 10 minutes and centrifuged 15 minutes at 12,000G at 4ºC. The bacteria pellet was resuspended in 80mL of sterile 50mM $CaCl_2$ and incubated on ice for 30 more minutes. The suspension is re-centrifuged 15 minutes at 12,000G at 4ºC. The final pellet is resuspended in 8mL of sterile 50mM $CaCl_2$ with 15% glycerol, in order to be aliquoted in 100 µL tubes and stocked at -80ºC.

For transformation, a vial of cryopreserved competent cells was thawed on ice and the whole ligation reaction mixture (10 µL) was inoculated. The tube was incubated in ice for 20 minutes without mixing. Then a 60 second 42ºC heatshock was performed in order to introduce the DNA

into the cells. After 5 minutes in ice, 500 µL of room temperature LB with no antibiotics were added and the mixture was incubated at 37ºC (or 30ºC if STBL3) for 30-90 minutes under agitation to allow recovery and expression of antibiotic resistance genes. Transformation culture was then spread into selection plates with antibiotic LB + 1.5% agar media. Antibiotics were used at different concentrations, 100 µg/mL for ampicillin and 50 µg/mL for kanamycin. Once seeded, the plates were incubated overnight at 37ºC (or 30ºC if STBL3). On the next day, colonies were picked for clone isolation, colony-PCR and/or miniprep (Sigma) plasmid extraction.

For colony-PCR analysis, a single colony was picked into 10 µL of water or LB. We use 1 µL of this mixture directly in the PCR reaction as template.

3.7.3 CRISPR knock-out vector generation

For generating knock-out cellular models, we used an all-in-one system, plentiCRISPRv2 (Sanjana et al., 2014) with puromycin resistance. This plasmid contains two expression cassettes, the humanized SpCas9 and the chimeric gRNA (containing the specific crRNA and the common tracrRNA). In order to get the two components assembled, the original vector containing the Cas9 must be digested and inserted with a synthetic sequence containing the crRNA part, that will complement the already present tracrRNA to form a full gRNA. This protocol was also employed when preparing plentigRNA (Cong et al., 2013), that only contain the gRNA part and pX330 (Stringer et al., 2019), non-lentiviral, plasmids.

The vector was digested with *BsmbI* restriction enzyme, for 2 hours at 55ºC. This digestion liberates a 2kb stuffer sequence, so the digested vector was gel purified and dephosphorylated. In parallel, in order to generate the crRNA, two oligonucleotides were designed to contain the crRNA sequence, while being complementary to each other and generating *BsmBI* compatible ends. The design process of the oligos is described later on. These two oligos were annealed by mixing 10 µM each and ramping down the temperature 5ºC/min in a thermocycler in presence of 1mM ATP (present in the T4 ligase buffer). The mixture of annealed oligos was then diluted 1/200 before using 1 µL as insert in the ligation reaction, together with 50ng of *BsmBI* digested vector. The ligation product

was transformed and amplified in STBL3 bacteria as described before. Lentiviral supernatants were produced in 293T cells and used to infect the cells of interest.

After infection, a verification of the editing efficiency is performed by extracting gDNA from the infected cells selected with puromycin. Then, a PCR was performed to amplify the editing region using specific primers, that were retained during the gRNA design process. The amplicon was then Sanger-sequenced and gene editing efficiency was calculated with TIDE (Brinkman et al., 2014) algorithms.

These are the primers used in CRISPR ko vector generation and analysis

ID	Name	Sequence
362	Fw-sgRNA1-ZsGreen	CACCGAAGTTCGTGATCACCGGCGA
363	Rev-sgRNA1-ZsGreen	AAACTCGCCGGTGATCACGAACTTC
364	Fw-sgRNA2-ZsGreen	CACCGACCATGAAGTACCGCATGG
365	Rev-sgRNA2-ZsGreen	AAACCCATGCGGTACTTCATGGTC
380	F-gRNA1-turboGFP	CACCGGAGATCGAGTGCCGCATCAC
381	R-gRNA1-turboGFP	AAACGTGATGCGGCACTCGATCTCC
382	F-gRNA2-turboGFP	CACCGGGTCATGCGGCCCTGCTCGG
383	R-gRNA2-turboGFP	AAACCCGAGCAGGGCCGCATGACCC
399	F-gRNA1-DUSP4 (human)	CACCGAAAGTGGTTTGGGCAGTCCG
400	R-gRNA1-DUSP4 (human)	AAACCGGACTGCCCAAACCACTTTC
401	F-gRNA2-DUSP4 (human)	CACCGTGGGACCCCACTACACGACC
402	R-gRNA2-DUSP4 (human)	AAACGGTCGTGTAGTGGGGTCCCAC
416	F-gRNA1-mouse DUSP4	CACCGCACAGCGCGGGCTACATCCG
417	R-gRNA1-mouse DUSP4	AAACCGGATGTAGCCCGCGCTGTGC
418	F-gRNA2-mouse DUSP4	CACCGGCAATACCATCGTGCGGCGG
419	R-gRNA2-mouse DUSP4	AAACCCGCCGCACGATGGTATTGCC
420	F-gRNA-lacZ	CACCGAGACGATCCGCTGGCCGTTA
421	R-gRNA-lacZ	AAACTAACGGCCAGCGGATCGTCTC
424	DUSP4 human gRNA1 amplification primer F	GAGATCCTTCCCTTCCTCTACC
425	DUSP4 human gRNA1 amplification primer R	GCTTACAGGGGTTCCTTATCCT
426	DUSP4 human gRNA2 amplification primer F	CTGGCTTAGTGACCCCATTAAC
427	DUSP4 human gRNA2 amplification primer R	CTCTGAAAAGAAGGCATCCACT
428	DUSP4 mouse gRNA1+2 amplification primer F	TGATGAACCGGGATGAGAAC
429	DUSP4 mouse gRNA1+2 amplification primer R	TAGACGATGACAGCCGAGTAGA
457	DUSP4 human gRNA3 amplification primer F	CAAGCACTTTACCCTCATGTCA
458	DUSP4 human gRNA3 amplification primer R	AGTGTCCTTCAAAGTGGTTTGG
473	F-gRNA3-mouse DUSP4	CACCGACATACCTGGTCGTGCAGCG
474	R-gRNA3-mouse DUSP4	AAACCGCTGCACGACCAGGTATGTC
475	F-gRNA4-mouse DUSP4	CACCGGGGACATGTTGGATGCCCTG
476	R-gRNA4-mouse DUSP4	AAACCAGGGCATCCAACATGTCCCC
477	DUSP4 mouse gRNA3 amplification F	CAGGTGGCTATGAGAGGTTTTC
478	DUSP4 mouse gRNA3 amplification R	GGATACTTTATGGACAGAGGCG
479	DUSP4 mouse gRNA4 amplification F	GCATCACTCATGTTTTGCCTAT
480	DUSP4 mouse gRNA4 amplification R	CAAAGTGATTGGGACAGTCTGA
508	F-gRNA1-human CSK	CACCGTGATGCTGGGCGATTACCGA
509	R-gRNA1-human CSK	AAACTCGGTAATCGCCCAGCATCAC
510	CSK human gRNA1 amplification F	GCCCTGAACATGAAGGAGCT
511	CSK human gRNA1 amplification R	CCTTCTCCTCCACGATCACG
512	F-gRNA2-human CSK	CACCGCAACTACGTCCAGAAGCGGG
513	R-gRNA2-human CSK	AAACCCCGCTTCTGGACGTAGTTGC
514	CSK human gRNA2 amplification F	ACCCCAACTGGTACAAAGCC
515	CSK human gRNA2 amplification R	GGCATTTGAGGCCCTCTTCT
516	F-gRNA3-human CSK	CACCGCGCACAGCGTGTAGTCTCCG
517	R-gRNA3-human CSK	AAACCGGAGACTACACGCTGTGCGC
518	CSK human gRNA3 amplification F	CTTCAGAAAGGGGAGCCAGG
519	CSK human gRNA3 amplification R	ACCAGCTGCATGAGGTTCTC
520	F-gRNA1-human TTC1	CACCGAGAGAGCACTAGACTAAAGG

521	R-gRNA1-human TTC1	AAACCCTTTAGTCTAGTGCTCTCTC
522	TTC1 human gRNA1 amplification F	TGTGCATAAGGAAAGCTCACCT
523	TTC1 human gRNA1 amplification R	AGGTACTGGGAAGCAACACTG
524	F-gRNA2-human TTC1	CACCGTTCTCAACCTTGTCCGCTCC
525	R-gRNA2-human TTC1	AAACGGAGCGGACAAGGTTGAGAAC
526	TTC1 human gRNA2 amplification F	CAGGAGGACCAGGGAGAAGA
527	TTC1 human gRNA2 amplification R	TCAAGTGCTTCCCTGTCACG
528	F-gRNA3-human TTC1	CACCGGCAGGATGGGCACATTTCGA
529	R-gRNA3-human TTC1	AAACTCGAAATGTGCCCATCCTGCC
530	TTC1 human gRNA3 amplification F	AGCTGTCAGTTCACCAAGCA
531	TTC1 human gRNA3 amplification R	TTCATCCTTGCTGCAGCTCT
532	F-gRNA1-human PAG1	CACCGAACTGTGAAAGAGATCAAGG
533	R-gRNA1-human PAG1	AAACCCTTGATCTCTTTCACAGTTC
534	PAG1 human gRNA1 amplification F	CGTGTCTGTGGCACTCTCTT
535	PAG1 human gRNA1 amplification R	AAGTGCTCAAGGACAGCTCC
536	F-gRNA2-human PAG1	CACCGTCACGGCGAGAAGTGTGGAC
537	R-gRNA2-human PAG1	AAACGTCCACACTTCTCGCCGTGAC
538	PAG1 human gRNA2 amplification F	TCCACCGAGGCATATTCAGC
539	PAG1 human gRNA2 amplification R	CTCGGATCTGCTGGATTCCC
540	F-gRNA1-human PPP4C	CACCGCGATCAGGATAGCGAACCTG
541	R-gRNA1-human PPP4C	AAACCAGGTTCGCTATCCTGATCGC
542	PPP4C human gRNA1 amplification F	AGTGGTTGTGAGGATGGCAG
543	PPP4C human gRNA1 amplification R	ATCTACAGGGGAGAGCAGGG
544	F-gRNA2-human PPP4C	CACCGGATTGTCCGAATCTGATCCA
545	R-gRNA2-human PPP4C	AAACTGGATCAGATTCGGACAATCC
546	PPP4C human gRNA2 amplification F	GCGCTACTGCACTGAGATCT
547	PPP4C human gRNA2 amplification R	GCTCCCTCTCTTTCCCAACC
548	F-gRNA3-human PPP4C	CACCGTCACCGAGCCGTACTTGCGC
549	R-gRNA3-human PPP4C	AAACGCGCAAGTACGGCTCGGTGAC
550	PPP4C human gRNA3 amplification F	GGTTCGCTATCCTGATCGCA
551	PPP4C human gRNA3 amplification R	ATCTACAGGGGAGAGCAGGG
684	F-gRNA3 DUSP4 human	CACCGAGCATGGTAGGCACTGCCG
685	R-gRNA3 DUSP4 human	AAACCGGCAGTGCCTACCATGCTC

Table 19. ***Table of oligonucleotides used for CRISPR knockout vector generation***

3.7.4 RNA interference (shRNA) vector generation

Knock-down of a particular gene's expression was achieved using shRNA vectors. Depending on the context, we chose to use constitutive or doxycycline inducible vectors, both had in common a pLKO backbone (Moffat et al., 2006) and shRNAs were cloned through the same process. The empty vector was digested with *EcoRI* and *AgeI,* liberating a 1.9kb stuffer. The remaining ends were compatible with designed annealed oligos containing the hairpin RNA loop in between the *EcoRI* and *AgeI* sites. The process of annealing, ligating, transforming, and expanding was the same as for the CRISPR vectors.

The shRNA sequences were directly obtained from the Broad Institute RNAi consortium (MISSION) list, from the validated selection list. This is the list of primers used for shRNA generation:

ID	Name	Sequence
562	GFP control shRNA 1 F	CCGGCAACAGCCACAACGTCTATATCTCGAGATATAGACGTTGTGGCTGTTGTTTTTG
563	GFP control shRNA 1 R	AATTCAAAAACAACAGCCACAACGTCTATATCTCGAGATATAGACGTTGTGGCTGTTG
591	TTC1 human shRNA1 F	CCGGCGGCTCGTACTCCATCAATTTCTCGAGAAATTGATGGAGTACGAGCCGTTTTTG
592	TTC1 human shRNA1 R	AATTCAAAAACGGCTCGTACTCCATCAATTTCTCGAGAAATTGATGGAGTACGAGCCG
593	TTC1 human shRNA2 F	CCGGCAGCTATATCAGGGCAATATTCTCGAGAATATTGCCCTGATATAGCTGTTTTTG
594	TTC1 human shRNA2 R	AATTCAAAAACAGCTATATCAGGGCAATATTCTCGAGAATATTGCCCTGATATAGCTG
595	TTC1 human shRNA3 F	CCGGCTGATGTAATGAACCTAATTTCTCGAGAAATTAGGTTCATTACATCAGTTTTTG
596	TTC1 human shRNA3 R	AATTCAAAAACTGATGTAATGAACCTAATTTCTCGAGAAATTAGGTTCATTACATCAG
709	DUSP4 human shRNA1 F	CCGGGGAGGCCTTCGAGTTCGTTAACTCGAGTTAACGAACTCGAAGGCCTCCTTTTTG
710	DUSP4 human shRNA1 R	AATTCAAAAAGGAGGCCTTCGAGTTCGTTAACTCGAGTTAACGAACTCGAAGGCCTCC
711	DUSP4 human shRNA2 F	CCGGACCACTTTGAAGGACACTATCCTCGAGGATAGTGTCCTTCAAAGTGGTTTTTTG
712	DUSP4 human shRNA2 R	AATTCAAAAAACCACTTTGAAGGACACTATCCTCGAGGATAGTGTCCTTCAAAGTGGT
713	DUSP4 human shRNA3 F	CCGGTTCGGTCAACGTGCGCTGTAACTCGAGTTACAGCGCACGTTGACCGAATTTTTG
714	DUSP4 human shRNA3 R	AATTCAAAAATTCGGTCAACGTGCGCTGTAACTCGAGTTACAGCGCACGTTGACCGAA
715	DUSP4 mouse shRNA1 F	CCGGCGAGTACATCGACGCAGTAAACTCGAGTTTACTGCGTCGATGTACTCGTTTTTG
716	DUSP4 mouse shRNA1 R	AATTCAAAAACGAGTACATCGACGCAGTAAACTCGAGTTTACTGCGTCGATGTACTCG
717	DUSP4 mouse shRNA2 F	CCGGACGGACATCTGCCTGCTTAAACTCGAGTTTAAGCAGGCAGATGTCCGTTTTTTG
718	DUSP4 mouse shRNA2 R	AATTCAAAAAACGGACATCTGCCTGCTTAAACTCGAGTTTAAGCAGGCAGATGTCCGT
719	DUSP4 mouse shRNA3 F	CCGGGCTGATGAACCGGGATGAGAACTCGAGTTCTCATCCCGGTTCATCAGCTTTTTG
720	DUSP4 mouse shRNA3 R	AATTCAAAAAGCTGATGAACCGGGATGAGAACTCGAGTTCTCATCCCGGTTCATCAGC

Table 20. ***Table of oligonucleotides used for shRNA generation in pLKO backbone vectors***

3.7.5 Ectopic and inducible expression of cDNAs

The lentiviral backbone used for expressing a cDNA, ectopically and only under the induction by doxycycline, was the pCW57, either in its puromycin resistant version (pCW57.1 Puro, Addgene #41393) or in its fluorescent alternative (pCW57-MCS1-P2A-MCS2 turboGFP, Addgene #80924). In both cases, the vector was digested using compatible enzymes (not present in the cDNA) from the multi-cloning site (MCS).

Human cDNAs were PCR amplified with primers containing these restriction sites. In the primers were included V5 and HA tag sequences for optimized protein detection. Two vectors were generated using this protocol, for the expression of human BRAF D594A mutant (pCW57-turboGFP, V5) and the expression of DUSP4 (pCW57.1 Puro, HA). The BRAF D594A cDNA was previously generated in the lab (Nieto et al., 2017) in a pLVX backbone. The cDNA of DUSP4 was extracted from pDONR223 plasmid from the human ORFeome collection v.8.1 (Horizon) (Yang et al., 2011). These cDNA amplicons were then digested with the corresponding enzymes and gel purified before using them as inserts in the pCW57 ligation and transformation in STBL3. Plasmids were digested and Sanger sequenced to ensure cDNA integrity.

This is the list of primers used for the ectopic expression vectors:

ID	Name	Sequence
371	BRAF human 5' NheI Kozak V5	AAGCTAGCAGCCATGGGTAAGCCTATCCCTAACCCTCTCCTCGGTCTCG ATTCTACGGCGGCGCTGAGCGGTGGCGG
372	BRAF human 3' MluI	AAACGCGTTCAGTGGACAGGAAACGCAC
481	DUSP4 cDNA human 5'XhoI/Kozak/HA	ATCTCGAGAGCCATGTACCCATACGATGTTCCAGATTACGCTGTGACGA TGGAGGAGCTGCG
482	DUSP4 cDNA human 3'BamHI	ATGGATCCCTAACAGCTGGGAGAGGTGG

Table 21. ***Table of oligonucleotides used for ectopic expression vectors of BRAF and DUSP4 cDNAs***

3.7.6 CRISPR-mediated knock-in of GFP-tag

A P2A-GFP reporter system was generated to monitor endogenous DUSP6 gene expression in the ATII cells. To this end, a CRISPR knock-in strategy was designed to target the DUSP6 locus and insert a P2A-d2eGFP co-expression cassette. This was the work of a Master student in the lab, Ana García Gimeno.

The d2eGFP is a modified version of the GFP that presents a reduced protein half-life, which is very useful to monitor transcription of the gene of interest even when not in fusion (ClonTech, Takara) (X. Li et al., 1998). The d2eGFP sequence was obtained by PCR from a pTOPO-TA d2eGFP-containing vector gifted by Sergio Ruiz Macías in the NIH. Then, it was cloned inside a pUC19 homology recombination matrix vector that we generated, as a means to flank it with DUSP6 locus homology arms of 1kb. This matrix was then transfected, together with a pX330 vector containing the SpCas9 and gRNAs targeting the DUSP6 region in-between the homology arms. Cells were then sorted by FACS for GFP fluorescence, obtaining single-cell clone populations that were expanded and verified for GFP protein expression by cytometry and PCR. Cells were tested for DUSP6-P2A-d2eGFP zygosity and showed to be only heterozygous for the knock-in, meaning that at least one DUSP6 allele remained completely wild-type.

This is the list of oligos used for generation of the DUSP6-GFP tag vector:

ID	Name	Sequence
485	F-gRNA1-KI-human DUSP6	CACCGTTCCAACCAGAATGTATACC
486	R-gRNA1-KI-human DUSP6	AAACGGTATACATTCTGGTTGGAAC
487	F-gRNA2-KI-human DUSP6	CACCGGGGCCAGACACATTCCAGCA
488	R-gRNA2-KI-human DUSP6	AAACTGCTGGAATGTGTCTGGCCCC
489	DUSP6 human gRNA1/2 KI amplification F	CTGTATTTTACCACCCCTTCCA
490	DUSP6 human gRNA1/2 KI amplification R	ACAGACAGCTGGTGTCATTTTG
491	DUSP6 Human-KI-HomologyArm 5' F	ATGACCATGATTACGCCAAGGAATTCCAGCATTGCTTT
492	DUSP6 Human-KI-HomologyArm 5' R	CGTAGATTGCAGAGAGTCCA
493	DUSP6 Human-KI-HomologyArm 3' F	AAGACCCCACACCCCT
494	DUSP6 Human-KI-HomologyArm 3' R	AAACGACGGCCAGTGAAGGAAAGAAACCAACCCAA
495	hDUSP6-P2A-d2eGFP-F	TGGACTCTCTGCAATCTACGGGCTCCGGAGCAACAAACTTCTCT CTGCTGAAACAAGCCGGAGATGTCGAAGAGAATCCTGGACCGA TGGTGAGCAAGGGC
496	hDUSP6-d2eGFP-R	AGGGGTGTGGGGTCTTCTACACATTGATCCTAGCAG
497	EcoRI-Kozak-d2eGFP F	AAAGAATTCAGCCATGGTGAGCAAGGGC
498	d2eGFP-BamHI R	AAAGGATCCCTACACATTGATCCTAGCAG
506	d2eGFP seq primer R	CCTTGATGCCGTTCTTCTGC

Table 22. ***Table of oligonucleotides used for DUSP6-GFP tag generation****.*

3.8 PROTEIN ANALYSIS

3.8.1 Western blot

In order to prepare cell pellets for protein extraction, cells were trypsinized and washed with PBS. Pellets were directly frozen down at -20ºC prior to extraction. Alternatively, cell plates were washed with PBS, frozen down at -20ºC and scraped. Lysis was performed with homemade RIPA buffer (10mM Tris HCl (pH 7.5), 1mM EDTA, 1% Triton X-100, 0.5% Sodium Deoxycholate, 0.1% SDS, 140nM NaCl) supplemented with a protein phosphatases inhibitor cocktail (Mix II, SERVA Cat# 39055.01) and a protease inhibitor cocktail (Halt™ EDTA-free, Thermo Scientific Cat# 78425). Sonication was performed for 10-15 seconds in order to complete cell lysis if necessary. The lysates were incubated 20 minutes on ice to allow proper shearing of all the cellular components. Clarification was performed by centrifugation at 14,000G for 15 minutes at 4ºC. Clarified supernatants were stored at -20ºC or -80ºC for long-term storage. Protein quantification was determined in 96-well plates either by Bradford colorimetric assay (Bio-Rad Cat# 5000006) or Pierce™ BCA protein assay (Thermo Scientific Cat# 23227).

Protein extracts were prepared in 6X denaturing-SDS Laemmli (10570021 bioPLUS™) and heated at 95ºC for 5 minutes prior to SDS-PAGE in acrylamide gels. Running buffer was 250 mM Tris-HCl, 200 mM glycine, 0.05% SDS. Proteins in separated gels were transferred to nitrocellulose membranes (Amersham™ Protran Cat# GE10600002) following a semi-dry protocol, 1h and 20 minutes at constant amperage in 10X Tris-Glycine buffer (500mM Tris, 400mM Glycine). A Ponceau-Red was performed to ensure proper transfer of the protein load. The membrane was washed in water and blocked for 45 minutes in 5% milk TBS-T (TBS (50 mM Tris-HCl pH 7.5, 150 mM NaCl) with 0.1% Tween). The membrane was washed with TBS-T and probed with primary antibody (details in 3.6.3. Antibodies table) in 5% BSA or milk TBS-T at 4ºC overnight. The next day, the blot was washed three times in TBS-T, then incubated with HRP-conjugated secondary antibody in 5% milk TBS-T, anti-mouse or anti-rabbit (Cell Signaling Cat# 7074 or Cat# 7076) at 1:3000 dilution for 1-2 hours. Finally, the membrane was washed three times in TBS-T and imaged with ECL peroxide substrate (Bio-Rad Clarity Cat# 1705061) in a ChemiDoc™ XRS+ System (Bio-Rad).

3.8.2 Antibodies used for protein detection

Primary antibody	Reference	Provider	Size	Dilution WB	Dilution IHC	Isotype
Actin β	4970S	Cell Signaling	44 kDa	1/1000	-	Rabbit
Akt1	sc-5298	Santacruz	60 kDa	1/500	-	Mouse
Akt1 Phospho Ser473	4060S	Cell Signaling	60kDa	1/1000	-	Rabbit
AKT1/2/3 PhosphoSer473/474/472	sc-514032	Santacruz	60kDa	1/500	-	Mouse
BRAF	sc-5284	Santacruz	90 kDa	1/1000	-	Mouse
Cas9	698302	BioLegend	160 kDa	1/1000	-	Mouse
Cas9 (N-ter)	14697	Cell Signaling	160kDa	1/1000	-	Mouse
Chk1	2348S	Novocastra Leica	56kDa	1/1000	-	Mouse
Cleaved Caspase 3 Asp175	9661S	Cell Signaling	17/19 kDa	1/1000	-	Rabbit
Cleaved Caspase 9 Asp300	7237P	Cell Signaling	37kDa	1/1000	-	Rabbit
Cleaved PARP	5625BC	Cell Signaling	89kDa	1/1000	-	Rabbit
CSK	4980S	Cell Signaling	50kDa	1/1000	-	Rabbit
DUSP4 human	5149S	Cell Signaling	42kDa	1/1000	-	Rabbit
DUSP4 mouse	ab216576	Abcam	42kDa	1/1000	-	Rabbit
DUSP4 mouse (48)	sc-135991	Santacruz	42kDa	1/500	-	Mouse
DUSP4 mouse (F-10)	sc-17821	Santacruz	42kDa	1/1000	-	Mouse
DUSP6	sc-377070	Santacruz	42kDa	1/1000	-	Mouse

ERK1	554100	BD	44 kDa	1/2000	-	Mouse
ERK1/2 Phospho T202/Y204	9101S	Cell Signaling	44/42 kDa	1/1000	-	Rabbit
ERK1/2 Total	4696S	Cell Signaling	44/42 kDa	1/1000	-	Mouse
ERK2	610103	BD	42 kDa	1/1000	-	Mouse
GFP	2555S	Cell Signaling	25kDa	1/1000	-	Rabbit
GFP10	-	-	25 kDa	1/25000	-	Rabbit
GFP11	-	-	25 kDa	1/10000	-	Rabbit
Guanosine, 8-Hydroxy-2'-deoxy	ab48508	Abcam	-	-	1/100	Mouse
HA	2367S	Cell Signaling	-	1/2000	-	Mouse
HA	3724S	Cell Signaling	-	1/2000	1/200	Rabbit
Histone H3 acetyl	06-599	Millipore Sigma	17kDa	1/500	-	Rabbit
Histone H3 phospho	3377T	Cell Signaling	17 kDa	1/500	-	Rabbit
Histone H3 total	4499T	Cell Signaling	17kDa	1/500	-	Rabbit
Histone γH2AX phospho	05-636-I	Millipore Sigma	17kDa	1/1500	1/200	Mouse
Histone γH2AX phospho	9718S	Cell Signaling	17kDa	1/1000	-	Rabbit
Hsp90	4877S	Cell Signaling	90 kDa	1/2000	-	Rabbit
MEK1/2 phospho Ser217/221	9154S	Cell Signaling				
MEK1/2 total	8727S	Cell Signaling				
p21	sc6246	Santacruz	21 kDa	1/500	-	Mouse
p21	2947S	Cell Signaling	21 kDa	1/500		
p90 RSK phospho-Thr359/Ser363	9344S	Cell Signaling	90kDa	1/1000	-	Rabbit
p90 RSK1/2/3 total	9355S	Cell Signaling	90kDa	1/1000	-	Rabbit
Pan-RAS	8832S	Cell Signaling	21 kDa	1/2000	-	Mouse
pChk1		Cell Signaling	56kDa	1/1000	-	Rabbit
p-RSK	sc-377526	Santacruz	90kDa	1/1000	-	Mouse
RSK	sc-393147	Santacruz	90kDa	1/1000	-	Mouse
SPRY2	14954S	Cell Signaling	35kDa	1/2000	-	Rabbit
SRC phospho family Tyr416	6943S	Cell Signaling	60kDa	1/1000	-	Rabbit
SRC total	2109S	Cell Signaling	60kDa	1/1000	-	Rabbit
TTC1	HPA036557	Prestige Sigma	33kDa	1/500	-	Rabbit
Tubulin α	T5168	Sigma	50 kDa	1/10000	-	Mouse
V5	BLE680602	BioLegend	-	1/2000	-	Mouse
V5	80076S	Cell Signaling	-	1/1000	-	Mouse
Secondary antibody	**Reference**	**Provider**	**Size**	**Dilution WB**	**Dilution IHC**	**Isotype**
Anti-rabbit	5127S	Cell Signaling	-	1/5000	-	Mouse
Anti-mouse	7074S	Cell Signaling	-	1/5000	-	Goat

Table 23. ***Table of antibodies used for protein detection techniques.***

4 HISTOLOGY AND IMMUNE STAINING TECHNIQUES

4.1 HISTOLOGY AND IMMUNOHISTOCHEMISTRY

To perform the histological analyses of mouse tissues, organs were extracted during the necropsy and incubated in formalin (4% formaldehyde stabilized with methanol) for 24h at room temperature. Lung lobes were disconnected from each other and inserted separately in the cassettes. Fixed tissues were embedded in paraffin and cut into 5 µm sections. Counterstaining was performed with hematoxylin/eosin (HE) or Nuclear Fast Red following standard protocols. Immunohistochemistry was performed following an automated protocol of the BenchMark ULTRA IHC/ISH System (Roche) in the Pathology unit. Microtome-dissected samples were deparaffinized and rehydrated on slides using standard protocols. Antigen retrieval was performed by immersing the slides in the antigen retrieval buffer, setting the temperature and time according to manufacturer recommendations. The slides were washed and blocked for non-specific binding by incubating the slides with a blocking solution for 30 minutes up to 1 hour. The primary antibody was diluted in an antibody-specific manner and applied to the tissue sections, ensuring complete coverage. Once the staining program was completed, the slides were removed and washed to remove any unbound antibodies or detection reagents. The secondary antibody conjugated to HRP enzyme was applied onto the tissue sections and incubated for the recommended time. Slides were finally washed and incubated with the DAB substrate to visualize the target antigen. Monitor the staining intensity and adjust the incubation time if needed to achieve optimal results. The reaction was stopped by rinsing the slides with distilled water. A compatible counterstaining, such as hematoxylin, was applied to the slides. The slides were dehydrated through a series of alcohol washes and cleared in xylene. Finally, the slides were mounted with coverslips, ensuring they were completely dry.

Slides were scanned using the NanoZoomer (Hamamatsu Photonics) located in the Bordeaux Imaging Center and the Olympus dotSlide system located in the Salamanca Comparative Molecular Pathology Unit at 20X resolution.

These techniques were developed in collaboration with the Compared Molecular Pathology unit at the CIC in Salamanca and the Pathology department of Bergonié Hospital in Bordeaux.

4.2 WHOLE MOUNT X-GAL STAINING

In vivo β-galactosidase activity was detected by whole mount X-gal staining. The organs and tissue were dissected and introduced into histology cassettes. The samples were fixed under a fixative solution (0.2% glutaraldehyde, 1.5% formalin, 2mM $MgCl_2$, 5mM EGTA, 0.1M Sodium phosphate buffer (pH 7.25)) for 60 minutes. The cassettes were then washed twice with PBS buffer and twice for 20 minutes in washing solution (0.2% Nonidet P-40 IGEPAL, 0.01% Sodium Deoxycholate, 2mM $MgCl_2$, 0.1M Sodium Phosphate buffer (pH 7.25)). Washed samples were stained with X-Gal staining solution (5mM Potassium hexacyanoferrate (II) trihydrate, $K_4Fe(CN)_6 \cdot 3H2O$, 5mM Potassium hexacyanoferrate (III), $K_3Fe(CN)_6$, 1mg/mL X-Gal/DMSO) at 37ºC overnight or even over weekend (as optimized for *Rosa26* locus promoter). Once the staining step was completed, cassettes were washed with PBS three times under agitation. The tissues were then fixed in formalin (formaldehyde 4% with methanol) at room temperature overnight.

Fixed tissues were then washed and immediately dehydrated through a series of ethanol and propanol washes, with no xylene clearing as it removes X-Gal staining from the cells. Finally, cassettes were inserted in a 1:1 propanol/paraffin bath at 60ºC overnight. The next day, paraffin embedded cassettes were included in serial baths of paraffin and finally inserted into molds. Paraffin samples were cut on a microtome generating 4 μm sections included in AAS coated slides and counter stained with Nuclear Fast Red.

5 FLUORESCENCE ANALYSIS

5.1 CYTOMETRY AND FACS

Cell-by-cell fluorescent analysis of cellular cultures and tissues was performed by flow-cytometry.

The following fluorescent proteins were used for live cell detection and/or sorting: eGFP (Ex488/Em507), ZsGreen (Ex493/Em505), turboGFP (Ex482/Em502), eYFP (Ex514/Em524), mCherry (Ex587/Em610)

The dyes used for cytometry analysis were: Annexin V – PE (Ex566/Em574, Immunostep, Cat# ANXVPE), 7-AAD (Ex549/Em648, from Apoptosis Detection Kit I, BD, Cat# 559763), propidium iodide (PI) at 50 µg/mL working solution (Ex535/Em615, Sigma, Cat# 81845). Amounts and concentrations for these dyes were applied following manufacturer recommendations.

Different systems were used for all the cytometry protocols, located in both TBM Core Facilities in the University of Bordeaux and the Microscopy and Cytometry Unit of the CIC at Salamanca. The systems used were BD Accuri™ C6+ (4 colors, Salamanca), BD FACSAria™ II (16 colors, Lecture mode, Salamanca) BD Canto™ II (8 colors, Bordeaux), BD LSRFortessa™ (16 colors, Bordeaux). Fluorescence activated cell sorting (FACS) was performed in a cell sorter under a biosafety cabinet. The sorters used during this thesis were BD FACSAria™ III (in Salamanca and Bordeaux), both able to separate more than 16 colors.

5.2 EPIFLUORESCENCE MICROSCOPY

Cells were imaged on an epifluorescence microscope Leica DM4 with Thunder Imaging System located in CIC-IBMCC facilities. Images were acquired with 40X and 60X objectives. The data was processed with Leica LAS X software and the analysis was performed in ImageJ Fiji software.

6 OMICS AND BIOINFORMATICS

6.1 ANALYSIS OF PATIENT DATA

All data was retrieved from The Cancer Genome Atlas repositories thanks to XenaBrowser (Goldman et al., 2020). The computed signature was calculated as previously described (Brant et al., 2017; Dry et al., 2010; Loboda et al., 2010), by averaging log2 normalized RSEM expression data of the selected genes (B. Li & Dewey, 2011), as the expression range for all of the genes was similar. The expression values were scaled by gene between 0 and 1, minimum and maximum levels across patients, respectively. The score represents the median value of the signature genes.

Survival was evaluated with coxph/survfit (Therneau, 2023) and survminer (Scrucca et al., 2007). Copy number alterations were computationally calculated with GISTIC2 (Mermel et al., 2011), computing 19401 gene variations at a time. Power analysis was computed with the R WebPower tool (Zhang & Yuan, 2018). Purity levels were re-estimated from the TCGA with ABSOLUTE (Carter et al., 2012) and from microarray with ESTIMATE (Yoshihara et al., 2013), tools that use somatic DNA calculations to select patients harboring scores above population median purity, in this case set at 0.44 as seen in the TCGA data.

Microarray dataset GSE72094 (Schabath et al., 2016) was RMA normalized (Carvalho & Irizarry, 2010; Irizarry et al., 2003) prior to the signature evaluation and survival analysis. Gene set enrichment analysis (ssGSEA) was performed with GSVA (Hänzelmann et al., 2013), and MsigDB (Liberzon et al., 2011) was used to evaluate multiple pathways.

The immune populations were estimated using a deconvolution method called quanTIseq (Finotello et al., 2019), where bulk RNAseq data was used to quantify the absolute fractions of 10 different types of immune cells. In parallel, we computed scores for a set of 14 immune signatures as described in (Danaher et al., 2017, 2018) to calculate individual immune cells fraction score. By performing an initial correlation analysis of these genes, we decided to remove those genes that did

not correlate with the rest in each immune set. We thus refined the signature by eliminating the genes CTSW, HSD11B1, CSF3R, S100A12, CEACAM3 and IL21R.

6.2 DESIGN OF SGRNAS

The crRNA part of the gRNA, specifically targeting the gene of interest, was designed using online algorithms that have been optimized for predicting gRNA efficiency through these applications. The rationale for the design had two priorities, the first one being avoiding off-target effects. We specifically retained gRNAs that, at the maximum, presented 1 off-target gene that scored 1 double mismatch (MM2), and no MM1 or MM0 off-targets. Thus, the off-target list of genes was also revised to confirm that none belonged to the same superfamily than the gene of interest. Second, the efficiency of the gRNA was evaluated, selecting guides that presented higher efficiency rates of >60-70%. The algorithms used for the selection were CHOPCHOP (MIT-Bergen) (Labun et al., 2019), CRISPOR-Tefor (UCSC) (Concordet & Haeussler, 2018) and CRISPick (Broad Institute) (Doench et al., 2016; Sanson et al., 2018).

6.3 NEXT GENERATION SEQUENCING (NGS)

6.3.1 RNAseq

Total RNA was extracted from cellular pellets with a commercial kit as previously described. RNA was stocked at -80ºC until arriving at the genomics facility at the Centro de Investigaciones Oncológicas (CNIO, Madrid), where it was processed. A labchip analysis was performed before processing the samples obtaining an RNA integrity score (RIN) between 9 and 10. A total of 250ng of RNA were processed into cDNA librares with the Quant-Seq 3' mRNA-Seq Kit for Illumina (Lexogen, Cat#015). Adapter sequences for Illumina sequencing were integrated at this step. A final PCR step was performed to complete the library. Single read (86bp) sequencing was performed in an Illumina NextSeq 550 with v2.5 reagents at the CNIO Genomics Unit. Delivered sequences in fastq format passed the Illumina quality filtering (PF).

For analyzing RNA-seq data obtained as described previously, we followed the next pipeline in a bioconductoR environment (Huber et al., 2015). Quality was assessed by FastQC analysis, checking sample integrity, and overall run performance. To remove adapter sequences and polyA tails, reads were trimmed with bbduk (BBMap package). Alignment was performed with STAR v2.5 (Dobin et al., 2013) and hisat2 (Kim et al., 2019). Read counting was performed with HTSeq (Putri et al., 2022) and differential gene expression was evaluated with DESeq2 (Love et al., 2014) and edgeR (Robinson et al., 2010). Gene ontology analysis and gene set enrichment analysis (GSEA) were performed with the clusterProfiler R package (Wu et al., 2021). Data visualization was generated with pheatmap and ggplot in R.

6.3.2 CRISPR Screening Deep Sequencing

In order to prepare the libraries containing Illumina adapters next to the gRNA sequences, we performed a nested PCR protocol, to first amplify the DNA and then insert the adapters and barcodes. Three different barcodes were used for the conditions of the screening (Pre, K and KB with Idx01, Idx03, Idx08 respectively). More details of the library preparation step by nested PCR are in the Nested PCR section of Materials & Methods. Nested PCR amplicons were gel purified with Monarch® DNA Gel Extraction Kit (NEB, Cat# T1020) and eluted in Ultrapure water. Product integrity was evaluated in a labchip Tape-station D1000 High Sensitivity (Agilent) and showed no signs of degradation and 90-92% purity. Single read (86pb) sequencing was performed in an Illumina NextSeq 500 with v2.5 reagent kits at the CNIO Genomics Unit. Delivered sequences in fastq format passed the Illumina quality filtering (PF). The final representation of the technical replicates was around 40X, making a total representation of the Brunello library of 200X per condition.

6.4 BIOINFORMATIC TOOLS FOR CRISPR SCREENING ANALYSIS

A series of bioinformatics tools were used for analyzing the raw fastq data obtained from the Illumina NGS CRISPR screening data. A first analysis was performed with CRISPR-Cloud2 (Jeong et al., 2017), a web-based interface that allows comparing conditions according to individual

sgRNA and/or gene counts. CRISPRAnalyzeR (DFKZ) (Winter et al., 2017) was also initially used to this end. Then, the Python-based PinAPL.py tool (Spahn et al., 2017) was used to run complex algorithms on the data, particularly gene ranking by specific metrics, such as RRA (Kolde et al., 2012) and STARS (Doench et al., 2016). Only STARS ranking metrics were taken into consideration for the PinAPL part of the manuscript, because the FDR system was more rewarding with genes that had more active sgRNAs, avoiding single sgRNA hits. Finally, we took advantage of MAGECK (W. Li et al., 2014) to perform an αRRA-based analysis. The STARS and MAGECK analyses were retained for selecting a candidate list, as positive control genes showed clear enrichment or depletion in the different conditions. Selection thresholds were retained according to the positioning of these controls and a significance value of an alpha equal to 0.05. Only genes that showed 3 or 4 significant sgRNAs enriched or depleted, when compared to the control conditions, were retained in the candidate list. Data visualization and enrichment analysis was elaborated with STRING database (Szklarczyk et al., 2022).

6.5 FLUORESCENCE MICROSCOPY ANALYSIS

Images were processed on ImageJ FIJI software to evaluate number of micronuclei per cell. A macro algorithm was designed to perform cell selection and counting. From this selection, the number of nuclei was established per cell and used to compute the CBMN score as described previously.

6.6 HISTOLOGY ANALYSIS

Immunohistochemistry slides containing tissular samples were scanned and digitalized as previously described. The digital images were analyzed in QuPath (Bankhead et al., 2017) 0.4.3 open-source software. DAB stain vector was recalculated for a group of slides prior to quantification. Positive cells were detected and counted with the automated *Positive cell detection* plugin. Cells were first detected on the Hematoxylin coloration. Then the intensity threshold was established on the DAB coloration, selecting Nuclear or Cytoplasmic scoring compartment depending on the staining. Necrotic parts of the tumor were not considered for the analysis.

7 STATISTICS

A minimum of three biological replicates was obtained for each experiment, unless indicated otherwise, with the proper technical replicates deemed necessary for each protocol. The results are indicated as mean or median ± standard deviation (SD) or standard error of the mean (SEM), as indicated in the figure legend. SD was generally used whereas SEM was preferentially used for populations carrying a large number of individuals. Different statistical tests were used to compare population means and/or distribution. If parametrical tests were employed, population distributions were previously tested for normal gaussian dispersion by a univariate Shapiro-Wilk. For comparing two groups, a Student's t-test (with Welch's correction for heteroscedastic samples) or the non-parametric alternative Mann-Whitney-Wilcoxon's test were used. For more than two groups' comparisons, analysis of the variance (ANOVA) was used with Dunnett's correction of p-value, unless the use of another correction is stated. The non-parametric alternative, Kruskal-Wallis H test was also used to compare ranks of the samples. Two-way ANOVA was used to test the influence and interaction of two different categorical variables on the numerical values of the samples, and Friedman's ranks test was used as the non-parametric alternative. Statistical significance was generally determined by an alpha of 0.05 to reject the null hypothesis. Thus, a p-value > 0.05 was considered not significant (n.s.). For significant one-to-one comparisons, p-value was noted with asterisks: * p-value <0.05, ** p-value <0.01, *** p-value <0.001, **** p-value <0.0001.

IC50s were calculated by computing a non-linear regression model fitting, by least squares method, the points obtained with increasing doses of the inhibitor. The data is normalized so the top plateau is 100%, while the bottom baseline is defined by the dataset shared values and often, but not always necessarily as cytostatic effect could exist, results in a value of 0. The slope of the IC50 curve is also shared by the dataset values. Confidence intervals of 95% were computed as a range with a symmetrical asymptotic method. Non-parametric Mann-Whitney-Wilcoxon sum rank test was used to compare the values of each condition independently with the control. The data and statistics management software used was GraphPad Prism 9 and further statistical analyses were performed in R. Additional pathway graphics and experiment layouts were elaborated in BioRender.

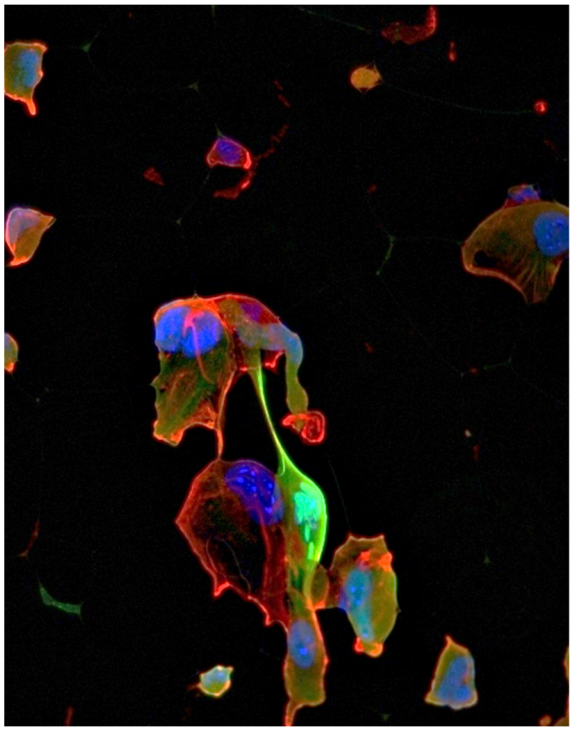

Picture IVV. Mouse lung tumoral cells harboring cytoplasmic GFP fluorescence, stained with Hoechst 33258 and Phalloidin conjugated to Alexa 647

Results

There is no inevitability so long as there is a willingness to contemplate what is happening.

Marshall McLuhan

1 RECAPITULATING MAPK ACTIVITY THROUGH A TRANSCRIPTIONAL SIGNATURE

1.1 MAPK TRANSCRIPTIONAL SIGNATURE DETERMINES PATIENT SURVIVAL IN TCGA COHORT

First, we sought to address the question on whether MAPK activity dictates KRAS mutant tumor outcome. These bioinformatic results have been generated in collaboration with Elodie Darbo (U1312 BRIC Bordeaux). We selected data from 162 patients from the KRAS mutant LUAD cohort of the TCGA, including clinical and transcriptomic data for each of the samples. In these patients, we assessed MAPK activity by computing a score that considered the expression of 6 genes whose expression was previously described to be MAPK specific in NSCLC (Brant et al., 2017). The expression of these six genes contributes equally to the computed score (see Methods for details on the normalization protocol): DUSP4, DUSP6, ETV4, ETV5, PHLDA1 and SPRY2 (**Figure 24**).

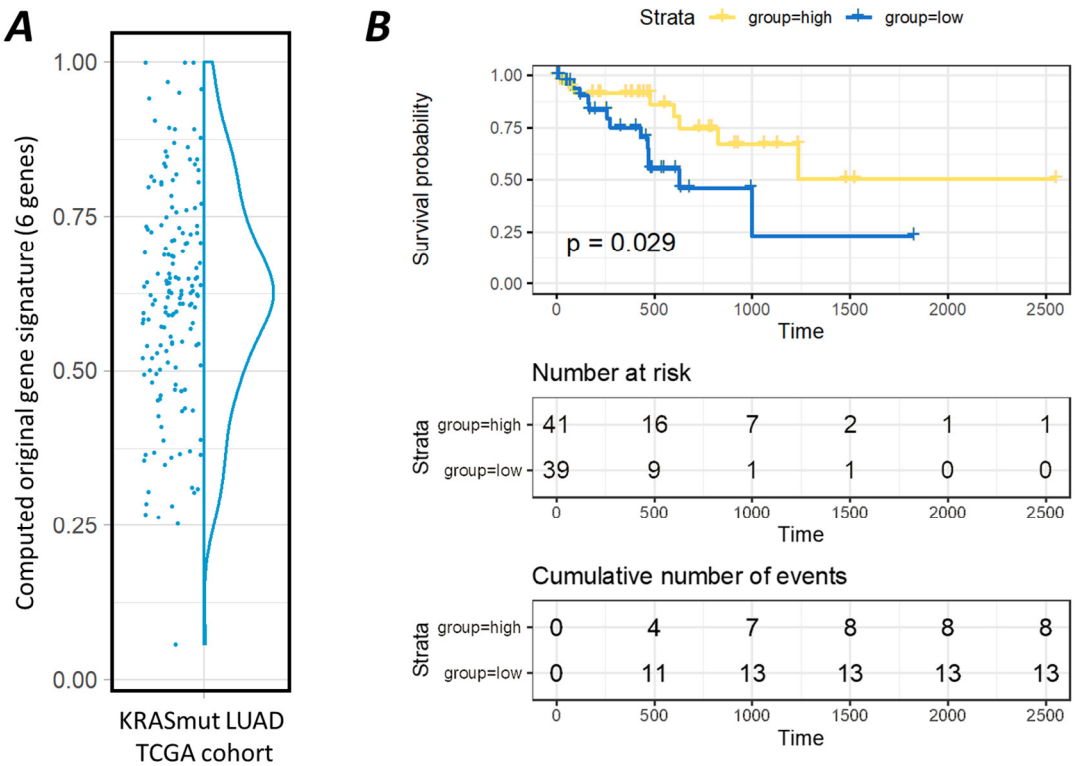

*Figure 24. **MAPK signature determines patient survival**. Analysis of TCGA KRAS mutant LUAD patient data. (A) Computed gene signature score of gene expression data of DUSP4, DUSP6, ETV4, ETV5, PHLDA1 and SPRY2. The top and bottom quartiles (41 patients) were used to form the high and low MAPK groups. (B) Kaplan Meier survival probability curve of the two groups (days since diagnosis). Survival differences are noted at the indicated p-value (Cox proportional hazard ratio).*

We classified the patients into two groups corresponding to the top and bottom quartiles (41 patients) of the signature score (**Figure 24A**), from now on depicted as the high and low MAPK groups. In order to assess how MAPK activity, recapitulated through this signature score, could impact patient outcome, we performed a survival analysis in the cohort, computing Kaplan-Meier estimators for these two patient categories. We observed clear survival differences between the two groups, surprisingly, noting a reduced survival probability in the low MAPK group (Hazard Ratio, HR=0.5, logrank p=0,029) (**Figure 24B**).

With this result in our hands, we wondered how tumors that harbor moderate MAPK levels present the most aggressiveness, while high MAPK tumors are linked to slower progression rates. Indeed, we hypothesized that this initial analysis presented clinical proof that high MAPK levels are detrimental in a KRAS driven LUAD context, and the tumor must limit its signaling levels in order to ensure its maximum fitness. We also evaluated the potential of the signature to compute survival differences among patients harboring other driver mutations(**Figure 25**).

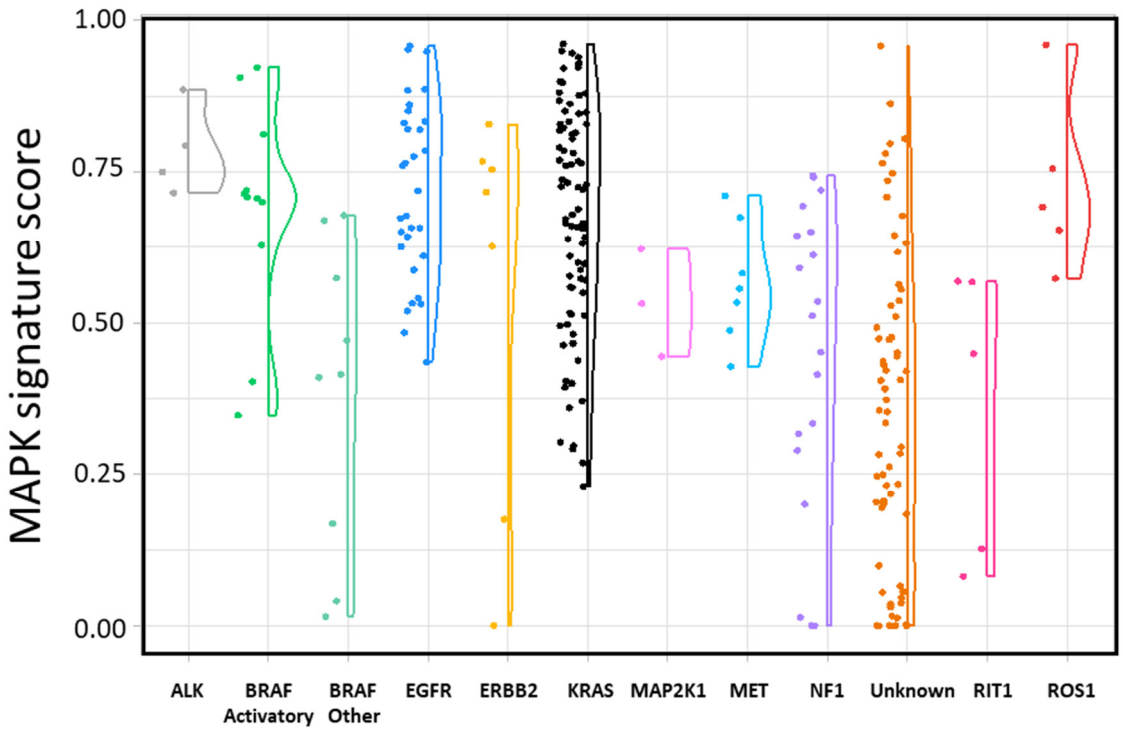

Figure 25. ***MAPK signature score across multiple LUAD TCGA cohorts.*** *We computed the MAPK signature score for tumors classified according to their driver mutation, revealing that scores are heterogeneous across all TCGA data.*

We analyzed TCGA cohorts of tumors driven by BRAF, EGFR, ERBB2, MET, NF1, RIT1, ROS1 and a last cohort with unknown driver mutations. None of these cohorts, other than KRAS, presented any statistical difference when studying survival differences between quartile groups clustered by the signature strategy presented here, suggesting that these differences observed are intrinsic to KRAS mutant tumors alone.

With the intention of confirming that these results were not an artifact from the patient data that we selected, we decided to evaluate tumor purity across these samples. Tumor purity is evaluated individually by a pathologist from the TCGA consortium to ensure that the samples can be included in the database. Although the original tumor purity threshold of the TCGA consortium was set at 80% of tumoral nuclei, in 2016 it was reduced down to 60%. With these new criteria, a non-negligible portion of the genomic data may present a significant stromal component (Aran et al., 2015), potentially altering biological interpretation of results. For this reason, we decided to implement a tumor purity filter on our cohort. We accepted only samples over the median purity of the cohort (**Figure 26A**), leaving a total of 79 samples (**Figure 26B**).

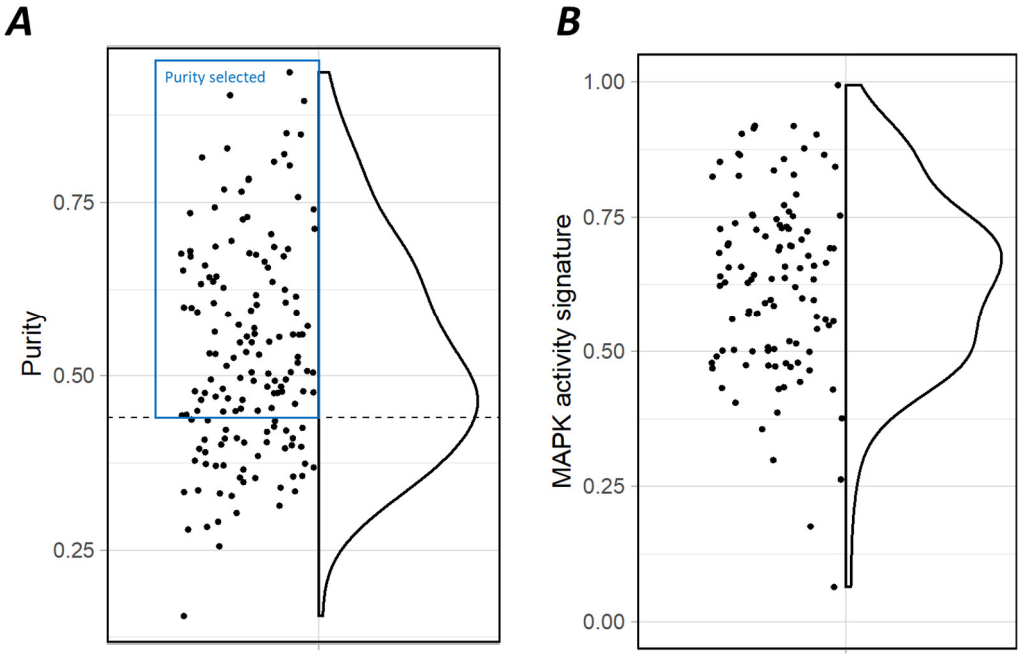

Figure 26. ***Patient distribution upon purity filtering****. (A) Computed ABSOLUTE purity distribution in TCGA LUAD cohort. Patients above purity threshold (0.44) were retained for the analysis. (B) Computed signature score for "pure" patients.*

In this new refined cohort, we sought to re-define the signature to evaluate MAPK to the best of our ability. First, we re-evaluated how patients were classified, as our aim is to compare the most divergent patients in MAPK levels. Although the initial analysis was performed in quartile-based groups, we calculated the ideal number of patients per group by applying a statistical power strategy. The best fit was set at 32 patients, that would be assigned symmetrically to each category in order to obtain the best statistical performance (**Figure 27**).

In these two new groups of 32 patients, we performed pairwise correlation analysis on the six genes of the signature, comparing side-by-side their expression (**Figure 28**). Although the majority of the genes showed positive Spearman correlation levels, we remarked that two of them, DUSP4 and PHLDA1, were not correlating properly with the rest of the signature. Most precisely, while PHLDA1 was only correlating with DUSP6 expression, DUSP4 expression anti-correlated systematically with the rest of the genes of the signature.

To corroborate these results, we computed the survival univariate hazard ratios (HR) for every possible combination of genes in the signature (**Figure 29**). The most statistically significant results were obtained with the combination of the remaining 4 genes, DUSP6, ETV4, ETV5 and SPRY2 (HR=0.2, logrank p=0.0012), confirming that neither DUSP4 nor PHLDA1 were contributing to the statistical power of the signature. Additionally, these results show that DUSP4 and PHLDA1 alone do not allow to stratify patients in a statistically relevant manner, contrarily to the rest of the signature. For these reasons, we discarded these two genes for further signature analyses.

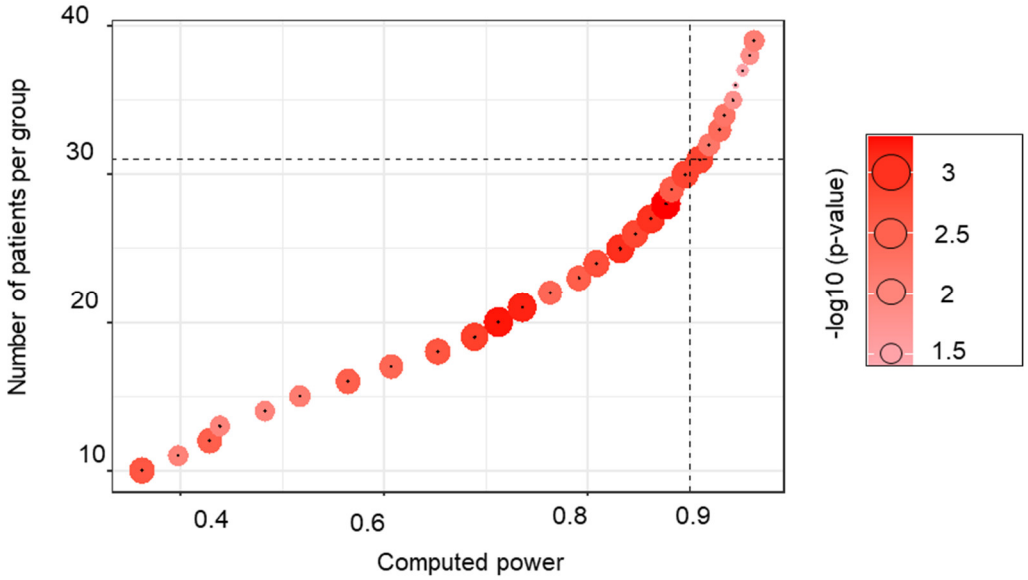

Figure 27. ***Power prediction strategy for determining number of patients per group****. The computed power assigns the minimal number of patients to formulate a significant predictive separation by comparing increasing group sizes and determining the consequent p-value.*

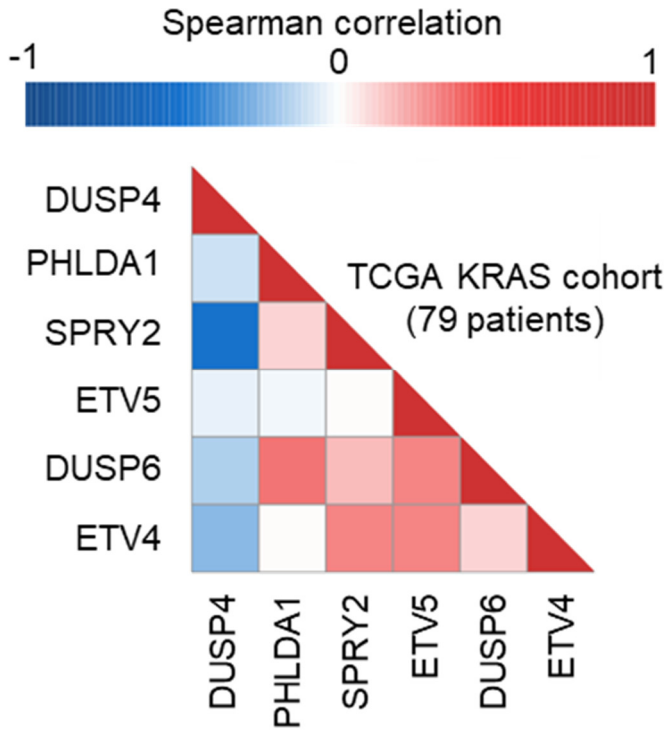

Figure 28. ***Correlation analysis of the 6 genes of the signature reveals opposite behavior of DUSP4 and PHLDA1****. Side by side comparison and computed Spearman correlation shows anti-correlation (negative, blue) and correlation (positive, red) between the median expression of each gene in the "pure" KRAS mutant LUAD cohort.*

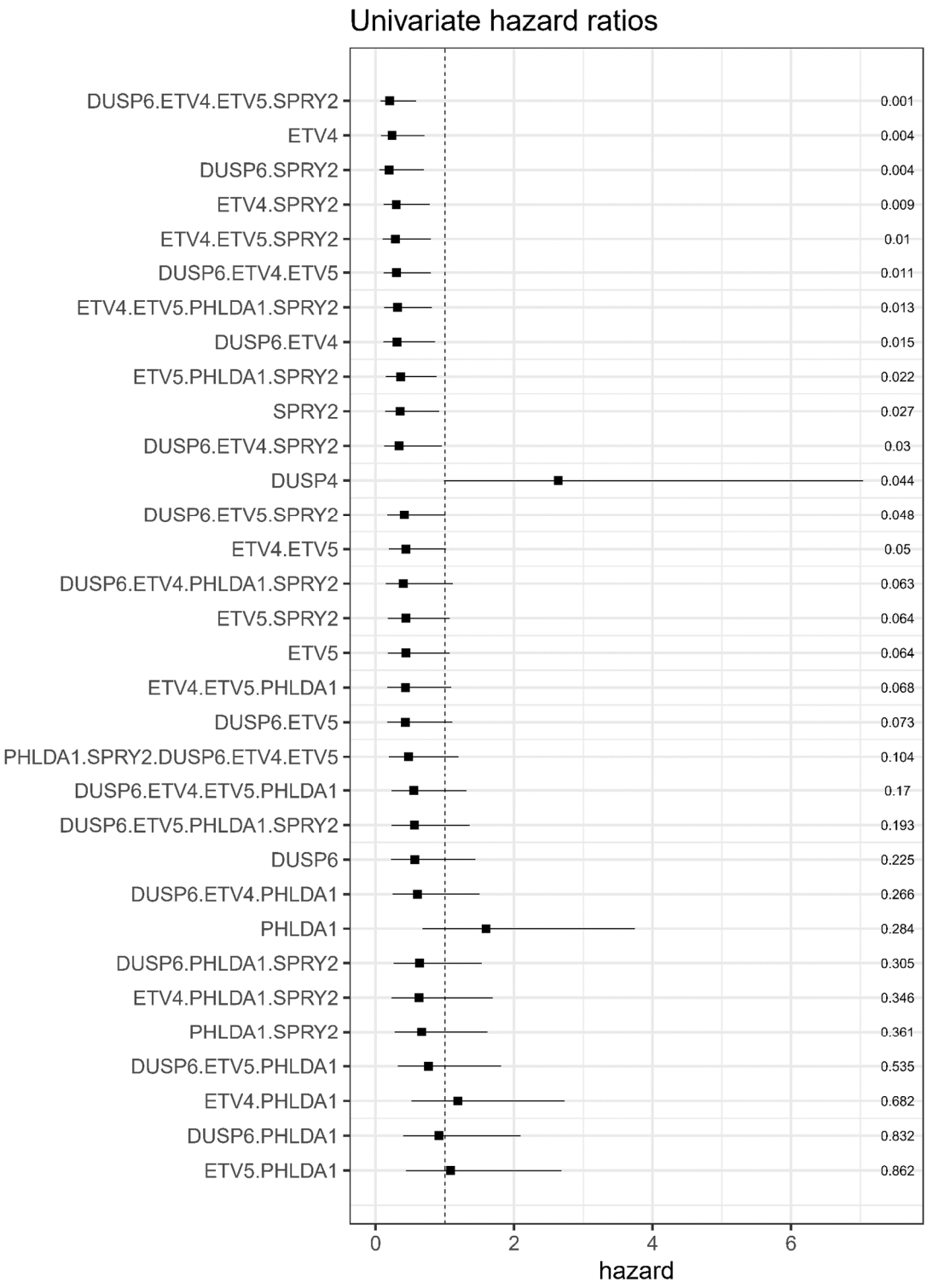

Figure 29. ***DUSP4 and PHLDA1 do not provide any predictive power to the signature****. Cox univariate hazard ratios comparison between multiple combinations of genes in the MAPK signature. Computed p-values (log-rank) are noted in the right. A value above the threshold of 1 indicates hazardous values suggesting no predictive value of that gene or combination of genes.*

At this point, we re-computed Kaplan-Meier estimators for survival analysis (**Figure 30**). The analysis of the newly "pure" cohort with the 4-gene signature confirmed the difference in survival, with low MAPK group presenting the most aggressive progression. Statistical significance was greater with this strategy refinement (HR=0.2, logrank p=0.0012).

To verify that our results were not specific to the intrinsic properties of the TCGA cohort, we confronted the predictive power of the signature to an additional independent cohort of patients. We performed a search for publicly available datasets containing KRAS mutant LUAD patients and only identified GSE72094, a transcriptomic microarray dataset including 154 KRAS mutant tumors (Schabath et al., 2016) that we used as a validation cohort. We normalized the microarray data and applied the same purity filters previously commented and proceeded to compute the 4-gene MAPK signature in the remaining patients (see Methods for additional details on the microarray analysis protocol). Through the same power analysis strategy previously mentioned, we classified patients from this validation cohort into high and low MAPK groups consisting of 15 individuals each (**Figure 31**). The signature score was significantly associated with better outcome (HR=0.11, logrank p=0.013), confirming the same survival results obtained with the TCGA cohort. Taking together these two cohorts, these results could imply that MAPK output may be a general predictive factor in KRAS mutant LUAD patients.

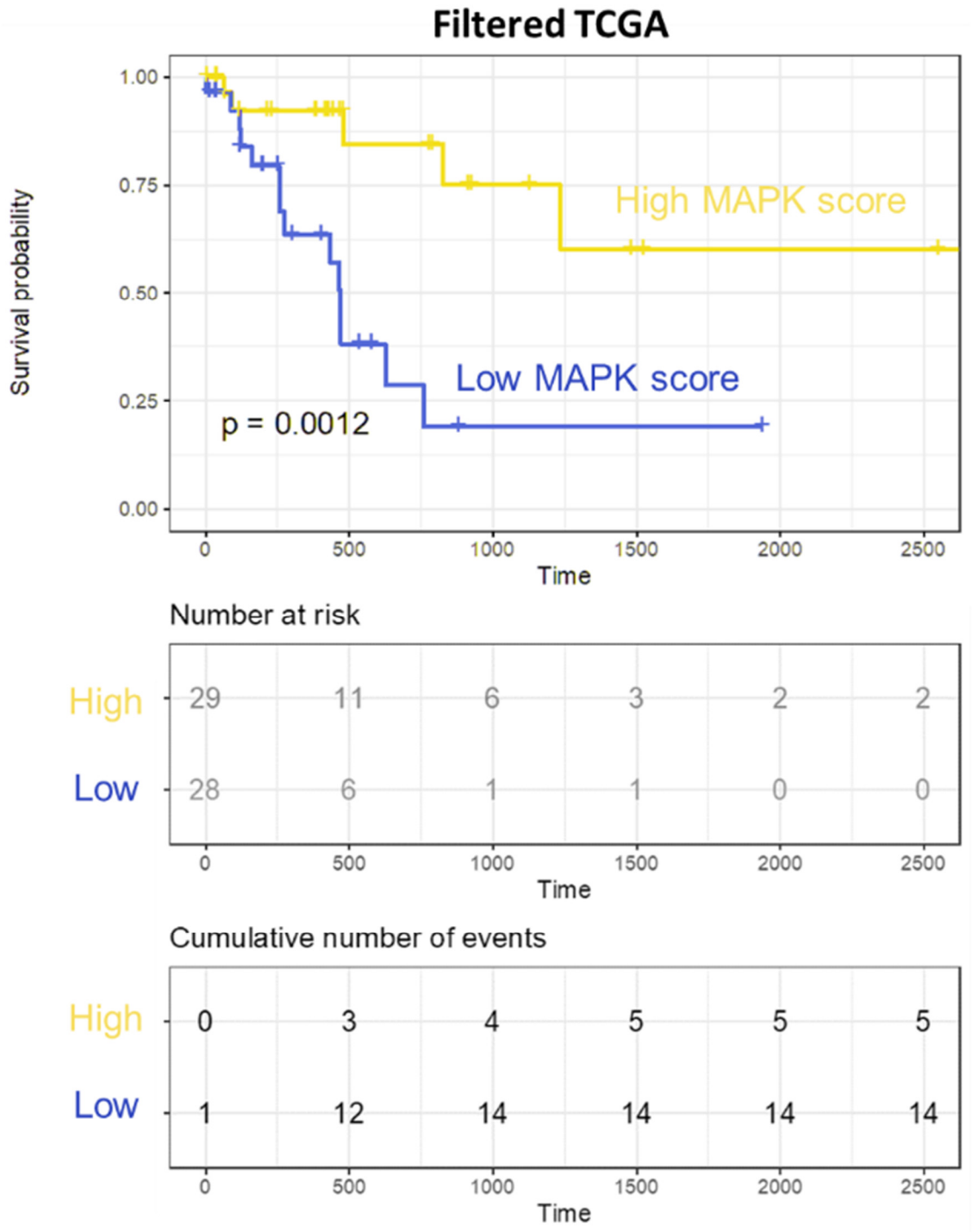

Figure 30. ***Refined MAPK signature determines patient survival in TCGA data****. Survival analysis of "pure" TCGA KRAS mutant LUAD patient data. Computed gene signature score of gene expression data of DUSP6, ETV4, ETV5 and SPRY2. The power-optimized groups (31 patients) were used to form the high and low MAPK groups.*

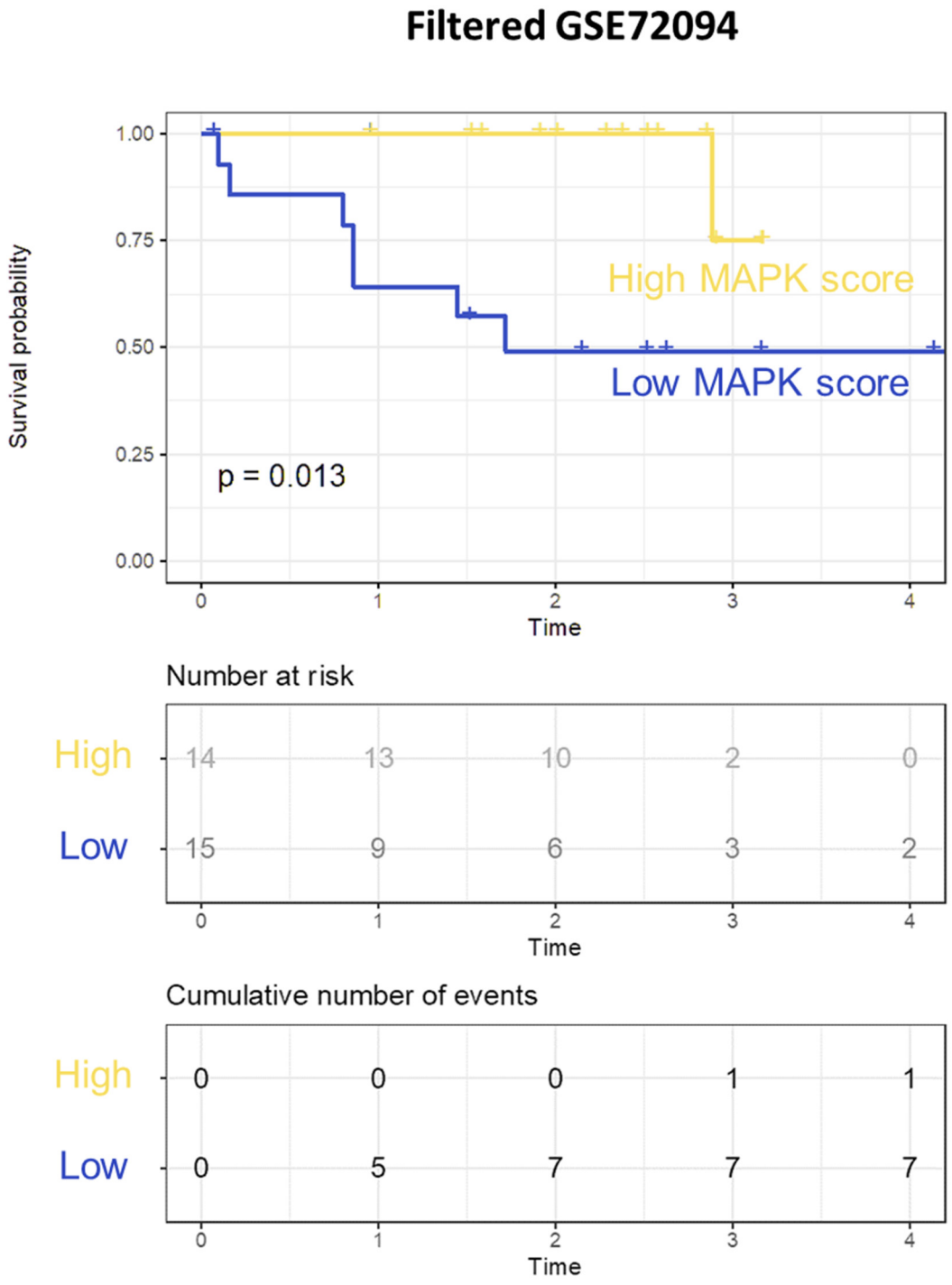

Figure 31. ***MAPK signature predicts survival in microarray validation cohort****. Survival analysis of "pure" microarray GSE72094 data, corresponding to a KRAS mutant LUAD cohort. Computed gene signature score of gene expression data of DUSP6, ETV4, ETV5 and SPRY2. The power-optimized groups (15 patients) were used to form the high and low MAPK groups.*

1.2 SIGNATURE CORRELATES WITH MAPK ACTIVITY

The resulting signature recapitulates the transcription levels of genes directly controlled by MAPK levels in the KRAS mutant cohort. We sought to confirm that the resulting classification correlated with MAPK activation state by applying single sample gene set enrichment analysis (ssGSEA) to the TCGA cohort. We evaluated scores for ontologies related to MAPK interactors and obtained a significantly higher activation of MAPK pathways GO:0070371 (ERK1/2 cascade) and GO:0000165 (MAPK cascade) (**Figure 32)**.

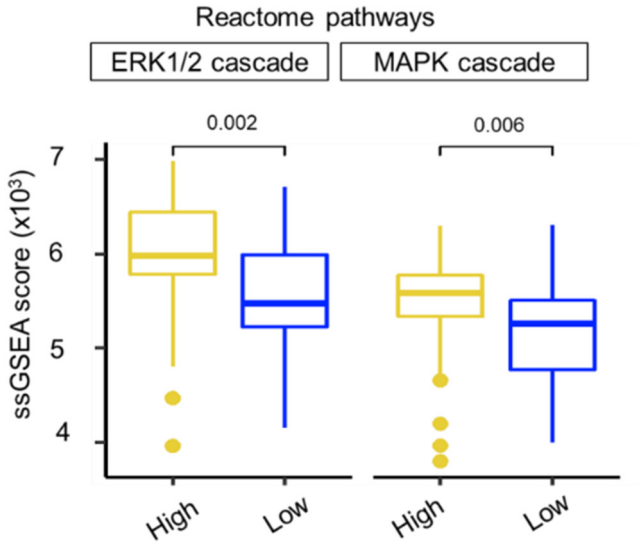

Figure 32. ***Signature recapitulates MAPK activity ontology terms****. MAPK-related single sample gene set enrichment analysis (ssGSEA) computed individually for each of the patients of the TCGA "pure" cohort. Two terms came out significantly different among patients of the two MAPK categories (Wilcox).*

Additionally, we analyzed the differentially expressed genes that could be a cause or consequence of the different levels of MAPK activity. We identified 129 genes significantly associated with low MAPK activity and 147 genes that correlate with high MAPK signature score **(Figure 33A)**. Among the genes that correlate with the high group we detected genes directly related to MAPK negative feedback, such as SPREDs (**Figure 33B**), suggesting that excessive MAPK levels activate compensatory mechanisms in an attempt to counteract hypersignaling to moderate levels.

A

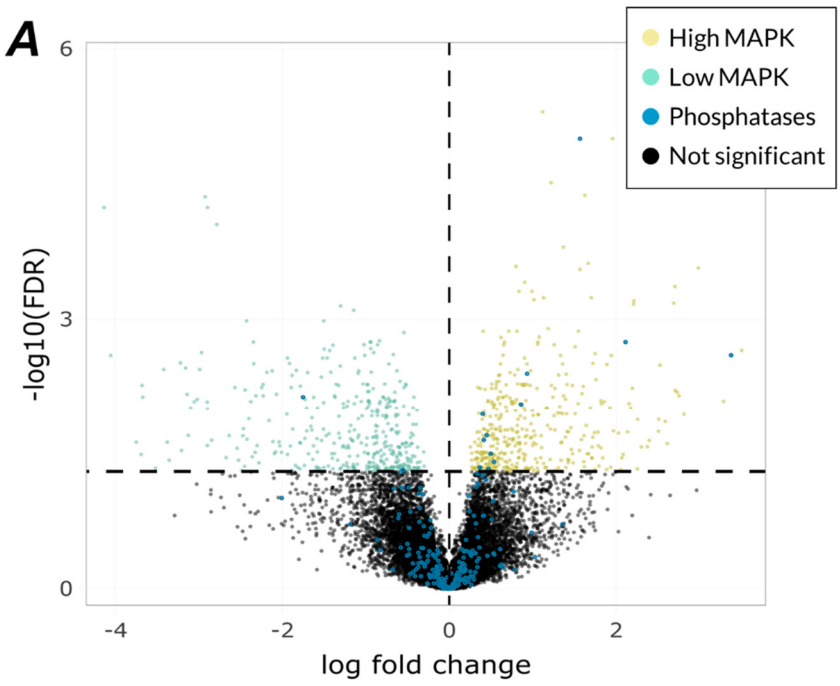

B

ID	logFC	adj.P.Val	differential
ETV5	1.83	1.52E-12	High
SPRY2	1.12	5.02E-06	High
DUSP6	1.57	9.94E-06	High
ETNK2	1.96	9.94E-06	High
SNX25	1.22	3.06E-05	High
ETV4	1.62	4.23E-05	High
RHOV	-2.93	4.38E-05	Low
KYNU	-2.9	5.77E-05	Low
HHIPL2	-4.14	5.77E-05	Low
LYPD3	-2.79	8.88E-05	Low
FLJ90757	1.37	1.58E-04	High
SESN3	1.66	2.40E-04	High
DHX40	0.8	2.59E-04	High
HOXD1	2.98	2.70E-04	High
ST3GAL5	1.57	2.80E-04	High
HDAC5	0.9	3.88E-04	High
HPCAL4	2.7	4.33E-04	High
EML4	0.83	4.91E-04	High
SPRED2	0.99	4.91E-04	High
USP27X	1.7	5.76E-04	High
STK39	1.13	5.76E-04	High
EPB41L5	1.01	6.08E-04	High
DPP4	2.21	6.26E-04	High
SPTB	2.69	6.63E-04	High
FIGNL2	2.21	6.79E-04	High
DUSP4	-1.75	7.33E-03	Low

Figure 33. ***Differentially expressed genes (DEGs) obtained from the comparison of High vs Low MAPK groups****. (A) Volcano plot depicting the DEGs. Highlighted genes are specific for each group (B) Table of top DEGs in the analysis. DUSP4 score is highlighted.*

In order to confirm that these differentially expressed genes directly affect MAPK pathway, we performed a pathway enrichment analysis by KEGG, focusing on the MAPK signaling pathway (**Figure 34**).

Indeed, we noticed that an important number of genes directly implicated in the pathway are modified and could probably explain the quantitative differences observed in the MAPK output. The expression of several main RAS/MAPK effectors, genes such as EGFR, SOS, BRAF, CRAF and RSK, was found to be enriched in the high MAPK group. These results would indeed imply that our refined signature correlates with high levels of MAPK activity in these tumors.

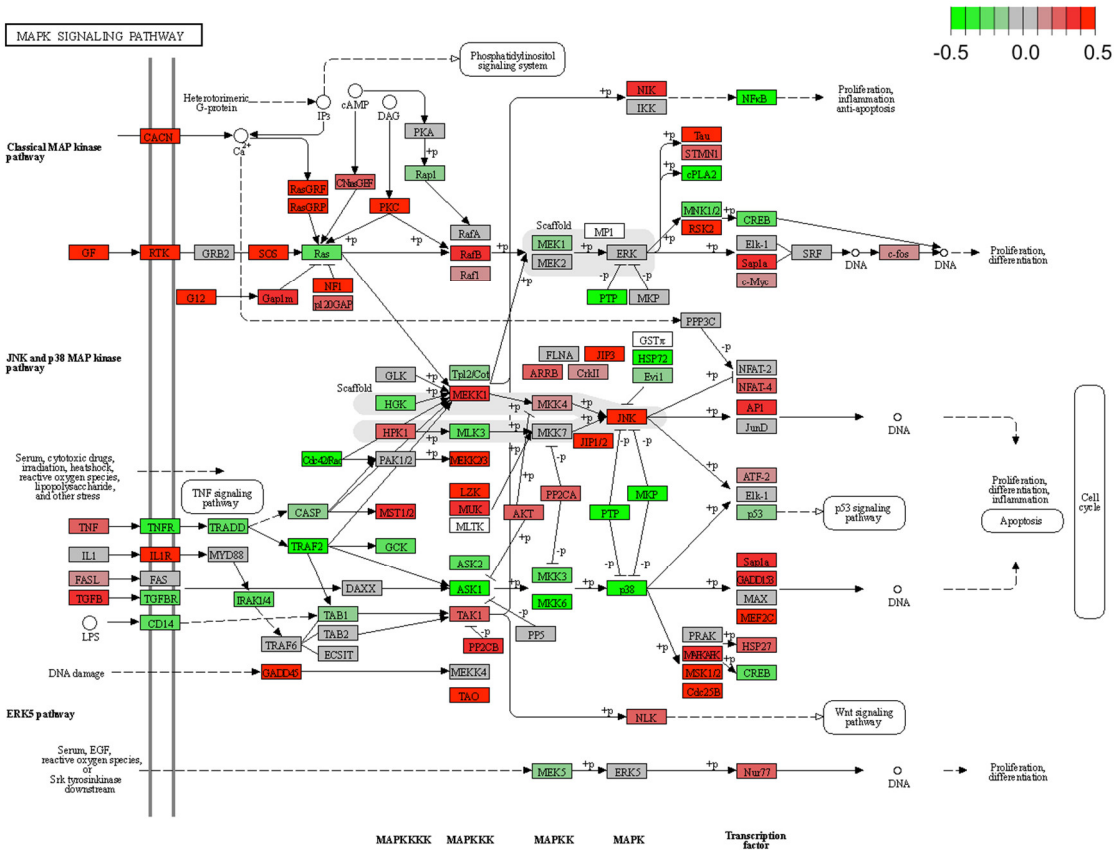

Figure 34. ***MAPK subgroups present dissimilar expression patterns of pathway-related genes****. Pathway enrichment analysis of KEGG MAPK signaling pathway (HSA04010). DEGs are highlighted in red or green when preferentially expressed in High or Low MAPK groups, respectively.*

1.3 MAPK SIGNATURE IS ASSOCIATED WITH GENOMIC INSTABILITY

In order to elucidate the biological characteristics intrinsic to these two extreme levels of MAPK activity, we evaluated whether these differences could derive from specific clinical features or genomic alterations.

The classification inferred from the MAPK signature was not associated with any particular clinical feature (age, gender, pathological stage nor tobacco history; Fisher exact test or Student t-test < 0.05). Furthermore, we did not observe any specific association between KRAS mutants distribution and the MAPK clustering (**Figure 35**), suggesting that the different potencies and functional differences among KRAS mutants (Haigis, 2017) are not behind the different MAPK levels.

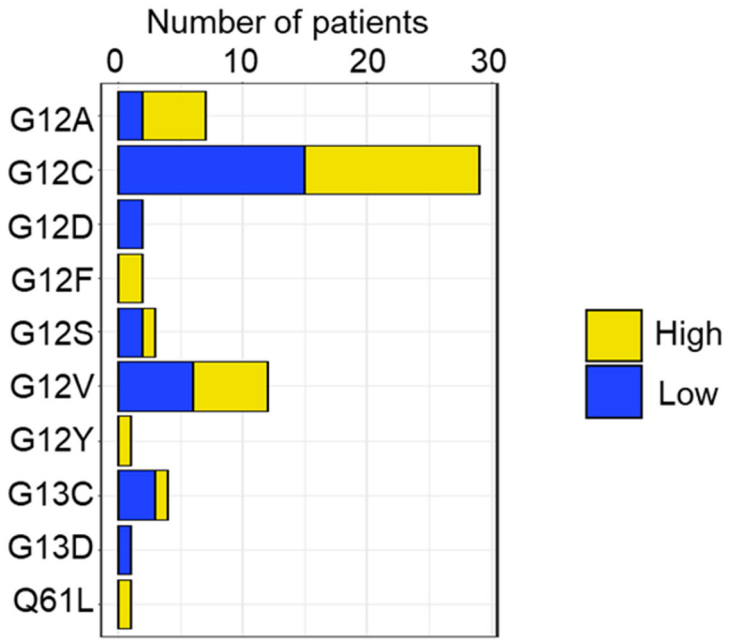

Figure 35. ***MAPK subgroups are not driven by any particular KRAS oncogenic mutation****. Oncogenic KRAS driver mutations found in the TCGA cohort patients. Distribution of the different mutations was found non-significant in each case (Fisher's exact test p-value >0.05).*

We then evaluated additional co-existing mutations that could be differentially present in the two groups (**Figure 36A**). To this respect, we observed a normal distribution of alterations in the two most common co-mutated genes in KRAS mutant LUAD, TP53 and STK11, with no difference between the two groups. However, we observed that half of the patients in the low MAPK group

presented KEAP1 mutations in a very high frequency (17 individuals, 55% of the group, Fisher exact p=0.0004) when compared to the high MAPK group (only 2 individuals).

We wondered if KEAP1 status could be linked to the survival differences seen between the high and low MAPK groups, so we computed survival hazard ratio for these co-occurrences (**Figure 36B**). We did not find any difference in survival among the different groups (high MAPK with WT KEAP1, low MAPK with WT KEAP1 and low MAPK with mutant KEAP1) suggesting that KEAP1 mutational status was not a determinant factor for survival in the low MAPK subgroup.

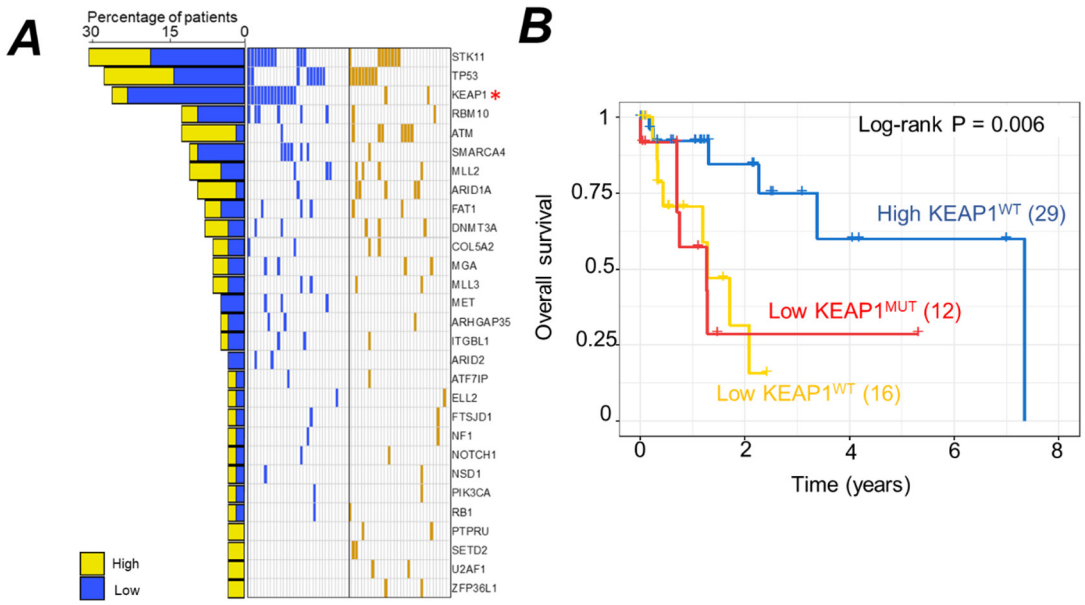

Figure 36. ***KEAP1 and other co-mutations found in MAPK subgroups are not determining survival differences****. Co-occurring mutations in the two MAPK sub-groups. (A) Table of mutations per patient, each patient representing one sub-column. The frequency is recapitulated on the left. The only gene mutation showing recurrent association was KEAP1 with the Low MAPK group (Fisher's exact p-value=0.0004). (B) Kaplan Meier curves recapitulating overall survival probabilities of the High MAPK group versus the Low MAPK group separated according to KEAP1 mutational status, wild-type or mutant. P-value (Cox) of the comparison between the three groups, proportional-hazard ratio between low MAPK KEAP1 WT and MUT was not appreciable.*

In parallel, we also analyzed gene-level copy number variation and compared differentially present abnormalities among the two groups genome-wide (**Figure 37A**). We remarked that most of the tumors, independently of the MAPK subgroup, presented a series of rearrangements in chr1q (70%) and chr19p (50%). Despite these common rearrangements, we did observe specific events happening, especially in the high MAPK group (**Figure 37B**).

We found a significant increase of the number of CNV occurring in the high MAPK group when compared to the low group, a total of 1017 significantly lost genes and 355 gene gains (Fisher's exact test $p<0.001$).

These alterations were present in more than 50% of the high MAPK tumors, while, in comparison, the low MAPK tumors did not present any statistically significant differential loss and only 2 differential gene gains. These findings would indicate that high MAPK tumors are more susceptible to genomic rearrangements and present a very complex and heterogeneous genomic landscape.

A

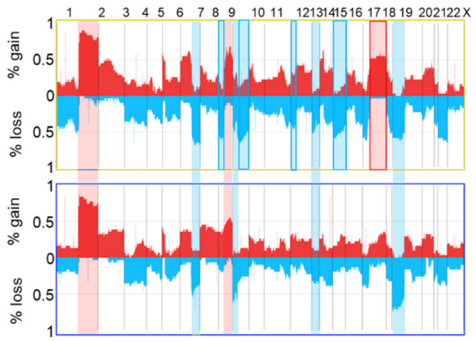

B

	High MAPK	Low MAPK
Differential CN gains	355 chr17q	2 ZNF395, PNOC
Differencial CN losses	1017 chr8p, chr15, chr9q	0

Figure 37. ***High MAPK tumors present a more complex genomic alteration profile****. Genomic alterations in the TCGA cohort. (A) Chromosomic map representing amplified and lost regions. In the lower blue square, alterations specific to Low MAPK group and in the yellow upper square alterations specific to High MAPK group. Significant amplifications are marked in red while significant deletions are marked in blue (ratio of patients). (B) Global estimates for CNVs of both groups. The main regions (or genes) involved are depicted.*

To confirm this hypothesis, and test if MAPK activity is linked to any kind of genomic stress that could be inferred from this data, we evaluated 30 fragile sites previously defined to be prone to rearrangements in cases of genomic stress (Beroukhim et al., 2010). Indeed, we observed that high MAPK tumors presented a significantly increased frequency of these fragile sites losses when compared to the low MAPK group (**Figure 38**). We deduce that this genomic instability is directly associated with MAPK activity, and it is probably linked to the replicative stress generated by pathway hypersignaling.

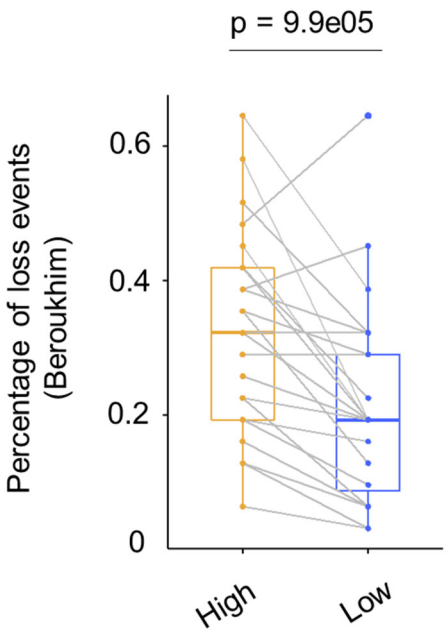

Figure 38. ***High MAPK tumors are more genomically instable****. Fragile sites described in (Beroukhim et al., 2010) were analyzed in the two subgroups. Each line represents a single chromosome, and how it is distributed in the two categories.*

1.4 AUGMENTED IMMUNE INFILTRATION IN THE HIGH MAPK POPULATION

The immune component could also play an important role in regulating these tumors evolution. We sought to investigate if MAPK activity was responsible for modifying the presence of immune populations in the tumor microenvironment. For this purpose, we performed two different bioinformatic methods to estimate tumor immune fractions.

First, we performed a deconvolution strategy, quanTIseq, to fractionate the TCGA's bulk RNAseq data into different immune cellular types (Finotello et al., 2019). By this method, we identified that the high MAPK patient group presented an increase in the immune component fraction, showing a global higher infiltration, all immune types confounded (**Figure 39A**).

In order to further dissect the individual populations that could be infiltrating these tumors, we evaluated the expression of a set of 10 immune transcriptional signatures, that we refined (see Methods), in order to fractionate immune populations and correlate them with the MAPK signature (Danaher et al., 2017, 2018). In this case, by comparing the immune populations between the high and low MAPK groups, we only identified that the high MAPK tumors presented a significantly increased frequency of CD8+ infiltrated T cells (**Figure 39B**).

Taken together, these results suggest that the high MAPK tumors present an active immune infiltration contexture, characterized by the increased presence of CD8+ lymphocytes when compared to low MAPK tumors.

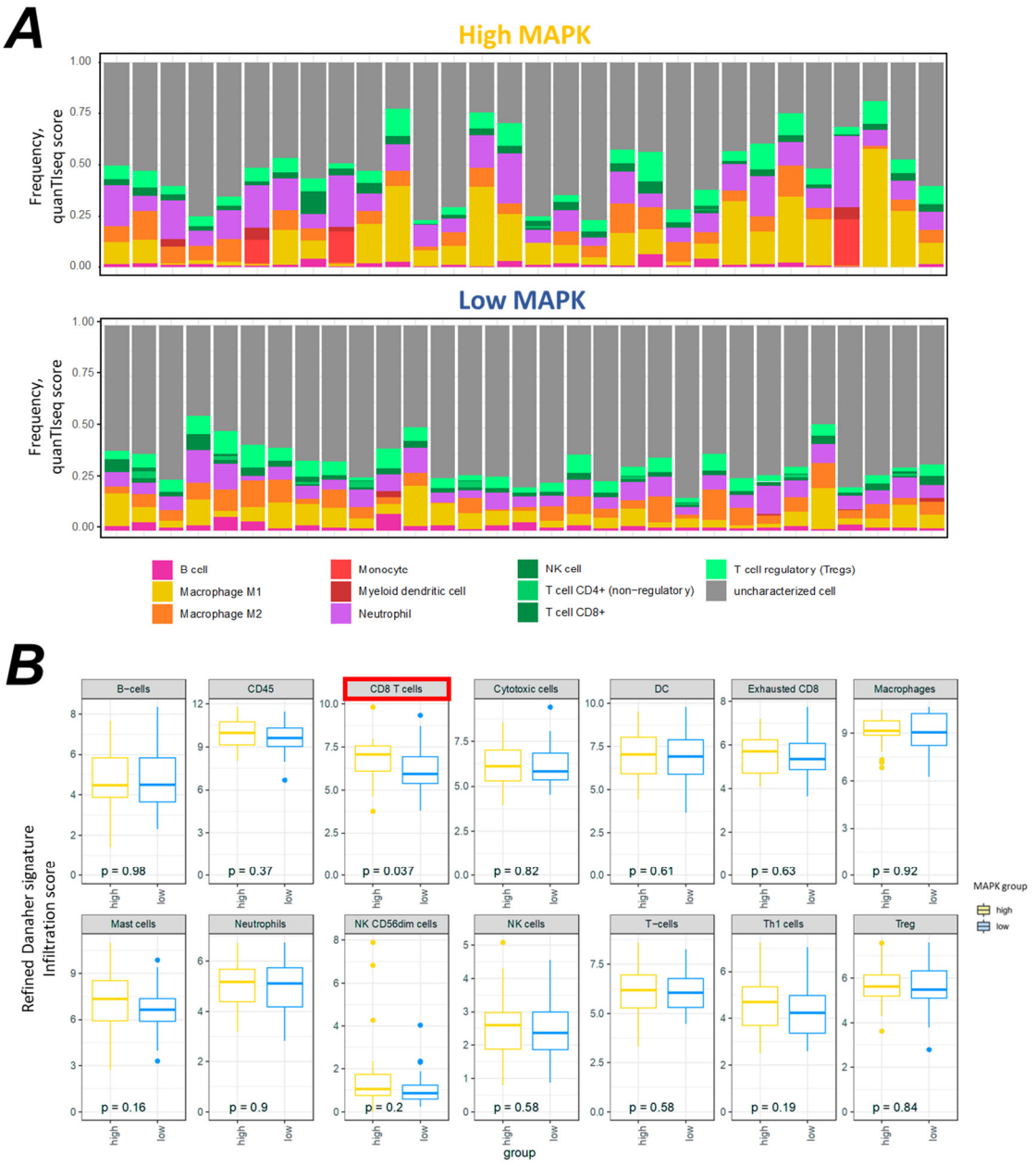

Figure 39. ***High MAPK tumors present increased immune infiltration****. We performed two independent methodologies to estimate and quantify the presence of immune populations in the TCGA KRAS mutant LUAD cohort. (A) The deconvolution strategy quanTIseq was performed to fractionate different immune populations. From the bulk RNAseq, frequencies of 10 different immune cells are estimated. The un-assigned fraction of reads is denominated "uncharacterized cell". (B) Individual components were re-evaluated through immune transcriptional signatures as described in Danaher. CD8+ T cells was the only compartment significantly different when compared among the MAPK subgroups with Wilcox test, p-value is indicated.*

2 DUSP4 AS A SENTINEL OF MAPK HYPERSIGNALING-DRIVEN TOXICITY

2.1 DUSP4 GENE IS ALTERED IN KRAS MUTANT TUMORS DEPENDING ON MAPK LEVELS

After discovering the complex genomic abnormalities that lined behind MAPK activation, we ought to decipher the biological relevance of these recurrent alterations and the molecular mechanisms that might be responsible for their frequency. A particular case retained our attention, the DUSP4 gene. As a gene directly involved in the negative feedback loop of ERK activation, DUSP4 transcription is activated by MAPK activity. However, as we previously remarked, DUSP4 expression anti-correlated with the rest of MAPK transcriptional targets. When taking a closer look on how DUSP4 behaves in the MAPK cohorts, we could indeed identify that DUSP4 expression was higher in the low MAPK group (**Figure 40A**). We understood that this paradoxical expression pattern was altered because of recurrent CNVs of the DUSP4 gene differentially present when comparing the two cohorts (**Figure 40B**).

Indeed, DUSP4 is genomically lost in the majority of the high MAPK tumors, making its global expression decrease. In parallel, a third of the low MAPK tumors do present genomic amplifications of the gene, suggesting that this group can also benefit from an enhanced expression coming from these copy number gains.

These findings are independent of any particular clinical feature. Furthermore, DUSP4 status did not correlate with any particular KRAS mutation. Interestingly, DUSP4 CNVs are observable along all the pathological stages present in the cohort (**Figure 41**). This would suggest that the alterations events affecting DUSP4 occur at early timepoints. The variants are retained until the very advanced stages, possibly by a mechanism of positive selection that grants an advantage to DUSP4 altered cells.

Intriguingly, DUSP4 expression anticorrelates with the MAPK signature also in EGFR and NF1 mutant cohorts from the TCGA (**Figure 42**), suggesting that this event extends further than the KRAS driver and may have an important biological relevance for every MAPK driven tumor.

Despite these findings, we did not observe any other particular rearrangement nor mutation that could be associated with DUSP4 genomic status.

A

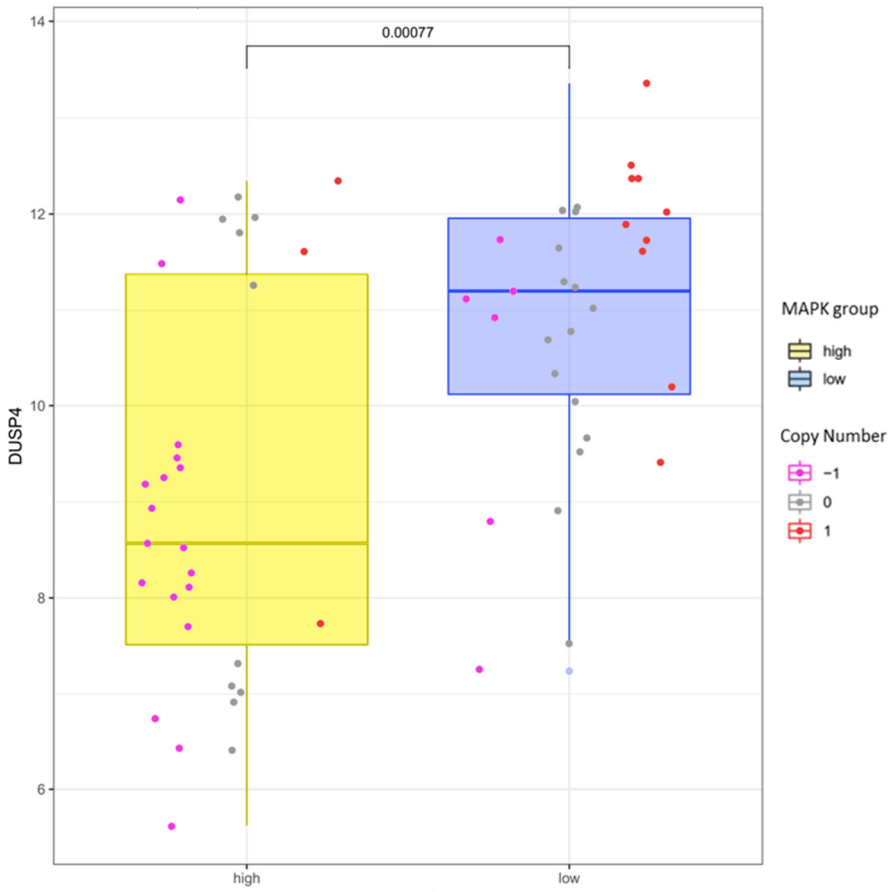

B

	Number of patients with CN gain (frequency, Fisher's p-value)	Number of patients with CN loss (frequency, Fisher's p-value)
High	3 (10%, 0.99)	**18** (58%, ***0.002)
Low	**10** (32%, *0.03)	6 (19%, 1)

Figure 40. ***DUSP4 gene is submitted to distinct CNVs in both MAPK subgroups****. (A) DUSP4 status drives its expression pattern. DUSP4 expression levels are indicated per patient in each group, reflected in the boxplot, (Wilcox p-value). Each dot represents a single tumor with a given DUSP4 expression level (y axis, Wilcoxon p-value is indicated for the comparison of high vs. low groups). Every patient is colored according to its DUSP4 copy number status: pink for copy number losses, gray for normal copy number and red for copy number gains. (B) Table recapitulating the status of DUSP4 in the two categories, indicating Fisher's exact test p-value.*

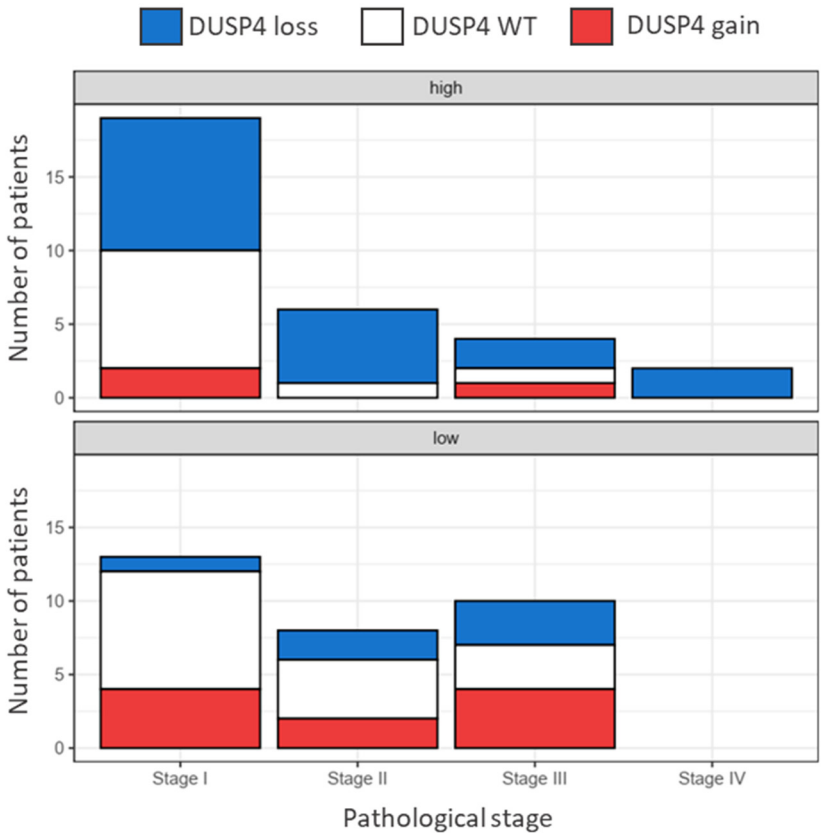

Figure 41. ***CNVs of DUSP4 gene are present since early stages of the disease****. DUSP4 status across pathological stages and MAPK subgroups. For both high and low MAPK subgroups, the frequency of copy number alterations of DUSP4 were equally distributed across tumor progression stages (Fisher's exact test p-value >0.05).*

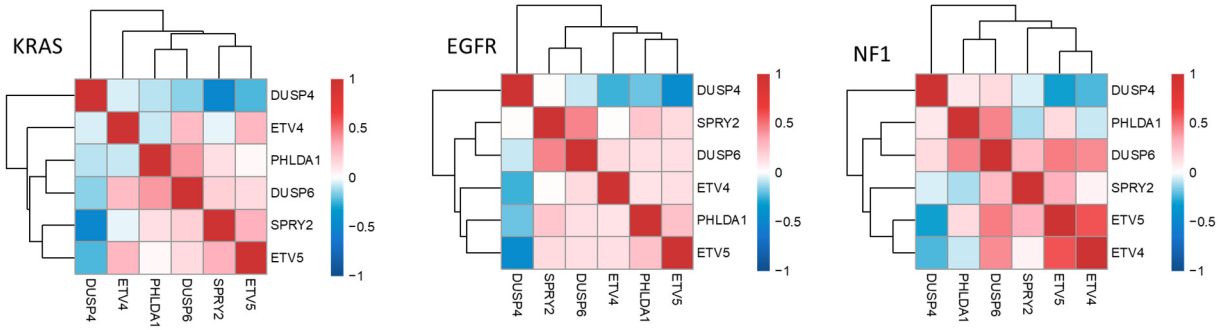

Figure 42. ***DUSP4 anti-correlates with the rest of the signature in MAPK driven tumors****. Correlation analysis of the six genes of the signature across TCGA LUAD different cohorts by driver mutation. Side by side comparison and computed Spearman correlation shows anti-correlation (negative, blue) and correlation (positive, red) between the median expression of each gene in "pure" LUAD cohorts.*

2.2 DUSP4 LOSS GENERATES HARMFUL HIGH MAPK ACTIVITY

2.2.1 Inducible loss of DUSP4 generates increased MAPK levels

The *in-silico* analysis of the clinical data has shown that DUSP4 status is substantially different across patients harboring divergent MAPK levels. In order to elucidate the biological impact of these CNVs, we focused on DUSP4 loss as a possible cause of a hyperactive MAPK pathway, hampering tumor progression.

As previously mentioned, DUSP4 has historically been described, experimentally, as a negative regulator of ERK in the nucleus (Chu et al., 1996; Guan & Butch, 1995). To validate that DUSP4 is able to control MAPK responses through ERK phosphorylation, we infected immortalized wild-type mouse embryonic fibroblasts (MEFs) with two plentiCRISPR constructs targeting DUSP4 mouse gene and one non targeting control vector against the bacterial gene lacZ (**Figure 43**).

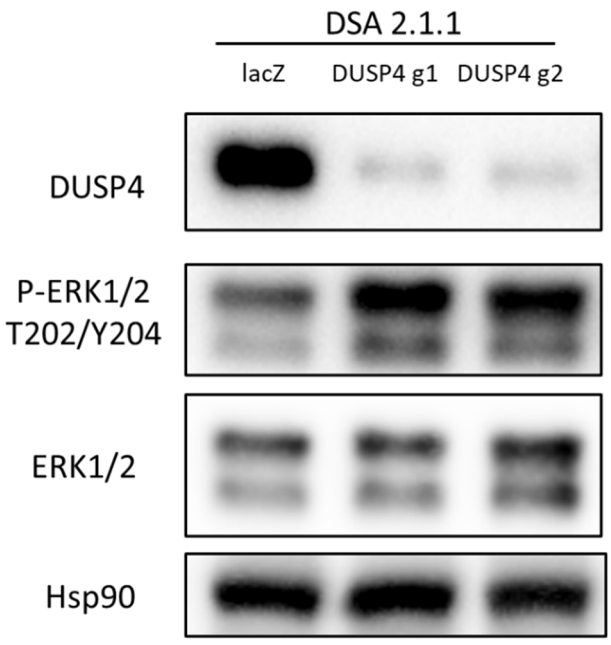

Figure 43. ***DUSP4 knock-out in mouse embryonic fibroblasts enhances MAPK activity****. Western blot depicting DUSP4 deletion with plentiCRISPR in the DSA 2.1.1 cell line (WT background, untreated).*

We confirmed that DUSP4 loss increases ERK phosphorylation in its activating residues T202 and Y204, reinforcing previous findings reporting that DUSP4 dephosphorylates ERK in the same residues that MEK targets (Guan & Butch, 1995).

After observing this MAPK increase driven by DUSP4 ablation, we ought to determine if DUSP4 loss could contribute to cellular transformation by synergizing with RAS oncogenes. We extracted additional MEFs from mouse embryos and performed retroviral infections with constructs harboring an oncogenic HRAS variant (G12V) and the E1A viral transforming sequence (**Figure 44**).

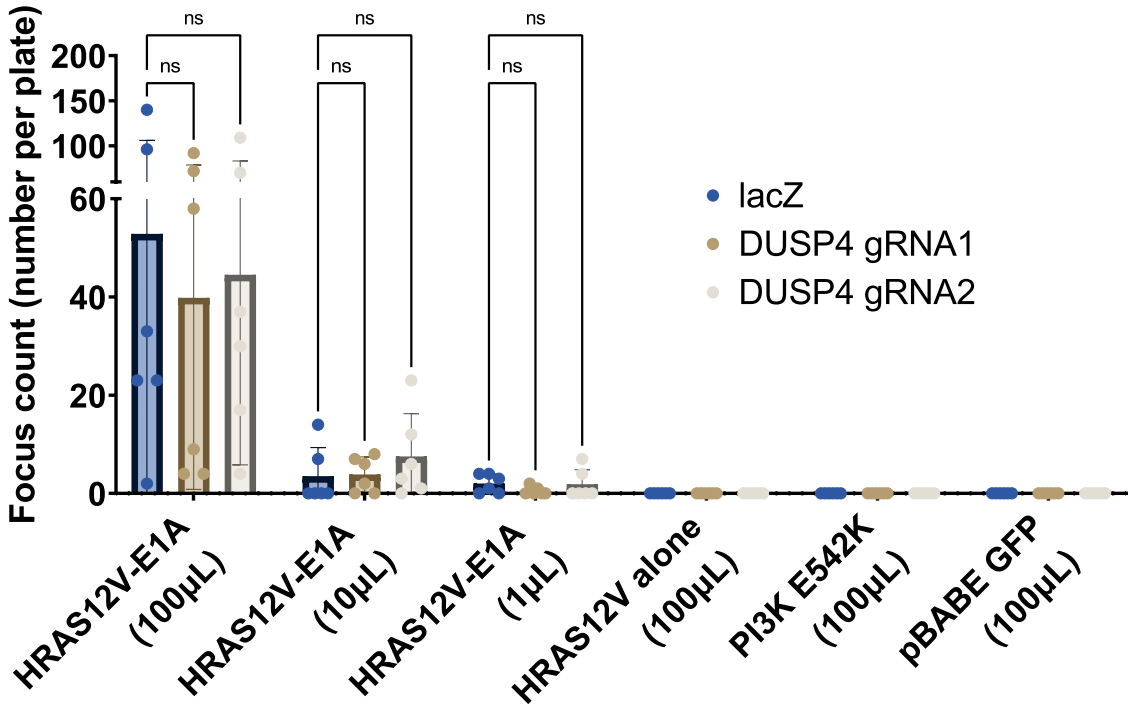

Figure 44. ***DUSP4 does not contribute to RAS-mediated transformation process****. Immortalization assay in MEFs combined with DUSP4 loss. We infected freshly extracted MEFs (WT DSD background, untreated) with retroviruses harboring oncogenic Ras and viral E1A cDNA. MEFs were previously infected and selected (puromycin) for plentiCRISPR against DUSP4 or a non-targeting control (lacZ). Focus formation was counted on 10mm plates, performing two-way ANOVA with Dunnett's multiple comparison test.*

MEFs were able to form focus colonies with increasing levels of $HRAS^{G12V}$ combined with the E1A protein. No colonies were observed in the infections harboring $HRAS^{G12V}$ alone nor with a GFP empty vector, showing that this transformation required the cooperation of both RAS oncogenic activity and p53 block by E1A.

We compared these results with cells previously infected and selected with plentiCRISPR constructs targeting DUSP4. In this experiment, DUSP4 status did not modify the transforming potential of $HRAS^{G12V}$ and E1A, and DUSP4 loss was not enough to induce transformation by itself. We also confirmed that DUSP4 could not collaborate with an alternate driver, in this case PI3K oncogenic mutant (E542K), to transform these MEFs.

These results suggest that DUSP4 loss is not an oncogenic driver event *per se*. Thus, the biological relevance of DUSP4 alterations probably resides only after KRAS transformation.

For this reason, we decided to evaluate how loss of DUSP4 affected KRAS-mutant tumor cell fitness. For this purpose, we engineered mouse KRAS mutant tumoral cells (14.9 cell line) with an inducible Cas9 whose expression is controlled by a tetracycline response element. Combined with a constitutive expression of gRNAs in a lentiviral form, we can induce DUSP4 knock-out by adding doxycycline to the system (**Figure 45A**). We successfully observed DUSP4 inducible ablation with two independent gRNAs. The inducible system generated a DUSP4 loss of function that resulted in increased phosphorylated ERK levels (**Figure 45B**).

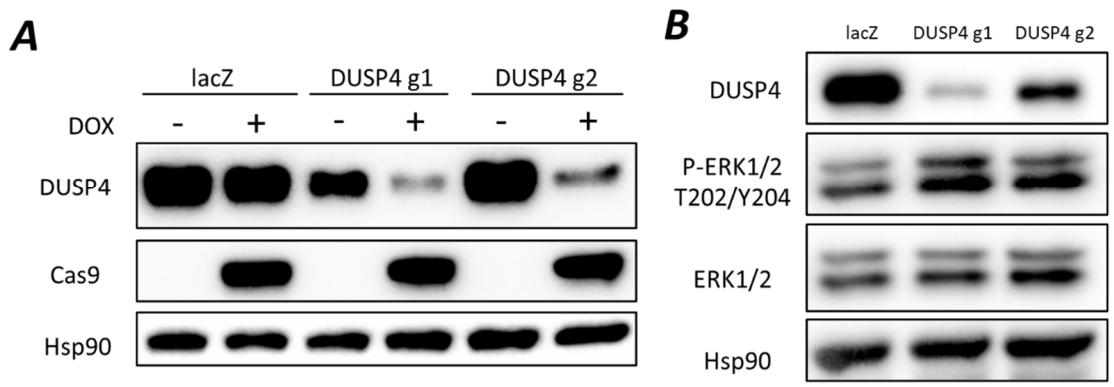

Figure 45. ***DUSP4 inducible ablation generates increased MAPK levels****. Mouse cell line 14.9 (KRAS G12V mutant, p53 WT/WT) were engineered with the inducible CRISPR/Cas9 system targeting DUSP4. (A) Western blot depicting doxycycline induction (1 µg/mL for 2 weeks) of Cas9 and mediated DUSP4 ablation. (B) Doxycycline induction (1 µg/mL for 1 week) enables DUSP4 editing and increases MAPK activity levels.*

2.2.2 Stress phenotypes driven by DUSP4 loss of function

We evaluated how DUSP4 ablation could contribute to a putative toxic event that may affect normal progression of the tumor. As MAPK activity has previously been described to affect and be affected

by oxidative stress (Son et al., 2011), we evaluated the presence of reactive oxygen species (ROS) in cells lacking DUSP4 (**Figure 46**). Indeed, we found that elimination of DUSP4 slightly augmented ROS levels in our *in vitro* tumoral model, suggesting that loss of DUSP4 is able to generate toxicity by directly increasing oxidative stress.

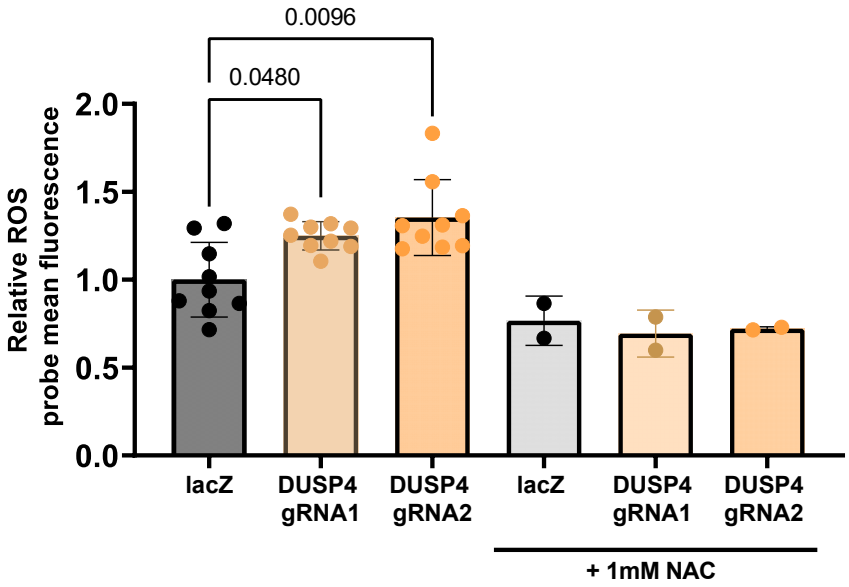

Figure 46. ***DUSP4 deletion induces cellular increase of ROS and oxidative stress levels.*** *14.9 mouse cell line engineered with the inducible CRISPR/Cas9 system targeting DUSP4 were cultured in presence of doxycycline for 2 weeks. At that point, ROS levels were measured with a fluorescent probe by flow cytometry. For comparison, the non-parametric Kruskal-Wallis test was performed with Dunn's multiple comparison correction, significant p-values are indicated, n=3.*

In order to better understand these toxicities in a more physiological setting, we used the previously described inducible knock-out cell line model to generate abrupt ablation of DUSP4 *in* vivo, in fully formed KRAS mutant tumors. We orthotopically injected the engineered cells by the mouse tail vein and waited for the forming tumors to appear before starting the doxycycline diet (**Figure 47A)**. We collected lung tumors from every mouse to perform histology analyses and IHC stainings. We observed that tumors lacking DUSP4 presented increased levels of γH2AX phosphorylation in non-necrotic areas, denoting precise cellular foci of genomic stress in these tumors (**Figure 47B**). Additionally, these tumors presented an increase in non-necrotic cleaved caspase 3 staining, a common marker for apoptosis, suggesting that DUSP4 loss generated localized cellular death (**Figure 47C**). We also evaluated oxidative stress marks that could corroborate the previous findings pointing to a ROS increase in DUSP4 knockout cells. We performed 8-hydroxyguanosine staining, a biomarker for oxidative damage to nucleic acids and lipids, and found no significant

difference between the tumors, although the relevance of this particular staining for our model is contestable and further oxidative stress markers need to be tested in the future.

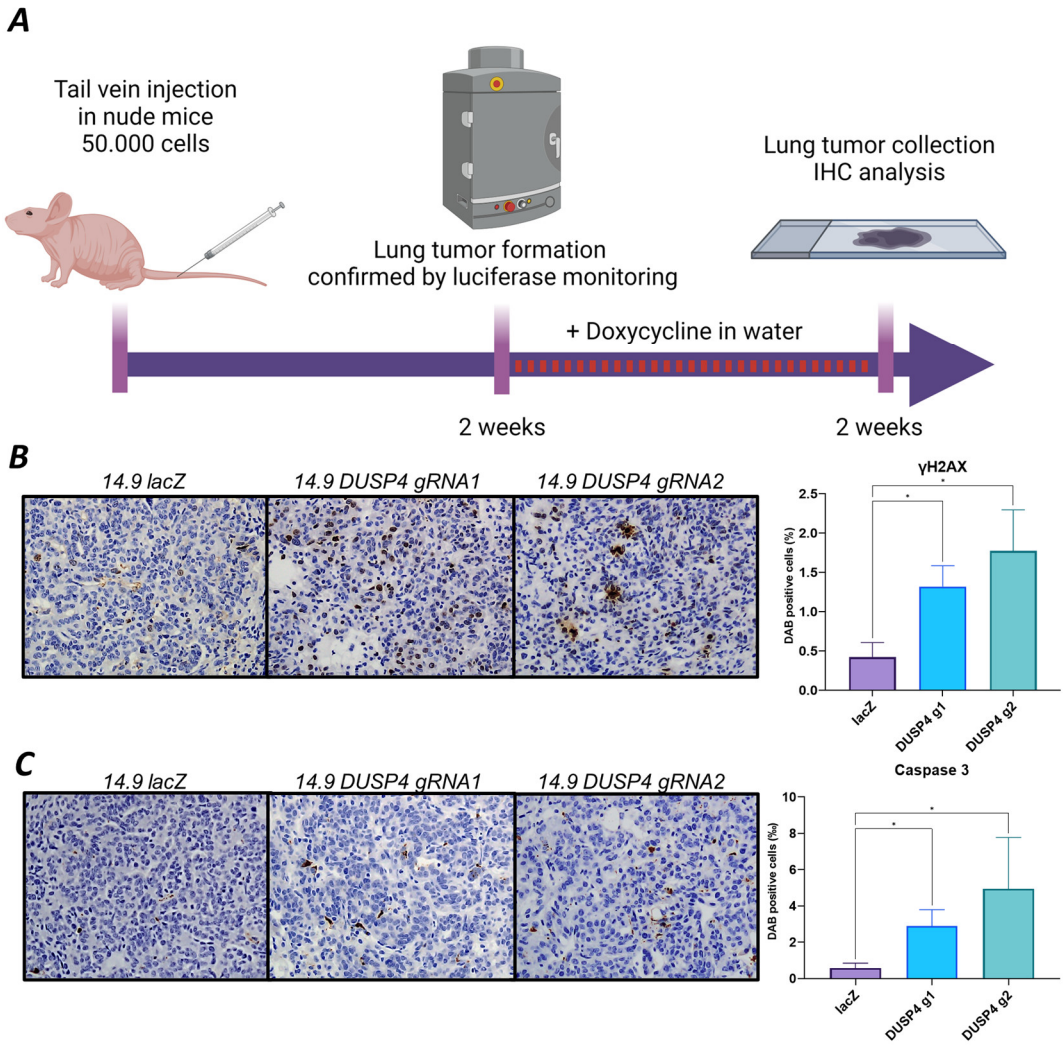

*Figure 47. **Abrupt deletion of DUSP4 in formed tumors increases genomic instability and apoptotic rate**. (A) In vivo strategy, DUSP4 ablation modelled in mice. Tumor formation was ensured by luciferase monitoring before starting doxycycline treatment. Immunohistochemistry staining of tumor samples revealed (B) more frequent marks of genomic stress by phosphorylated γH2AX and (C) increased number of apoptotic cleaved-caspase 3 positive cells. Non-parametric Kruskal-Wallis test was used to compare the number of positive cells for each staining, the quantification avoided necrotic and hypoxic areas, p-value *<0.05.*

2.3 DUSP4 LOSS GRANTS AN INITIAL ADVANTAGE TO KRAS-DRIVEN CELLS

From the clinical data, we confirmed that DUSP4 losses are observed in the majority of high MAPK patients since the early stages of the disease. This high frequency of copy number losses could imply that these inactivation events are being selected at early stages. We hypothesized that one possible way DUSP4 deletion could be positively selected early on is by conferring an initial

MAPK-driven proliferative advantage to KRAS mutant cell lines. In order to understand this putative process, we designed an *in vivo* model that could mimic this early timepoint (**Figure 48**).

Alveolar type II (ATII) cells are the most predominant cellular type in the lung, and they are considered to be the cell of origin for lung adenocarcinoma development (Aja et al., 2021). We developed an *in vivo* model from a human immortalized ATII cell line, a generous gift from Julian Downward, that harbors a tamoxifen-activatable KRAS oncogenic mutant, thanks to a fusion with the estrogen receptor (KRASG12V-ER). These cells were infected with plentiCRISPR constructs targeting DUSP4, validated by western blot (**Figure 48A)**. We did not obtain significant difference in phosphorylated ERK in between the conditions. However, we evaluated the MAPK transcriptional signature response to KRAS activation by tamoxifen treatment and observed that DUSP4 knockout cells presented increased levels of expression of the MAPK-dependent genes (**Figure 48B**). Finally, the cell lines were orthotopically injected by tail-vein injection in NSG immunodeficient mice that were already under tamoxifen diet. Only mice that retained the tamoxifen during the whole process developed a positive luciferase signal (**Figure 48C**), demonstrating that this was a KRAS-dependent phenotype.

We followed luciferase signals across multiple months (**Figure 48D**), that were almost undetectable until 10 weeks after the injection of the cells. From that point on, signals from DUSP4 knock-out cells started to emerge. This phenomenon occurred significantly earlier than the control cells, that took another additional two weeks to start. DUSP4 knockout cells presented a significantly increased luciferase signal for several weeks. However, during the last weeks, lacZ control tumor development was abruptly accelerated, even reaching higher luciferase levels than the knockouts. These mice had to be sacrificed at 20 weeks post-implantation due to old age and the presence of hepatic tumors derived from the ATII cells. We did not see any significant difference in tumor burden at the end timepoint (data not shown).

These results would contribute to the hypothesis derived from the clinical data, suggesting that DUSP4 deletion events are positively selected during early stages of the disease, as DUSP4 loss seems advantageous for initial malignant growth. However, we have observed that DUSP4

knockouts progressively lose the conferred advantage and are overcome by DUSP4-proficient cells, suggesting that, at a latter point, DUSP4 integrity may be more beneficial.

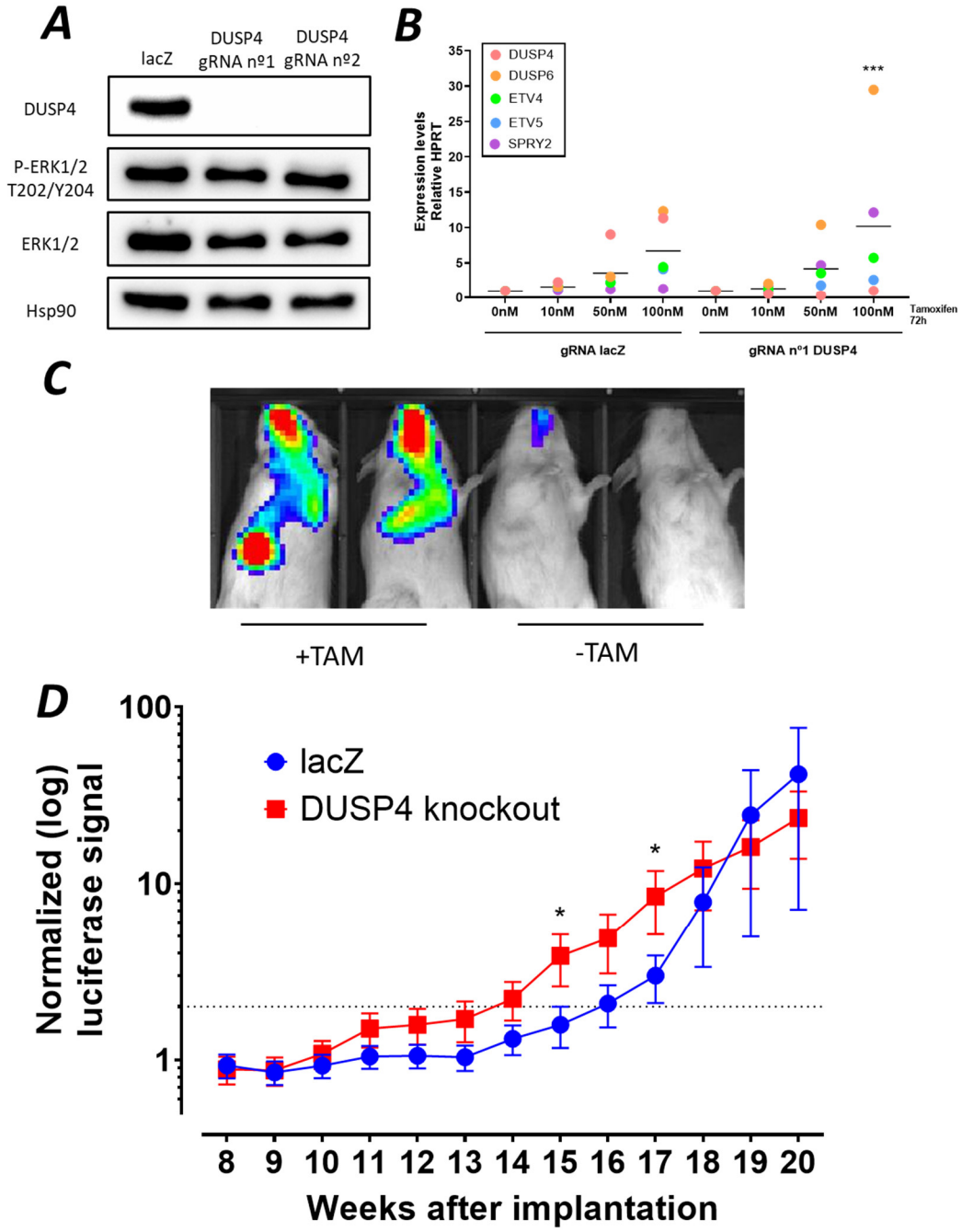

*Figure 48. **An inducible KRAS tumor formation model reveals that DUSP4 loss initially grants a selective advantage**. (A) The human ATII KRASG12V-ER cell line was infected with plentiCRISPR targeting DUSP4. (B) RTqPCR analysis was performed on the ATII cell line, either harboring plentiCRISPR lacZ control or DUSP4 targeting gRNA n°1. Cells were exposed to increasing levels of tamoxifen for 72h before lysis and RNA extraction. Two-way ANOVA was performed, the only significant comparison (*** p-value<0.001) is shown (vs. Untreated lacZ control). (C) These lines were orthotopically injected by the tail vein in NSG mice. Only mice under tamoxifen diet presented luciferase signal. (D) Follow-up of luciferase signal across several months. Luciferase signal is normalized to the 8th week post-implantation (as no significant signal was observed previously) and log represented. Each timepoint is represented as mean ± SEM, multiple Mann-Whitney tests were performed for each timepoint to compare ranks, applying FDR multiple correction of p-value (*<0.05) (n=9 for control and n=19 for knockouts).*

2.4 RECAPITULATING CLINICAL DUSP4 STATUS IN VIVO

The clinical data, together with these last experimental observations, may indicate towards a dual role of DUSP4 in tumorigenesis. In order to better understand how DUSP4 globally affects the malignant process, we sought to generate a more comprehensive model where we could recapitulate the entirety of the tumor initiation and development process of KRAS mutant cells harboring (or not) DUSP4 alterations.

2.4.1 Conditional KRAS activation combined with DUSP4 ablation in vivo in pSECC model

For this particular model, we took advantage of the *K-ras*$^{+/lox\text{-}Stop\text{-}lox\text{-}G12V\text{-}geo}$ mouse strain (see **Figure 12** in Methods). The STOP cassette flanked by the *loxP* sites will prevent KRAS oncogenic mutant G12V expression until a recombination event is mediated by a CRE recombinase. We opted for an intranasal infection of lentiviral particles in order to couple *Cre* activity with gene-targeting technology that could model DUSP4 ablation, locally targeting the lung tissue after instillation. For this purpose, we took advantage of the pSECC lentiviral plasmid (Sanchez-Rivera et al., 2014). This vector allows for parallel co-expression of a sgRNA of interest, the Cas9 protein and the Cre recombinase. We generated plasmids that allowed CRISPR/Cas9 targeting of DUSP4 gene, as well as a turboGFP non-targeting control vector.

In order to ensure that this system was working efficiently, we used the *Rosa26*$^{lox\text{-}Stop\text{-}lox\text{-}YFP}$ allele for fluorescence reporting. For verification purposes, we infected immortalized MEFs derived from this same mouse model with the pSECC lentiviruses in vitro. Upon CRE recombination, the STOP cassette in between the *loxP* sites will be ablated and expression of both KRAS^{G12V} and the YFP will take place. As this plasmid does not have any selectable marker, we collected the cells seven days after infection. We detected a majority of YFP positive cells in the population and performed FACS sorting of these cells, harboring pSECC constructs with gRNAs targeting DUSP4 (**Figure 49A and 49B**). We recovered the cell pellets to perform gDNA extraction, purification and PCR amplification of the genomic region targeted by the gRNAs. We sequenced the resulting PCR product and performed a CRISPR performance analysis to determine the efficiency of the gRNAs

(**Figure 49C and 49D**). The results were satisfactory for both gRNAs, as they presented 55 and 56% knock-out score in the sequence pool (standards usually recommend 40-90% of indels for this verification process).

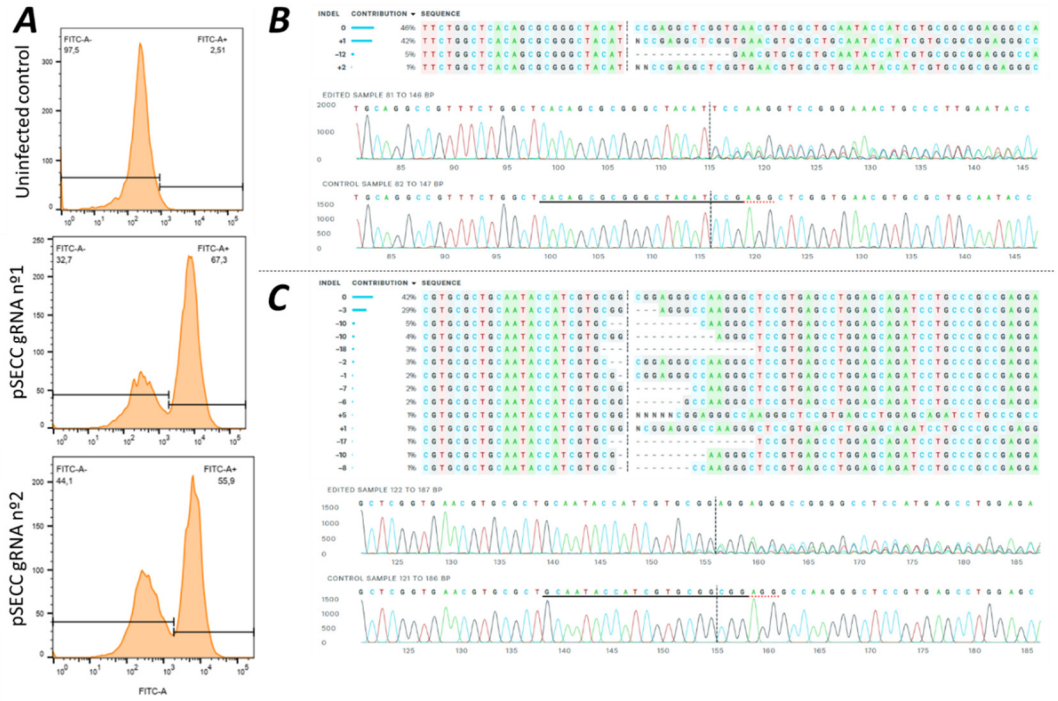

Figure 49. ***pSECC model allows for direct DUSP4 genome editing combined with Cre activity****. MEFs were infected with pSECC lentiviral particles at a rate of a theoretical MOI of 1. (A) Cells infected with pSECC gRNAs nº1 and nº2 were FACS sorted for YFP (FITC channel) fluorescence. DNA was extracted to perform PCR amplification of the genomic region targeted by the gRNA nº1 (B) and nº2 (C), and Sanger sequencing. The CRISPR analysis results (B,C) show the frequency of the different editing products, estimating by deconvolution the knock-out rate at around 50%. The chromatograms represent the sequence of the region and underline the cutting point of the gRNA, at which point the sequence becomes blurry due to the heterogeneity of the products upon editing.*

As the verification process was successful, we started infecting mice with the pSECC particles intra-nasally, using identical titers per mouse. We determined that the experiment should be one year long, as this is the general off-set for KRAS tumors generated by this strategy (DuPage et al., 2009), with different reference timepoints separated by 3-months' time. At each timepoint, we collected lung lobes and tumors for IHC (**Figure 50**). The goal of this experiment was to compare and analyze the quantitative differences in tumor progression that a DUSP4 knockout could produce when compared to the turboGFP non-targeting control. The initial comparison that we used was the quantification of the number of cells that underwent KRAS recombination and were proliferating

in the lung. For this purpose, we opted to utilize the *Rosa26*$^{lox\text{-}Stop\text{-}lox\text{-}YFP}$ reporter to quantify the lesions, performing IHC against the fluorescent protein.

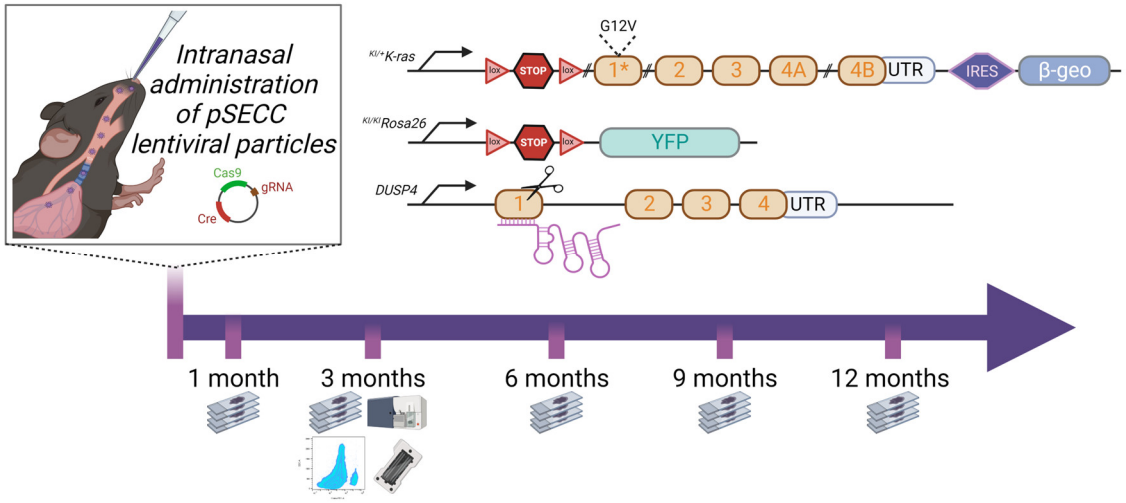

Figure 50. ***Experimental plan for the pSECC experiments****. Mice harboring heterozygous K-ras*$^{+/lox\text{-}Stop\text{-}lox\text{-}G12V\text{-}geo}$ *and Rosa26*$^{lox\text{-}Stop\text{-}lox\text{-}YFP}$ *alleles were selected for the experiment. Each mouse got an intranasal dose (see Methods) of pSECC lentiviral particles. Upon integration, the Cre recombinase would activate KRAS oncogenic mutant, concomitantly with the YFP reporter. In parallel, with the Cas9-mediated system, DUSP4 knockout would co-occur, simulating the situation seen in the clinic. During the experiment, lung lobes were collected to perform IHC every 3 months and monitor the evolution of the positive cells. Furthermore, we performed a 3-month experiment to collect positive cells and perform RNA-sequencing, in order to investigate the transcriptional changes that depend on DUSP4 function.*

2.4.2 DUSP4 loss of function accelerates growth of initial KRAS mutant lesions

The first timepoint to be analyzed for this experiment was the 1-month reference (**Figure 51A**). This was an internal control to the experiment, as we wanted to ensure that mice did not present any initial bias coming from the infection protocol. Indeed, at this timepoint there were no differences in the number of positive cells, validating the procedure and confirming the infection rates were comparable.

The next experimental timepoint was at 3 months after infection (**Figure 51B and 51C**). Quantification results showed that mice having received particles targeting DUSP4 presented an increase (although not significant for gRNA nº1) in the number of positive cells. As this was not a consequence of the infection itself, we suggest that DUSP4 loss synergizes with KRAS oncogenic activity to enhance tumor burden in this spatio-temporal context.

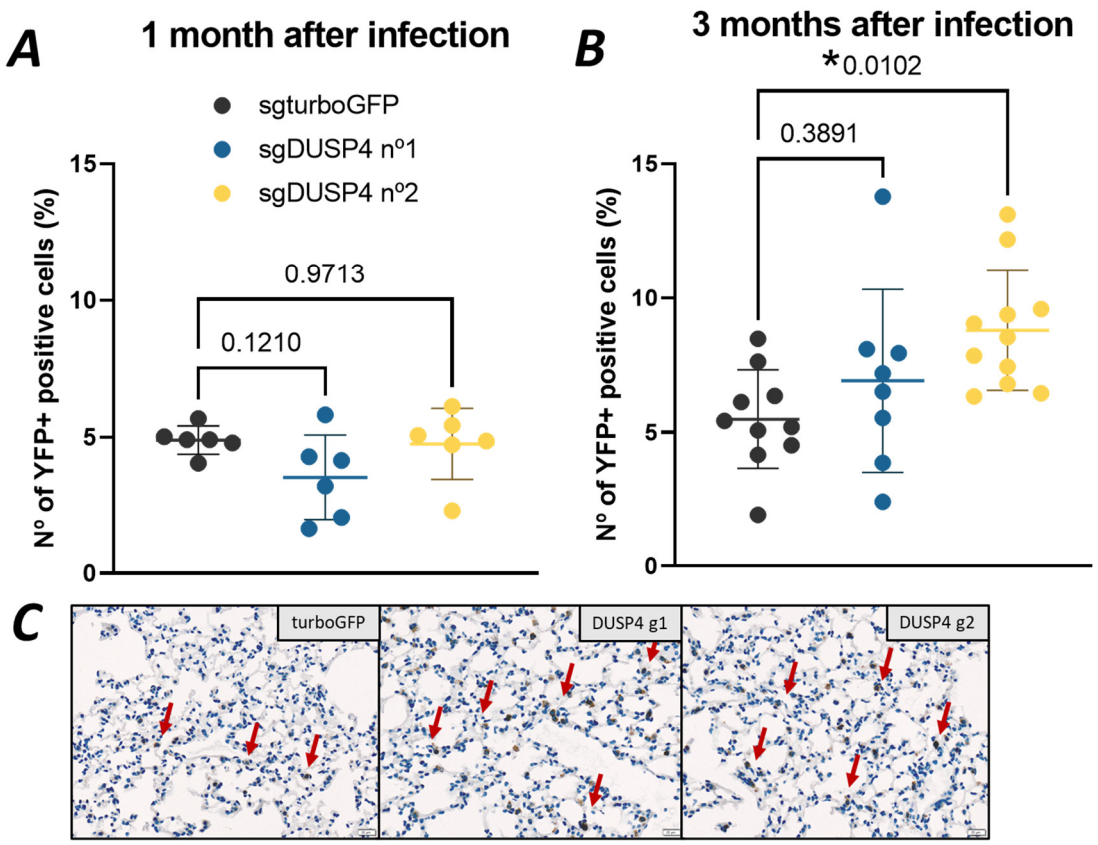

Figure 51. ***DUSP4 loss increases the frequency of early lesions****. K-ras$^{+/lox\text{-}Stop\text{-}lox\text{-}G12V\text{-}geo}$ mice were infected with lentiviral pSECC particles (expression vector for CRE, Cas9 and gRNAs) targeting turboGFP, as a non-targeting control, or DUSP4. Hematoxylin slides were counter-stained against YFP expression, which acts as a surrogate marker for KrasG12V-expressing cells. Slides were scanned and analyzed using QuPath software. One-way ANOVA with Dunnett's multiple comparisons test, p-value is indicated. (A) One month after the infection, there is no visible difference suggesting that infection rates were comparable. (B) Three months after infection, quantitative differences appear. (C) Representative images of the 3-month timepoint.*

2.4.3 KRAS-driven tumors lacking DUSP4 present impaired tumor growth at advanced stages

We proceeded to continue the IHC quantification of the following timepoints, which consisted in the analysis of established visible lesions (**Figure 52**). At 6 months post-infection, we counted the number of lesions and noticed that tumor frequency in the non-targeting control condition was higher (**Figure 52A**). These results were confirmed with the following timepoint at 9 months post-infection (**Figure 52B**).

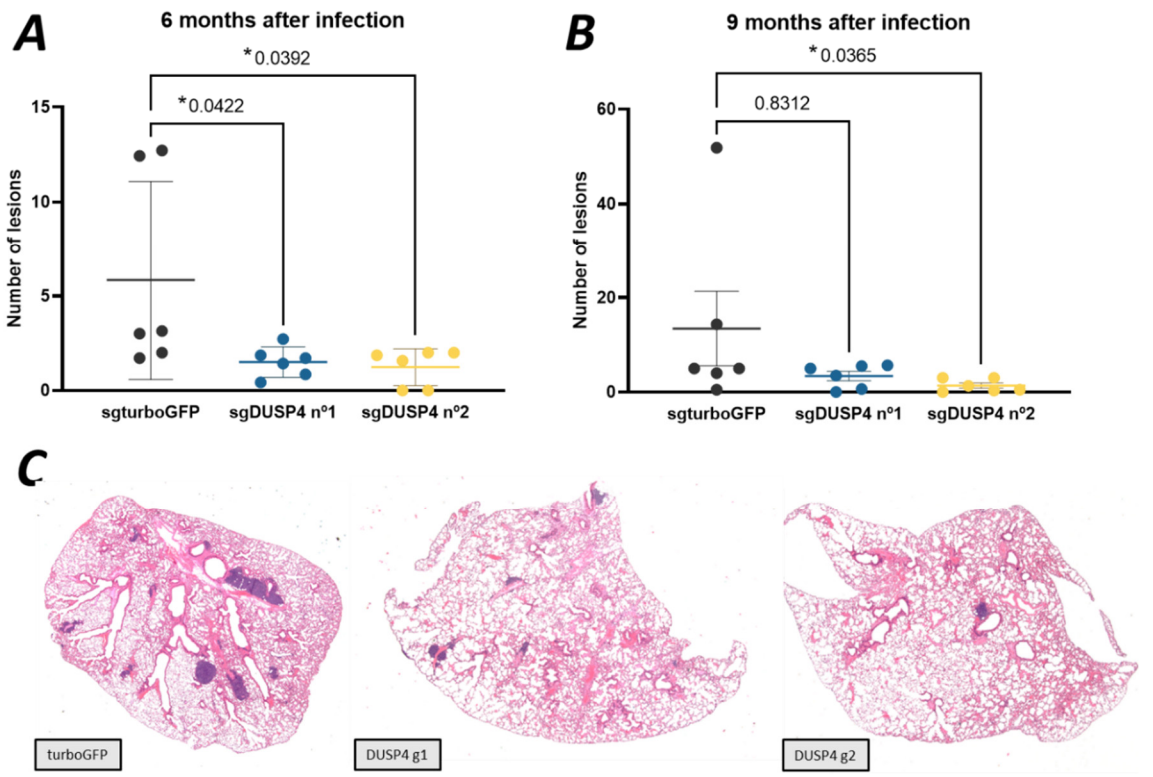

Figure 52. ***Limited tumor frequency upon DUSP4 ablation.*** *K-ras$^{+/lox\text{-}Stop\text{-}lox\text{-}G12V\text{-}geo}$ mice were infected with lentiviral pSECC particles targeting turboGFP, as a non-targeting control, or DUSP4. Lesions were counted on hematoxylin/eosin slides, with a total of 7 sections per mouse, with 6 mice per condition. Each dot represents the mean of lesions per mouse, the bar represents the grand mean +/- SD for each condition. Non-parametric Kruskal-Wallis with Dunn's multiple comparisons test, p-value is indicated. Lesions counted at (A) 6 months post-infection and (B) 9-months post-infection. Representative images of the left lobe for each condition at 9 months timepoint (C).*

The next and last timepoint obtained was at 12-months post-infection (**Figure 53**). At this moment, all the mice, independent of the condition, presented fully invaded organs. For this reason, the counting does no longer seem to represent any difference among tumors with or without DUSP4 function (**Figure 53A**). However, we did observe a difference in the physical characteristics of these tumors when DUSP4 was deleted. Tumors lacking DUSP4 present smaller sizes, reflected both in their radius and surface area (**Figure 53B and 53C**). These findings may suggest that DUSP4 loss decreases the probabilities of generating substantial and more advanced neoplasms.

In summary, considering the whole experiment series, these findings may indicate that, as we hypothesized, DUSP4 loss becomes detrimental during KRAS-driven tumor progression, as DUSP4 ablation results in enhanced tumor formation at early time points following the activation of a resident KRAS^{G12V} but subsequently decreases tumor progression rates.

In order to further understand the stress phenotype generated by DUSP4 ablation at late stages, we will perform additional histology analyses of these lesions to determine if tumors are affected by apoptotic, genomic and/or oxidative toxicities.

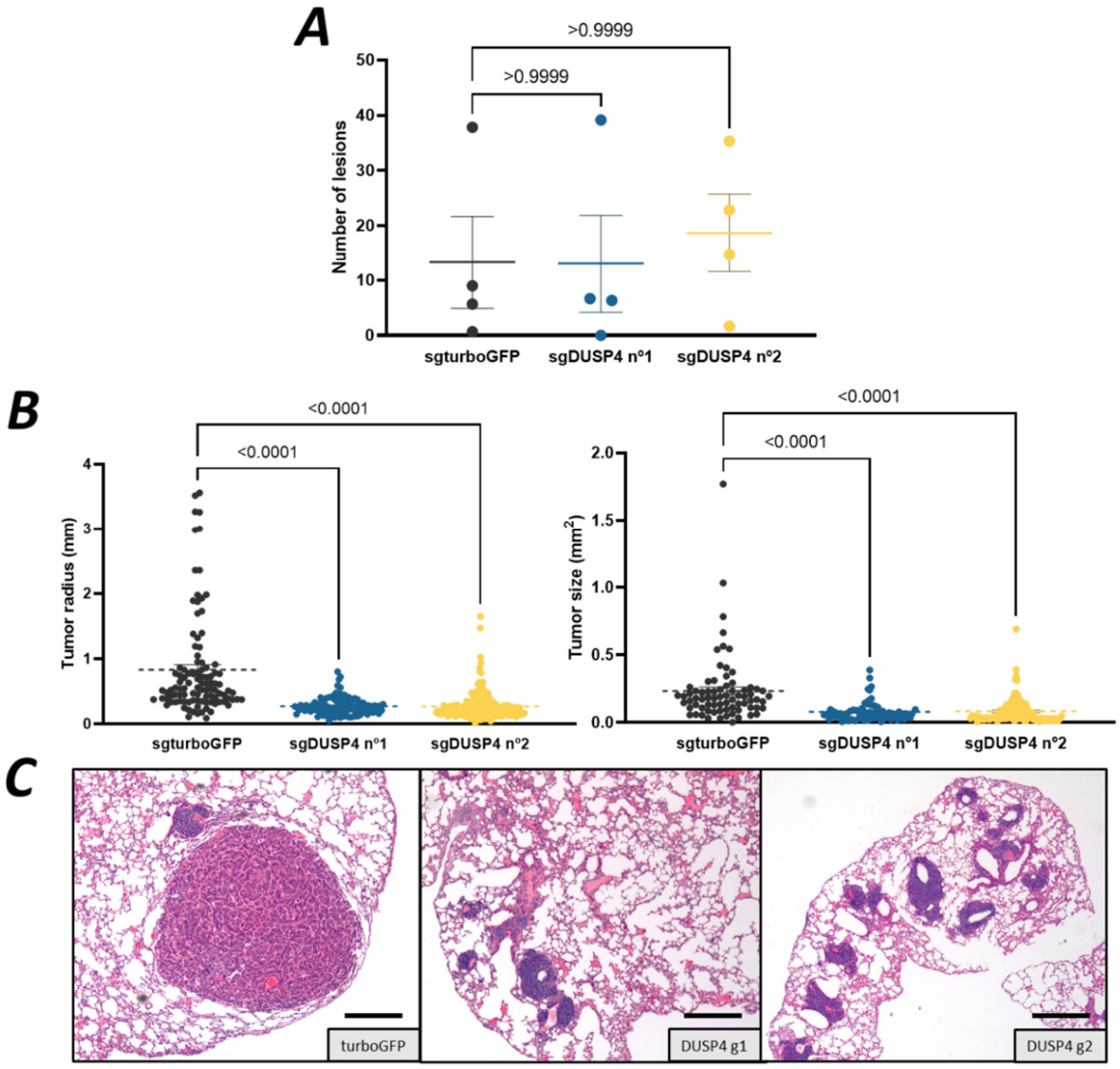

Figure 53. ***Tumoral burden is lessened by DUSP4 deletion.*** *12-month timepoint. K-ras$^{+/lox\text{-}Stop\text{-}lox\text{-}G12V\text{-}geo}$ mice were infected with pSECC lentiviral particles targeting turboGFP, as a non-targeting control, or DUSP4. Lesions were counted and measured directly (long and small radius; surface area) on hematoxylin/eosin slides, with a total of 6 sections per mouse and 6 mice per condition. Each dot represents (A) the mean number of lesions per slide per mouse (B) the size of a single lesion, more than 50 lesions were counted per condition (n=74, 68, and 85, respectively), the bar represents the grand mean +/- SD for each condition. (C) Representative images were represented on the HE slides, the scale-bar represents 500µm. Non-parametric Kruskal-Wallis with Dunn's multiple comparisons test, p-value is indicated*

2.5 CHANGES IN DUSP4 EXPRESSION PROMOTE ALTERED SENSITIVITIES TO MAPK INHIBITORS

We previously identified that DUSP4 alterations are present in a considerable amount of KRAS mutant tumors. Preferentially, we found copy number losses in high MAPK, while locus gains are enriched in low MAPK patients. In this section, we sought to investigate how these alterations could contribute to the clinical outcome of these patients. We were particularly interested in how DUSP4 alterations may modulate response to targeted treatment strategies. Specifically, we speculate that DUSP4 differential status could alter the response to MEK inhibitors and the recently developed $KRAS^{G12C}$ specific inhibitors.

We generated a panel of DUSP4 knock-out and inducible expression models of KRAS mutant human LUAD cell lines in order to evaluate how DUSP4 modulation could specifically alter MAPK inhibitor responses.

LUAD tumors are characterized by an intrinsic high heterogeneity, even when dealing with tumors sharing KRAS mutations. Especially when working with tumoral cell lines, we took this into account and performed these experiments in several cell lines, including A549, H2030, H23, H358 and H460. In these cell lines we generated constitutive knock-out models of DUSP4 (**Figure 54**). First, we successfully characterized almost total DUSP4 protein loss using three independent CRISPR/Cas9 gRNAs in all these cell lines by western blot analysis. In these results, we can observe that both DUSP4 human isoforms are depleted: the canonical isoform of 42 kDa, and a short isoform lacking functional MAPK phosphatase activity of 34kDa.

Then, in these cell lines, we evaluated sensitivity to MAPK inhibitors, including MEK inhibitor trametinib, and the most recent KRAS inhibitors adagrasib and sotorasib (for the $KRAS^{G12C}$ mutant cell lines only). Three of these cell lines (A549, H460 and H358) presented a decreased sensitivity to trametinib when DUSP4 was deleted, increasing the IC50 from 2 to 3-fold (**Figure 55**). The other two cell lines, H2030 and H23, did not show any significative IC50 shift.

In our hands, $KRAS^{G12C}$ inhibitor sensitivity was not altered by DUSP4 deletion in the cell lines H23 and H358 (results not shown).

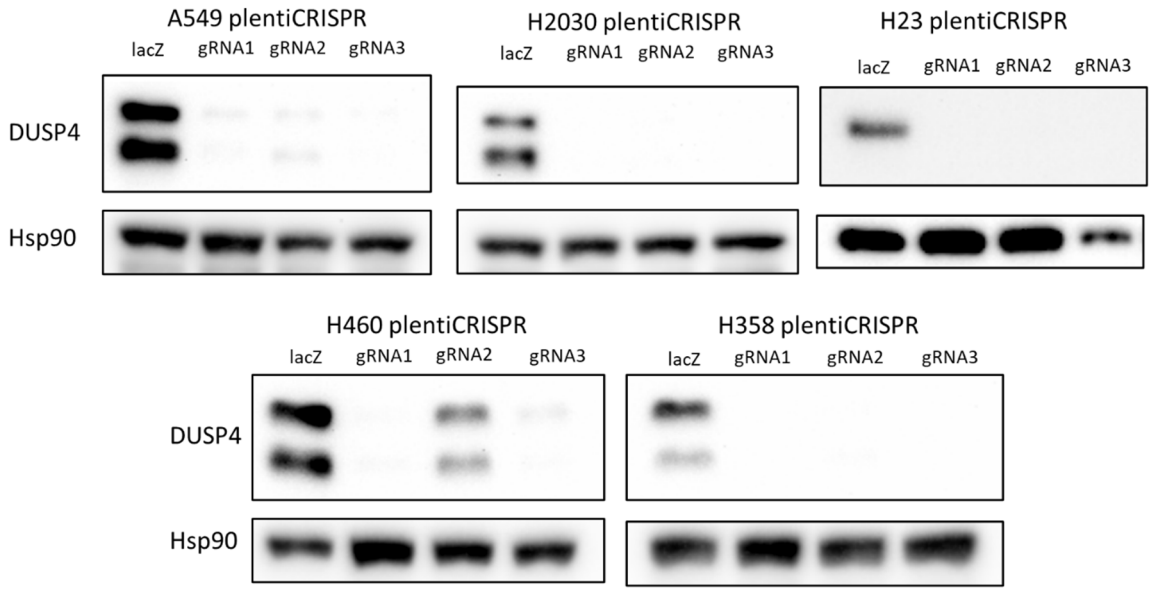

Figure 54. ***Knockout of DUSP4 in a panel of LUAD human KRAS mutant cell lines.*** *Western blot analysis revealed complete or partial deletion of the protein levels of DUSP4 two main isoforms, the canonical one at 42kDa and the secondary one at 34kDa.*

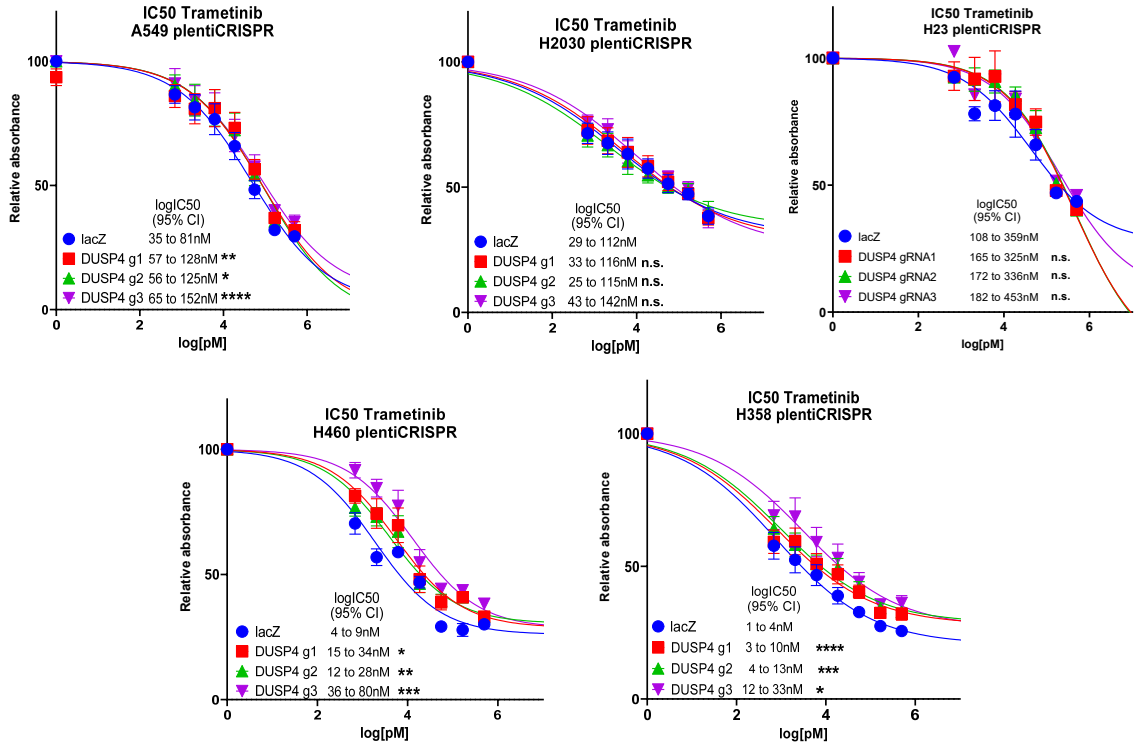

Figure 55. ***DUSP4 deletion results in an increased resistance to MEK inhibitor trametinib in a panel of human LUAD cell lines****. IC50s reflecting the sensitivity of each cell line in presence of plentiCRISPR DUSP4. Cells previously infected with the viral CRISPR vector were plated and treated with trametinib for 72h at increasing concentrations to determine the IC50, depicted as 95% asymptotic confidence intervals (CI). Mann-Whitney-Wilcoxon rank sum test comparing gRNA vs. Control, n=4. ****, p<0,0001; ***, p<0,001; **, p<0,01; *, p<0,05.*

Differential sensitivities to trametinib may derive from the altered MAPK levels generated by DUSP4 ablation (**Figure 56**). We analyzed response to trametinib at the phosphorylated ERK protein level and found that DUSP4 knockout H358 cells present increased levels of active ERK. Although the increase of phosphorylated ERK was less evident in presence of trametinib, this difference may explain the increased resistance in a subset of these cells to MAPK inhibitors.

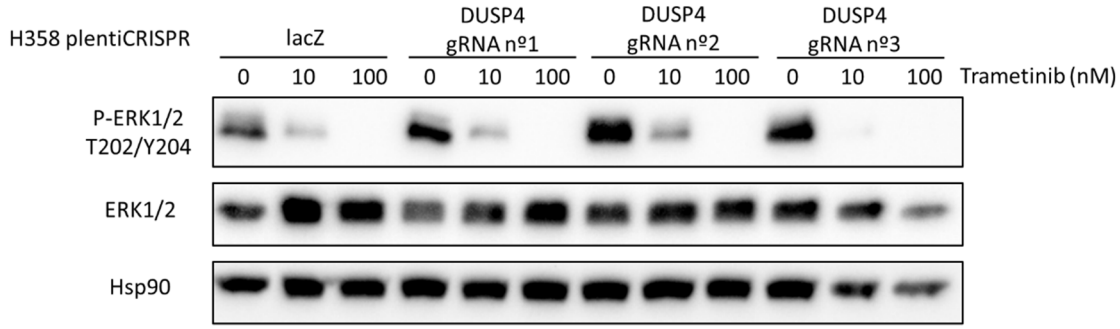

Figure 56. ***DUSP4 knockout cell lines have increased MAPK levels, presenting increased trametinib resistance****. H358 cell line infected with plentiCRISPR constructs targeting DUSP4 were submitted to increasing concentrations of trametinib.*

DUSP4 copy number gains are also frequent, in this case in the low MAPK cohort presenting the poorest prognosis. We wondered if, in the opposite direction than the knockout experiments, the gain of function of this protein could affect MAPK inhibitor response. For this purpose, we generated cell lines overexpressing a DUSP4 protein in a doxycycline inducible manner (**Figure 57**).

Overexpression of DUSP4 was achieved in H23 and H358 cell lines at 72h post-doxycycline addition. These levels of DUSP4 reduced the fraction of active phosphorylated ERK, confirming that DUSP4 is functionally reducing MAPK levels in this setting.

In these two cell lines, we evaluated the same set of inhibitors, including MEK inhibitor trametinib, and the most recent KRAS inhibitors adagrasib and sotorasib (as both cell lines are G12C mutant) (**Figure 58**).

The overexpression of DUSP4 sensitized only the H358 cells to trametinib. The H23 cell line presented a slight but non-significant alteration of the IC50 for trametinib. Surprisingly, we did also observe significant differences in resistance to $KRAS^{G12C}$ inhibitors, being the overexpression of

DUSP4 also a sensitizing agent, however we found notable differences between adagrasib and sotorasib agents depending on the cell line.

Taken together, these results may indicate that DUSP4 status may be a determinant factor for the efficacy of response to $KRAS^{G12C}$ MAPK inhibitors. High MAPK tumors that lack DUSP4 function, that may present a better prognosis than the average population, may present an increased resistance to these inhibitors and may benefit from alternative therapeutic strategies. However, the low MAPK tumors showing copy number gains of DUSP4, that show a poor prognosis, may be more susceptible to responding to MAPK inhibition.

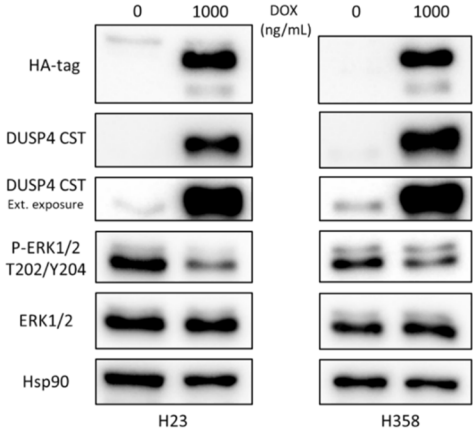

Figure 57. ***DUSP4 overexpression leads to reduced levels of MAPK activity****. Cell lines H23 and H358 were infected with a doxycycline inducible construct pCW57.1 harboring an HA-tagged DUSP4 cDNA. Puromycin resistant cells were then treated with 1 µg/mL of doxycycline for 72h.*

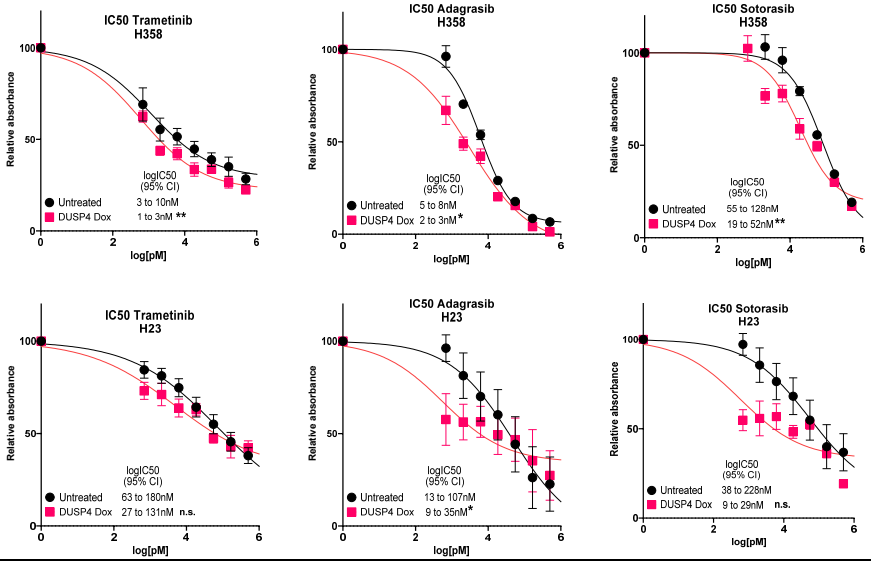

Figure 58. ***DUSP4 overexpression sensitizes LUAD cell lines to MAPK inhibitors****. IC50s reflecting the sensitivity of each cell line harboring the inducible DUSP4 in presence of 1 µg/mL of doxycycline. Cells previously infected with the viral pCW57.1 DUSP4-HA vector were plated, pre-treated for 72h with 1 µg/mL of doxycycline and then treated with increasing concentrations of the inhibitors for 72h. The IC50 is depicted as 95% asymptotic confidence intervals (CI). Mann-Whitney-Wilcoxon rank sum test comparing doxycycline-treated vs. Control, n=3. ****, p<0,0001; ***, p<0,001; **, p<0,01; *, p<0,05.*

3 TOXICITY DRIVEN BY MAPK HYPER-SIGNALING

The previously described DUSP4 results reinforce the importance of MAPK negative regulation during tumor initiation and progression. In this section, we sought to unveil the consequences of lacking proper MAPK negative regulation mechanisms, by overdriving MAPK activity and exploiting its consequent toxicities. Taking advantage of these phenotypes, we sought to perform an unbiased search for novel MAPK regulators that could help unravel the complex regulatory network that controls it all.

3.1 COMBINED KRAS AND BRAF INCREASE ON MAPK ACTIVITY IS LETHAL

3.1.1 Inducible KRAS activation drives MAPK hypersignaling in presence of $BRAF^{D594A}$

For this objective, we engineered an immortalized alveolar type II (ATII) cell line to harbor an inducible KRAS oncogenic mutant. This $KRAS^{G12V}$ mutant is fused to the estrogen receptor (ER) so its activatable by the presence of tamoxifen in the media. We combined this construct with the constitutive expression of $BRAF^{D594A}$ mutant that is able to enhance MAPK activity despite lacking kinase activity by transactivating CRAF during the dimerization process (Heidorn et al., 2010; Nieto et al., 2017). used previously (**Figure 59**).

In the absence of the kinase dead mutant, induction by tamoxifen generates an increase in KRAS effectors as seen by both phosphorylated ERK and phosphorylated AKT. Conversely, tamoxifen induction combined with the expression of BRAF D594A synergizes with KRAS activation and enhances MAPK responses, with further phosphorylated ERK levels, without generating an increase in phosphorylated AKT.

The ATII cells expressing BRAF D594A did not present any particular phenotype in the absence of tamoxifen (**Figure 60**).

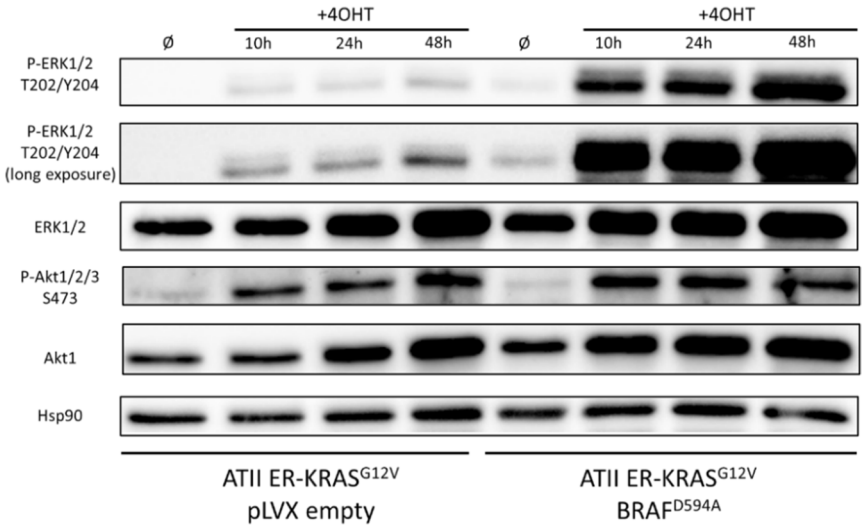

Figure 59. ***MAPK induction by the combined action of tamoxifen activatable KRAS and BRAF D594A.*** *Western blot analysis of the alveolar type II cells harboring KRASG12V-ER and BRAF D594A (or the empty backbone). Cells were treated for different timepoints with a single dose of 600nM 4-hydroxytamoxifen (4-OHT).*

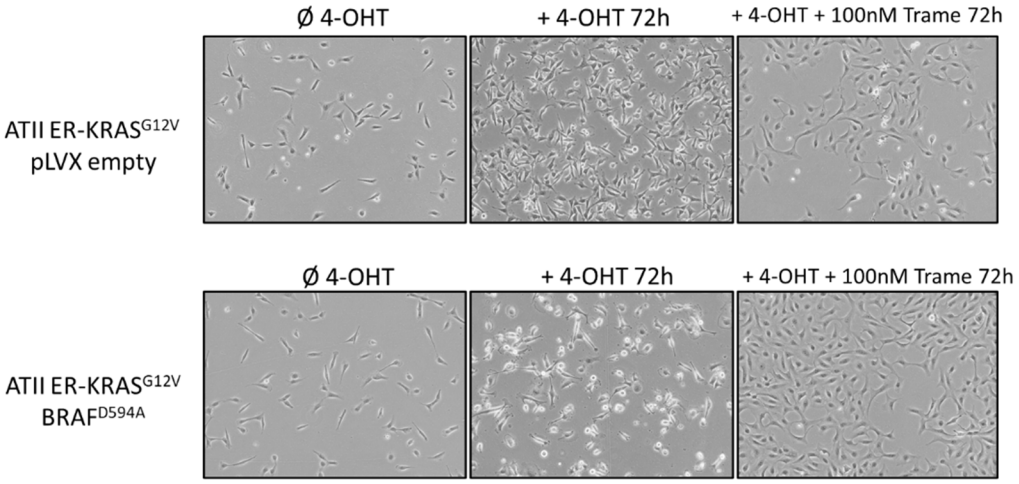

Figure 60. ***Activation of KRAS in presence of BRAF kinase dead results in a MAPK dependent cell death****. Inverted microscope image of a culture of the ATII cell line (10x), cultured in presence of tamoxifen 600nM and 100nM of trametinib for 72h.*

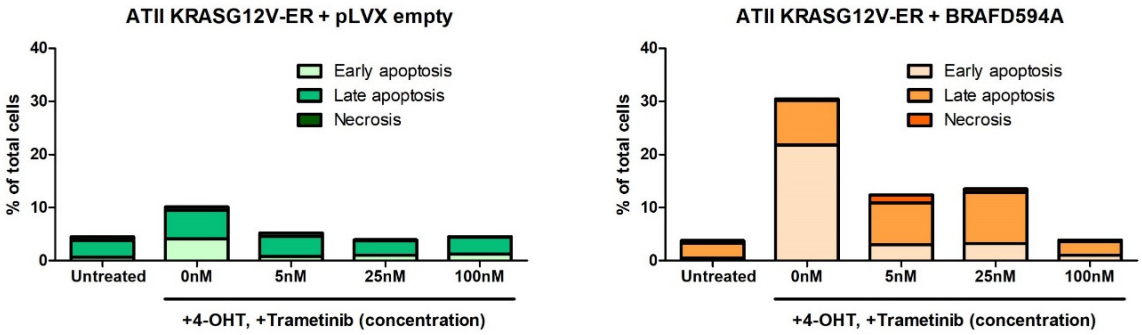

Figure 61. ***KRAS and BRAF activation leads to apoptosis in ATII cells.*** *ATII cells were treated with tamoxifen 600nM, and/or trametinib at the indicated concentration for 72h. AnnexinV-7AAD staining was used to determine apoptotic phenotype by flow cytometry [AnnV+/7AAD-, early apoptosis; AnnV+/7AAD+, late apoptosis; AnnV-/7AAD+, necrosis].*

In presence of tamoxifen, KRAS activity increases refringence of these cells, probably consequence of acquiring a malignant transformation phenotype. In contrast, when expressing the kinase dead mutant, cells start dying in a matter of 72h. While the KRAS active phenotype can still be seen in these cultures, the toxicity is such that no cells are able to survive long term tamoxifen induction. When trametinib is supplemented to the tamoxifen induction, the viability of these cells is rescued, confirming that this cell death was a MAPK-dependent phenotype driven by hypersignaling.

To illustrate this phenotype, we performed Annexin V/7AAD staining for apoptotic cell detection (**Figure 61**).

While little effect was seen by the single induction of KRAS, BRAF D59A ATII presented a considerable increase in the apoptotic fraction upon tamoxifen induction. Interestingly, increasing levels of trametinib were able to rescue these cells in a dose dependent manner, suggesting that MAPK-dependent apoptosis is controlled by tunable hypersignaling.

In an attempt to characterize the phenotypic cell death, we performed γH2AX detection in these cell lines to evaluate genomic stress (**Figure 62**).

Indeed, we were able to detect H2AX phosphorylation in the presence of both active KRAS G12V and BRAF D594A. Even the single activation of KRAS presented lesser levels of γH2AX, suggesting that KRAS activation can also present toxicities in these non-malignant cell settings.

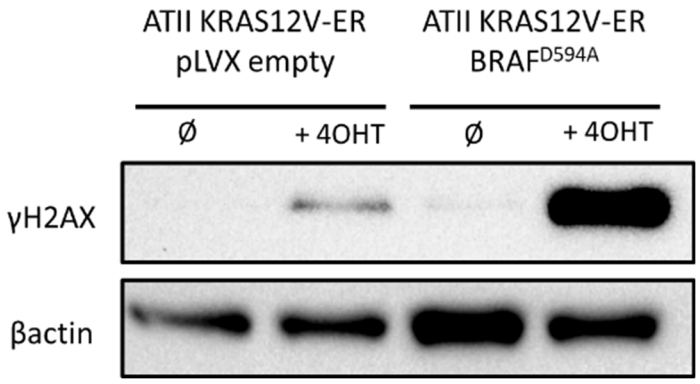

Figure 62. ***Triggered MAPK activity generates oncogenic stress.*** *Western blot image obtained after treatment of the ATII cell lines with 72h of tamoxifen.*

3.1.2 Dosing KRAS and BRAF up to mild MAPK-driven toxicities

Although the previous model allowed us to generate MAPK specific toxicities, these may not be amenable enough for finely detecting subtle changes driven by gain or loss of putative MAPK modulators. For the purpose of achieving further control on MAPK activity and the derived phenotypes, we introduced a doxycycline inducible version of the BRAF kinase dead D594A (**Figure 63A**). In this setting, we can achieve double control on KRAS and BRAF activity by dosing tamoxifen and doxycycline, respectively. We performed synergy matrixes to analyze how the combination could cooperate to enhance MAPK activity up to a toxic point (**Figure 63B**). An excessive tamoxifen concentration, resulting in overactive KRAS levels, results toxicity on its own, so we determined that the combination of 10nM of tamoxifen combined with 10ng/mL of doxycycline was the most appropriate for achieving a mild toxicity, but not fatal, driven specifically by MAPK. This mild toxicity will be required in the following part, for the screening, where the phenotype could be either rescued or aggravated in presence of gRNAs targeting specific MAPK regulators.

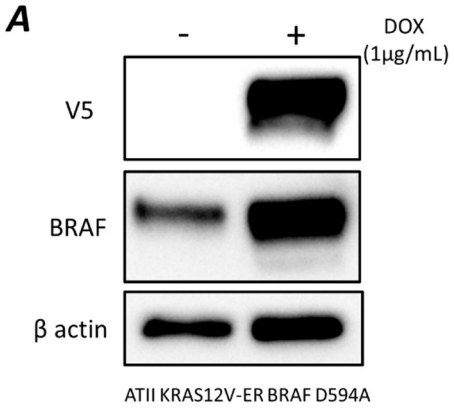

B

Synergy matrix (Normalized cell death)		Tamoxifen (nM)					
		40.0	20.0	10.0	5.0	2.5	0.0
Doxycycline (ng/mL)	40.0	0.17	0.37	0.63	0.85	0.84	0.99
	20.0	0.18	0.24	0.67	0.79	0.87	0.99
	10.0	0.07	0.11	**0.43**	0.96	0.86	0.95
	5.0	0.07	0.14	0.61	1.01	0.98	1.01
	2.5	0.10	0.19	0.73	0.99	0.96	0.98
	0.0	0.09	0.14	0.82	0.94	1.00	1.00

Figure 63. ***Inducible and precise doxycycline BRAF activation cooperates with KRAS induction and triggers mild toxicities.*** *(A) ATII KRASG12V-ER were infected with a doxycycline inducible BRAF D594A kinase dead mutant V5-tagged. (B) A synergy matrix was performed to compare the cell death produced by the combination of tamoxifen (inducing KRAS) and doxycycline (inducing BRAF). Cell death was evaluated at 1 week and normalized to the untreated condition, the value of 1.00 (green) refers to 100% of viability while a value of 0.00 (red) refers to 0% of living cells. The retained concentration was 10nM tamoxifen and 10ng/mL of doxycycline.*

Next, we evaluated if these concentrations recapitulated the desired MAPK activity by RT-qPCR, where we monitored the six-gene MAPK signature (**Figure 64A**). Upon tamoxifen induction, KRAS induces by its own the signature expression levels. However, combination of both tamoxifen

and doxycycline significantly escalates further the transcription of the six genes. The signature expression levels can be reverted by addition of trametinib in a dose-dependent manner, significantly abolishing the induction effect. These results were recapitulated at the protein level (**Figure 64B**).

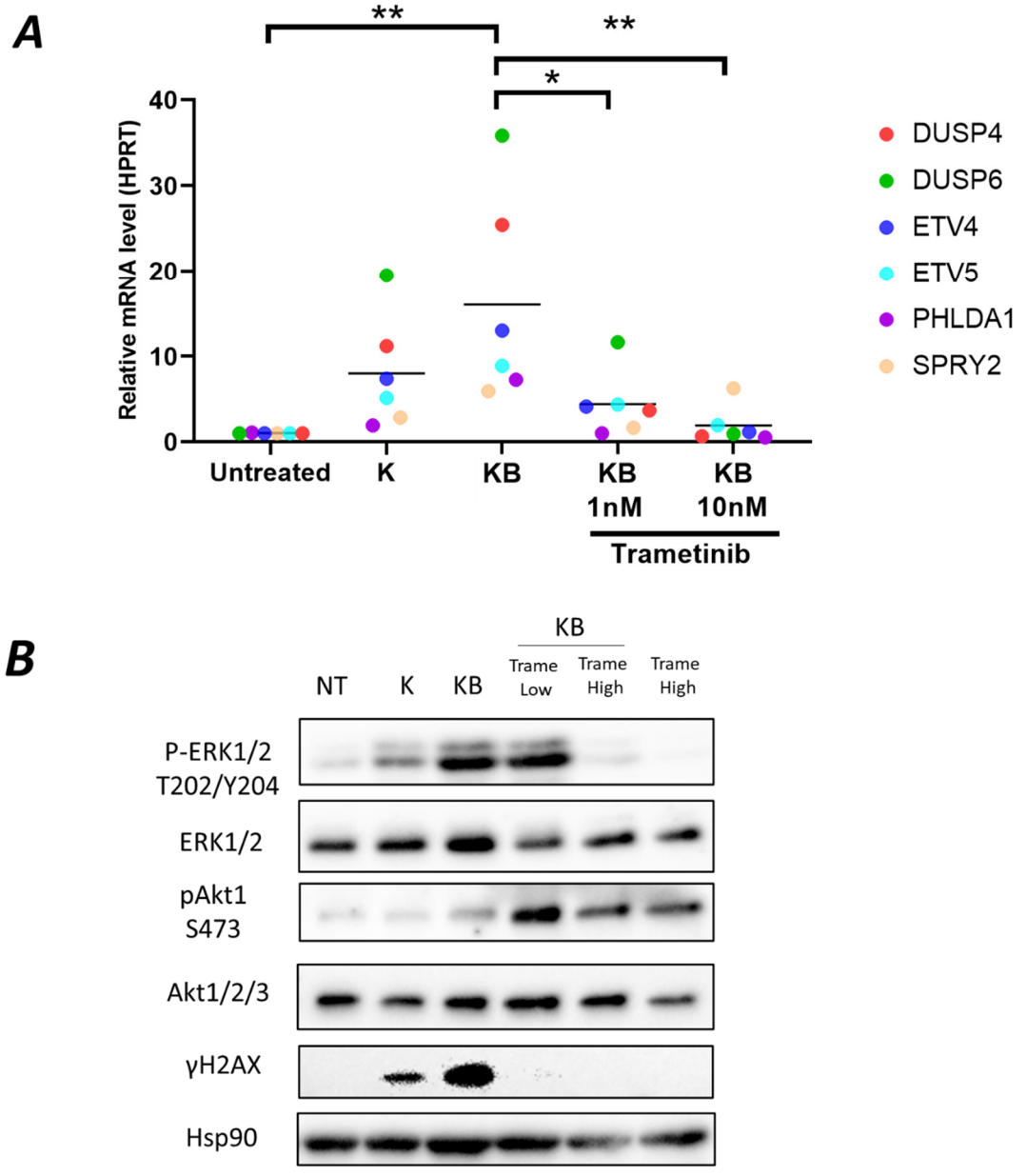

Figure 64. ***Combined induction of KRAS and BRAF induces MAPK levels and generates MAPK dependent genomic stress.*** *ATII KRAS12V-ER pCW57 BRAFD594A cell line was treated for 1 week [K, 10nM tamoxifen; KB, 10nM tamoxifen, 10ng/mL doxycycline; each condition in presence of Trametinib (low 1nM or high 10nM)]. (A) RTqPCR was performed on total RNA extracts, quantifying MAPK signature expression data normalized to HPRT expression and the untreated control. Each dot represents the mean of each gene's expression in three independent experiments (n=3). The great mean between the 6-gene signature is plotted. For multiple comparison analyses, one-way ANOVA followed by Tukey's **, p<0,01;*, p<0,05.*

Phosphorylated ERK levels increase with KRAS activity but are further enhanced in BRAF presence. Furthermore, trametinib action regresses phosphorylated ERK levels in all cases. We observed a sudden increase in phosphorylated AKT upon treatment with trametinib, that has already been described in the literature to be a crosstalk compensatory effect of increasing EGFR/PI3K activity upon MEK inhibition (Chandarlapaty, 2012; Novoplansky et al., 2023). On top of that, we detected γH2AX phosphorylation levels correlating with MAPK activity. This marker of genomic stress disappears in the presence of trametinib, reiterating over the fact that MAPK is the main producer of this stress phenotype.

Following this, we evaluated if the observed MAPK hypersignaling correlated with the appearance of stress phenotypes, as we had detected before. We performed apoptotic staining of these cells (**Figure 65**) to corroborate that apoptosis was dependent on both KRAS and BRAF activity, and that the viability could be rescued with trametinib in a dose dependent manner.

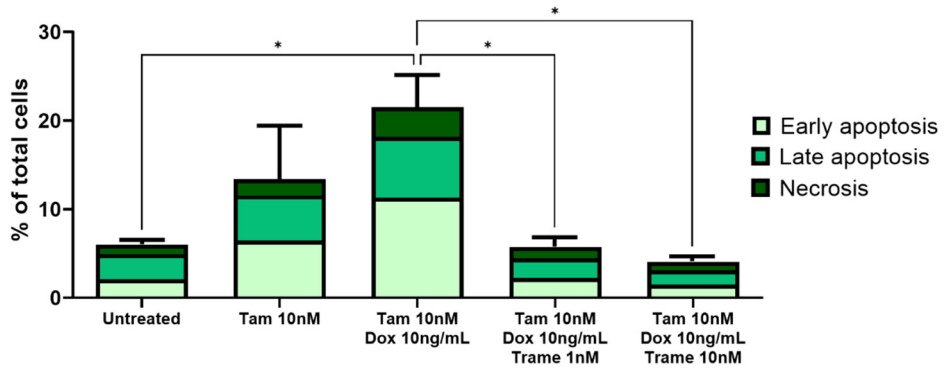

Figure 65. ***MAPK hypersignaling obtained from KRAS and BRAF induction generates MEK dependent apoptosis.*** *ATII cells were treated with tamoxifen, doxycycline and or trametinib for 1 week. AnnexinV-7AAD staining was used to determine apoptotic phenotype by flow cytometry [AnnV+/7AAD-, early apoptosis; AnnV+/7AAD+, late apoptosis; AnnV-/7AAD+, necrosis]. Total cell death was used for multiple comparison analyses, one-way ANOVA followed by Tukey's multiple comparison correction. *, p<0,05. n=3*

In consequence, these cells present a slower growth profile, resulting in almost arrested development (**Figure 66A**). MAPK hypersignaling hinders colony formation, and restoring endogenous MAPK levels completely rehabilitates cellular capabilities, as induced cells thrive in presence of trametinib (**Figure 66B**). We performed a cell cycle analysis of these populations and remarked a slight non-significant increase in the G2 fraction upon MAPK induction (**Figure 66C**), suggesting that the differences in growth and colony formation that are being described here are certainly more due to cell death than from a putative G2/M cell cycle arrest.

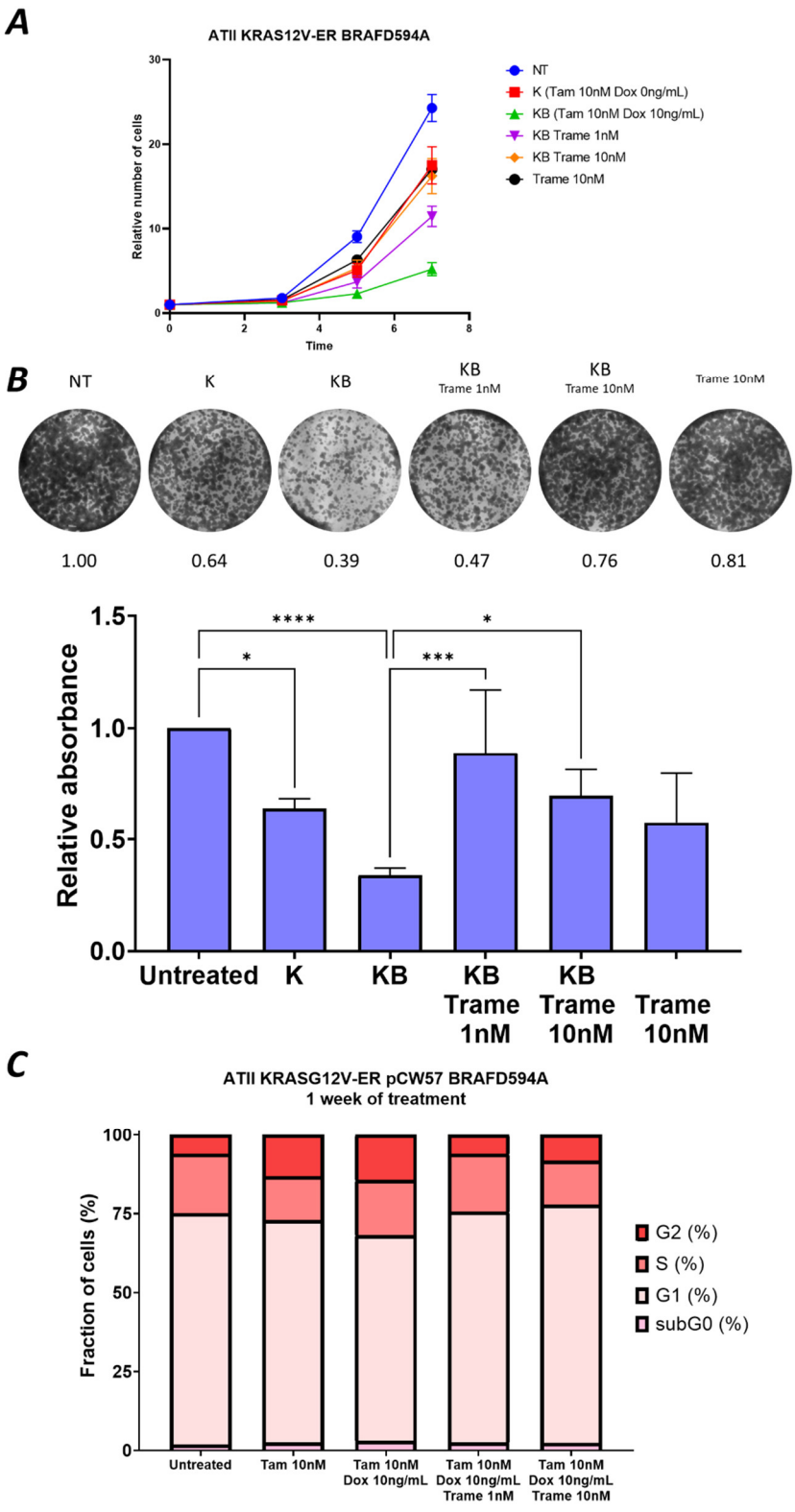

Figure 66. ***Excessive MAPK activity impairs cellular growth and limits colony formation without significantly affecting cell cycle****. ATII KRASG12V-ER BRAFD594A cell line growth was monitored by (A) MTT assay in presence of tamoxifen 10nM, doxycycline 10ng/mL and/or trametinib 1nM or 10nM. The same conditions were used to perform a colony formation assay at low density plating (B). 5000 cells were seeded in 6-well plates and were stained on Crystal violet at 2 weeks' time. The plates were lysed, and absorbance was measured for quantification. For multiple comparison analyses, one-way ANOVA followed by Tukey's ****, p<0,0001; ***, p<0,001; *, p<0,05. Quantitative levels are normalized to untreated control. n=5. Also, these conditions were used to follow cell cycle population distribution by propidium iodide staining.*

Taking together all the results obtained with the ATII cell line, we can conclude that our model generates high MAPK levels by an inducible KRAS and BRAF activation that generates mild toxicities. We will exploit these toxicities in the model to identify further MAPK candidate regulators in the next part of the manuscript.

3.2 INDUCTION OF MAPK ACTIVITY IS TOXIC IN A KRAS MUTANT CONTEXT

Building on the previous findings, we ought to confirm that these MAPK signals are coordinated and generate these toxicities also in a KRAS mutant tumoral context. To recapitulate the results previously observed with a BRAF kinase dead in presence of a KRAS mutant, we engineered the A549 KRAS mutant human cell line with the same inducible BRAF kinase dead D594A mutant.

With increasing doses of doxycycline, we are able to induce BRAF kinase dead protein levels significantly, having a quick impact in MAPK activation seen by ERK phosphorylation at 24h post treatment (**Figure 67**).

Effectively, this short induction is also capable of generating the transcription of the MAPK signature genes, with even the lowest concentrations presenting moderate induction of the expression of these genes (**Figure 68**).

Despite reaching these moderately increased MAPK levels, the pathway is not able to maintain this increase without consequence. Overexpression of this BRAF kinase dead protein is toxic in the A549 KRAS mutant context. We performed clonogenic assay from the lowest concentrations of doxycycline and remarked that these cells presented impaired growth from increasing concentrations of BRAF D594A (**Figure 69**), suggesting that these artificial levels of MAPK reach out from the *sweet spot* and result toxic.

We also performed a transcriptomic analysis of these cells overexpressing BRAF D594A, induced at 1 µg/mL for 24h. We confirmed activation of the MAPK pathway as the genes of the signature presented coordinated transcriptional expression (**Figure 70A**). In parallel, we performed gene set enrichment analysis and found the term *ERK1 and ERK2 cascade* (GO:0070371) significantly

enriched from the comparison of the treated cells versus the control (**Figure 70B**). All these results confirmed that MAPK hypersignaling by an hyperactive BRAF results is detrimental in a KRAS mutant cellular context.

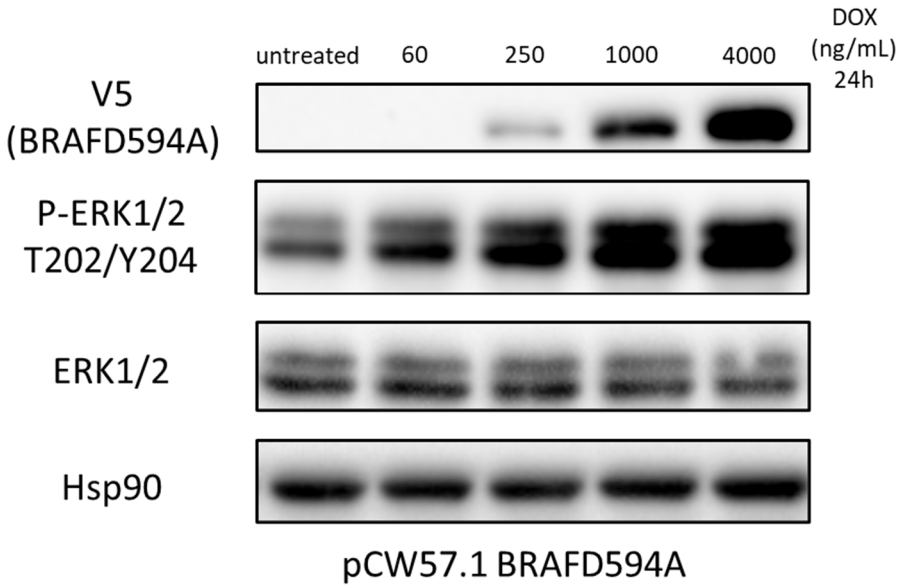

Figure 67. ***MAPK induction by BRAF kinase dead inducible expression****. A549 cell line infected with a lentiviral inducible BRAF kinase dead D594A mutant were treated with increasing doses of doxycycline for 24h.*

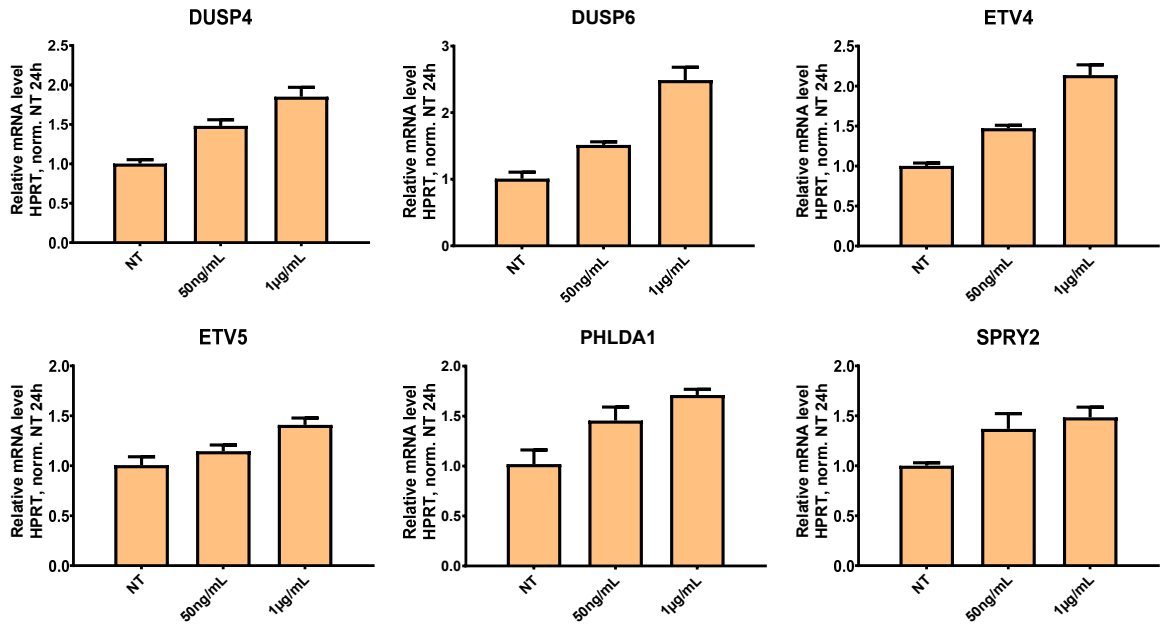

Figure 68. ***The transcriptional signature recapitulates how BRAF kinase dead mutant is able to activate MAPK levels****. A549 cell line harboring the inducible BRAF D594A mutant were submitted to 50 and 1000 ng/mL of doxycycline for 24 hours prior to evaluating MAPK signature expression by RTqPCR*

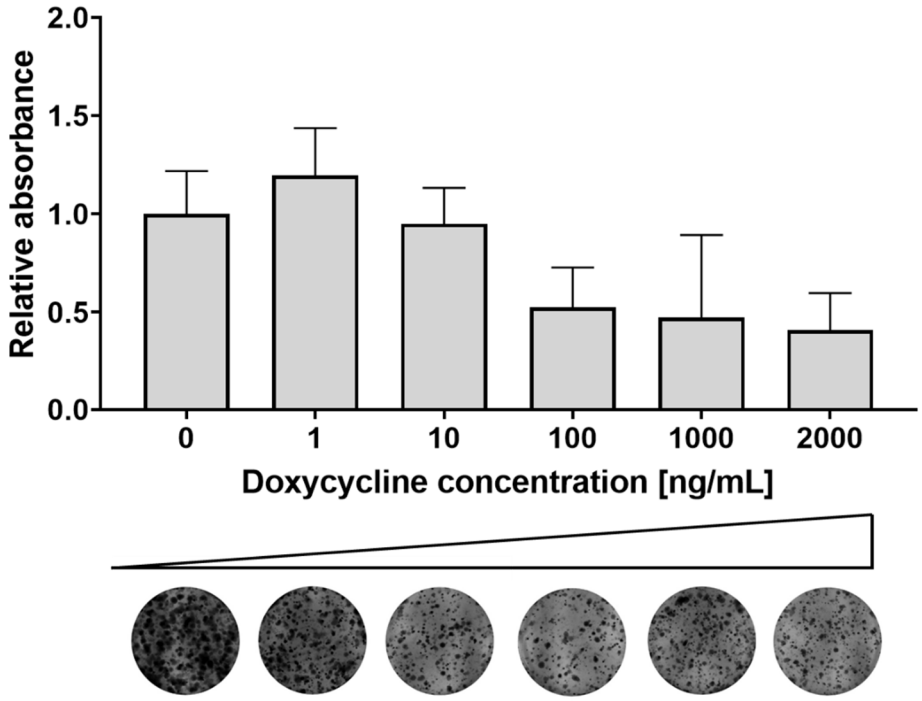

Figure 69. ***Overexpression of BRAF D594A results toxic in a KRAS mutant context****. Clonogenic assay of A549 cell line harboring the inducible BRAF D594A mutant treated with increasing concentrations of doxycycline for 1 week. Colonies were formed and pictures were obtained, then the wells were lysed and quantified.*

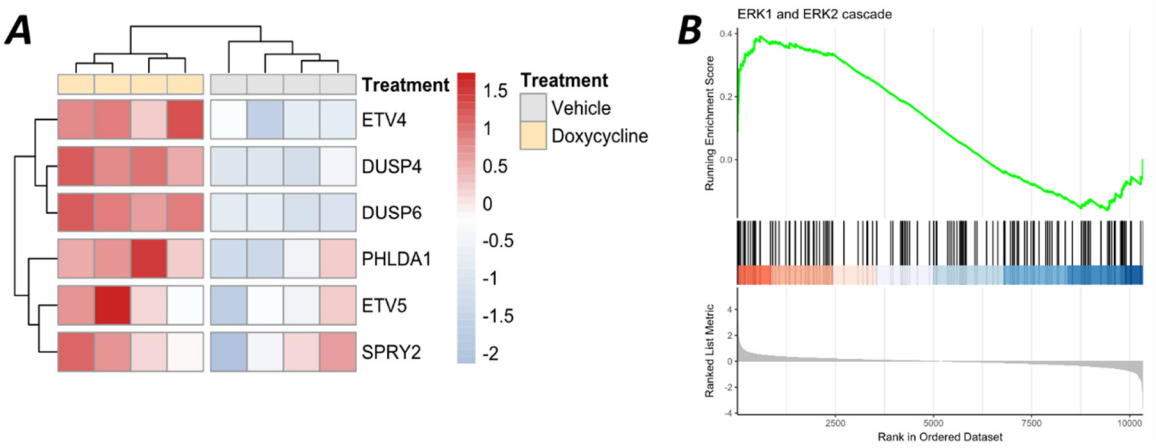

Figure 70. ***BRAF kinase dead activity conveys MAPK output****. (A) Heatmap depicting transcriptional signature levels with the BRAF D594A induction (scaled counts). (B) Gene set enrichment analysis obtained from the comparison of doxycycline versus control. We found that gene ontology term GO:0070371 was significantly divergent in the two populations.*

4 WHOLE GENOME SCREENING FOR MAPK REGULATORS

4.1 CRISPR/CAS9 MODEL ESTABLISHMENT

In our ATII model, we have achieved MAPK dependent mild toxicities by carefully titrating both the KRAS and BRAF components. In order to better understand the MAPK network and regulation, we sought to exploit this characteristic of the model to identify additional candidate regulators of the pathway. Indeed, we designed a CRISPR/Cas9 whole genome knockout screening using these toxicities to target potential MAPK regulators that could modulate these responses (**Figure 71**).

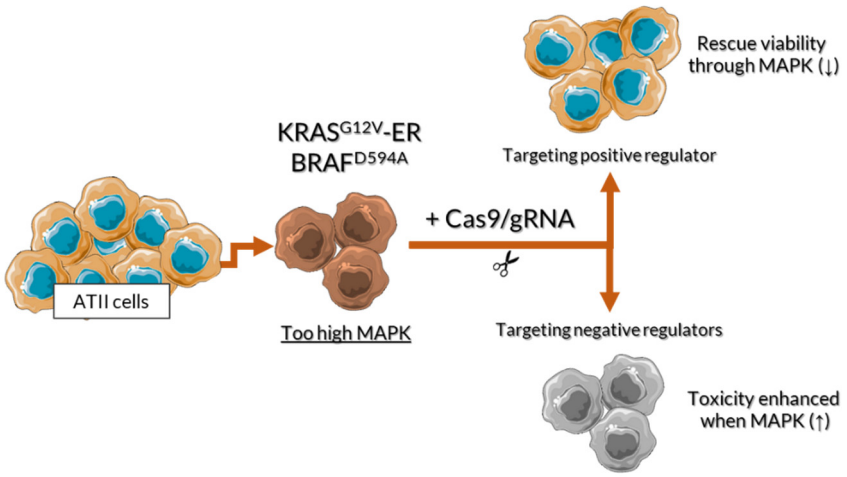

Figure 71. ***Exploiting the toxic effect of over-driving MAPK activity with CRISPR/Cas9****. Biological and functional principle of the enrichment and depletion of gRNAs depending on their effect on MAPK activity and/or toxicities.*

If we use a gRNA targeting a positive regulator of the pathway, the toxicity would be decreased and viability would be rescued, similarly as previously seen by trametinib treatment. On the contrary, a gRNA targeting negative regulators will enhance MAPK activity and the consequential toxicities. In the CRISPR screening scenario, the representation of these two types of gRNAs will evolve differently, being respectively enriched or depleted as selective pressures are established depending on the resulting MAPK levels. The following part of the manuscript will explain the strategy and the results obtained by this CRISPR screening.

We engineered the ATII cells, harboring the tamoxifen activatable KRAS and the inducible BRAF kinase mutant, to express the Cas9 protein. We performed the infection at different multiplicity of

infection (MOIs) concentrations (**Figure 72A**). While both presented correct Cas9 expression levels, we opted to select the cells infected with MOI 2.5, in order to avoid at a maximum any possible Cas9 mediated toxicities caused by non-specific activity of the endonuclease (Álvarez et al., 2022). For validating Cas9 activity function, we infected two gRNAs targeting a fluorescent reporter already present in the BRAF expressing vector, turboGFP, and monitored fluorescence decrease along two weeks (**Figure 72B**).

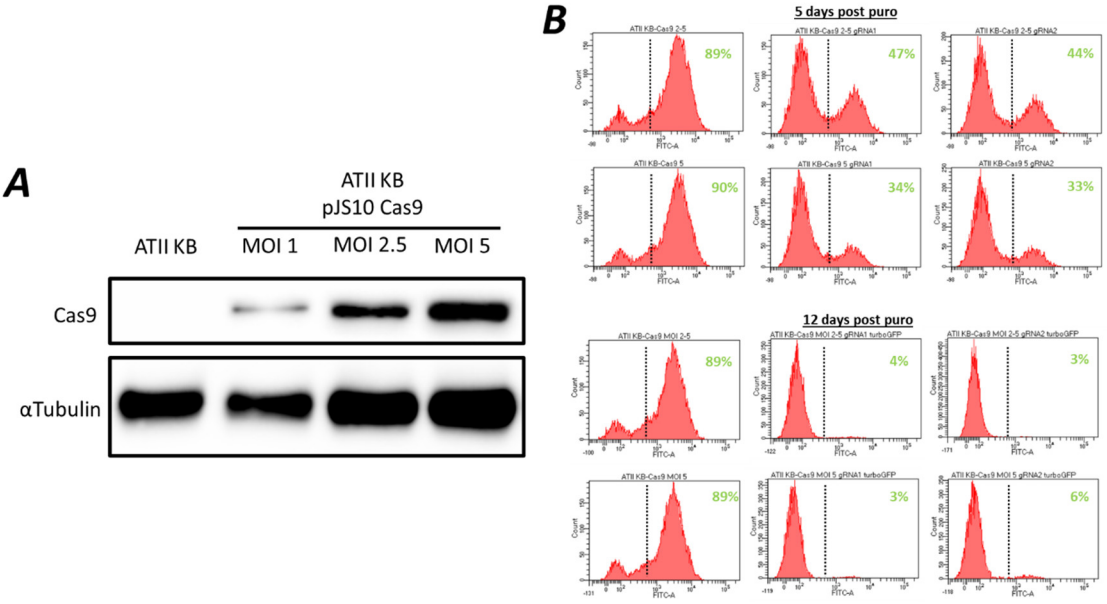

Figure 72. ***Cas9 editing function in ATII cell line.*** *(A) Western blot depicting the expression of the Cas9 protein in the ATII cell line, three different MOIs were used. (B) Flow cytometry analysis of turboGFP fluorescence across two weeks. ATII cell line (MOI 2.5 of lenti-Cas9) harboring a control gRNA (left column), gRNA n°1 (middle column) and gRNA n°2 (right column) against turboGFP.*

After puromycin selection of the lentiviral gRNA plasmid, we observed a considerable decrease of the number of fluorescent positive cells already at 5 days post-puromycin. This effect reached its peak at 12 days post-puromycin, as almost the entirety of the population ended being negative for the fluorescence. Thus, we determined that the time for the Cas9 to complete the editing and silencing function was two weeks. Cas9 expression did not alter the phenotypic characterization of the cell line through tamoxifen and doxycycline induction, obtaining the same MAPK dependent toxicity results as those obtained with the cells not harboring the Cas9 (results not shown).

4.2 SCREENING

4.2.1 In vitro establishment of screening conditions

Cas9-containing cells were thawed and infected with the Brunello library (Doench et al., 2016; Sanson et al., 2018), a lentiviral library harboring 4 gRNAs per gene, targeting the whole genome (see Methods for more details on the library). In order to ensure proper representation of the gRNA library, we decided to perform the screening at a 500X depth, meaning that each gRNA will be represented at least 500 times in the population before starting the screening.

Three different conditions were carried out in parallel, in order to compare their gRNA populations at the end (**Figure 73**).

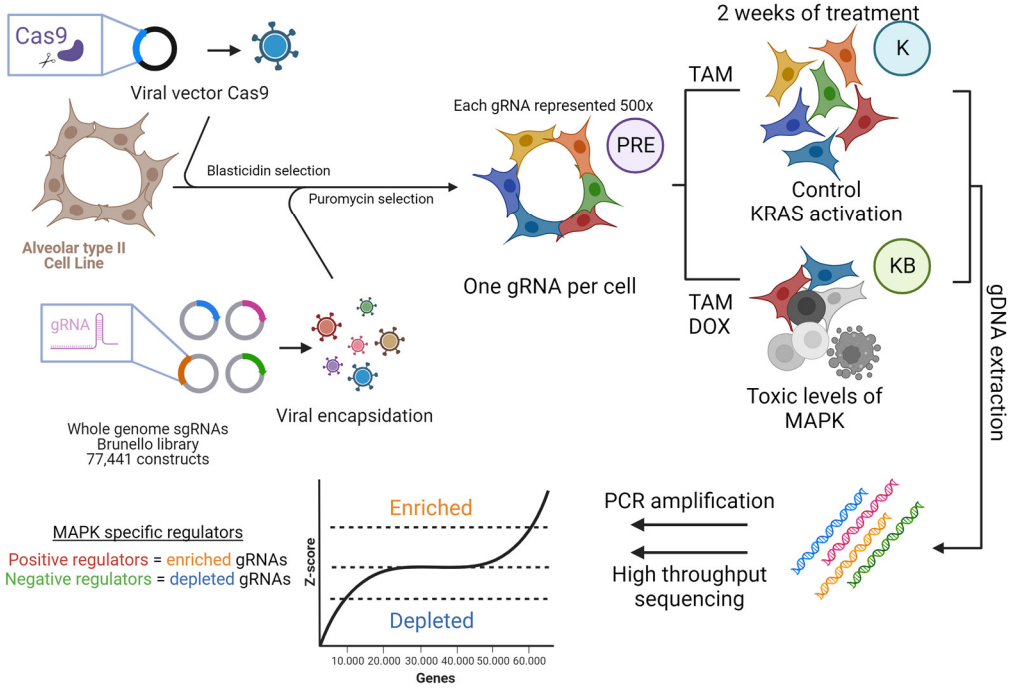

Figure 73. ***CRISPR screening strategy for identifying MAPK putative regulators in ATII cell line.*** *ATII cell line was infected with lentiviral particles for Cas9 expression and selected with blasticidin. Then, the lentiviral form of the Brunello library was used to infect the cells at an MOI of 3 to ensure that only one gRNA was present per cell. Puromycin selection was used to generate the screening cell line, that will always contain a representation greater than 500X during the whole process. The PRE condition represented the initial population, before treatment. Cells were treated with tamoxifen 10nM only (K) or tamoxifen 10nM and doxycycline 10ng/mL (KB) for two weeks. The gDNA of these cells was then extracted and PCRs were performed to extract the gRNAs. Then, Illumina sequencing was performed on the amplified fragments. According to our hypotheses, gRNAs enriched in the KB population when compared to the K condition would target positive regulations as they alleviate the toxicity generated by MAPK. On the other hand, gRNAs depleted in the KB condition would target negative regulators as they enhance MAPK levels and their subsequent toxicities.*

The first population, called PRE, did not undergo the treatment period as it will represent the status of representation of the gRNAs in the starting population, having eliminated gRNAs targeting common essential genes. The K population will act as a control of single KRAS activation, as it will be compared to the KB condition, that accounts for the double KRAS and BRAF activation. While the PRE condition will only serve to control gRNA population biases that could have been selected since the beginning, the comparison of KB vs. K conditions will result in the selection of gRNAs, either enriched or depleted in these conditions, that are specific for regulating the toxicity driven by the MAPK activity.

After genomic DNA extraction of all the conditions, we decided to opt for a nested PCR approach for amplifying the gRNAs prior to sequencing (**Figure 16**, more details in Methods). The protocol was optimized prior to performing the amplification directly from the entirety of the gDNA drawn from the screening. After purification of the last PCR products, the amplicons were used to perform targeted Illumina sequencing of the region of interest of the gRNAs.

4.2.2 Analysis reveals putative candidate MAPK regulators

After performing quality controls for the sequencing reads, we proceeded to the CRISPR screening specific bioinformatic analysis. We analyzed the three conditions in 4 series of sequencing samples. Principal component analysis of these samples efficiently separated the three different conditions, being the KB the most different one (**Figure 74A**). Then, we retained only gRNAs significantly enriched or depleted in either K or KB, when comparing with the control PRE (**Figure 74B**).

The bioinformatic analysis of the screening has been carried out through two different strategies. Two different algorithms (STARS and MAGECK, see Methods) have been used to compare the results and ensure that no statistical bias was introduced.

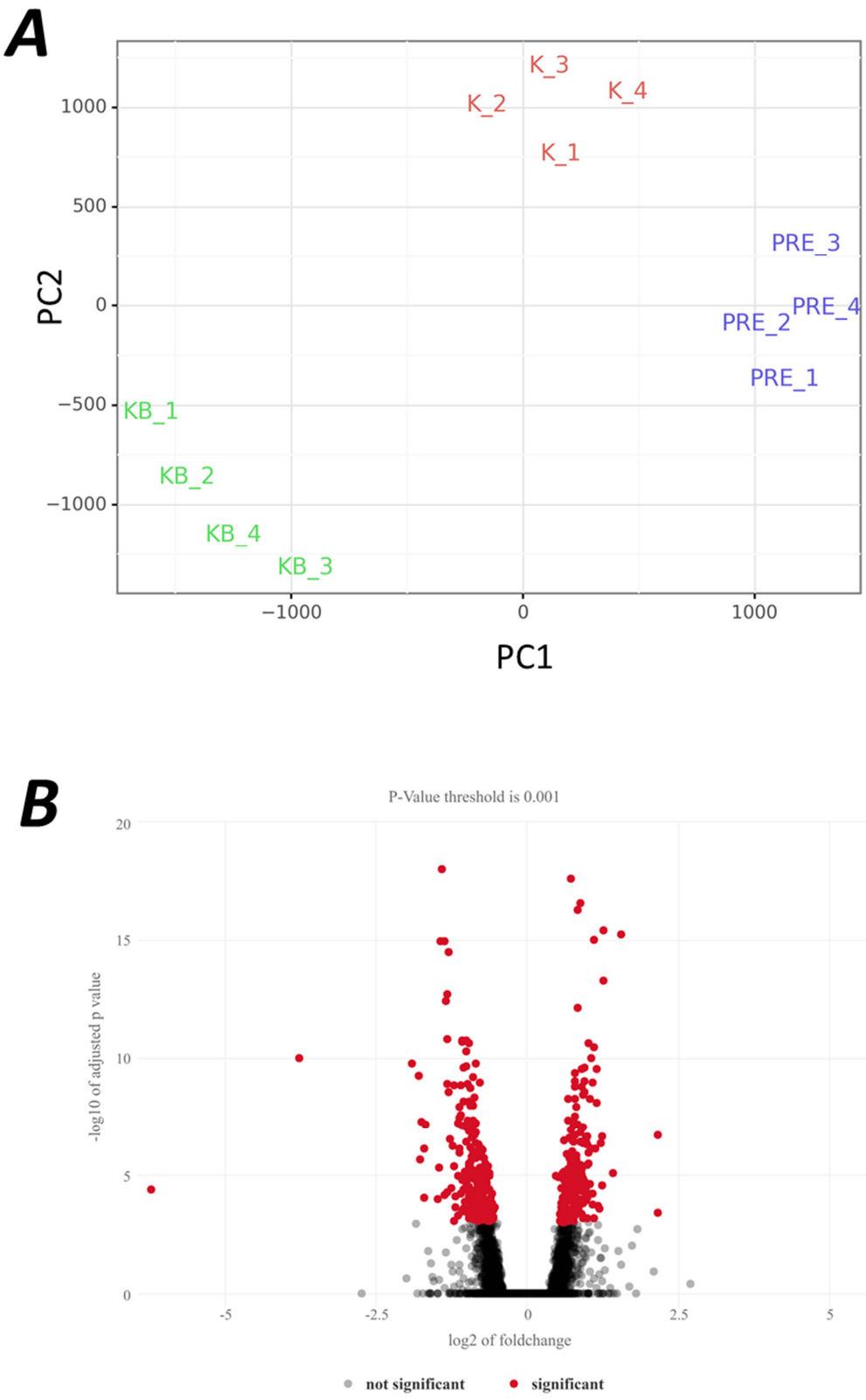

Figure 74. ***Screening results depict distinct gRNA enrichment patterns.*** *(A) Principal component analysis depicting the 4 series of sequencing batches per condition. (B) Differential volcano plot comparing gRNAs between PRE and KB conditions. In red are depicted the significantly enriched or depleted gRNAs.*

4.2.3 Enriched gRNAs

The enriched gRNAs have been selected through the screening process as they allegedly rescue the viability of the cells by targeting mediators of the apoptotic phenotype, either directly by controlling MAPK, or indirectly by other means. This hypothesis would suggest that a subset of genes obtained through this process could be potential positive regulators of the pathway.

By performing the STARS analysis, we obtained 273 sets of gRNAs to be significantly enriched. From those, we only accounted for 164 gRNAs, those that were present in the KB condition, as we wished to select for MAPK specific (and not only KRAS-mediated) gRNAs (**Figure 75A and 75B**).

In order to ensure that our analysis was coherent with our biological question, we searched and identified genes that directly affect MAPK activity, such as BRAF and CRAF, gRNAs that could unmistakably alleviate the selective pressure, thus validating our analysis.

Next, we performed enrichment analysis to identify several pathways directly related to RAS activity and cell cycle and mitosis hallmarks (**Figure 75C**), suggesting that these targets may mediate cellular process directly involved in relieving the replicative stress undergoing during KRAS and BRAF activation. Additionally, MAGECK analysis revealed a complementary list of targets, also containing the positive controls already mentioned, but including 40 novel genes that were also retained for literature search (**Figure 75D**). Additionally, we also identified enriched gRNAs targeting CDKN2A, a gene encoding for ARF and INK4A, two proteins directly regulating p53-mediated apoptosis (Honda & Yasuda, 1999; Schmitt et al., 2002). This result confirms the hypothesis that genes directly promoting cell death could also be selected in the gRNA depletion analysis.

Figure 75 (Right page). ***CRISPR screening KB enrichment analyses****. (A) STRING network depicting the enriched selection of gRNAs obtained from the STAR algorithm. (B) Venn diagram showing the shared gRNAs between the conditions K and KB. For the STARS analysis, only those present in the KB were considered as we want to work with MAPK specific targets. (C) Enrichment analysis obtained from the list of gRNAs coming from the STARS algorithm. (D) List of genes obtained from the MAGECK analysis. In red are positive controls for effectors of the MAPK pathway. In yellow, effectors of p53-mediated apoptotic signals, such as CDKN2A. TTC1 candidate is highlighted in purple.*

A **Enriched gRNAs**

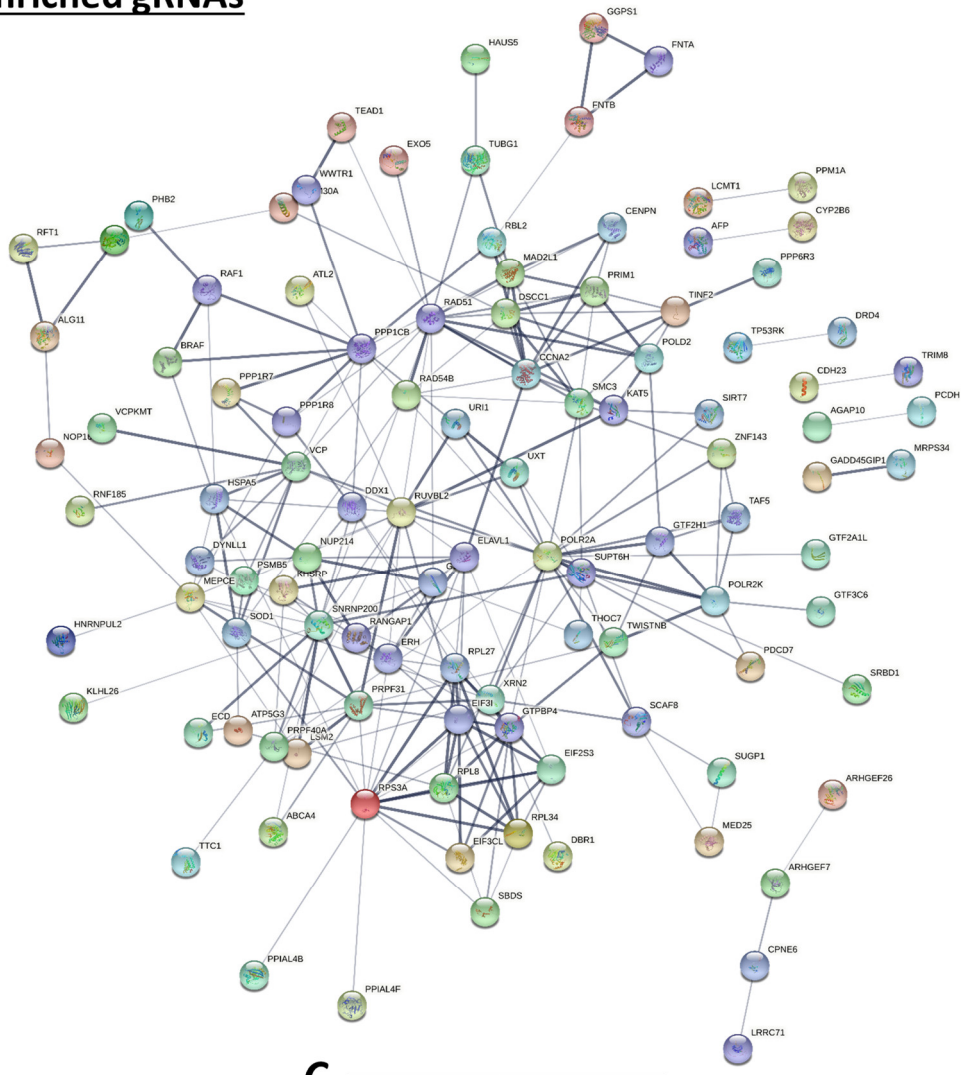

B

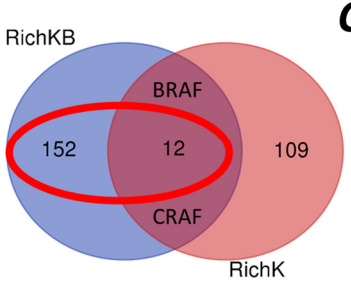

C

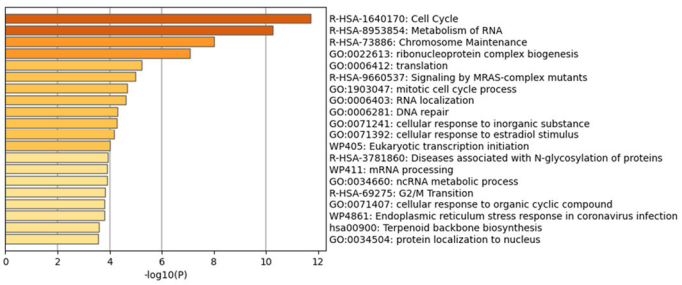

D **STARS**

ABCA4	AFP	AGAP9	ALG11	ALS2CR12	AQP5	ARL2	ARHGEF26	ARHGEF7	ARHGEF7	ATP1A1
ATP5G3	ATL2	BRAF	CDKN2A	CCNA2	CDH23	CENPN	CEP350	CF1A	CLCC1	CPNE6
CREB5	CREG2	CSF1	CYP20A1	CYP2B6	DDX1	DRD4	DSCC1	EIF2S3	EIF3CL	EIF3I
ELAVL1	ERH	EXO5	FAM161B	FNTA	FNTB	GADD45GIP1	GALNTL5	GAREML	GDF9	GGGX
GLE1	GOLGA6L1	GPR135	GPR151	GTF2A1L	GTF2H1	GTF3C6	GZMA	HAUS5	HEMGN	HNRNPUL2
KAT5	KHSRP	KIAA0895L	KLHL26	LCMT1	LOC100144595	LOXL3	LRRC71	MAD2L1	MED25	MEPCE
MPV17L	MRPS34	NFKBID	NIPAL1	NPIPB6	NOP16	NUP214	ORAOV1	PCDHB12	PDCD7	PHB2
PPIAL4A	PPIAL4E	PPP1CB	PPP1R7	PPP1R8	PPP6R3	PRIM1	PRPF31	PRPF40A	PSMB5	PSMG4
RAF1	RANGAP1	RBM26	RBL2	RILP	RNF148	RNF185	SCAF8	SCGB2A2	SDCCAG3	SH3D21
SIRT7	SLC13A3	SLC25A15	SMR3B	SMC3	SNRNP200	SOX4	SOD1	SSTR2	STC2	TEAD1
THOC7	TMEM101	TMEM30A	TINF2	TP53RK	TRIM8	TTC1	TWISTNB	UXT	URI1	USP17L30
VCP	VCPKMT	WNK1	WWTR1	XRN2	YARS2	ZNF143	ZNF185	ZNF626	ZNF841	C17orf74

E **MAGECK**

APOBR	ATL2	ATP1A1	ATP5G3	BRAF	C5AR2	C8orf44	CCNL1	CCT2	CDH23
CENPN	CEP97	CLEC19A	CLSTN1	CNNM2	CSTL1	CYP4F2	DDX46	DUSP4	EIF2S3
EIF3CL	ERH	FAM132B	FKTN	FZD8	GDF9	GOLGA6A	GOLGA8M	GPR135	GZMA
GZMB	HIBADH	HNRNPUL2	HSPA12A	HSPA5	IFNA13	IFNA21	IGSF3	IK	KAT5
KHSRP	KIF11	KIN	KRAS	KRT19	KRTAP9-3	LIN37	LINGO4	LUC7L3	MAPK1
MEF2D	MEPCE	MPV17L	MYO15A	MYO18A	NAPG	NDOR1	NF2	NPBWR2	NPIPA2
NPIPB6	NSMCE4A	OBSL1	PCDHB12	PEX6	POLD2	PPIAL4A	PPP1R7	PSMB5	RAD51
RAD54B	RAF1	RBL2	RILP	RPL38	RPL4	RPS10-NUDT3	RPS3A	RRP9	SDCCAG3
SLC13A3	SMC2	SMR3B	SNIP1	SNRPD3	STAT1	SUPT4H1	SYS1	TAF6L	TEX37
TLDC2	TMEM92	TTC1	TTC16	UCHL1	URB2	VCP	ZCCHC14	ZNF185	ZNF783

4.2.4 Depleted gRNAs

Depletion of gRNAs is a more complex process than the selective enrichment that we previously described. The only process where a complete set of gRNAs can be exhausted in this case is that the target gene is contributing to the viability of the cells during KRAS and BRAF activation, either directly by controlling MAPK, or indirectly by other means. This hypothesis would suggest that some of these targets could be negative regulators of the pathway.

Through the STARS analysis we obtained a total of 577 sets of gRNAs to be significantly depleted. Only 167 gRNAs were depleted in the KB condition only (**Figure 76A and 76B**), as we wanted to retain MAPK specific gRNAs.

Enrichment analysis detected hallmarks related with p38 MAPK and ferroptosis to be significantly modified in these samples (**Figure 76C**). The complementary list obtained by MAGECK introduced 30 additional genes for the literature search (**Figure 76D**).

In this case, we also sought to identify positive controls for our biological hypothesis, already known negative MAPK regulators whose gRNAs would be depleted. We noticed the presence of several phosphatases genes and regulatory subunits that could mediate important roles in regulating MAPK hypersignaling. Among these, we identified PP6, a MEK direct negative regulator that was recently described for its putative role in trametinib resistance (Cho et al., 2021), validating our hypothesis on having MAPK negative regulators gRNAs depleted. Additionally, we also identified gRNAs targeting MDM2, a negative regulator of p53-mediated apoptosis (Chen et al., 1998), to be depleted in the KB condition, confirming that genes directly inhibiting cell death could also be selected in the gRNA depletion analysis.

Figure 76 (right page). ***CRISPR screening KB depletion analysis*** *(A) STRING network depicting the depleted selection of gRNAs obtained from the STAR algorithm. (B) Venn diagram showing the shared gRNAs between the conditions K and KB. For the STARS analysis, only those present in the KB were considered. (C) Enrichment analysis obtained from the list of gRNAs coming from the STARS algorithm. (D) List of genes obtained from the MAGECK analysis. In red are positive controls for negative regulators of the MAPK pathway. In yellow, inhibitors of p53-mediated apoptotic signals, such as MDM2. TTC1 candidate is highlighted in purple.*

A

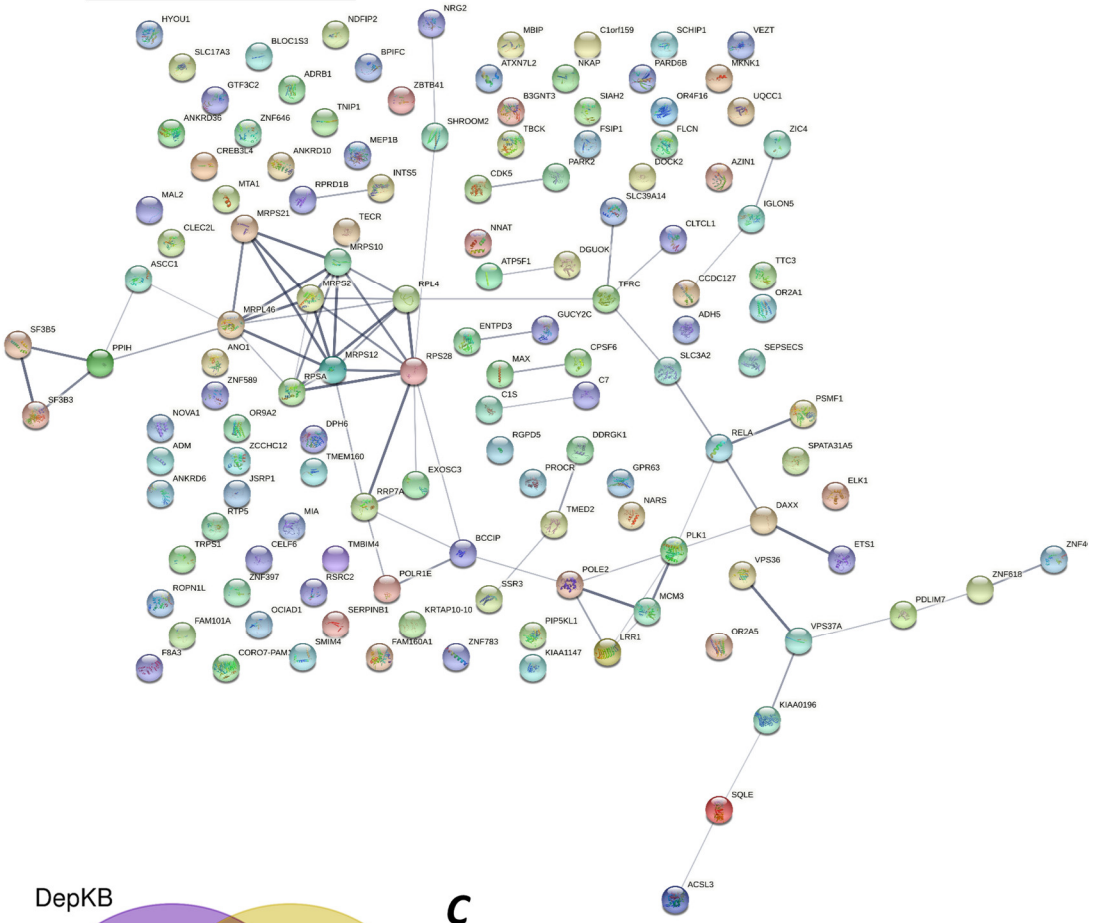

B

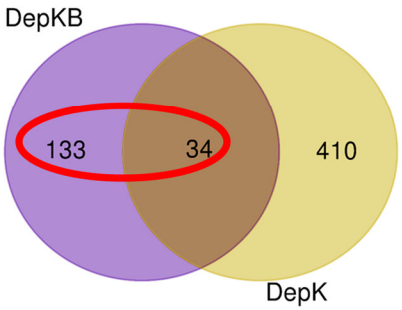

C

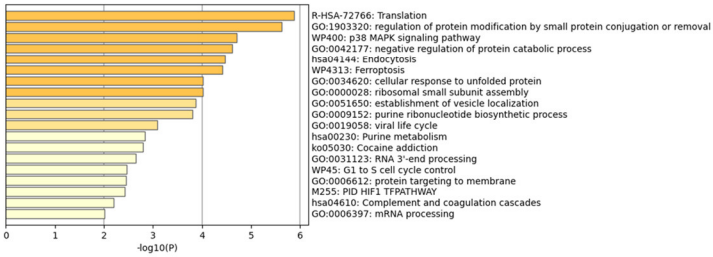

D

STARS

ACSL3	ADH5	ADM	ANKRD10	ANKRD36	ANO1	ATXN7L2	ATP5F1	B3GNT3
BCCIP	CDK5	CLEC2L	CLTCL1	CORO7-PAM16	CPSF6	CREB3L4	CSK	DAXX
DDRGK1	DGUOK	DOCK2	FAM101A	FAM160A1	FLCN	FSIP1	GPR63	GTF3C2
GUCY2C	HYOU1	IGLON5	INTS5	JSRP1	KIAA0196	KIAA1147	KRTAP10-10	LRR1
MCM3	MAX	MBIP	MEP1B	MIA	MKNK1	MRPL46	MRPS10	MRPS12
MRPS2	NARS	NDFIP2	NNAT	NOVA1	OR2A1	OR2A5	OR4F16	PARD6B
PARK2	PDLIM7	PIP5KL1	PLK1	POLE2	POLR1E	PROCR	RELA	RGPD5
ROPN1L	RPRD1B	RSRC2	SIAH2	SCHIP1	SEPSECS	SERPINB1	SF3B3	SF3B5
SHROOM2	SLC17A3	SLC39A14	SLC3A2	SMIM4	SNAI2	SPATA31A5	SSR3	TBCK
TECR	TFRC	TNIP1	TRPS1	TTC3	TSPY8	UQCC1	VEZT	VPS36
ZCCHC12	ZIC4	ZNF397	ZNF404	ZNF404	ZNF404	ZNF404	ZNF404	ZNF404
ZNF589	ZNF618	ZNF646	ZNF783	MDM2				

E

MAGECK

ABCA13	ABHD17B	ABHD6	AHRR	AMELY	ANKRD6	AZIN1	B2M	BLOC1S3	BMP10
C16orf95	C1S	C2orf44	C4BPA	CACNG2	CAPN6	CCDC152	CEP44	CFHR3	CRCT1
CSK	CT45A6	CTAGE8	CTBP1	CTBP2	DCAF16	DCDC5	DLK1	DOCK2	DTNA
EBF1	ELK1	EML4	ENKUR	FBXO44	FERD3L	FITM1	FKBPL	FOXP3	FRAS1
GUCA2A	GUCY2C	HSFY2	HTRA3	IGLON5	IGSF9B	KIF20B	KRTAP10-10	LDHAL6B	LZTFL1
MAB21L1	MGAT4A	MIA	MSMO1	MSR1	MTUS2	NR1H2	NRG2	OR2Z1	OR4B1
OR51G1	PARK2	PASD1	PCDHB10	PCDHGA11	PPP2R2A	PPP4CA	PPP6CA	RASA3	RBMY1J
RCAN3	RFX8	ROCK1	ROPN1L	RPA4	RWDD3	SCRN1	SERPINB1	SHC3	SLC15A4
SLC25A36	SLC38A9	SLC39A14	SSR3	TFPT	TFRC	TOP2B	TOR1B	TPD52L1	TPO
TREH	TRIM50	TTLL2	TTPAL	YWHAG	ZMYND10	ZNF397	ZNF404	ZNF813	ZP4

4.3 POTENTIAL NOVEL POSITIVE REGULATORS

Although the list of targets obtained through this process is large, some of them captivated our attention. After a literature search, we focused on genes that, based on the collected information, could potentially mediate MAPK signaling responses either directly regulating MAPK effectors or indirectly having an impact on a MAPK driven phenotype. From the enriched gRNAs list, we studied putative MAPK effectors and/or mediators of the toxicities obtained during the KB activation.

First, the occurrence of several orphan G protein coupled receptors (GPCR), GPR135, 151, 152, all proteins that present a wide number of alterations in cancer (Sriram et al., 2019); in the enriched gRNA list coming from the STARS analysis made us wonder if there was a GPCR contribution to the RAS/MAPK output. Several studies have pointed to the possibility of these particular GPCRs contributing to MAPK/ERK activity (Jiang et al., 2021; Morri et al., 2018), however GPCRs account for 4% of the genes in the genome and the redundancy between genes makes difficult to assess which GPCR could directly have an impact on the pathway. In the TCGA KRAS mutant LUAD cohort, we evaluated how the expression of these three genes affected patient prognosis. Only GPR135 presented a difference in patient survival, patients having low expression levels presenting better prognosis (**Figure 77**). However, these differences in expression did not present any correlation with the MAPK signature nor significant differential expression among the high or low MAPK patients (results not shown).

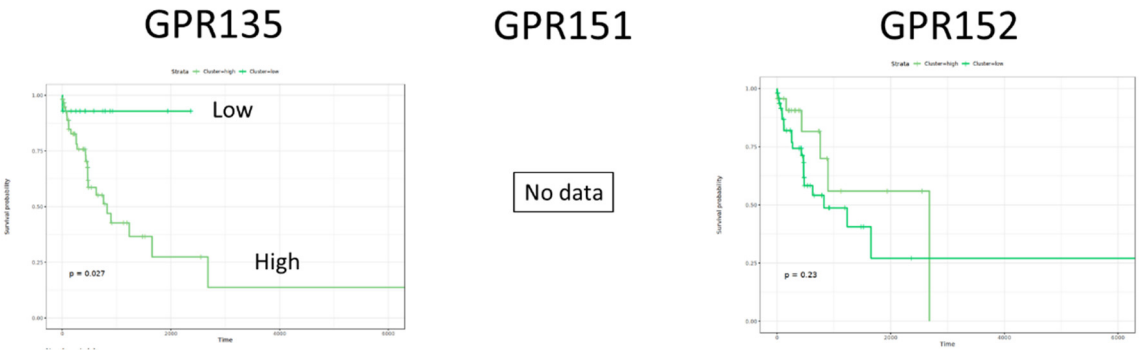

Figure 77. ***GPCRs effect on KRAS mutant LUAD patient prognosis are independent of MAPK signature effect.*** *We evaluated survival of patients from the TCGA cohort depending on the expression levels of GPR135, GPR151 and GPR152 (computed by the top and bottom expression quartiles in the population). GPR151 was not annotated in the transcriptomic data. Indicated p-value is from a Cox proportional hazards model.*

Because of the lack of evidence of these GPCRs possibly contributing to the MAPK signaling and the unapproachable redundance of this protein family, we decided to focus on an alternate candidate gene as a positive regulator of the pathway, TTC1.

4.4 REGULATORY ROLE OF THE ESSENTIAL GENE TTC1

Tetratricopeptide Repeat Domain 1, TTC1, is a membrane adaptor protein able to mediate RAS activation through alternative membrane signaling complex involving, for example, GPCRs (Kwan et al., 2012). The gRNAs targeting TTC1 were found significantly enriched in the KB condition, suggesting that this protein could act as a mediator of MAPK activity and could potentially contribute to the hypersignaling mediated toxicity.

For this gene, we also enquired the TCGA cohort and found that TTC1 expression (quartiles) separates two distinct populations in a survival analysis. Tumors that express high levels of TTC1 present worse prognosis than those that express lower levels of the gene (**Figure 78**), suggesting that TTC1 expression is a determinant event for KRAS mutant LUAD progression. Based on these results, we proceeded to the functional characterization of the protein in our biological model.

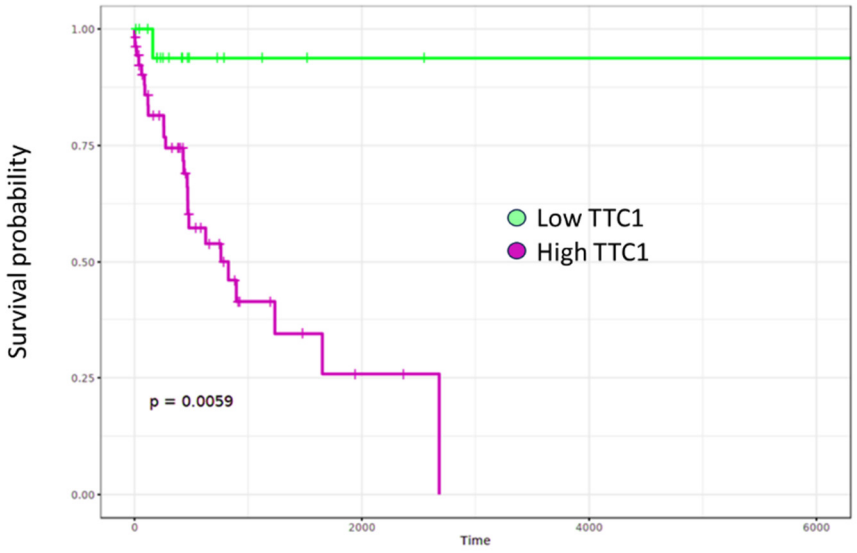

Figure 78. ***TTC1 shapes KRAS mutant LUAD patient prognosis.*** *We evaluated survival of patients from the TCGA cohort depending on the expression levels of TTC1 (computed by the top and bottom expression quartiles in the population). Indicated p-value is from a Cox proportional hazards model.*

To validate the hit, we engineered the ATII KB cells from the screening to contain three independent plentiCRISPR constructs targeting TTC1, different than those of Brunello library (**Figure 79**).

Concerning the MAPK effect of depleting TTC1, we observed a slight reduction in the fraction of phosphorylated ERK. These results would suggest that TTC1 exerts a MAPK effector role. However, we were not able to confirm these results when monitoring the signature levels by RTqPCR, as TTC1 deletion did not modify the expression of the 6-gene signature in the asynchronous ATII cell line (results not shown).

We continued to validate the effect of TTC1 deletion by evaluating if the screening conditions could be recapitulated, meaning that TTC1 depletion should contribute to relieving the toxic pressure of excessive MAPK levels (**Figure 80**).

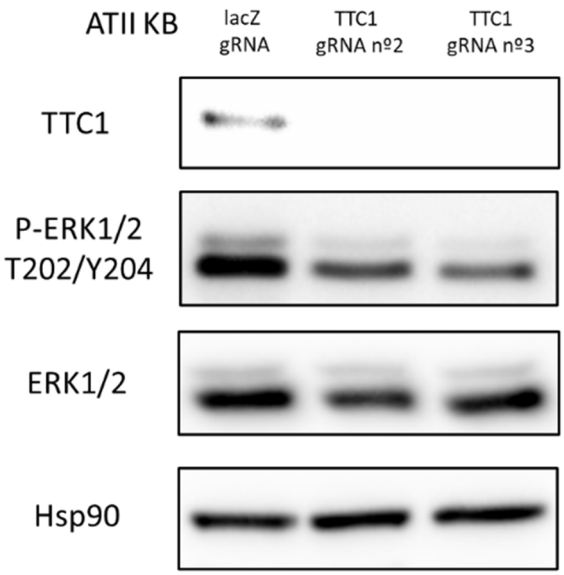

Figure 79. ***TTC1 deletion in ATII KB cell line****. Western blot analysis of alveolar type II cell line harboring the KB constructs infected with plentiCRISPR gRNAs targeting TTC1. The cells were infected then selected with puromycin for a week before generating the lysates from the asynchronous cell culture. A construct harboring non-targeting gRNAs against the bacterial lacZ was used as a control.*

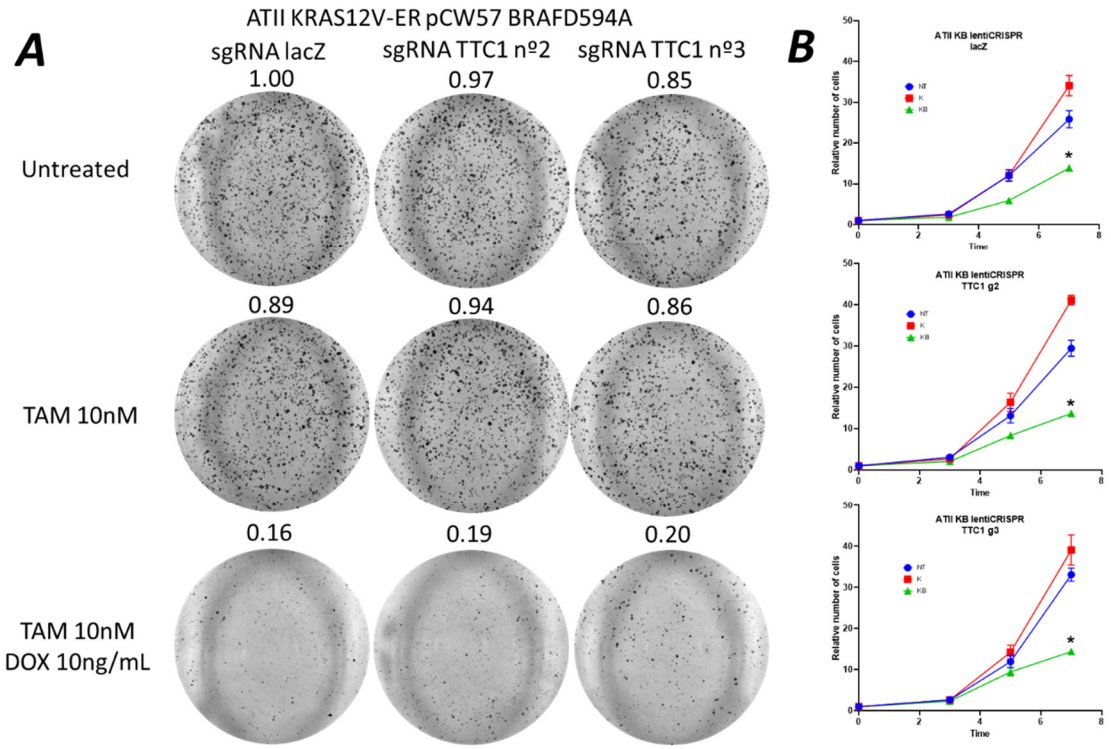

Figure 80. ***TTC1 depletion does not modify the effect of MAPK dependent toxicities.*** *ATII cell lines harboring gRNAs targeting TTC1 were submitted to tamoxifen and doxycycline conditions that induce toxicity. (A) Colony formation assay in 2D, cells were plated in 10mm plates and treated for 2 weeks with the selected concentrations of tamoxifen and doxycycline. Then the colonies were stained with crystal violet and the picture was taken. The number of colonies obtained was quantified by ImageJ and normalized to the untreated lacZ control (B) Cell growth (number of cells) was monitored in the same conditions during a week with an MTT assay. For comparison, one-way ANOVA with Dunnett's multiple comparisons test (with the NT control), * p-value < 0.01, n=3. No difference was observed when comparing the gRNAs vs. lacZ control.*

To our surprise, TTC1 depletion did not affect the sensitivity of the ATII cells to MAPK activation. We treated the cells with the same concentrations previously established in the cell line to generate MAPK inducible cell death. By combining tamoxifen and doxycycline at these concentrations, lacZ control cells presented the expected cell death phenotype. However, the cells carrying TTC1 targeting constructs presented the same toxicities, and cell death was not aggravated nor relieved by TTC1 absence, both in colony formation assay (**Figure 80A**) or asynchronous growth in presence of the activating agents (**Figure 80B**). These results do not recapitulate the biological meaning behind our screening.

To better understand how TTC1 could have been selected in the screening process, we decided to perform the knockout in KRAS mutant LUAD cell lines (**Figure 81**).

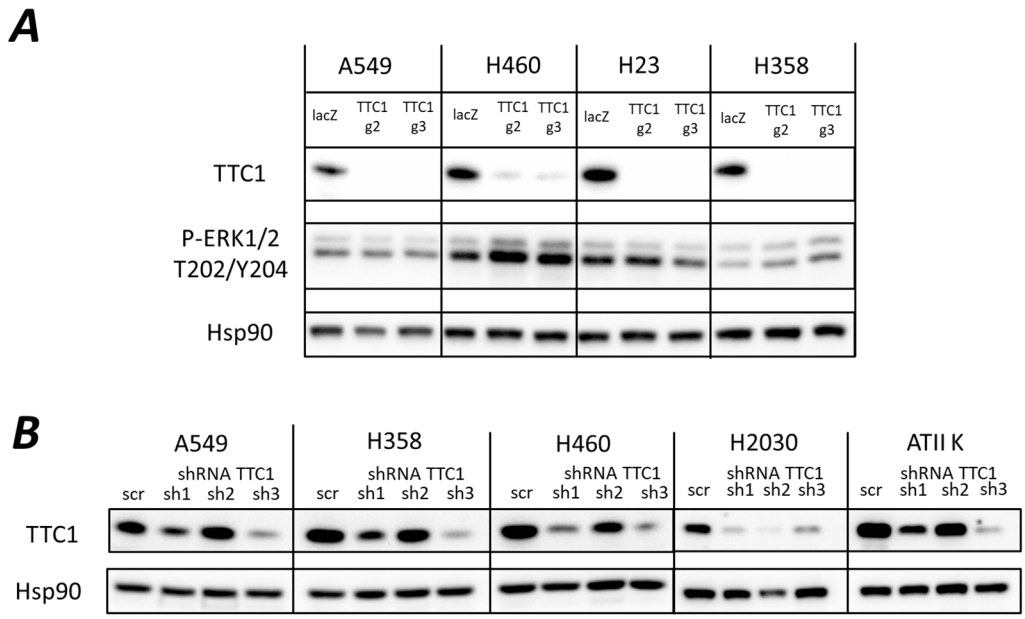

Figure 81. ***Validation of TTC1 depletion both gRNAs and shRNAs on LUAD cell lines.*** *Cell lines were infected with lentiviral constructs (A) plentiCRISPR and (B) Doxycycline inducible shRNA Tet pLKO targeting TTC1, where cells were treated with doxycycline 1 µg/mL for 72h.*

An efficient depletion of TTC1 was achieved with the constructs carrying gRNAs. However, we evaluated how TTC1 depletion could affect phosphorylated ERK levels and realized that ERK activity was inconsistently modified depending on the cell line (**Figure 81A**). Indeed, only in the H460 cell line we were able to detect that the deletion of TTC1 increased phosphorylated ERK levels, while the rest of the cell lines were unmodified. This was in contradiction with the results obtained in the ATII cell line and with our initial hypothesis of TTC1 possibly acting as a positive effector of the MAPK pathway.

To confirm these results, we performed TTC1 inhibition by doxycycline inducible shRNAs (**Figure 81B**). Upon doxycycline induction, TTC1 decrease was either incomplete or inexistant. During this experiment, we realized that this incomplete inhibition could be partially explained as we noticed that shRNA induction was systematically toxic.

This toxicity was confirmed in a 2D growth assay (**Figure 82**). In this assay, we confirmed that activation of the shRNAs targeting TTC1 at a standard dose of doxycycline was toxic in every KRAS mutant cell line that we tested. These results were also confirmed in the cell lines carrying the CRISPR gRNA constructs (results not shown).

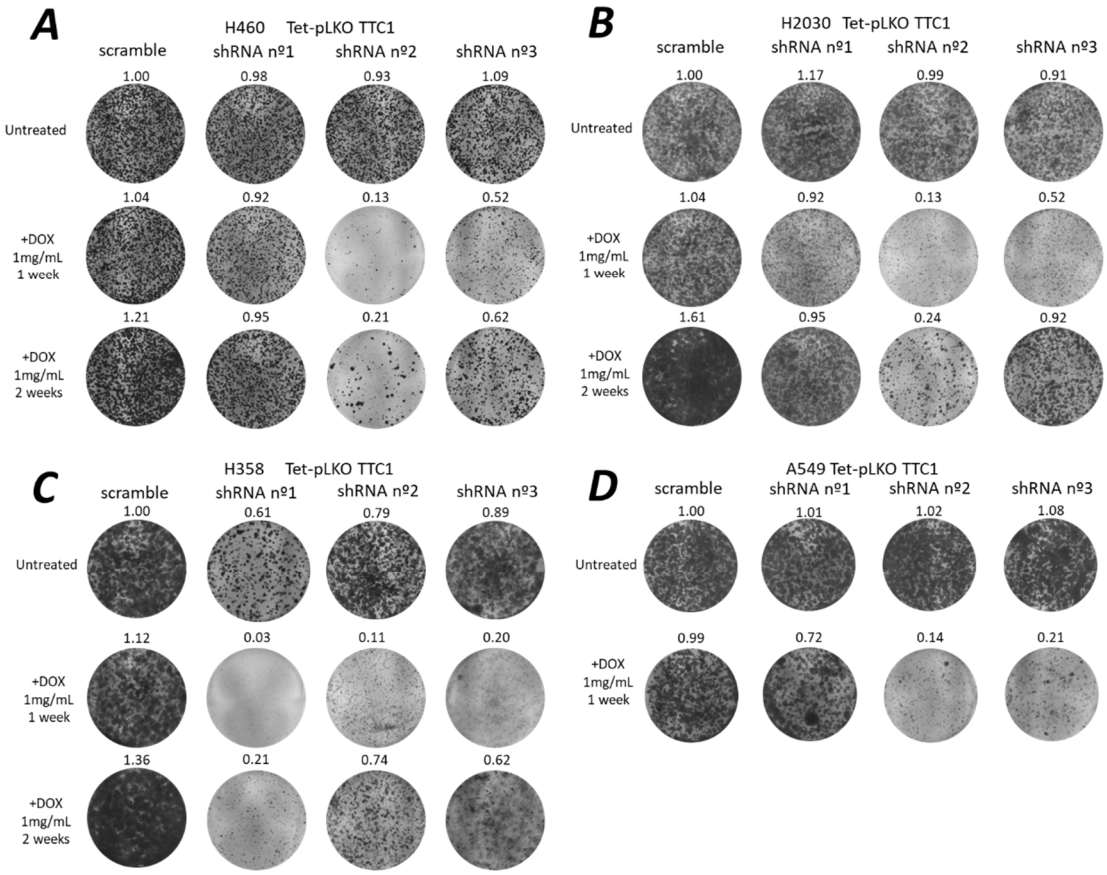

Figure 82. ***TTC1 inhibition by inducible shRNA is toxic in a panel of KRAS mutant LUAD cell lines.*** *Cells were infected with the Tet pLKO to express in a doxycycline inducible manner three different validated shRNAs obtained from the MISSION initiative from the Broad Institute. Cell lines (A) H460, (B) H2030, (C) H358, (D) A549 were plated at low density to perform colony formation assays and crystal violet staining. For a 1-week assay, 5.000 cells were plated, while for a 2-week assay 1.000 cells were plated. The control depicted here corresponds to a 1-week untreated condition. Quantification was performed and normalized to the untreated condition.*

In the screening PRE condition, we confirmed that TTC1 gRNAs were not depleted after the puromycin selection of the library of the ATII cells. This information suggests that this gene may not be essential in this cell line, but we still wondered about the essentiality of this gene in tumoral cell lines. We consulted both the DepMap repository and the Database of Essential Genes for TTC1 dependency data in a vast panel of cell lines. The CERES CRISPR score for TTC1 indicates that the effect of this gene is strongly selective, and the DepMap study concluded that 99% of the cell

lines presented at least a moderate dependency on the gene. Furthermore, the Database of Essential Genes has flagged TTC1 as a common essential gene in some human cell lines (Luo et al., 2020).

After this finding, we concluded that TTC1 was not a suitable candidate for further analysis. The fact that ATII finished the screening treatment with enriched levels of TTC1 gRNAs may be related to a selectivity based on essentiality and not MAPK activity.

4.5 Alternative Negative regulators

From the depleted gRNAs list, we studied genes that could negatively affect MAPK activity and/or be gatekeepers of the KB mediated toxicities.

We identified RASA3, a RAS-GAP that processes the active GTP-bound form of RAS and renders it inactive (Kitajima & Barbie, 2018; Li et al., 2019). Although RASA3 may not be exclusively involved in MAPK activity, KB cells presented RASA3 gRNAs depletion while K cells did not.

We also identified DOCK2 as a depleted gene. DOCK2 is a RAS like-protein that activates RAC GTPase and could even mediate the activation of MAPKs (Ji et al., 2022). Although DOCK2 presents multiple alterations across many tumor types, its activity is highly dependent on chemokines and activated by the immune compartment in a context-dependent manner (Guo & Chen, 2017), making it difficult to dissect its putative role as a MAPK regulator.

Finally, we focused on C-terminal SRC kinase, CSK. This protein is a key negative regulator of the non-receptor membrane SRC family kinases (SFKs). CSK is a kinase that phosphorylates inhibitory residues of SFKs, including the Y527 residue located in the protein c-SRC (Okada, 2012). We wondered if CSK functions were limited to SRC inactivation, and, even if RAS-SRC pathway crosstalk can occur, we sought to evaluate if CSK was able to modulate MAPK activity as suggested in the screening results.

4.6 CSK ENGAGES IN MAPK MODULATION (IN)DEPENDENTLY OF SRC

4.6.1 Hit validation in ATII KB

The gRNAs targeting CSK were found to be significantly depleted in the KB condition, suggesting that this protein could act as a negative regulator of MAPK activity and could therefore have a pro-survival function in the context of elevated MAPK activity.

First, we validated the screening results in the same ATII cell line. We engineered the cells with a plentiCRISPR plasmid targeting CSK with three independent gRNAs (**Figure 83A**), successfully eliminating CSK at the protein level.

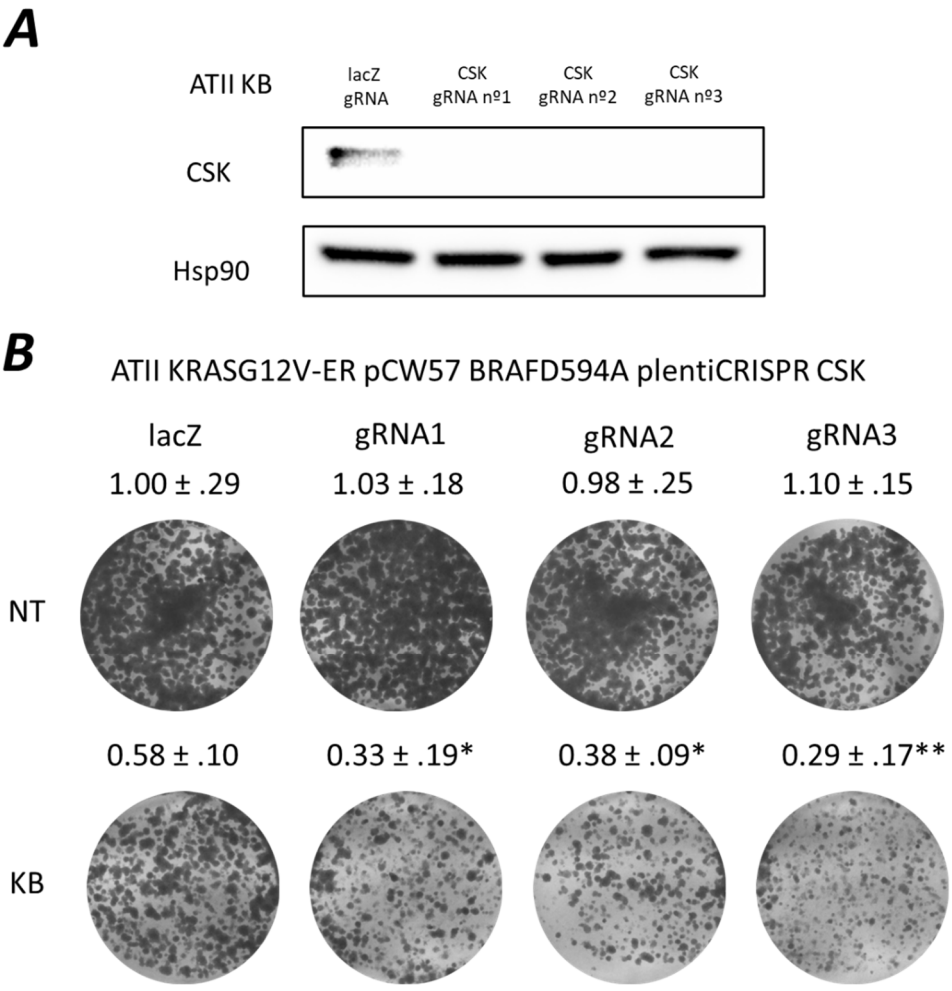

Figure 83. ***CSK deletion sensitizes cells to MAPK activation.*** *ATII cell line was infected with plentiCRISPR targeting CSK, with three independent gRNAs. (A) Western blot analysis for verification of CSK deletion after puromycin selection. (B) Colony formation assay in 2D culture in presence of tamoxifen 10nM and doxycycline 10ng/mL (KB condition). Cells were plated at low density to perform colony formation assays and crystal violet staining. Plates were lysed and mean absorbance is indicated ± SD. Two-way ANOVA with Sidak's multiple comparisons test, against lacZ, p-value **<0.01, *<0.05; n=3.*

The first validation with these cells consisted in studying the effect of CSK deletion in the toxicity generated by high MAPK levels. For all the tested gRNAs, we obtained an increased sensitivity of the CSK knockouts to KRAS and BRAF activation compared to the control (**Figure 83B**), confirming indeed that CSK could play a protection role by mitigating MAPK activity and/or its consequential toxicities.

To evaluate whether CSK activity could actually control MAPK output, we performed a transcriptomic MAPK signature evaluation in the context of the screening KRAS and BRAF activation (**Figure 84**).

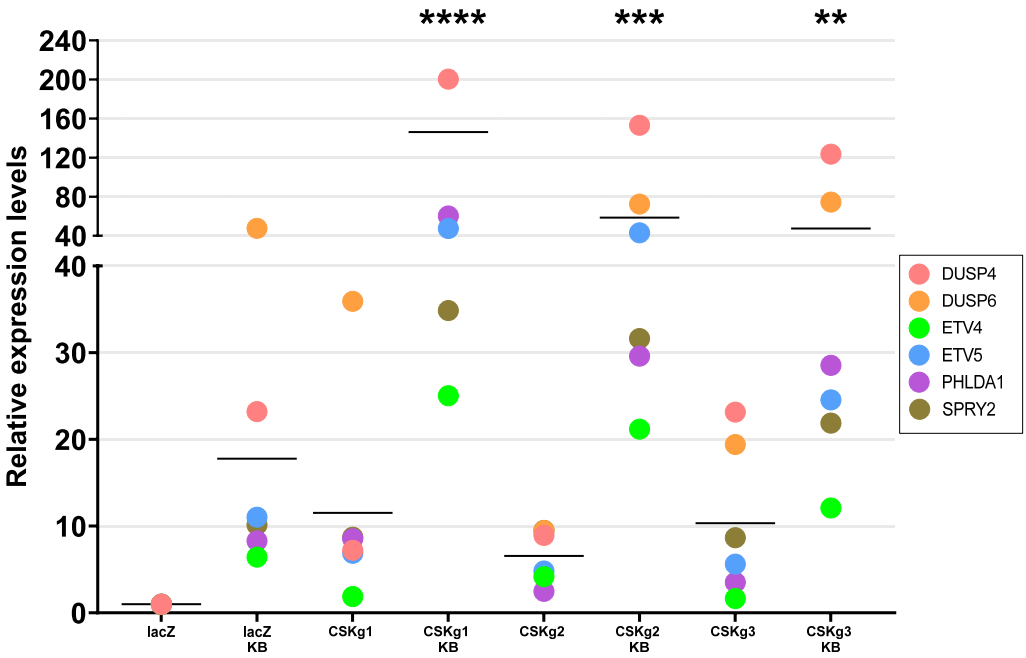

Figure 84. ***Knockout of CSK significantly enhances and overdrives MAPK signature levels.*** *RTqPCR analysis of the ATII cell line infected with plentiCRISPR targeting CSK. Cells were treated with tamoxifen 10nM and doxycycline 10ng/mL for KRAS and BRAF activation, respectively, for 1 week. The signature score, the grand mean combining the expression of the 6 MAPK dependent genes, is marked by a line. The non-parametric Kruskal-Wallis test was used to compare the samples with Dunn's multiple comparison correction, p-value is indicated as follows, ****, p<0,0001; ***, p<0,001; **, p<0,01, n=3. Quantitative levels are normalized to untreated control and HPRT house-keeping gene.*

We remarked that CSK ablation strongly induced increased MAPK activity, observed by the gene signature expression levels, even at non-induced baseline levels. Upon KRAS and BRAF activation, the transcription of the six MAPK-dependent genes increased up to 10-fold. These results suggest that CSK loss of function compromises MAPK negative regulation and these increased signaling levels could be responsible for the increased toxicity of the cells to hypersignaling.

4.6.2 CSK role in modulating MAPK inhibitor responses in LUAD cell lines

Now that the screening hit was functionally validated and we understood how CSK got selected upon MAPK activation, we wondered if CSK negative effect could be translated to a KRAS mutant context, where CSK activity or loss of function could enhance or mitigate the effect of MAPK inhibitors.

We took advantage of the KRAS mutant LUAD H358 cell line and inserted the same plentiCRISPR constructs to mediate CSK deletion (**Figure 85**).

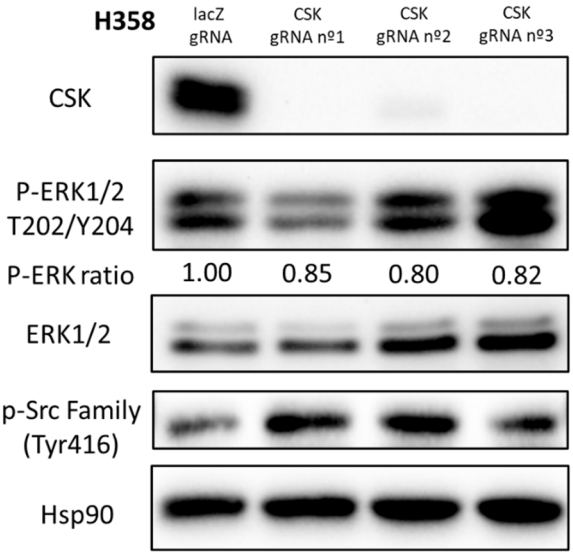

Figure 85. ***CSK ablation in a KRAS mutant context.*** *Western blot analysis of H358 cell line infected with plentiCRISPR constructs targeting CSK with three independent guides. Phosphorylated ERK levels were quantified and normalized to total ERK levels.*

In this cell line, we were not able to confirm the previous results as we observed that phosphorylated ERK levels were not significantly increased in absence of CSK. We also confirmed that, as an already described modulator of SRC activity, CSK enhanced the levels of phosphorylated SRC at the residue Y416.

To further evaluate MAPK effect on CSK deletion, we evaluated CSK knockouts sensitivity to MAPK inhibitor trametinib and the first $KRAS^{G12C}$ inhibitor to have come to the market, sotorasib. We performed IC50s for both compounds and identified that tumoral cells lacking CSK were 2 to 10 times more resistant to trametinib (**Figure 86A**) and 5 to 10 times more resistant to sotorasib (**Figure 86B**). These results were confirmed in a 2D culture colony formation assay, where

treatment with the control's IC50s resulted in a 50-100% increase in cell growth for both compounds (**Figure 86C and 86D**). We evaluated ERK activation at the protein level in presence of sotorasib and identified that CSK knockouts presented increased phosphorylation of ERK in presence of high doses of sotorasib, when compared to the treated control (**Figure 86E**). These results could contribute to the hypothesis that CSK loss enhances MAPK levels, either directly or indirectly, resulting in a decreased sensitivity to RAS/MAPK inhibitors.

Nevertheless, we still were interested in the possible involvement of SFKs in the MAPK regulation phenotype that we were observing upon CSK ablation. First, in order to better understand SRC-MAPK crosstalk, we evaluated how sotorasib treatment affected SRC activity (**Figure 87A**). Certainly, $KRAS^{G12C}$ inhibition generated a slower decrease in phosphorylated ERK levels in the CSK knockout cells. However, this was accompanied by a rapid increase in phosphorylated SRC levels, that were already enhanced by CSK loss of function. Although this increase was less evident in the sotorasib treated control cells, this feedback phosphorylation could suggest that there exist underlying compensatory mechanisms.

Indeed, if the main biological function of CSK is to phosphorylate SRC and its related kinases, we have to evaluate how a CSK-independent inhibition of SRC could affect the resistance phenotype that we are currently observing. For this purpose, we took advantage of a common SFK inhibitor, the PP2 molecule (Hanke et al., 1996) (**Figure 87B**). In this case, we evaluated PP2 action in the control setting to avoid any effect of CSK, in order to just analyze the effect of SRC inhibition *per se*. SRC was clearly inactivated by PP2, reaching a molecular EC50 of around 125nM. At these concentrations, phosphorylated ERK levels did not appear altered, being deeply inhibited only at high concentrations of the inhibitor. These results would suggest that, at a working concentration of 125nM of PP2, MAPK is not altered by SRC.

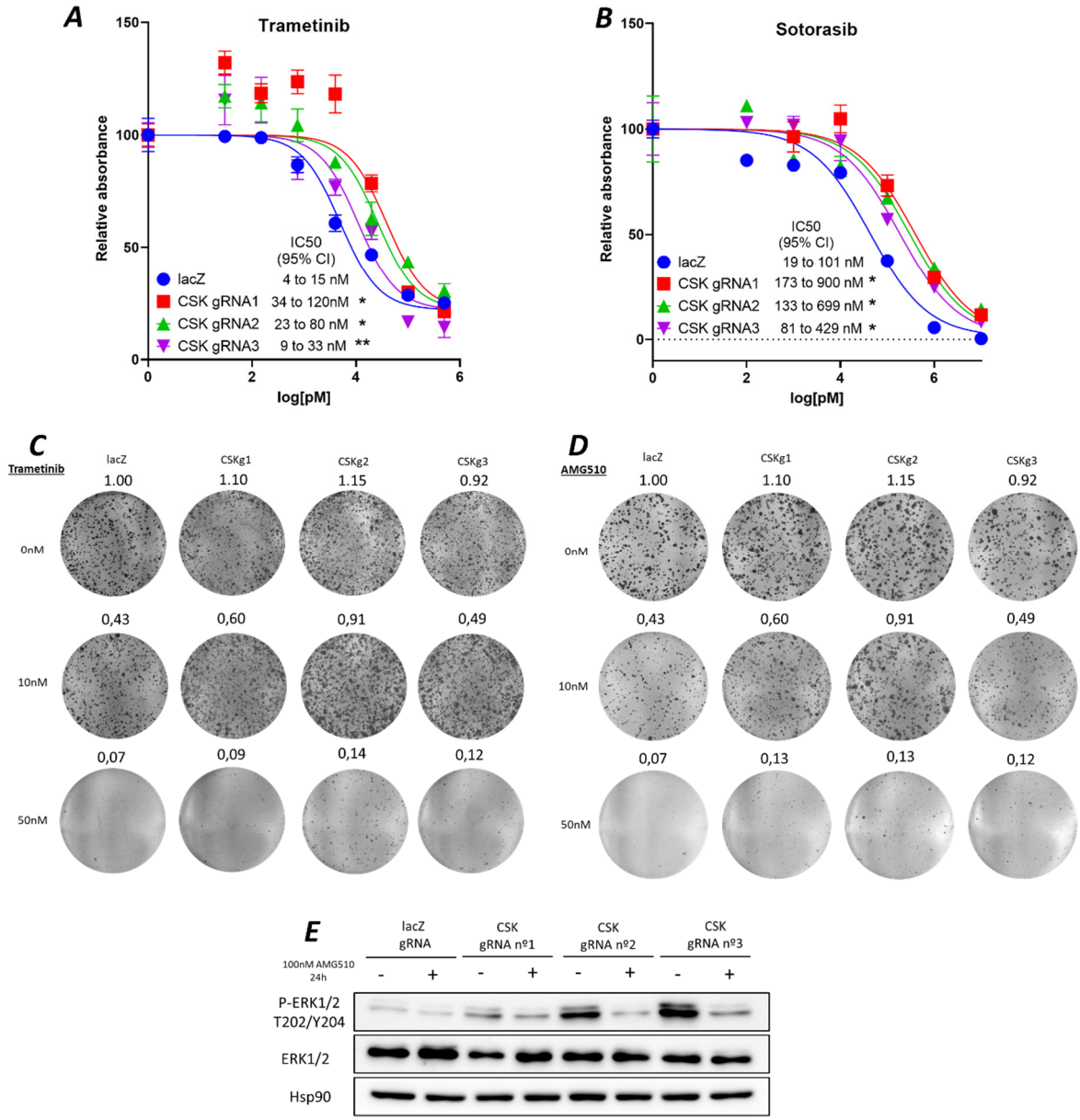

Figure 86. ***Elimination of CSK activity results in a decreased sensitivity to RAS/MAPK inhibitors.*** *H358 cell line was engineered with plentiCRISPR and was submitted to increasing levels of inhibitors to calculate the IC50s of both (A) trametinib and (B) sotorasib for 72h. The computed IC50 is depicted as 95% asymptotic confidence intervals (CI). Mann-Whitney-Wilcoxon rank sum test comparing gRNA vs. Control, n=4. ****, p<0,0001; ***, p<0,001; **, p<0,01; *, p<0,05, n=3. Colony formation assays were performed in presence of (C) trametinib and (D) sotorasib inhibitors at doses corresponding to the control's IC50 (around 10nM) and 5 times higher than the IC50 (50nM). Plates were stained with crystal violet and then lysed to obtain the quantification data. (E) H358 cell line was then subjected to a dose 10 times higher than the IC50 of sotorasib (AMG-510) to evaluate the effect on MAPK activity.*

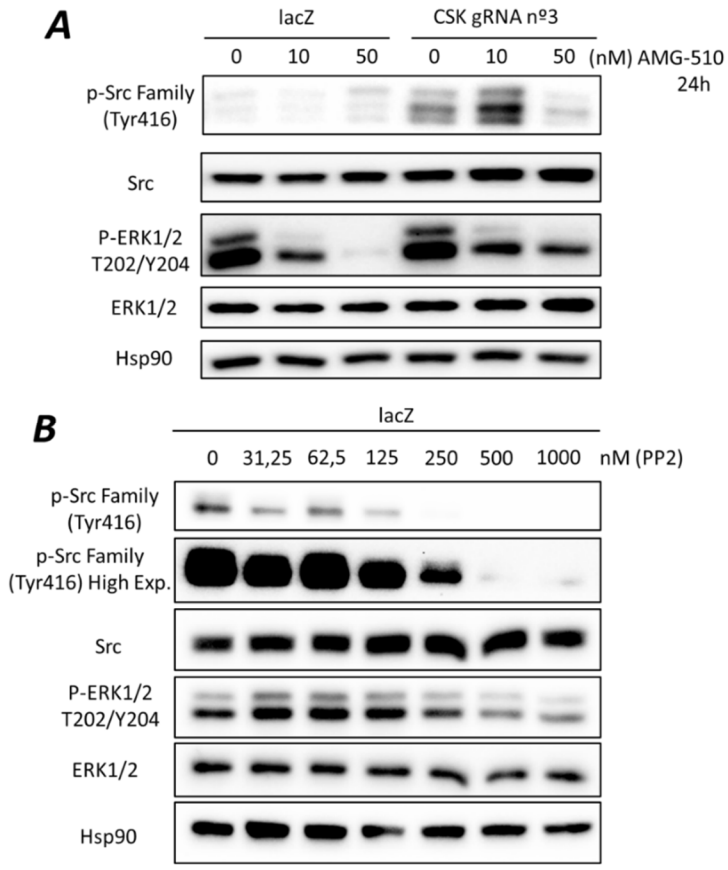

Figure 87. ***CSK-SRC interplay with MAPK pathway in a KRAS mutant LUAD cell line.*** *H358 cell line was treated with increasing levels of (A) sotorasib to evaluate the response of SRC family kinases activation; and (B) PP2 SFK inhibitor to evaluate MAPK response to a SRC inhibition independent of CSK.*

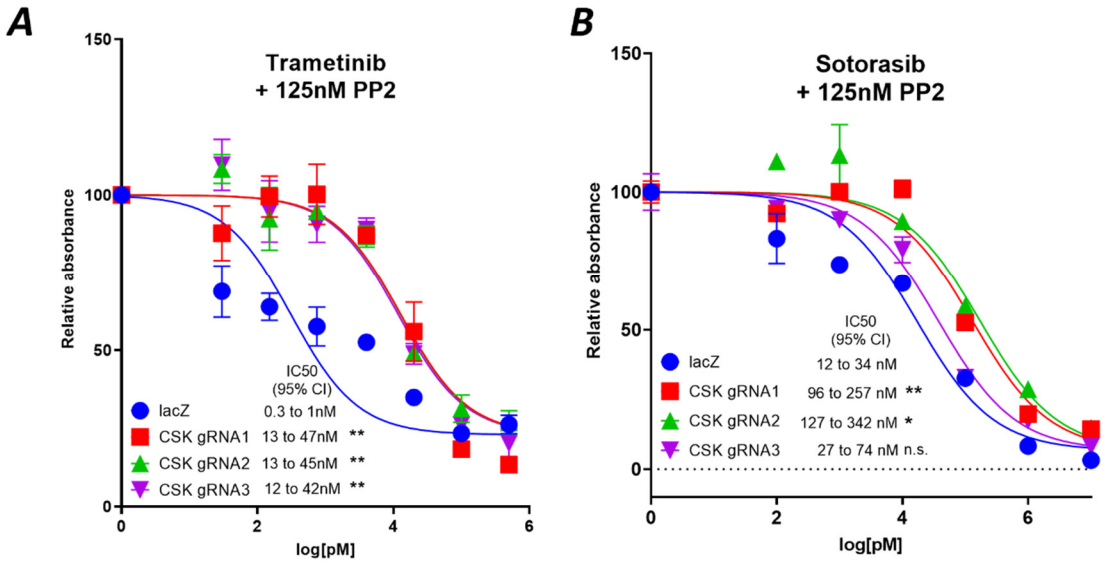

Figure 88. ***RAS-MAPK increased resistance in absence of CSK is not altered by PP2 inhibitor.*** *H358 cell line engineered with plentiCRISPR targeting CSK was submitted to increasing levels of inhibitors to calculate the IC50s of both (A) trametinib and (B) sotorasib in presence of 125nM of PP2 at the estimated EC50 dose for 72h. The computed IC50 is depicted as 95% asymptotic confidence intervals (CI). Mann-Whitney-Wilcoxon rank sum test comparing gRNA vs. Control, n=4. ****, p<0,0001; ***, p<0,001; **, p<0,01; *, p<0,05, n=3.*

Thus, the functional relevance of CSK in the context of MAPK regulation should not be affected in presence of the PP2 inhibitor. In order to confirm this hypothesis, we decided to re-calculate the IC50s of both trametinib and sotorasib in presence of PP2 at this working concentration (**Figure 88**).

The co-treatment with PP2 resulted in a slight increase of sensitivity of all of the cell lines to both inhibitors, reducing the IC50s by around a 2-fold for the trametinib (**Figure 88A**) and very slightly for sotorasib (**Figure 88B**). While all the IC50s were reduced, the increased resistance difference among the CSK knockouts and the control was conserved, making CSK absence a resistance-inducing agent even in presence of the inhibitor PP2. While, in this case, most probable synergies reducing global IC50s may arise from non-specific targets of PP2, ablation of CSK resulted in a beneficial reduction of the sensitivity to RAS-MAPK inhibitors.

Taken together, all these results point to putative MAPK negative regulation properties underlying CSK function. Whether if these imply the involvement of SRC or any additional SFK, additional studies will have to address the implication of CSK in regulating RAS-MAPK signaling levels both *in vivo* and in the clinical setting.

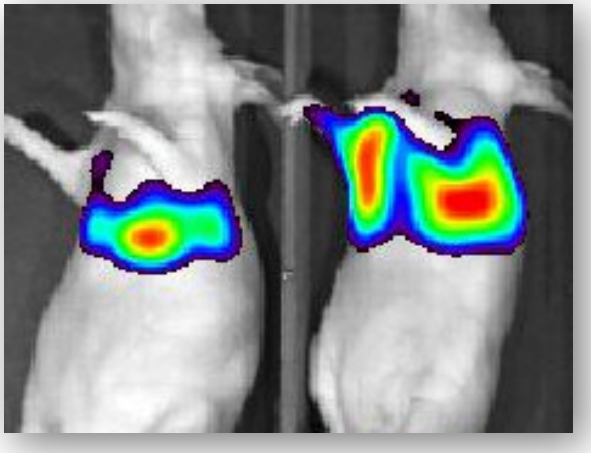

Picture V. Mouse in vivo visualization of lung tumoral invasive cells harboring luciferase. Image obtained by bioluminescence observation in an IVIS platform at the Universidad de Salamanca (Nucleus).

Discussion

Mi verdad básica es que todo tiempo es un ahora en expansión.

Severo Ochoa

1 HYPERSIGNALING IMPAIRS TUMORAL DEVELOPMENT

1.1 MAPK EXCESS PARADOXICALLY IMPAIRS KRAS DRIVEN TUMOR PROGRESSION

In this essay, we have revised and discussed the significance of MAPK regulation, highlighting how excessive MAPK levels are toxic in a KRAS mutant context. The paradoxical survival results obtained from the TCGA data, validated in an alternate cohort, only confirm that there exists a narrow window where RAS/MAPK signaling can promote tumor growth, while avoiding toxicity. These toxicities are still far from being understood, given that lots of different cellular processes could be triggered by oncogenic hypersignaling.

First, the functional status of DNA damage response (DDR) elements, such as p53, may be key to understanding the toxic effect of MAPK hypersignaling. From the patient data, we learn that MAPK distribution of tumors is independent of p53 mutational state, with half of the tumors being P53 mutant.

In the case of p53 WT high MAPK patients, with overactive signaling and a functional DDR, hypersignaling may promote apoptosis or induce senescence mechanisms that delay tumor progression. This hypothesis is supported by existing research, showing that RAS activation can trigger regulatory processes that modulate oncogene-induced senescence functions, mediated by proteins like MDM2 or FOXO in a p53 proficient context (Courtois-Cox et al., 2006; Serrano et al., 1997).

In the context of these same responses, the presence of the wild-type RAS isoforms is a determinant factor, with both HRAS and NRAS being able of activating ATR-Chk1 mediated DDR (Grabocka et al., 2014). The exact biological sense of these functions is still poorly understood. DDR processes are thought to act as a protective mechanism in response to oncogenic signals. Senescence responses curtail the development of cancer, letting senescent cells accumulate while slowing down tumor progression. According to this hypothesis, low MAPK tumors that are able to limit pathway activity

remain “silent” and somehow evade senescence. However, our *in-silico* analysis did not provide evidence supporting this hypothesis, as the senescence signatures previously described (Jochems et al., 2021) did not correlate with MAPK activity in the cohort. Most probably, high MAPK activity generates multiple stress reactions, including senescence-like mechanisms, that may only be detected in a fraction of the tumor, at a given time.

Nevertheless, the nature of the toxicities in tumors that lack a functional DDR remains unexplained by this hypothesis. It is very possible that cellular stress may be an accidental consequence of overdriving MAPK signals. Recent work has proven that MAPK activity, dependent on RAS hypersignaling, stimulates a network of kinetochore kinases that compromises chromosome segregation and prone to genomic instability (Herman et al., 2022). Furthermore, there exists a multitude of mechanisms related to the replicative stress, generated by mitogen signaling, that could explain how high MAPK tumors present unstable genomic landscapes (Kotsantis et al., 2018). Upon DSBs formation, during endogenous damages such as apoptosis and oxidative stress, γH2AX is phosphorylated in an ATM/ATR dependent manner (Kuo & Yang, 2008; Rogakou et al., 1998). Both in our cellular models and *in vivo*, we have presented evidence of γH2AX accumulation in a context of high MAPK signaling, suggesting that the toxicities generated by hypersignaling directly affect genome integrity. In patients, we confirmed that high MAPK results in more frequent heterogeneous genomic rearrangements, resulting in recurrent losses of chromosomal fragile sites.

Additionally, limiting oxidative species is another important factor to consider. Detoxification of ROS has proven to be an increasingly evident mediator of oncogenesis in KRAS mutant tumors (DeNicola et al., 2011). We identified that KEAP1 mutations are particularly prevalent in low MAPK tumors, which may be implying a directed activation mechanism of the NRF2 antioxidant program in these patients. Low MAPK tumors may rely on these antioxidant responses to perpetuate tumor progression. Therefore, targeting NRF2-mediated detoxification programs may be a specific vulnerability of low MAPK tumors.

All these toxicities become a burden for the tumoral cells, that, in turn, present impaired growth when compared to cells harboring moderate levels of MAPK. Tumors that suffer from high MAPK

levels do try to come back to the sweet spot by triggering the pathway regulatory mechanisms. We observed that high MAPK tumors present increased expression of SPRED proteins, in addition to the other transcriptional targets accounting for the negative feedback machinery.

1.2 MAPK ACTIVITY CORRELATES WITH AN IMMUNE HOT CONTEXTURE

Beyond the heterogeneous intrinsic landscape of the high and low MAPK, another variable to consider is the effect of the immune component and the broader cellular microenvironment existing in these tumors. Indeed, oncogenic KRAS/MAPK activity inside of the tumor not only shapes cell-autonomous mechanisms. A large panel of secretory and cellular communications with the stroma depends on the tumor's ability to produce MAPK levels. Factors such as TNFα, secreted by tumor cells, act in an autocrine manner to enhance MAPK levels in response of abrupt modifications of the pathway (Gray-Schopfer et al., 2007; Sabio & Davis, 2014). These agents also mediate paracrine responses controlling immune recruitment, macrophage activation and inflammation (Smith et al., 2014). On the opposite side, cells in the tumor microenvironment are able to shape signaling responses of tumoral cells. MAPK activity can be altered by cancer-associated fibroblasts (CAFs) by secretion of a panel of factors including EREG, POSTN or CXCL12 (Cavallaro, 2013; Lu Chen et al., 2019; Neufert et al., 2013; Wu et al., 2021). Furthermore, these mechanisms mediate the tumor's physical constraints, angiogenesis, invasion, and metastasis.

In the TCGA cohort, we have detected an increased immune infiltration in the high MAPK tumors, specifically with an augmented presence of CD8+ cytotoxic T lymphocytes. These results may imply that these tumors exist in an *immune hot* context. In such a scenario, it is very possible that high MAPK tumors may activate immune evasion mechanisms, such as PD-L1 and/or B7-1/2 (Buchbinder & Desai, 2016; Juneja et al., 2017). Therefore, these tumors could be vulnerable to immune checkpoint inhibitor therapy, potentially re-activating cytotoxic anti-tumor responses (Hirano et al., 2005; Leach et al., 1996). Further experiments must be conducted in order to confirm the *hotness* of these tumors, checking the expression of PD-L1 in a context of high MAPK.

Additionally, it would be interesting to investigate how additional immune compartments are regulated, and control tumor evolution according to MAPK signaling output.

1.3 CLINICAL IMPACT IN OTHER MAPK DRIVEN COHORTS

The MAPK signature score is not only applicable to KRAS mutant patients. There exists a vast heterogeneity in the dispersion of the MAPK signature score, proving the existence of different MAPK outputs across the oncogenic drivers. For this reason, the refined MAPK transcriptional signature could be translated to other non-KRAS mutant cohorts.

The most interesting one may be the study of how MAPK activity levels shape clinical outcomes of BRAF mutant patients. In this case, the 4-gene signature is also biologically relevant, as these transcriptional targets are shared between KRAS and BRAF oncogenic activities (Dry et al., 2010; Pratilas et al., 2009). Furthermore, our *in vitro* results confirm this relationship between BRAF oncogenic mutant activity and the transcriptional levels of the signature.

Although we could not evaluate MAPK levels clinical relevance in BRAF mutant patients in the TCGA, mainly because of a lack of samples to reach a statistically relevant analysis, previous work in the literature have reiterated that BRAF mutant tumors do not tolerate hyperactivation of MAPK. BRAF and RAS mutant, and not wild-type, melanoma models with excessive MAPK levels suffer from ER stress, DNA damage and, finally, apoptosis (Gutierrez-Prat et al., 2022; Leung et al., 2019). In melanoma patients, transcriptional signatures recapitulating MAPK levels have shown that tumors with low MAPK levels presented decreased survival when compared to higher MAPK tumors (Wagle et al., 2018). The evidence suggests that it would be of interest to extend our analysis to LUAD BRAF mutant cohorts and confirm the clinical relevance of MAPK activity levels.

2 DUSP4 STATUS DICTATES TUMOR FITNESS BY CONTROLLING MAPK ACTIVITY

2.1 DUSP4 DELETION GRANTS AN INITIAL ADVANTAGE

Surprisingly, DUSP4 has been found to be a systematically altered MAPK regulator in KRAS mutant LUAD tumors. The differential copy numbers status of DUSP4 in the high and low MAPK cohorts is consequence of a selective process happening since early stages of LUAD. Additionally, we the rest of known negative and positive regulators of the pathway do not show any kind of significant alteration, suggesting that DUSP4 biology is unique amid the MAPK network.

We have demonstrated that DUSP4 loss of function allows for an increased frequency of KRAS transformed cells, suggesting that there exists a particular advantage to early neoplasias that lost DUSP4. A possible explanation could be that transformation thresholds, primarily directed by KRAS oncogenic activity, are modified in presence of MAPK-altering events (Nieto et al., 2017; Simón-Carrasco et al., 2017). In absence of DUSP4, a threshold of KRAS activity normally benign for ATII cells could finally result in an efficient transformation of these cells. In the same way, additional cell types present in the lung, that normally are refractory to KRAS oncogenic activity, may be more easily transformed when DUSP4 deletion co-occurs with KRAS mutations.

In our *in vivo* models, KRAS activation combined with DUSP4 ablation does not result in a differential spatial origin of the tumors, further suggesting that a differential, more accessible, transformation threshold exist for murine ATII cells in absence of DUSP4. This putative modification of the malignant onset might explain why DUSP4 deficient cells are overrepresented and selected at initial stages of LUAD.

2.2 ABLATION OF DUSP4 RESULTS IN TOXIC MAPK LEVELS

Our *in vivo* data has proven that DUSP4 deletion, selected at early timepoints, is a detrimental event that affects tumor progression. Ablation of DUSP4 resulted in increased apoptosis, possibly due to genomic instability. As mentioned in the last paragraph, p53 status may be partially responsible for driving the apoptotic phenotype that we identified. Our pSECC model has been carried out in a WT

p53 background, reflecting how DUSP4 ablation occurs in at least half of the patients that did not present p53 co-occurring mutations.

We also identified a direct increase of ROS presence upon DUSP4 ablation in our cellular models. It is also possible that the oxidative stress may be a direct cause of the genomic instability in the high MAPK context. Recent studies have shown that deletion of DUSP activity is capable of generating increased levels of ROS, that, in turn, are responsible for DNA damage accumulation (Ecker et al., 2023). Moreover, work in EGFR mutant LUAD also revealed that DUSP4 alterations were concomitant with p16 and CDKN2A deletions, suggesting that these tumors drive selection for loss of known mediators of senescence (Chitale et al., 2009).

In order to further study which are the molecular phenotypes triggered by DUSP4 ablation, we are currently performing a transcriptomic analysis to evaluate the stress responses of KRAS mutant pSECC tumors with concomitant DUSP4 inactivation.

As previously mentioned, the immune component and microenvironment are also factors that could account for a considerable part of the phenotypes that are observed, as DUSP4 has important functions in both innate and adaptive immune cells (Lang & Raffi, 2019). BRCA cells silenced of DUSP4 present increased production of pro-inflammatory cytokines IL-4, IL-6, CD-40L and IL-21 (Balko et al., 2013; Yu et al., 2012), while DUSP4 overexpressing cells have decreased production of pro-inflammatory cytokine IL-2 (Lu et al., 2015). In this respect, further secretory and antigen presentation phenotypes might be modified upon DUSP4 alterations in the tumor and should be revisited.

Likewise, DUSP4 deletion could contribute to the reception of cell-to-cell communication signals, by mediating phosphorylation events in other MAPK pathways such as JNK/p38, that participate in a variety of process including cellular motility (Denhez et al., 2019), EMT (Al-Mutairi & Habashy, 2022; Boulding et al., 2016; Guler et al., 2022) or induction of autophagy (He et al., 2021).

To integrate all these possibilities, we are currently studying the potential role that the immune component could play in modulating the stress phenotypes that we see in mouse models. An elevation in MAPK activity resulting from the deletion of DUSP4 may suggest, as observed in the high MAPK patient group, that it may exist an enhanced immune recruitment in the knockout tumors. To explore this matter, we will study the immune contexture and the inflammatory responses that may be differentially represented in DUSP4 knockout tumors.

2.3 DUSP4 IN MAPK REGULATION ACROSS TUMOR TYPES

The expression of DUSP4 also anti-correlated with the MAPK signature in the TCGA EGFR mutant cohort. Although we did not see any effect on survival, MAPK signaling and regulatory proteins such as DUSP4 may play important roles in coordinating tumor progression in this context. It is reported that EGFR mutant LUAD tumors with functional, copy neutral DUSP4 also correlate with more aggressive features and poor prognosis (Chitale et al., 2009).

Still, even in these contexts, DUSP4 is not a MAPK gatekeeper. In spite of presenting an impaired progression, tumors harboring DUSP4 deletions do continue onto very advanced stages. Because of MAPK complex network of regulators, DUSP4 function in regulating ERK activity could eventually be partially compensated by some other redundant proteins, including phosphatases.

For example, both DUSP4 and DUSP6 coordinate their function as a digenic dependency to mitigate excessive MAPK signaling driven by oncogenic mutations in BRAF melanoma (Ito et al., 2021). The nature of the crosstalk mechanisms and redundancies between DUSPs is certainly unclear. Some recent work in melanoma suggests that DUSP6 may even be responsible for MAPK rebound effects when DUSP4 is absent (Kamada et al., 2022). Similarly, in an EGFR mutant context, DUSP4 deletion can result in a paradoxical inactivation of the pathway, possibly by triggering negative feedback loops that may interrupt EGFR signal transduction (Britson et al., 2009).

In our DUSP4 knockout models, we did not observe any kind of reactivation of negative feedback systems of the MAPK pathway. However, it will still be interesting to perform sequential DUSP4

and DUSP6 deletions to better understand why DUSP4 copy number losses are selected, and not DUSP6, in KRAS mutant LUAD.

2.4 DUSP4 AMPLIFICATIONS, CAUSE OR CONSEQUENCE OF MAPK ACTIVITY

The mystery remains unsolved for how DUSP4 copy number gains are selected for since early stages of the low MAPK group. According to the patients transcriptomic data, DUSP4 amplifications do correlate with increased expression levels, suggesting that these are, indeed, operational gains of function of the protein. Locally increasing DUSP4 concentrations could be a failsafe mechanism to keep active ERK levels at a minimum and, overall, maintaining low MAPK activity. Alternatively, it may create a much more adaptable MAPK rheostat.

In this line of thought, DUSP4 high expression has proven to be a relevant biomarker in some tumor types, suggesting that some tumors may recur to different levels of DUSP4 to modulate oncogenic processes. In melanoma, DUSP4 expression levels are increased when compared to normal skin (Mamoor, 2023), and DUSP4 expression is associated with good clinical response to MAPK inhibitors (Gupta et al., 2020). In CRC, high DUSP4 has been frequently linked to both being a good prognosis marker (Armes et al., 2004; Saigusa et al., 2013), and a sign of bad outlook (Gröschl et al., 2013; Sim et al., 2015; Varela et al., 2020; Vriendt et al., 2013). None of these studies have attempted to correlate DUSP4 status with MAPK activity nor with any other MAPK component, so it is very difficult to understand which are the precise conditions where DUSP4 could contribute to a MAPK mediated tumor progression.

Additionally, not to omit that DUSP4 is still among the main transcriptional targets of the MAPK pathway, therefore, in a non-negligible number of tumors, high DUSP4 expression levels will correlate with high MAPK activity.

Whether it exerts a tumor suppressor, or an oncogenic role, DUSP4 presents a completely context dependent functionality. As previously discussed, DUSP4 may be differentially altered according

to particular needs, such as transforming thresholds, that may vary depending on both the tumor type, the oncogenic driver, and the malignancy stage, among others.

2.5 RAS/MAPK INHIBITOR SENSITIVITY ALTERED BY DUSP4 STATUS

The role of DUSP4 seems to extend further than tumor development, but also may have a profound impact on treatment responses. The resistance to MAPK inhibitors observed with DUSP4 deletion may also be indicating that high MAPK tumors harboring these alterations could gain additional potential malignancy upon targeted therapy. This hypothesis is supported by work in melanoma, where DUSP4 inhibition results in a toxic phenotype, correlating with increased levels of MAPK activity. In this case, MAPK inhibitors enhance the viability of DUSP4-depleted cells in both drug-naïve and drug-resistance settings (Gutierrez-Prat et al., 2022), suggesting that DUSP4 deletion not only could be a resistance-triggering event, but an oncogenic catalyst in presence of these inhibitors.

Previous clinical studies using MAPK inhibitors, such as selumetinib in the SELECT trials, roundly failed to obtain a clinical benefit in KRAS mutant NSCLC (Jänne et al., 2017; Soria et al., 2017). One of the main limitations of the study was that, although the study only included KRAS driven tumors, there was no segregation of patients according to potential concomitant genomic alterations. It will be interesting to investigate, together with the other genes of the signature to evaluate MAPK levels, if DUSP4 alterations may allow to differentiate responders from non-responders.

As a MAPK-modifying component, it is understandable that DUSP4 locus could be compromised in MAPKi, or even KRASi, resistant settings. It would also be interesting to identify if DUSP4 alterations are enriched in patients that develop resistances to these inhibitors, as DUSP4 could become an interesting vulnerability to exploit at these stages.

3 UNDERSTANDING NEGATIVE REGULATION OF MAPK TUMORS

3.1 MODELING MAPK HYPERSIGNALING IN THE LABORATORY

Given the tumor characteristics that rely on the collective MAPK output, identifying novel players capable of orchestrating overall signaling could be of clinical relevance. In this project, we sought to develop and exploit a MAPK hypersignaling model in order to perform the whole genome CRISPR screening in search of putative novel regulators of the pathway.

In our ATII cellular model, we have combined the effect of both KRAS and BRAF oncogenic mutants to induce MAPK toxicities. The toxicities that we have selected in the double inducible model, combining tamoxifen and doxycycline, have a mild effect on cellular growth, approximately reducing by half cellular viability. This careful selection of concentrations was focused on finding a KRAS and MAPK dependent phenotype, not relying on one more than the other. ATII cells do not tolerate increased concentrations of tamoxifen as KRAS activation quickly becomes toxic. BRAF induction synergizes with KRAS activation only at the doses that we determined, as increasing doxycycline concentrations rescues the viability of these cells. We hypothesize that BRAF stoichiometry and its effect on heterodimerization with CRAF could explain this phenotype. Indeed, in presence of a hyperactive KRAS, only $BRAF^{D594A}$-CRAF dimers are able to convey hypersignaling. When BRAF kinase dead mutant is overdosed, only homodimers are formed, which are incompetent in transducing KRAS signaling. We then suggest that the dosing of this particular $BRAF^{D594A}$, as well as the rest of the MAPK components, is an essential factor driving the MAPK dependent toxicities. For this reason, dosing of the individual components might also be a key tumoral ability for controlling and maintaining proficient MAPK activity levels.

Additionally, these models for MAPK hyperactivation replicate, at least to a certain extent, situations that can be seen in the clinic. LUAD tumors harboring KRAS mutations, and co-occurring BRAF kinase dead mutations are observed quite frequently (Carter et al., 2015; M. T. Chang et al., 2016; Nieto et al., 2017). Hence, this is evidence that KRAS mutant tumors must

possess additional regulatory mechanisms that compensate the high MAPK activity that, otherwise, could be detrimental. Identifying which are these regulatory factors could unveil tumor vulnerabilities related to MAPK hypersignaling.

3.2 NOVEL ROLES FOR OLD NAMES: CSK TO BE PLAYING IN MAPK TERRAIN?

The CRISPR screening approach has proven to be a very useful technique to identify a broad spectrum of targets likely involved in mediating MAPK signals and regulation. One of the most interesting, and surprising, hits that we identified, as a MAPK negative regulator, was CSK.

CSK biology is quite complex and has been primarily studied by focusing on SRC-related functions of the protein. As a negative regulator of SRC family kinases (SFKs), CSK is located in the membrane and collaborates with adaptor proteins such as PAG in precise lipid rafts to phosphorylate SFKs (Hrdinka & Horejsi, 2014). PAG is a poorly described protein, with few other functions that some scaffolding roles at the membrane for CSK and SFK proteins. Surprisingly, PAG expression can be inactivated with increased levels of MAPK activity, as described in the literature (Smida et al., 2007). It will be interesting to evaluate how PAG contributes to the negative regulator functions of CSK at the MAPK level, and, similarly to previously described functions of the protein, if it serves as a scaffold for the RAS signalosome or other MAPK components.

The major concern that is raised with the putative role of CSK as a negative regulator, is the possible direct involvement of SRC and SFKs. Being quite a pleiotropic protein, SRC kinase mediates multiple signaling pathways that could easily involve a certain degree of crosstalk with MAPKs. While there exist clear evidence pointing on p38/JNK MAPK pathway being a target of SRC (Yoshizumi et al., 2000), it is still unclear how SRC could directly contribute to ERK output other than mediating RAS switch properties. Indeed, SRC kinase is able to regulate RAS switch activity by phosphorylation of tyrosine residues that reduce GEF sensitivity, directly compromising RAS signaling (Gebregiworgis et al., 2021; Kano et al., 2019). Additionally, it may be possible that scaffolding proteins such as β-arrestin, that escort SRC to its putative targets upon GPCR activation,

also recruit RAF proteins, leading to a non-canonical phosphorylation of MAPK proteins by the scaffolding complex (Bourquard et al., 2015; Q. Wang et al., 2006; Zang et al., 2021).

In order to exclude the fact that SRC could be behind the regulatory role of CSK, SFK inhibitors could prove very useful. In our experiments, we used PP2 inhibitor, which is very pleiotropic, and has been flagged as a multi-kinase inhibitor, being able to reduce activity of RTKs, such as EGFR, still at nM concentrations (Brandvold et al., 2012). Still, we demonstrated that CSK function on negatively regulating MAPK inhibitor sensitivity potentially exists in an SFK-independent manner. Our conclusions could be supported by additional experimental data taking advantage of alternative inhibitors such as dasatinib, which is also a pleiotropic multi-kinase inhibitor, until better and more specific inhibitors are found.

CSK activities still prove interesting and could be explored in KRAS driven oncogenesis models. A study reports that, by eliminating CSK, $KRAS^{G12D}$ pancreatic tumors show increased progression with increased levels of phosphorylated ERK, suggesting that the loss of CSK could cooperate with KRAS mutations to increase malignancy (Shields et al., 2011). Indeed, this close collaboration of CSK inactivation with KRAS oncogenic mutants may be a subject of interest in LUAD biology. *In vivo* data, combining these two events, could give further evidence on the role of CSK in controlling KRAS driven oncogenesis.

Moreover, we have evidence that CSK alterations mediate RAS/MAPK inhibitor responses, as CSK deletion increases tolerance to MEK inhibitor trametinib and $KRAS^{G12C}$ inhibitor sotorasib. The fact that CSK deletion is able to modify $KRAS^{G12C}$ inhibitor responses opens the possibility of CSK regulating KRAS biology, possibly at the membrane by modifying the local presence of scaffolding factors such as PAG. This possibility could also explain increased downstream MAPKi resistances.

In order to further investigate the role of CSK at this level, we are interested in evaluating CSK status in patients treated with sotorasib, or other inhibitors, that developed resistance. We will explore patient data in search of CSK alterations, and other potentially compromised genes during the development of resistances, thanks to an ongoing collaboration with Mark Awad and Biagio

Ricciuti in the DFCI in Boston. Given that CSK loss of function de-sensitizes LUAD cell lines to $KRAS^{G12C}$ inhibitors, the presence of CSK mutations or deletions might already evidence a compensatory mechanism in patients presenting sotorasib, or any KRAS inhibitor, resistance.

3.3 MAPK NETWORK IS FAR FROM BEING COMPLETELY DISSECTED

Despite having identified CSK in the screening, there exist some limitations to our CRISPR screening approach. Even if our MAPK induction system was very controlled and the toxicities generated in our cellular model were MAPK dependent, as they were rescued by trametinib, we contemplated that the putative targets obtained through the screening may not directly reflect an effect on MAPK activity.

Some of the targets presence could also be explained by an indirect effect on the toxicity itself, for example, if a gRNA is able to reduce apoptosis it could also have been enriched without having a direct effect on MAPK. For example, we identified that gRNAs targeting negative regulator of p53, MDM2 (Lihong Chen et al., 1998), were depleted in the KB condition. On the other hand, gRNAs targeting CDKN2A, a gene encoding for p53-activating proteins ARF and INK4A (Honda & Yasuda, 1999; Schmitt et al., 2002), were found enriched in KB cells. Both these findings would suggest that regulation of p53, probably for its apoptosis-inducing functions, also generates a selective pressure in the MAPK screening. More precisely, mechanisms inducing p53 activation and apoptosis are shut down by enrichment of gRNAs targeting these genes; while p53 inhibitors, silencing apoptosis triggers, remain untouched as their gRNAs are depleted when MAPK is high.

In consequence, validation of the hits remained the most important part of the process. In the case of TTC1, we were never able to replicate the functional process that allegedly got this hit selected in the screening. The functional role of TTC1, as described in the literature, is to coordinate GPCR signals by acting as an adaptor protein to downstream effectors. In this role, it is preconized that RAS proteins could interact with TTC1 in order to funnel GPCR signaling onto ERK cascade (Kwan et al., 2012; Liu et al., 2010). All this information reinforced the idea of TTC1 being a novel positive regulator that could mediate RAS/MAPK responses, as it was suggested by the screening.

Since gRNAs targeting TTC1 were significantly enriched in the KB condition, when compared to the K and PRE conditions, we argue that there was likely a selective pressure to retain these gRNAs throughout the screening process. Indeed, TTC1 gRNAs might have contributed, in an unclear manner, to reducing RAS/MAPK activation levels and/or rescuing the viability of KB cells that were suffering from excessive MAPK signaling.

Upon further validation, essentiality could only help explain one part of the incoherence behind our results. The ATII cell line does not seem to rely on TTC1, as seen in the validation steps after the screening. Furthermore, TTC1 gRNAs were present and conserved after puromycin selection, which, as we considered, was clear-cut proof of a gene not being essential prior to the screening. Plus, if the gRNAs were targeting an essential gene, during the treatment period the gRNA could only become depleted, and not enriched.

Still, the survival analysis of the TCGA datasets pointed to TTC1 being of extreme importance for LUAD progression. While in the ATII cells it may not have been a common essential gene, it seems that TTC1 is part of the fundamental machinery of KRAS mutant cells, a necessity probably originated by the adaptor protein functions that we have already described. Because of these reasons, the study of TTC1 in KRAS mutant LUAD escapes our understanding, as, for the moment, we cannot exploit the current models that we have in order to fully explain TTC1's role in MAPK activation.

Having acknowledged this, we do not discard the existence of additional MAPK regulators in the resulting final list of the screening. We decided to focus our limited efforts in TTC1 and CSK because of a particular interest developed from the literature, which is clearly a biased approach on how to target a list of putative regulators. Future research efforts should take advantage of our results and explore the functionalities in MAPK regulation of additional targets. One very interesting approach to be followed could be the dissection of the compendium of phosphatases that was obtained from the screening. For example, we identified that PPP4C was depleted in the KB condition, suggesting a negative MAPK regulator role, as it was proven for its homologous PPP6C (Cho et al., 2021), that was also depleted in this condition. Interestingly, a vast set of protein

phosphatases and regulatory subunits has also been curated with the results obtained in the differentially expressed gene analysis of the TCGA data. All these putative targets, when validated, could contribute to a better understanding of the complex regulation of the MAPK pathway.

Finally, we also found several protein scaffolds to be either depleted or enriched in the KB condition. In our lab, we have an interest on studying the clustering and/or dimerization properties of KRAS, a process that strongly requires the presence of unknown protein scaffolds that might mediate the assembly of a RAS signalosome, a compendium of proteins recruited at the membrane, in proximity to RAS, that coordinate effector recruitment and signal transduction (Mysore et al., 2021; Sarkar-Banerjee et al., 2017). Interestingly, scaffolding proteins SHOC2, FLOT2 and IQGAP1 were significantly enriched, while NPM1, NCL or PHB were significantly depleted. These targets might be involved in forming, maintaining, or regulating KRAS clustering, so future experiments should tackle their putative involvement as dimerization scaffolds and their subsequent input to MAPK pathway.

4 CLINICAL IMPLICATIONS OF HYPERSIGNALING, TAKING INTO THE CONTROVERSY

Treatments that arise from the idea of driving cells towards hypersignaling have historically been overlooked, while being called “unrealistically dangerous”. Despite of the fear that these alternative therapeutical approaches may arise, the scientific community is starting to re-consider hyperactivation of oncogenic pathway signaling for achieving toxicity (Bernards, 2023; L. Chang et al., 2023; Wood, 2023). The earliest example is René Bernards currently proposing using PP2A inhibitors in order to enhance oncogenic signaling and drive toxicity.

Over the years, this trend has already been proposed for other hallmarks in cancer. Potentiating mitotic pressure had moderate therapeutic success with the arrival of PARP inhibitors, that were able to restore DNA damage responses in order to enhance apoptosis (Bhamidipati et al., 2023). Enhancing oxidative stress may be key to synergize or reinforce the effectiveness of the chemo or radiotherapies (Diehn et al., 2009; Nogueira & Hay, 2013).

In the same way, inhibition of negative regulators of MAPK, such as DUSPs or SPRYs, could recreate the toxicities that we are describing, in this manuscript and in the literature, and open a new therapeutic window in multiple tumor types (Gutierrez-Prat et al., 2022; Leung et al., 2019; Shojaee et al., 2015; Unni et al., 2018; Wittig-Blaich et al., 2017; Zhao et al., 2015).

A successful MAPK targeted therapy will be more complex than just either reducing or increasing the activity of individual components. In the case of MAPK inhibition, oscillatory use of BRAF or MEK inhibitors forestalls the onset of resistance by inducing hyperactive-MAPK toxicities to drug-tolerant cells (Hong et al., 2017; L. Wang et al., 2018; Yang et al., 2021). For these reasons, we will also have to integrate rational designs of therapeutic strategies, combining withdrawal (or drug holiday) with drug usage.

In summary, the ultimate therapies will need to learn from previous mistakes and will have to present innovative solutions to 21st century problems, such as resistances to small molecule inhibitors, toxicities, patient comorbidities, and many more.

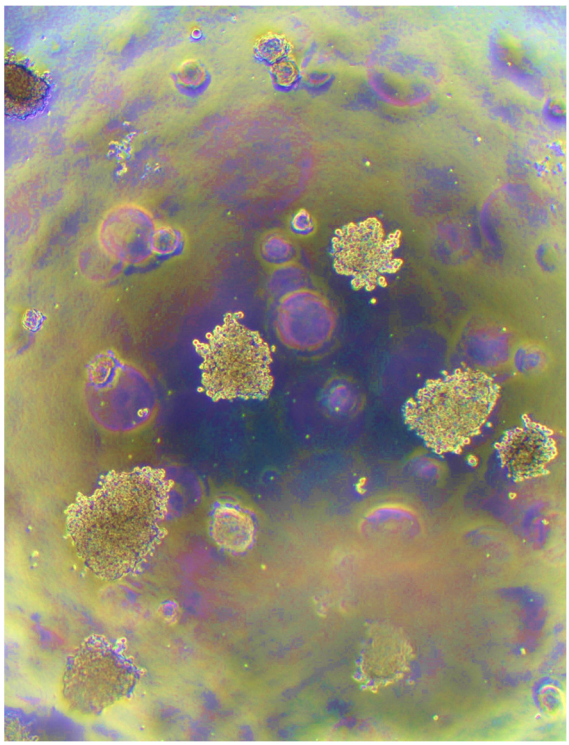

Picture VI. 3D cultures of H460 cell line in a semi-solid soft agar matrix. Images were obtained in an inverted microscope without phase contrast illumination. Colorized.

Conclusions

Science is made with facts, just as a house is made with stones; but a mere accumulation of facts is no more science than a pile of stones is a house

Henri Poincaré

Conclusions

Based on the objectives of this research, we achieved valuable insights into how MAPK pathway regulation affects tumor progression, demonstrating that alterations in modulators of the pathway can play a pivotal role in clinical prognosis.

The global conclusions of this work are the following:

1. The analysis of LUAD transcriptomic data through our refined MAPK signature revealed that MAPK activity determines KRAS mutant patient survival, being low MAPK levels a sign of poor prognosis.
2. High MAPK activity in KRAS mutant LUAD is correlated with stress phenotypes, including genomic stress, apoptosis, and oxidative toxicities.
3. DUSP4 is a negative MAPK regulator altered differently according to MAPK activity levels in KRAS mutant LUAD. High MAPK patients present deletions of DUSP4 while low MAPK patients present amplifications of DUSP4.
4. The loss of DUSP4 enhances MAPK activation. DUSP4 loss is an event selected in early stages because it may grant an initial advantage to KRAS-driven neoplasias. In advanced tumors, this increased signaling correlates with toxic events that suggest that long-term loss of DUSP4 may compromise normal tumor progression.
5. From the CRISPR screening, we identified CSK as a potential additional regulator that may function in an SRC-independent manner mediating negative regulation of the pathway. Further research may be needed to complete and better understand how CSK could contribute to different stages of tumor development.
6. We also identified a compendium of proteins, including phosphatases and regulatory subunits, that could function as putative positive or negative regulators of the pathway and might play a role in MAPK driven tumor evolution of KRAS mutant LUAD.

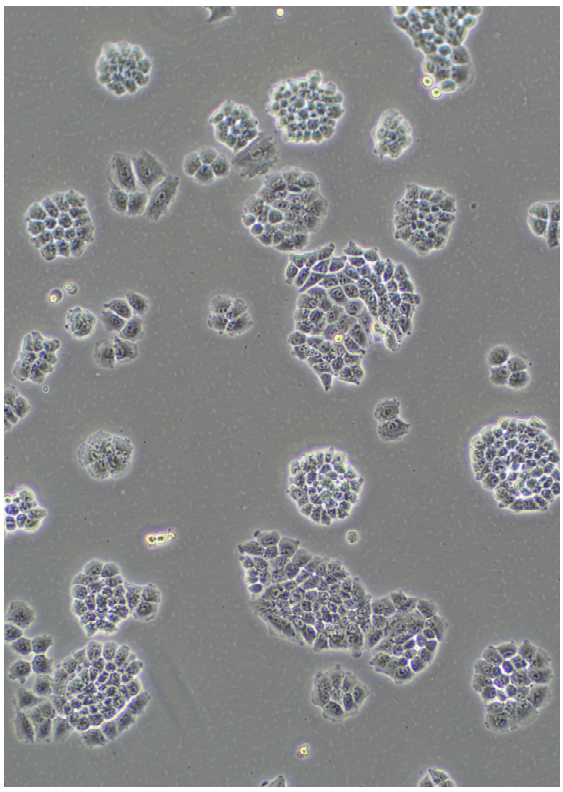

Picture VII. H460 cell line in culture, photography obtained from an inverted microscope with phase contrast illumination and a 10X magnification.

References

References (APA style)

Ablain, J., Liu, S., Moriceau, G., Lo, R. S. & Zon, L. I. (2020). *SPRED1 deletion confers resistance to MAPK inhibition in melanoma*. *218*(3).

Adachi, Y., Ito, K., Hayashi, Y., Kimura, R., Tan, T. Z., Yamaguchi, R. & Ebi, H. (2020). Epithelial-to-Mesenchymal Transition is a Cause of Both Intrinsic and Acquired Resistance to KRAS G12C Inhibitor in KRAS G12C–Mutant Non–Small Cell Lung Cancer. *Clinical Cancer Research*, *26*(22), 5962–5973. https://doi.org/10.1158/1078-0432.ccr-20-2077

Aelst, L. V., Barr, M., Marcus, S., Polverino, A. & Wigler, M. (1993). Complex formation between RAS and RAF and other protein kinases. *Proceedings of the National Academy of Sciences*, *90*(13), 6213–6217. https://doi.org/10.1073/pnas.90.13.6213

Aja, J. S. de, Dost, A. F. M. & Kim, C. F. (2021). Alveolar progenitor cells and the origin of lung cancer. *Journal of Internal Medicine*, *289*(5), 629–635. https://doi.org/10.1111/joim.13201

Albeck, J. G., Mills, G. B. & Brugge, J. S. (2013). Frequency-Modulated Pulses of ERK Activity Transmit Quantitative Proliferation Signals. *Molecular Cell*, *49*(2), 249–261. https://doi.org/10.1016/j.molcel.2012.11.002

Alessi, D. R., Saito, Y., Campbell, D. G., Cohen, P., Sithanandam, G., Rapp, U., Ashworth, A., Marshall, C. J. & Cowley, S. (1994). Identification of the sites in MAP kinase kinase-1 phosphorylated by p74raf-1. *The EMBO Journal*, *13*(7), 1610–1619. https://doi.org/10.1002/j.1460-2075.1994.tb06424.x

Alexandrov, L. B., Ju, Y. S., Haase, K., Loo, P. V., Martincorena, I., Nik-Zainal, S., Totoki, Y., Fujimoto, A., Nakagawa, H., Shibata, T., Campbell, P. J., Vineis, P., Phillips, D. H. & Stratton, M. R. (2016). Mutational signatures associated with tobacco smoking in human cancer. *BioRxiv*, 051417. https://doi.org/10.1101/051417

Aljanabi, S. M. & Martinez, I. (1997). Universal and rapid salt-extraction of high quality genomic DNA for PCR-based techniques. *Nucleic Acids Research*, *25*(22), 4692–4693. https://doi.org/10.1093/nar/25.22.4692

Al-Mutairi, M. S. & Habashy, H. O. (2022). DUSP4 Silencing Enhances the Sensitivity of Breast Cancer Cells to Doxorubicin through the Activation of the JNK/c-Jun Signalling Pathway. *Molecules*, *27*(19), 6146. https://doi.org/10.3390/molecules27196146

Álvarez, M. M., Biayna, J. & Supek, F. (2022). TP53-dependent toxicity of CRISPR/Cas9 cuts is differential across genomic loci and can confound genetic screening. *Nature Communications*, *13*(1), 4520. https://doi.org/10.1038/s41467-022-32285-1

Ambrogio, C., Barbacid, M. & Santamaría, D. (2017). In vivo oncogenic conflict triggered by co-existing KRAS and EGFR activating mutations in lung adenocarcinoma. *Oncogene*, *36*(16), 2309–2318. https://doi.org/10.1038/onc.2016.385

Ambrogio, C., Köhler, J., Zhou, Z. W., Wang, H., Paranal, R., Li, J., Capelletti, M., Caffarra, C., Li, S., Lv, Q., Gondi, S., Hunter, J. C., Lu, J., Chiarle, R., Santamaría, D., Westover, K. D. & Jänne, P. A. (2018). KRAS Dimerization Impacts MEK Inhibitor Sensitivity and Oncogenic Activity of Mutant KRAS. *Cell*, *172*(4), 857-868.e15. https://doi.org/10.1016/j.cell.2017.12.020

American-Cancer-Society. (2022). *Cancer Facts & Figures 2022*.

Amodio, V., Yaeger, R., Arcella, P., Cancelliere, C., Lamba, S., Lorenzato, A., Arena, S., Montone, M., Mussolin, B., Bian, Y., Whaley, A., Pinnelli, M., Murciano-Goroff, Y. R., Vakiani, E., Valeri, N., Liao, W.-L., Bhalkikar, A., Thyparambil, S., Zhao, H.-Y., … Misale, S. (2020). EGFR Blockade Reverts Resistance to KRAS G12C Inhibition in Colorectal Cancer. *Cancer Discovery*, *10*(8), 1129–1139. https://doi.org/10.1158/2159-8290.cd-20-0187

Aoki, K., Kumagai, Y., Sakurai, A., Komatsu, N., Fujita, Y., Shionyu, C. & Matsuda, M. (2013). Stochastic ERK Activation Induced by Noise and Cell-to-Cell Propagation Regulates Cell Density-Dependent Proliferation. *Molecular Cell*, *52*(4), 529–540. https://doi.org/10.1016/j.molcel.2013.09.015

Aran, D., Sirota, M. & Butte, A. J. (2015). Systematic pan-cancer analysis of tumour purity. *Nature Communications*, *6*(1), 8971. https://doi.org/10.1038/ncomms9971

Armes, J. E., Hammet, F., Silva, M. de, Ciciulla, J., Ramus, S. J., Soo, W.-K., Mahoney, A., Yarovaya, N., Henderson, M. A., Gish, K., Hutchins, A.-M., Price, G. R. & Venter, D. J. (2004). Candidate tumor-suppressor genes on chromosome arm 8p in early-onset and high-grade breast cancers. *Oncogene*, *23*(33), 5697–5702. https://doi.org/10.1038/sj.onc.1207740

Awad, M. M., Liu, S., Rybkin, I. I., Arbour, K. C., Dilly, J., Zhu, V. W., Johnson, M. L., Heist, R. S., Patil, T., Riely, G. J., Jacobson, J. O., Yang, X., Persky, N. S., Root, D. E., Lowder, K. E., Feng, H., Zhang, S. S., Haigis, K. M., Hung, Y. P., … Aguirre, A. J. (2021). Acquired Resistance to KRASG12C Inhibition in Cancer. *New England Journal of Medicine*, *384*(25), 2382–2393. https://doi.org/10.1056/nejmoa2105281

Balko, J. M., Schwarz, L. J., Bhola, N. E., Kurupi, R., Owens, P., Miller, T. W., Gómez, H., Cook, R. S. & Arteaga, C. L. (2013). Activation of MAPK Pathways due to DUSP4 Loss Promotes Cancer Stem Cell-like Phenotypes in Basal-like Breast Cancer. *Cancer Research*, *73*(20), 6346–6358. https://doi.org/10.1158/0008-5472.can-13-1385

Bankhead, P., Loughrey, M. B., Fernández, J. A., Dombrowski, Y., McArt, D. G., Dunne, P. D., McQuaid, S., Gray, R. T., Murray, L. J., Coleman, H. G., James, J. A., Salto-Tellez, M. & Hamilton, P. W. (2017). QuPath: Open source software for digital pathology image analysis. *Scientific Reports*, *7*(1), 16878. https://doi.org/10.1038/s41598-017-17204-5

Bear, A. S., Blanchard, T., Cesare, J., Ford, M. J., Richman, L. P., Xu, C., Baroja, M. L., McCuaig, S., Costeas, C., Gabunia, K., Scholler, J., Posey, A. D., O'Hara, M. H., Smole, A., Powell, D. J., Garcia, B. A., Vonderheide, R. H., Linette, G. P. & Carreno, B. M. (2021). Biochemical and functional characterization of mutant KRAS epitopes validates this oncoprotein for immunological targeting. *Nature Communications*, *12*(1), 4365. https://doi.org/10.1038/s41467-021-24562-2

Begum, P., Goldin, R. D., Possamai, L. A. & Popat, S. (2021). Severe Immune Checkpoint Inhibitor Hepatitis in KRAS G12C-Mutant NSCLC Potentially Triggered by Sotorasib: Case Report. *JTO Clinical and Research Reports*, *2*(9), 100213. https://doi.org/10.1016/j.jtocrr.2021.100213

Bernards, R. (2023, 14. September). *New ideas to target RAS*. Targeting RAS Symposium Salamanca 2023.

Beroukhim, R., Mermel, C. H., Porter, D., Wei, G., Raychaudhuri, S., Donovan, J., Barretina, J., Boehm, J. S., Dobson, J., Urashima, M., Henry, K. T. M., Pinchback, R. M., Ligon, A. H., Cho, Y.-J., Haery, L., Greulich, H., Reich, M., Winckler, W., Lawrence, M. S., … Meyerson, M. (2010). The landscape of somatic copy-number alteration across human cancers. *Nature*, *463*(7283), 899–905. https://doi.org/10.1038/nature08822

Bery, N., Miller, A. & Rabbitts, T. (2020). A potent KRAS macromolecule degrader specifically targeting tumours with mutant KRAS. *Nature Communications*, *11*(1), 1–14. https://doi.org/10.1038/s41467-020-17022-w

Bhamidipati, D., Haro-Silerio, J. I., Yap, T. A. & Ngoi, N. (2023). PARP inhibitors: enhancing efficacy through rational combinations. *British Journal of Cancer*, *129*(6), 904–916. https://doi.org/10.1038/s41416-023-02326-7

Blumenschein, G. R., Smit, E. F., Planchard, D., Kim, D.-W., Cadranel, J., Pas, T. D., Dunphy, F., Udud, K., Ahn, M.-J., Hanna, N. H., Kim, J.-H., Mazieres, J., Kim, S.-W., Baas, P., Rappold, E., Redhu, S., Puski, A., Wu, F. S. & Jänne, P. A. (2015). A randomized phase II study of the MEK1/MEK2 inhibitor trametinib (GSK1120212) compared with docetaxel in KRAS-mutant advanced non-small-cell lung cancer (NSCLC). *Annals of Oncology*, *26*(5), 894–901. https://doi.org/10.1093/annonc/mdv072

Blüthgen, N., Legewie, S., Kielbasa, S. M., Schramme, A., Tchernitsa, O., Keil, J., Solf, A., Vingron, M., Schäfer, R., Herzel, H. & Sers, C. (2009). A systems biological approach suggests that transcriptional feedback regulation by dual-specificity phosphatase 6 shapes extracellular signal-related kinase activity in RAS-transformed fibroblasts. *The FEBS Journal*, *276*(4), 1024–1035. https://doi.org/10.1111/j.1742-4658.2008.06846.x

Bollag, G., Hirth, P., Tsai, J., Zhang, J., Ibrahim, P. N., Cho, H., Spevak, W., Zhang, C., Zhang, Y., Habets, G., Burton, E. A., Wong, B., Tsang, G., West, B. L., Powell, B., Shellooe, R., Marimuthu, A., Nguyen, H., Zhang, K. Y. J., … Nolop, K. (2010). Clinical efficacy of a RAF inhibitor needs broad target blockade in BRAF-mutant melanoma. *Nature*, *467*(7315), 596–599. https://doi.org/10.1038/nature09454

Bollu, L. R., Mazumdar, A., Savage, M. I. & Brown, P. H. (2017). Molecular Pathways: Targeting Protein Tyrosine Phosphatases in Cancer. *Clinical Cancer Research*, *23*(9), 2136–2142. https://doi.org/10.1158/1078-0432.ccr-16-0934

Bond, M. J., Chu, L., Nalawansha, D. A., Li, K. & Crews, C. M. (2020). Targeted Degradation of Oncogenic KRASG12C by VHL-Recruiting PROTACs. *ACS Central Science*, *6*(8), 1367–1375. https://doi.org/10.1021/acscentsci.0c00411

Boulding, T., Wu, F., McCuaig, R., Dunn, J., Sutton, C. R., Hardy, K., Tu, W., Bullman, A., Yip, D., Dahlstrom, J. E. & Rao, S. (2016). Differential Roles for DUSP Family Members in Epithelial-to-Mesenchymal Transition and Cancer Stem Cell Regulation in Breast Cancer. *PLoS ONE*, *11*(2), e0148065. https://doi.org/10.1371/journal.pone.0148065

Bourquard, T., Landomiel, F., Reiter, E., Crépieux, P., Ritchie, D. W., Azé, J. & Poupon, A. (2015). Unraveling the molecular architecture of a G protein-coupled receptor/β-arrestin/Erk module complex. *Scientific Reports*, *5*(1), 10760. https://doi.org/10.1038/srep10760

Boykevisch, S., Zhao, C., Sondermann, H., Philippidou, P., Halegoua, S., Kuriyan, J. & Bar-Sagi, D. (2006). Regulation of Ras Signaling Dynamics by Sos-Mediated Positive Feedback. *Current Biology*, *16*(21), 2173–2179. https://doi.org/10.1016/j.cub.2006.09.033

Brandvold, K. R., Steffey, M. E., Fox, C. C. & Soellner, M. B. (2012). Development of a Highly Selective c-Src Kinase Inhibitor. *ACS Chemical Biology*, *7*(8), 1393–1398. https://doi.org/10.1021/cb300172e

Brant, R., Sharpe, A., Liptrot, T., Dry, J. R., Harrington, E. A., Barrett, J. C., Whalley, N., Womack, C., Smith, P. & Hodgson, D. R. (2017). Clinically viable gene expression assays with potential for predicting benefit from MEK inhibitors. *Clinical Cancer Research*, *23*(6), 1471–1480. https://doi.org/10.1158/1078-0432.ccr-16-0021

Brennan, D. F., Dar, A. C., Hertz, N. T., Chao, W. C. H., Burlingame, A. L., Shokat, K. M. & Barford, D. (2011). A Raf-induced allosteric transition of KSR stimulates phosphorylation of MEK. *Nature*, *472*(7343), 366–369. https://doi.org/10.1038/nature09860

Brinkman, E. K., Chen, T., Amendola, M. & van Steensel, B. (2014). Easy quantitative assessment of genome editing by sequence trace decomposition. *Nucleic Acids Research*, *42*(22), e168–e168. https://doi.org/10.1093/nar/gku936

Britson, J. S., Barton, F., Balko, J. M. & Black, E. P. (2009). Deregulation of DUSP activity in EGFR-mutant lung cancer cell lines contributes to sustained ERK1/2 signaling. *Biochemical and Biophysical Research Communications*, *390*(3), 849–854. https://doi.org/10.1016/j.bbrc.2009.10.061

Brondello, J.-M., Brunet, A., Pouysségur, J. & McKenzie, F. R. (1997a). The Dual Specificity Mitogen-activated Protein Kinase Phosphatase-1 and -2 Are Induced by the p42/p44MAPK Cascade*. *Journal of Biological Chemistry*, *272*(2), 1368–1376. https://doi.org/10.1074/jbc.272.2.1368

Brondello, J.-M., Brunet, A., Pouysségur, J. & McKenzie, F. R. (1997b). The Dual Specificity Mitogen-activated Protein Kinase Phosphatase-1 and -2 Are Induced by the p42/p44MAPK Cascade*. *Journal of Biological Chemistry*, *272*(2), 1368–1376. https://doi.org/10.1074/jbc.272.2.1368

Buchbinder, E. I. & Desai, A. (2016). CTLA-4 and PD-1 Pathways. *American Journal of Clinical Oncology*, *39*(1), 98–106. https://doi.org/10.1097/coc.0000000000000239

Buday, L. & Downward, J. (1993). Epidermal growth factor regulates p21ras through the formation of a complex of receptor, Grb2 adapter protein, and Sos nucleotide exchange factor. *Cell*, *73*(3), 611–620. https://doi.org/10.1016/0092-8674(93)90146-h

Burgess, M. R., Hwang, E., Mroue, R., Bielski, C. M., Wandler, A. M., Huang, B. J., Firestone, A. J., Young, A., Lacap, J. A., Crocker, L., Asthana, S., Davis, E. M., Xu, J., Akagi, K., Beau, M. M. L., Li, Q., Haley, B., Stokoe, D., Sampath, D., … Shannon, K. (2017). KRAS Allelic Imbalance Enhances Fitness and Modulates MAP Kinase Dependence in Cancer. *Cell*, *168*(5), 817-829.e15. https://doi.org/10.1016/j.cell.2017.01.020

Cannataro, V. L., Gaffney, S. G., Stender, C., Zhao, Z.-M., Philips, M., Greenstein, A. E. & Townsend, J. P. (2018). Heterogeneity and mutation in KRAS and associated oncogenes: evaluating the potential for the evolution of resistance to targeting of KRAS G12C. *Oncogene*, *37*(18), 2444–2455. https://doi.org/10.1038/s41388-017-0105-z

Canon, J., Rex, K., Saiki, A. Y., Mohr, C., Cooke, K., Bagal, D., Gaida, K., Holt, T., Knutson, C. G., Koppada, N., Lanman, B. A., Werner, J., Rapaport, A. S., Miguel, T. S., Ortiz, R., Osgood, T., Sun, J., Zhu, X., Mccarter, J. D., … Paca-, M. I. A. (2019). The clinical KRAS(G12C)

inhibitor AMG 510 drives anti-tumour immunity. *Nature*, *575*(March), 1–8. https://doi.org/10.1038/s41586-019-1694-1

Carrot-Zhang, J., Soca-Chafre, G., Patterson, N., Thorner, A. R., Nag, A., Watson, J., Genovese, G., Rodriguez, J., Gelbard, M. K., Corrales-Rodriguez, L., Mitsuishi, Y., Ha, G., Campbell, J. D., Oxnard, G. R., Arrieta, O., Cardona, A. F., Gusev, A. & Meyerson, M. (2021). Genetic Ancestry Contributes to Somatic Mutations in Lung Cancers from Admixed Latin American Populations. *Cancer Discovery*, *11*(3), 591–598. https://doi.org/10.1158/2159-8290.cd-20-1165

Carter, J., Tseng, L.-H., Zheng, G., Dudley, J., Illei, P., Gocke, C. D., Eshleman, J. R. & Lin, M.-T. (2015). Non-p.V600E BRAF Mutations Are Common Using a More Sensitive and Broad Detection Tool. *American Journal of Clinical Pathology*, *144*(4), 620–628. https://doi.org/10.1309/ajcp85atmjozoudj

Carter, S. L., Cibulskis, K., Helman, E., McKenna, A., Shen, H., Zack, T., Laird, P. W., Onofrio, R. C., Winckler, W., Weir, B. A., Beroukhim, R., Pellman, D., Levine, D. A., Lander, E. S., Meyerson, M. & Getz, G. (2012). Absolute quantification of somatic DNA alterations in human cancer. *Nature Biotechnology*, *30*(5), 413–421. https://doi.org/10.1038/nbt.2203

Carvalho, B. S. & Irizarry, R. A. (2010). A framework for oligonucleotide microarray preprocessing. *Bioinformatics*, *26*(19), 2363–2367. https://doi.org/10.1093/bioinformatics/btq431

Castellano, E. & Downward, J. (2011). RAS Interaction with PI3K: More Than Just Another Effector Pathway. *Genes & Cancer*, *2*(3), 261–274. https://doi.org/10.1177/1947601911408079

Castellano, E., Sheridan, C., Thin, M. Z., Nye, E., Spencer-Dene, B., Diefenbacher, M. E., Moore, C., Kumar, M. S., Murillo, M. M., Grönroos, E., Lassailly, F., Stamp, G. & Downward, J. (2013). Requirement for Interaction of PI3-Kinase p110α with RAS in Lung Tumor Maintenance. *Cancer Cell*, *24*(5), 617–630. https://doi.org/10.1016/j.ccr.2013.09.012

Cavallaro, S. (2013). CXCR4/CXCL12 in Non-Small-Cell Lung Cancer Metastasis to the Brain. *International Journal of Molecular Sciences*, *14*(1), 1713–1727. https://doi.org/10.3390/ijms14011713

Cesare, D. D., Jacquot, S., Hanauer, A. & Sassone-Corsi, P. (1998). Rsk-2 activity is necessary for epidermal growth factor-induced phosphorylation of CREB protein and transcription of c-fos gene. *Proceedings of the National Academy of Sciences*, *95*(21), 12202–12207. https://doi.org/10.1073/pnas.95.21.12202

Chandarlapaty, S. (2012). Negative Feedback and Adaptive Resistance to the Targeted Therapy of Cancer. *Cancer Discovery*, *2*(4), 311–319. https://doi.org/10.1158/2159-8290.cd-12-0018

Chang, L., Jung, N. Y., Atari, A., Rodriguez, D. J., Kesar, D., Song, T.-Y., Rees, M. G., Ronan, M., Li, R., Ruiz, P., Chaturantabut, S., Ito, T., Tienen, L. M. van, Tseng, Y.-Y., Roth, J. A. & Sellers, W. R. (2023). Systematic profiling of conditional pathway activation identifies context-dependent synthetic lethalities. *Nature Genetics*, 1–12. https://doi.org/10.1038/s41588-023-01515-7

Chang, M. T., Asthana, S., Gao, S. P., Lee, B. H., Chapman, J. S., Kandoth, C., Gao, J., Socci, N. D., Solit, D. B., Olshen, A. B., Schultz, N. & Taylor, B. S. (2016). Identifying recurrent

mutations in cancer reveals widespread lineage diversity and mutational specificity. *Nature Biotechnology*, *34*(2), 155–163. https://doi.org/10.1038/nbt.3391

Chardin, P., Camonis, J. H., Gale, N. W., Aelst, L. van, Schlessinger, J., Wigler, M. H. & Bar-Sagi, D. (1993). Human Sos1: a Guanine Nucleotide Exchange Factor for Ras that Binds to GRB2. *Science*, *260*(5112), 1338–1343. https://doi.org/10.1126/science.8493579

Chen, Lihong, Agrawal, S., Zhou, W., Zhang, R. & Chen, J. (1998). Synergistic activation of p53 by inhibition of MDM2 expression and DNA damage. *Proceedings of the National Academy of Sciences*, *95*(1), 195–200. https://doi.org/10.1073/pnas.95.1.195

Chen, Lu, Tian, X., Gong, W., Sun, B., Li, G., Liu, D., Guo, P., He, Y., Chen, Z., Xia, Y., Song, T. & Guo, H. (2019). Periostin mediates epithelial-mesenchymal transition through the MAPK/ERK pathway in hepatoblastoma. *Cancer Biology & Medicine*, *16*(1), 89–100. https://doi.org/10.20892/j.issn.2095-3941.2018.0077

Chesnokov, M. S., Yadav, A. & Chefetz, I. (2022). Optimized Transcriptional Signature for Evaluation of MEK/ERK Pathway Baseline Activity and Long-Term Modulations in Ovarian Cancer. *International Journal of Molecular Sciences*, *23*(21), 13365. https://doi.org/10.3390/ijms232113365

Chitale, D., Gong, Y., Taylor, B. S., Broderick, S., Brennan, C., Somwar, R., Golas, B., Wang, L., Motoi, N., Szoke, J., Reinersman, J. M., Major, J., Sander, C., Seshan, V. E., Zakowski, M. F., Rusch, V., Pao, W., Gerald, W. & Ladanyi, M. (2009). An integrated genomic analysis of lung cancer reveals loss of DUSP4 in EGFR-mutant tumors. *Oncogene*, *28*(31), 2773–2783. https://doi.org/10.1038/onc.2009.135

Cho, E., Lou, H. J., Kuruvilla, L., Calderwood, D. A. & Turk, B. E. (2021). PPP6C negatively regulates oncogenic ERK signaling through dephosphorylation of MEK. *Cell Reports*, *34*(13), 108928–108928. https://doi.org/10.1016/j.celrep.2021.108928

Chu, Y., Solski, P. A., Khosravi-Far, R., Der, C. J. & Kelly, K. (1996). The Mitogen-activated Protein Kinase Phosphatases PAC1, MKP-1, and MKP-2 Have Unique Substrate Specificities and Reduced Activity in Vivo toward the ERK2 sevenmaker Mutation (∗). *Journal of Biological Chemistry*, *271*(11), 6497–6501. https://doi.org/10.1074/jbc.271.11.6497

Chuderland, D., Konson, A. & Seger, R. (2008). Identification and Characterization of a General Nuclear Translocation Signal in Signaling Proteins. *Molecular Cell*, *31*(6), 850–861. https://doi.org/10.1016/j.molcel.2008.08.007

Cisowski, J., Sayin, V. I., Liu, M., Karlsson, C. & Bergo, M. O. (2016). Oncogene-induced senescence underlies the mutual exclusive nature of oncogenic KRAS and BRAF. *Oncogene*, *35*(10), 1328–1333. https://doi.org/10.1038/onc.2015.186

Clark, R., Wong, G., Arnheim, N., Nitecki, D. & McCormick, F. (1985). Antibodies specific for amino acid 12 of the ras oncogene product inhibit GTP binding. *Proceedings of the National Academy of Sciences*, *82*(16), 5280–5284. https://doi.org/10.1073/pnas.82.16.5280

Colombino, M., Capone, M., Lissia, A., Cossu, A., Rubino, C., Giorgi, V. D., Massi, D., Fonsatti, E., Staibano, S., Nappi, O., Pagani, E., Casula, M., Manca, A., Sini, M., Franco, R., Botti, G., Caracò, C., Mozzillo, N., Ascierto, P. A. & Palmieri, G. (2012). BRAF/NRAS Mutation Frequencies Among Primary Tumors and Metastases in Patients With Melanoma. *Journal of Clinical Oncology*, *30*(20), 2522–2529. https://doi.org/10.1200/jco.2011.41.2452

Concordet, J.-P. & Haeussler, M. (2018). CRISPOR: intuitive guide selection for CRISPR/Cas9 genome editing experiments and screens. *Nucleic Acids Research*, *46*(Web Server issue), W242–W245. https://doi.org/10.1093/nar/gky354

Cong, L., Ran, F. A., Cox, D., Lin, S., Barretto, R., Habib, N., Hsu, P. D., Wu, X., Jiang, W., Marraffini, L. A. & Zhang, F. (2013). Multiplex Genome Engineering Using CRISPR/Cas Systems. *Science*, *339*(6121), 819–823. https://doi.org/10.1126/science.1231143

Corcoran, R. B., Cheng, K. A., Hata, A. N., Faber, A. C., Ebi, H., Coffee, E. M., Greninger, P., Brown, R. D., Godfrey, J. T., Cohoon, T. J., Song, Y., Lifshits, E., Hung, K. E., Shioda, T., Dias-Santagata, D., Singh, A., Settleman, J., Benes, C. H., Mino-Kenudson, M., … Engelman, J. A. (2013). Synthetic Lethal Interaction of Combined BCL-XL and MEK Inhibition Promotes Tumor Regressions in KRAS Mutant Cancer Models. *Cancer Cell*, *23*(1), 121–128. https://doi.org/10.1016/j.ccr.2012.11.007

Corcoran, R. B., Ebi, H., Turke, A. B., Coffee, E. M., Nishino, M., Cogdill, A. P., Brown, R. D., Pelle, P. D., Dias-Santagata, D., Hung, K. E., Flaherty, K. T., Piris, A., Wargo, J. A., Settleman, J., Mino-Kenudson, M. & Engelman, J. A. (2012). EGFR-Mediated Reactivation of MAPK Signaling Contributes to Insensitivity of BRAF-Mutant Colorectal Cancers to RAF Inhibition with Vemurafenib. *Cancer Discovery*, *2*(3), 227–235. https://doi.org/10.1158/2159-8290.cd-11-0341

Courtois-Cox, S., Williams, S. M. G., Reczek, E. E., Johnson, B. W., McGillicuddy, L. T., Johannessen, C. M., Hollstein, P. E., MacCollin, M. & Cichowski, K. (2006). A negative feedback signaling network underlies oncogene-induced senescence. *Cancer Cell*, *10*(6), 459–472. https://doi.org/10.1016/j.ccr.2006.10.003

Creighton, C. J. (2007). A gene transcription signature of the Akt/mTOR pathway in clinical breast tumors. *Oncogene*, *26*(32), 4648–4655. https://doi.org/10.1038/sj.onc.1210245

Cuevas-Navarro, A., Wagner, M., Van, R., Swain, M., Mo, S., Columbus, J., Allison, M. R., Cheng, A., Messing, S., Turbyville, T. J., Simanshu, D. K., Sale, M. J., McCormick, F., Stephen, A. G. & Castel, P. (2023). RAS-dependent RAF-MAPK hyperactivation by pathogenic RIT1 is a therapeutic target in Noonan syndrome–associated cardiac hypertrophy. *Science Advances*, *9*(28), eadf4766. https://doi.org/10.1126/sciadv.adf4766

Damnernsawad, A., Kong, G., Wen, Z., Liu, Y., Rajagopalan, A., You, X., Wang, J., Zhou, Y., Ranheim, E. A., Luo, H. R., Chang, Q. & Zhang, J. (2016). Kras is Required for Adult Hematopoiesis. *STEM CELLS*, *34*(7), 1859–1871. https://doi.org/10.1002/stem.2355

Danaher, P., Warren, S., Dennis, L., D'Amico, L., White, A., Disis, M. L., Geller, M. A., Odunsi, K., Beechem, J. & Fling, S. P. (2017). Gene expression markers of Tumor Infiltrating Leukocytes. *Journal for ImmunoTherapy of Cancer*, *5*(1), 18. https://doi.org/10.1186/s40425-017-0215-8

Danaher, P., Warren, S., Lu, R., Samayoa, J., Sullivan, A., Pekker, I., Wallden, B., Marincola, F. M. & Cesano, A. (2018). Pan-cancer adaptive immune resistance as defined by the Tumor Inflammation Signature (TIS): results from The Cancer Genome Atlas (TCGA). *Journal for ImmunoTherapy of Cancer*, *6*(1), 63. https://doi.org/10.1186/s40425-018-0367-1

Denhez, B., Rousseau, M., Dancosst, D.-A., Lizotte, F., Guay, A., Auger-Messier, M., Côté, A. M. & Geraldes, P. (2019). Diabetes-Induced DUSP4 Reduction Promotes Podocyte Dysfunction and Progression of Diabetic Nephropathy. *Diabetes*, *68*(5), 1026–1039. https://doi.org/10.2337/db18-0837

DeNicola, G. M., Karreth, F. A., Humpton, T. J., Gopinathan, A., Wei, C., Frese, K., Mangal, D., Yu, K. H., Yeo, C. J., Calhoun, E. S., Scrimieri, F., Winter, J. M., Hruban, R. H., Iacobuzio-Donahue, C., Kern, S. E., Blair, I. A. & Tuveson, D. A. (2011). Oncogene-induced Nrf2 transcription promotes ROS detoxification and tumorigenesis. *Nature*, *475*(7354), 106–109. https://doi.org/10.1038/nature10189

Der, C. J., Finkel, T. & Cooper, G. M. (1986). Biological and biochemical properties of human rasH genes mutated at codon 61. *Cell*, *44*(1), 167–176. https://doi.org/10.1016/0092-8674(86)90495-2

Dhawahir, A. (2009). *Generación y caracterización de modelos murinos deficientes en los genes ras*. Universidad Autónoma de Madrid.

Diehn, M., Cho, R. W., Lobo, N. A., Kalisky, T., Dorie, M. J., Kulp, A. N., Qian, D., Lam, J. S., Ailles, L. E., Wong, M., Joshua, B., Kaplan, M. J., Wapnir, I., Dirbas, F. M., Somlo, G., Garberoglio, C., Paz, B., Shen, J., Lau, S. K., … Clarke, M. F. (2009). Association of reactive oxygen species levels and radioresistance in cancer stem cells. *Nature*, *458*(7239), 780–783. https://doi.org/10.1038/nature07733

Dobin, A., Davis, C. A., Schlesinger, F., Drenkow, J., Zaleski, C., Jha, S., Batut, P., Chaisson, M. & Gingeras, T. R. (2013). STAR: ultrafast universal RNA-seq aligner. *Bioinformatics*, *29*(1), 15–21. https://doi.org/10.1093/bioinformatics/bts635

Doench, J. G., Fusi, N., Sullender, M., Hegde, M., Vaimberg, E. W., Donovan, K. F., Smith, I., Tothova, Z., Wilen, C., Orchard, R., Virgin, H. W., Listgarten, J. & Root, D. E. (2016). Optimized sgRNA design to maximize activity and minimize off-target effects of CRISPR-Cas9. *Nature Biotechnology*, *34*(2), 184–191. https://doi.org/10.1038/nbt.3437

Dogan, S., Shen, R., Ang, D. C., Johnson, M. L., D'Angelo, S. P., Paik, P. K., Brzostowski, E. B., Riely, G. J., Kris, M. G., Zakowski, M. F. & Ladanyi, M. (2012). Molecular Epidemiology of EGFR and KRAS Mutations in 3,026 Lung Adenocarcinomas: Higher Susceptibility of Women to Smoking-Related KRAS-Mutant Cancers. *Clinical Cancer Research*, *18*(22), 6169–6177. https://doi.org/10.1158/1078-0432.ccr-11-3265

Douville, E. & Downward, J. (1997). EGF induced SOS phosphorylation in PC12 cells involves P90 RSK-2. *Oncogene*, *15*(4), 373–383. https://doi.org/10.1038/sj.onc.1201214

Drosten, M., Dhawahir, A., Sum, E. Y. M., Urosevic, J., Lechuga, C. G., Esteban, L. M., Castellano, E., Guerra, C., Santos, E. & Barbacid, M. (2010). Genetic analysis of Ras signalling pathways in cell proliferation, migration and survival. *The EMBO Journal*, *29*(6), 1091–1104. https://doi.org/10.1038/emboj.2010.7

Dry, J. R., Pavey, S., Pratilas, C. A., Harbron, C., Runswick, S., Hodgson, D., Chresta, C., McCormack, R., Byrne, N., Cockerill, M., Graham, A., Beran, G., Cassidy, A., Haggerty, C., Brown, H., Ellison, G., Dering, J., Taylor, B. S., Stark, M., … Smith, P. D. (2010). Transcriptional pathway signatures predict MEK addiction and response to selumetinib (AZD6244). *Cancer Research*, *70*(6), 2264–2273. https://doi.org/10.1158/0008-5472.can-09-1577

DuPage, M., Dooley, A. L. & Jacks, T. (2009). Conditional mouse lung cancer models using adenoviral or lentiviral delivery of Cre recombinase. *Nature Protocols*, *4*(7), 1064–1072. https://doi.org/10.1038/nprot.2009.95

Dy, G. K., Govindan, R., Velcheti, V., Falchook, G. S., Italiano, A., Wolf, J., Sacher, A. G., Takahashi, T., Ramalingam, S. S., Dooms, C., Kim, D.-W., Addeo, A., Desai, J., Schuler, M., Tomasini, P., Hong, D. S., Lito, P., Tran, Q., Jones, S., … Li, B. T. (2023). Long-Term Outcomes and Molecular Correlates of Sotorasib Efficacy in Patients With Pretreated KRAS G12C-Mutated Non–Small-Cell Lung Cancer: 2-Year Analysis of CodeBreaK 100. *Journal of Clinical Oncology*, *41*(18), 3311–3317. https://doi.org/10.1200/jco.22.02524

East, P., Kelly, G. P., Biswas, D., Marani, M., Hancock, D. C., Creasy, T., Sachsenmeier, K., Swanton, C., consortium, Tracer., Downward, J. & Trécesson, S. de C. (2022). RAS oncogenic activity predicts response to chemotherapy and outcome in lung adenocarcinoma. *Nature Communications*, *13*(1), 5632. https://doi.org/10.1038/s41467-022-33290-0

Ecker, V., Brandmeier, L., Stumpf, M., Giansanti, P., Moreira, A. V., Pfeuffer, L., Fens, M. H. A. M., Lu, J., Kuster, B., Engleitner, T., Heidegger, S., Rad, R., Ringshausen, I., Zenz, T., Wendtner, C.-M., Müschen, M., Jellusova, J., Ruland, J. & Buchner, M. (2023). Negative feedback regulation of MAPK signaling is an important driver of chronic lymphocytic leukemia progression. *Cell Reports*, *42*(10), 113017. https://doi.org/10.1016/j.celrep.2023.113017

Egan, S. E., Giddings, B. W., Brooks, M. W., Buday, L., Sizeland, A. M. & Weinberg, R. A. (1993). Association of Sos Ras exchange protein with Grb2 is implicated in tyrosine kinase signal transduction and transformation. *Nature*, *363*(6424), 45–51. https://doi.org/10.1038/363045a0

Ekerot, M., Stavridis, M. P., Delavaine, L., Mitchell, M. P., Staples, C., Owens, D. M., Keenan, I. D., Dickinson, R. J., Storey, K. G. & Keyse, S. M. (2008). Negative-feedback regulation of FGF signalling by DUSP6/MKP-3 is driven by ERK1/2 and mediated by Ets factor binding to a conserved site within the DUSP6/MKP-3 gene promoter. *Biochemical Journal*, *412*(Pt 2), 287–298. https://doi.org/10.1042/bj20071512

Ender, P., Gagliardi, P. A., Dobrzyński, M., Frismantiene, A., Dessauges, C., Höhener, T., Jacques, M.-A., Cohen, A. R. & Pertz, O. (2022). Spatiotemporal control of ERK pulse frequency coordinates fate decisions during mammary acinar morphogenesis. *Developmental Cell*, *57*(18), 2153-2167.e6. https://doi.org/10.1016/j.devcel.2022.08.008

Evan, G. I., Wyllie, A. H., Gilbert, C. S., Littlewood, T. D., Land, H., Brooks, M., Waters, C. M., Penn, L. Z. & Hancock, D. C. (1992). Induction of apoptosis in fibroblasts by c-myc protein. *Cell*, *69*(1), 119–128. https://doi.org/10.1016/0092-8674(92)90123-t

Evdokimov, A. G., Pokross, M. E., Egorov, N. S., Zaraisky, A. G., Yampolsky, I. V., Merzlyak, E. M., Shkoporov, A. N., Sander, I., Lukyanov, K. A. & Chudakov, D. M. (2006). Structural basis for the fast maturation of Arthropoda green fluorescent protein. *EMBO Reports*, *7*(10), 1006–1012. https://doi.org/10.1038/sj.embor.7400787

Fedele, C., Li, S., Teng, K. W., Foster, C. J. R., Peng, D., Ran, H., Mita, P., Geer, M. J., Hattori, T., Koide, A., Wang, Y., Tang, K. H., Leinwand, J., Wang, W., Diskin, B., Deng, J., Chen, T., Dolgalev, I., Ozerdem, U., … Neel, B. G. (2020). SHP2 inhibition diminishes KRASG12C cycling and promotes tumor microenvironment remodeling. *Journal of Experimental Medicine*, *218*(1), e20201414. https://doi.org/10.1084/jem.20201414

Fenech, M. (2007). Cytokinesis-block micronucleus cytome assay. *Nature Protocols*, *2*(5), 1084–1104. https://doi.org/10.1038/nprot.2007.77

Feng, T., Golji, J., Li, A., Zhang, X., Ruddy, D. A., Rakiec, D. P., Geyer, F. C., Gu, J., Gao, H., Williams, J. A., Stuart, D. D. & Meyer, M. J. (2019). Distinct Transcriptional Programming Drive Response to MAPK Inhibition in BRAFV600-Mutant Melanoma Patient-Derived Xenografts. *Molecular Cancer Therapeutics*, *18*(12), 2421–2432. https://doi.org/10.1158/1535-7163.mct-19-0028

Ferguson, B. S., Harrison, B. C., Jeong, M. Y., Reid, B. G., Wempe, M. F., Wagner, F. F., Holson, E. B. & McKinsey, T. A. (2013). Signal-dependent repression of DUSP5 by class I HDACs controls nuclear ERK activity and cardiomyocyte hypertrophy. *Proceedings of the National Academy of Sciences*, *110*(24), 9806–9811. https://doi.org/10.1073/pnas.1301509110

Finotello, F., Mayer, C., Plattner, C., Laschober, G., Rieder, D., Hackl, H., Krogsdam, A., Loncova, Z., Posch, W., Wilflingseder, D., Sopper, S., Ijsselsteijn, M., Brouwer, T. P., Johnson, D., Xu, Y., Wang, Y., Sanders, M. E., Estrada, M. V., Ericsson-Gonzalez, P., … Trajanoski, Z. (2019). Molecular and pharmacological modulators of the tumor immune contexture revealed by deconvolution of RNA-seq data. *Genome Medicine*, *11*(1), 34. https://doi.org/10.1186/s13073-019-0638-6

Flaherty, K. T., Robert, C., Hersey, P., Nathan, P., Garbe, C., Milhem, M., Demidov, L. V., Hassel, J. C., Rutkowski, P., Mohr, P., Dummer, R., Trefzer, U., Larkin, J. M. G., Utikal, J., Dreno, B., Nyakas, M., Middleton, M. R., Becker, J. C., Casey, M., … Group, M. S. (2012). Improved Survival with MEK Inhibition in BRAF-Mutated Melanoma. *New England Journal of Medicine*, *367*(2), 107–114. https://doi.org/10.1056/nejmoa1203421

Franza, B. R., Maruyama, K., Garrels, J. I. & Ruley, H. E. (1986). In vitro establishment is not a sufficient prerequisite for transformation by activated ras oncogenes. *Cell*, *44*(3), 409–418. https://doi.org/10.1016/0092-8674(86)90462-9

García, Z., Kumar, A., Marqués, M., Cortés, I. & Carrera, A. C. (2006). Phosphoinositide 3-kinase controls early and late events in mammalian cell division. *The EMBO Journal*, *25*(4), 655–661. https://doi.org/10.1038/sj.emboj.7600967

Gardner, A. M., Vaillancourt, R. R., Lange-Carter, C. A. & Johnson, G. L. (1994). MEK-1 phosphorylation by MEK kinase, Raf, and mitogen-activated protein kinase: analysis of phosphopeptides and regulation of activity. *Molecular Biology of the Cell*, *5*(2), 193–201. https://doi.org/10.1091/mbc.5.2.193

Gebregiworgis, T., Kano, Y., St-Germain, J., Radulovich, N., Udaskin, M. L., Mentes, A., Huang, R., Poon, B. P. K., He, W., Valencia-Sama, I., Robinson, C. M., Huestis, M., Miao, J., Yeh, J. J., Zhang, Z.-Y., Irwin, M. S., Lee, J. E., Tsao, M.-S., Raught, B., … Ikura, M. (2021). The Q61H mutation decouples KRAS from upstream regulation and renders cancer cells resistant to SHP2 inhibitors. *Nature Communications*, *12*(1), 6274. https://doi.org/10.1038/s41467-021-26526-y

George, J., Lim, J. S., Jang, S. J., Cun, Y., Ozretić, L., Kong, G., Leenders, F., Lu, X., Fernández-Cuesta, L., Bosco, G., Müller, C., Dahmen, I., Jahchan, N. S., Park, K.-S., Yang, D., Karnezis, A. N., Vaka, D., Torres, A., Wang, M. S., … Thomas, R. K. (2015). Comprehensive genomic profiles of small cell lung cancer. *Nature*, *524*(7563), 47–53. https://doi.org/10.1038/nature14664

Germann, U. A., Furey, B. F., Markland, W., Hoover, R. R., Aronov, A. M., Roix, J. J., Hale, M., Boucher, D. M., Sorrell, D. A., Martinez-Botella, G., Fitzgibbon, M., Shapiro, P., Wick, M. J., Samadani, R., Meshaw, K., Groover, A., DeCrescenzo, G., Namchuk, M., Emery, C. M., … Welsch, D. J. (2017). Targeting the MAPK Signaling Pathway in Cancer: Promising

Preclinical Activity with the Novel Selective ERK1/2 Inhibitor BVD-523 (ulixertinib). *Molecular Cancer Therapeutics*, *16*(11), molcanther.0456.2017. https://doi.org/10.1158/1535-7163.mct-17-0456

Goldman, M. J., Craft, B., Hastie, M., Repečka, K., McDade, F., Kamath, A., Banerjee, A., Luo, Y., Rogers, D., Brooks, A. N., Zhu, J. & Haussler, D. (2020). Visualizing and interpreting cancer genomics data via the Xena platform. *Nature Biotechnology*, *38*(6), 675–678. https://doi.org/10.1038/s41587-020-0546-8

Goswami, D., Chen, D., Yang, Y., Gudla, P. R., Columbus, J., Worthy, K., Rigby, M., Wheeler, M., Mukhopadhyay, S., Powell, K., Burgan, W., Wall, V., Esposito, D., Simanshu, D., Lightstone, F. C., Nissley, D. V., McCormick, F. & Turbyville, T. (2020). Membrane interactions of the globular domain and the hypervariable region of KRAS4b define its unique diffusion behavior. *ELife*, *9*, e47654. https://doi.org/10.7554/elife.47654

Goulart, B. H. L., Larkins, E., Beaver, J. A. & Singh, H. (2023). Continuation of Third-Generation Tyrosine Kinase Inhibitors in Second-Line Trials for EGFR-Mutated Non–Small-Cell Lung Cancer: Regulatory Considerations. *Journal of Clinical Oncology*, *41*(23), 3905–3908. https://doi.org/10.1200/jco.23.00154

Grabocka, E., Pylayeva-Gupta, Y., Jones, M. J. K., Lubkov, V., Yemanaberhan, E., Taylor, L., Jeng, H. H. & Bar-Sagi, D. (2014). Wild-Type H- and N-Ras Promote Mutant K-Ras-Driven Tumorigenesis by Modulating the DNA Damage Response. *Cancer Cell*, *25*(2), 243–256. https://doi.org/10.1016/j.ccr.2014.01.005

Gray-Schopfer, V. C., Karasarides, M., Hayward, R. & Marais, R. (2007). Tumor Necrosis Factor-α Blocks Apoptosis in Melanoma Cells when BRAF Signaling Is Inhibited. *Cancer Research*, *67*(1), 122–129. https://doi.org/10.1158/0008-5472.can-06-1880

Gröschl, B., Bettstetter, M., Giedl, C., Woenckhaus, M., Edmonston, T., Hofstädter, F. & Dietmaier, W. (2013). Expression of the MAP kinase phosphatase DUSP4 is associated with microsatellite instability in colorectal cancer (CRC) and causes increased cell proliferation. *International Journal of Cancer*, *132*(7), 1537–1546. https://doi.org/10.1002/ijc.27834

Guan, K.-L. & Butch, E. (1995). Isolation and Characterization of a Novel Dual Specific Phosphatase, HVH2, Which Selectively Dephosphorylates the Mitogen-activated Protein Kinase (∗). *Journal of Biological Chemistry*, *270*(13), 7197–7203. https://doi.org/10.1074/jbc.270.13.7197

Guerra, C., Mijimolle, N., Dhawahir, A., Dubus, P., Barradas, M., Serrano, M., Campuzano, V. & Barbacid, M. (2003). Tumor induction by an endogenous K-ras oncogene is highly dependent on cellular context. *Cancer Cell*, *4*(2), 111–120. https://doi.org/10.1016/s1535-6108(03)00191-0

Guler, S., Altunok, T. H., Sarioglu, A., Zik, B., Asmaz, D., Kayapunar, N., Sonmez, O., Tepedelen, B. E. & Yalcin, A. (2022). Overexpression of dual-specificity phosphatases 4 and 13 attenuates transforming growth factor β1-induced migration and drug resistance in A549 cells in vitro. *Biochemical and Biophysical Research Communications*, *606*, 35–41. https://doi.org/10.1016/j.bbrc.2022.03.090

Guo, X. & Chen, S. (2017). Dedicator of Cytokinesis 2 in Cell Signaling Regulation and Disease Development. *Journal of Cellular Physiology*, *232*(8), 1931–1940. https://doi.org/10.1002/jcp.25512

Gupta, A., Towers, C., Willenbrock, F., Brant, R., Hodgson, D. R., Sharpe, A., Smith, P., Cutts, A., Schuh, A., Asher, R., Myers, K., Love, S., Collins, L., Wise, A., Middleton, M. R. & Macaulay, V. M. (2020). Dual-specificity protein phosphatase DUSP4 regulates response to MEK inhibition in BRAF wild-type melanoma. *British Journal of Cancer*, *122*(4), 506–516. https://doi.org/10.1038/s41416-019-0673-5

Gupta, S., Ramjaun, A. R., Haiko, P., Wang, Y., Warne, P. H., Nicke, B., Nye, E., Stamp, G., Alitalo, K. & Downward, J. (2007). Binding of Ras to Phosphoinositide 3-Kinase p110α Is Required for Ras- Driven Tumorigenesis in Mice. *Cell*, *129*(5), 957–968. https://doi.org/10.1016/j.cell.2007.03.051

Gutierrez-Prat, N., Zuberer, H. L., Mangano, L., Karimaddini, Z., Wolf, L., Tyanova, S., Wellinger, L. C., Marbach, D., Griesser, V., Pettazzoni, P., Bischoff, J. R., Rohle, D., Palladino, C. & Vivanco, I. (2022). DUSP4 protects BRAF- and NRAS-mutant melanoma from oncogene overdose through modulation of MITF. *Life Science Alliance*, *5*(9), e202101235. https://doi.org/10.26508/lsa.202101235

Haigis, K. M. (2017). KRAS Alleles: The Devil Is in the Detail. *Trends in Cancer*, *3*(10), 686–697. https://doi.org/10.1016/j.trecan.2017.08.006

Hallin, J., Engstrom, L. D., Hargis, L., Calinisan, A., Aranda, R., Briere, D. M., Sudhakar, N., Bowcut, V., Baer, B. R., Ballard, J. A., Burkard, M. R., Fell, J. B., Fischer, J. P., Vigers, G. P., Xue, Y., Gatto, S., Fernandez-Banet, J., Pavlicek, A., Velastagui, K., … Christensen, J. G. (2020). The KRASG12C Inhibitor MRTX849 Provides Insight toward Therapeutic Susceptibility of KRAS-Mutant Cancers in Mouse Models and Patients. *Cancer Discovery*, *10*(1), 54–71. https://doi.org/10.1158/2159-8290.cd-19-1167

Hanafusa, H., Torii, S., Yasunaga, T., Matsumoto, K. & Nishida, E. (2004). Shp2, an SH2-containing Protein-tyrosine Phosphatase, Positively Regulates Receptor Tyrosine Kinase Signaling by Dephosphorylating and Inactivating the Inhibitor Sprouty*. *Journal of Biological Chemistry*, *279*(22), 22992–22995. https://doi.org/10.1074/jbc.m312498200

Hanafusa, H., Torii, S., Yasunaga, T. & Nishida, E. (2002). Sprouty1 and Sprouty2 provide a control mechanism for the Ras/MAPK signalling pathway. *Nature Cell Biology*, *4*(11), 850–858. https://doi.org/10.1038/ncb867

Hanahan, D. & Weinberg, R. A. (2000). The Hallmarks of Cancer. *Cell*, *100*(1), 57–70. https://doi.org/10.1016/s0092-8674(00)81683-9

Hanke, J. H., Gardner, J. P., Dow, R. L., Changelian, P. S., Brissette, W. H., Weringer, E. J., Pollok, B. A. & Connelly, P. A. (1996). Discovery of a Novel, Potent, and Src Family-selective Tyrosine Kinase Inhibitor STUDY OF Lck- AND FynT-DEPENDENT T CELL ACTIVATION (∗). *Journal of Biological Chemistry*, *271*(2), 695–701. https://doi.org/10.1074/jbc.271.2.695

Hänzelmann, S., Castelo, R. & Guinney, J. (2013). GSVA: gene set variation analysis for microarray and RNA-Seq data. *BMC Bioinformatics*, *14*(1), 7. https://doi.org/10.1186/1471-2105-14-7

Hatzivassiliou, G., Haling, J. R., Chen, H., Song, K., Price, S., Heald, R., Hewitt, J. F. M., Zak, M., Peck, A., Orr, C., Merchant, M., Hoeflich, K. P., Chan, J., Luoh, S.-M., Anderson, D. J., Ludlam, M. J. C., Wiesmann, C., Ultsch, M., Friedman, L. S., … Belvin, M. (2013). Mechanism of MEK inhibition determines efficacy in mutant KRAS- versus BRAF-driven cancers. *Nature*, *501*(7466), 232–236. https://doi.org/10.1038/nature12441

Hatzivassiliou, G., Liu, B., O'Brien, C., Spoerke, J. M., Hoeflich, K. P., Haverty, P. M., Soriano, R., Forrest, W. F., Heldens, S., Chen, H., Toy, K., Ha, C., Zhou, W., Song, K., Friedman, L. S., Amler, L. C., Hampton, G. M., Moffat, J., Belvin, M. & Lackner, M. R. (2012). ERK Inhibition Overcomes Acquired Resistance to MEK Inhibitors. *Molecular Cancer Therapeutics*, *11*(5), 1143–1154. https://doi.org/10.1158/1535-7163.mct-11-1010

Hatzivassiliou, G., Song, K., Yen, I., Brandhuber, B. J., Anderson, D. J., Alvarado, R., Ludlam, M. J. C., Stokoe, D., Gloor, S. L., Vigers, G., Morales, T., Aliagas, I., Liu, B., Sideris, S., Hoeflich, K. P., Jaiswal, B. S., Seshagiri, S., Koeppen, H., Belvin, M., … Malek, S. (2010). RAF inhibitors prime wild-type RAF to activate the MAPK pathway and enhance growth. *Nature*, *464*(7287), 431–435. https://doi.org/10.1038/nature08833

He, H., Du, Z., Lin, J., Wu, W. & Yu, Y. (2021). DUSP4 inhibits autophagic cell death in PTC by inhibiting JNK–BCL2–Beclin1 signaling. *Biochemistry and Cell Biology*, *99*(5), 554–561. https://doi.org/10.1139/bcb-2020-0636

Heidorn, S. J., Milagre, C., Whittaker, S., Nourry, A., Niculescu-Duvas, I., Dhomen, N., Hussain, J., Reis-Filho, J. S., Springer, C. J., Pritchard, C. & Marais, R. (2010). Kinase-Dead BRAF and Oncogenic RAS Cooperate to Drive Tumor Progression through CRAF. *Cell*, *140*(2), 209–221. https://doi.org/10.1016/j.cell.2009.12.040

Hendriks, W. J. A. J., Elson, A., Harroch, S., Pulido, R., Stoker, A. & Hertog, J. den. (2013). Protein tyrosine phosphatases in health and disease. *The FEBS Journal*, *280*(2), 708–730. https://doi.org/10.1111/febs.12000

Herbst, R. S., Heymach, J. V. & Lippman, S. M. (2008). Lung Cancer. *The New England Journal of Medicine*, *359*(13), 1367–1380. https://doi.org/10.1056/nejmra0802714

Herman, J. A., Romain, R. R., Hoellerbauer, P., Shirnekhi, H. K., King, D. C., DeLuca, K. F., Nishimura, E. O., Paddison, P. J. & DeLuca, J. G. (2022). Hyper-active RAS/MAPK introduces cancer-specific mitotic vulnerabilities. *Proceedings of the National Academy of Sciences*, *119*(41), e2208255119. https://doi.org/10.1073/pnas.2208255119

Herrero, A., Pinto, A., Colón-Bolea, P., Casar, B., Jones, M., Agudo-Ibáñez, L., Vidal, R., Tenbaum, S. P., Nuciforo, P., Valdizán, E. M., Horvath, Z., Orfi, L., Pineda-Lucena, A., Bony, E., Keri, G., Rivas, G., Pazos, A., Gozalbes, R., Palmer, H. G., … Crespo, P. (2015). Small Molecule Inhibition of ERK Dimerization Prevents Tumorigenesis by RAS-ERK Pathway Oncogenes. *Cancer Cell*, *28*(2), 170–182. https://doi.org/10.1016/j.ccell.2015.07.001

Herrmann, C., Martin, G. A. & Wittinghofer, A. (1995). Quantitative Analysis of the Complex between p21 ras and the Ras-binding Domain of the Human Raf-1 Protein Kinase (∗). *Journal of Biological Chemistry*, *270*(7), 2901–2905. https://doi.org/10.1074/jbc.270.7.2901

Hill, W., Lim, E. L., Weeden, C. E., Lee, C., Augustine, M., Chen, K., Kuan, F.-C., Marongiu, F., Evans, E. J., Moore, D. A., Rodrigues, F. S., Pich, O., Bakker, B., Cha, H., Myers, R., Maldegem, F. van, Boumelha, J., Veeriah, S., Rowan, A., … Swanton, C. (2023). Lung adenocarcinoma promotion by air pollutants. *Nature*, *616*(7955), 159–167. https://doi.org/10.1038/s41586-023-05874-3

Hirano, F., Kaneko, K., Tamura, H., Dong, H., Wang, S., Ichikawa, M., Rietz, C., Flies, D. B., Lau, J. S., Zhu, G., Tamada, K. & Chen, L. (2005). Blockade of B7-H1 and PD-1 by Monoclonal Antibodies Potentiates Cancer Therapeutic Immunity. *Cancer Research*, *65*(3), 1089–1096. https://doi.org/10.1158/0008-5472.1089.65.3

Hiratsuka, T., Fujita, Y., Naoki, H., Aoki, K., Kamioka, Y. & Matsuda, M. (2015). Intercellular propagation of extracellular signal-regulated kinase activation revealed by in vivo imaging of mouse skin. *ELife*, *4*, e05178. https://doi.org/10.7554/elife.05178

Holderfield, M., Merritt, H., Chan, J., Wallroth, M., Tandeske, L., Zhai, H., Tellew, J., Hardy, S., Hekmat-Nejad, M., Stuart, D. D., McCormick, F. & Nagel, T. E. (2013). RAF Inhibitors Activate the MAPK Pathway by Relieving Inhibitory Autophosphorylation. *Cancer Cell*, *23*(5), 594–602. https://doi.org/10.1016/j.ccr.2013.03.033

Honda, R. & Yasuda, H. (1999). Association of p19ARF with Mdm2 inhibits ubiquitin ligase activity of Mdm2 for tumor suppressor p53. *The EMBO Journal*, *18*(1), 22–27. https://doi.org/10.1093/emboj/18.1.22

Hong, A., Moriceau, G., Sun, L., Lomeli, S., Piva, M., Damoiseaux, R., Holmen, S. L., Sharpless, N. E., Hugo, W. & Lo, R. S. (2017). Exploiting drug addiction mechanisms to select against MAPKi-resistant melanoma. *Cancer Discovery*, *8*(1), CD-17-0682. https://doi.org/10.1158/2159-8290.cd-17-0682

Hong, D. S., Fakih, M. G., Strickler, J. H., Desai, J., Durm, G. A., Shapiro, G. I., Falchook, G. S., Price, T. J., Sacher, A., Denlinger, C. S., Bang, Y.-J., Dy, G. K., Krauss, J. C., Kuboki, Y., Kuo, J. C., Coveler, A. L., Park, K., Kim, T. W., Barlesi, F., … Li, B. T. (2020). KRASG12C Inhibition with Sotorasib in Advanced Solid Tumors. *New England Journal of Medicine*, *383*(13), 1207–1217. https://doi.org/10.1056/nejmoa1917239

Hong, D. S., Hollebecque, A., Gordon, M. S., Flaherty, K. T., Shapiro, G., Rodon, J., Millward, M., Ramdas, N., Zhang, W., Gao, L., Sykes, A., Willard, M. D., Yu, D., Schade, A., Flynn, D. L., Kaufman, M., Peng, S.-B., Conti, I., Tiu, R. V. & Sullivan, R. J. (2017). A first-in-human dose phase 1 study of LY3009120 in advanced cancer patients. *Journal of Clinical Oncology*, *35*(15_suppl), 2507–2507. https://doi.org/10.1200/jco.2017.35.15_suppl.2507

Hood, F. E., Sahraoui, Y. M., Jenkins, R. E. & Prior, I. A. (2023). Ras protein abundance correlates with Ras isoform mutation patterns in cancer. *Oncogene*, *42*(15), 1224–1232. https://doi.org/10.1038/s41388-023-02638-1

Hoshino, R., Chatani, Y., Yamori, T., Tsuruo, T., Oka, H., Yoshida, O., Shimada, Y., Ari-i, S., Wada, H., Fujimoto, J. & Kohno, M. (1999). Constitutive activation of the 41-/43-kDa mitogen-activated protein kinase signaling pathway in human tumors. *Oncogene*, *18*(3), 813–822. https://doi.org/10.1038/sj.onc.1202367

Houben, R., Vetter-Kauczok, C. S., Ortmann, S., Rapp, U. R., Broecker, E. B. & Becker, J. C. (2008). Phospho-ERK Staining Is a Poor Indicator of the Mutational Status of BRAF and NRAS in Human Melanoma. *Journal of Investigative Dermatology*, *128*(8), 2003–2012. https://doi.org/10.1038/jid.2008.30

Hrdinka, M. & Horejsi, V. (2014). PAG - a multipurpose transmembrane adaptor protein. *Oncogene*, *33*(41), 4881–4892. https://doi.org/10.1038/onc.2013.485

Hu, J., Stites, E. C., Yu, H., Germino, E. A., Meharena, H. S., Stork, P. J. S., Kornev, A. P., Taylor, S. S. & Shaw, A. S. (2013). Allosteric Activation of Functionally Asymmetric RAF Kinase Dimers. *Cell*, *154*(5), 1036–1046. https://doi.org/10.1016/j.cell.2013.07.046

Huang, C.-Y. & Tan, T.-H. (2012). DUSPs, to MAP kinases and beyond. *Cell & Bioscience*, *2*(1), 24. https://doi.org/10.1186/2045-3701-2-24

Huang, H., Daniluk, J., Liu, Y., Chu, J., Li, Z., Ji, B. & Logsdon, C. D. (2014). Oncogenic K-Ras requires activation for enhanced activity. *Oncogene*, *33*(4), 532–535. https://doi.org/10.1038/onc.2012.619

Huang, J., Dibble, C. C., Matsuzaki, M. & Manning, B. D. (2008). The TSC1-TSC2 Complex Is Required for Proper Activation of mTOR Complex 2. *Molecular and Cellular Biology*, *28*(12), 4104–4115. https://doi.org/10.1128/mcb.00289-08

Huber, W., Carey, V. J., Gentleman, R., Anders, S., Carlson, M., Carvalho, B. S., Bravo, H. C., Davis, S., Gatto, L., Girke, T., Gottardo, R., Hahne, F., Hansen, K. D., Irizarry, R. A., Lawrence, M., Love, M. I., MacDonald, J., Obenchain, V., Oleś, A. K., … Morgan, M. (2015). Orchestrating high-throughput genomic analysis with Bioconductor. *Nature Methods*, *12*(2), 115–121. https://doi.org/10.1038/nmeth.3252

Hunter, J. C., Manandhar, A., Carrasco, M. A., Gurbani, D., Gondi, S. & Westover, K. D. (2015). Biochemical and Structural Analysis of Common Cancer-Associated KRAS Mutations. *Molecular Cancer Research*, *13*(9), 1325–1335. https://doi.org/10.1158/1541-7786.mcr-15-0203

Irizarry, R. A., Hobbs, B., Collin, F., Beazer-Barclay, Y. D., Antonellis, K. J., Scherf, U. & Speed, T. P. (2003). Exploration, normalization, and summaries of high density oligonucleotide array probe level data. *Biostatistics*, *4*(2), 249–264. https://doi.org/10.1093/biostatistics/4.2.249

Ito, T., Young, M. J., Li, R., Jain, S., Wernitznig, A., Krill-Burger, J. M., Lemke, C. T., Monducci, D., Rodriguez, D. J., Chang, L., Dutta, S., Pal, D., Paolella, B. R., Rothberg, M. V., Root, D. E., Johannessen, C. M., Parida, L., Getz, G., Vazquez, F., … Sellers, W. R. (2021). Paralog knockout profiling identifies DUSP4 and DUSP6 as a digenic dependence in MAPK pathway-driven cancers. *Nature Genetics*, *53*(12), 1664–1672. https://doi.org/10.1038/s41588-021-00967-z

Jackson, E. L., Willis, N., Mercer, K., Bronson, R. T., Crowley, D., Montoya, R., Jacks, T. & Tuveson, D. A. (2001). Analysis of lung tumor initiation and progression using conditional expression of oncogenic K-ras. *Genes & Development*, *15*(24), 3243–3248. https://doi.org/10.1101/gad.943001

Janknecht, R., Ernst, W. H., Pingoud, V. & Nordheim, A. (1993). Activation of ternary complex factor Elk-1 by MAP kinases. *The EMBO Journal*, *12*(13), 5097–5104. https://doi.org/10.1002/j.1460-2075.1993.tb06204.x

Jänne, P. A., Heuvel, M. M. van den, Barlesi, F., Cobo, M., Mazieres, J., Crinò, L., Orlov, S., Blackhall, F., Wolf, J., Garrido, P., Poltoratskiy, A., Mariani, G., Ghiorghiu, D., Kilgour, E., Smith, P., Kohlmann, A., Carlile, D. J., Lawrence, D., Bowen, K. & Vansteenkiste, J. (2017). Selumetinib Plus Docetaxel Compared With Docetaxel Alone and Progression-Free Survival in Patients With KRAS-Mutant Advanced Non–Small Cell Lung Cancer: The SELECT-1 Randomized Clinical Trial. *JAMA*, *317*(18), 1844–1853. https://doi.org/10.1001/jama.2017.3438

Jänne, P. A., Riely, G. J., Gadgeel, S. M., Heist, R. S., Ou, S.-H. I., Pacheco, J. M., Johnson, M. L., Sabari, J. K., Leventakos, K., Yau, E., Bazhenova, L., Negrao, M. V., Pennell, N. A., Zhang, J., Anderes, K., Der-Torossian, H., Kheoh, T., Velastegui, K., Yan, X., … Spira, A. I. (2022). Adagrasib in Non–Small-Cell Lung Cancer Harboring a KRASG12C Mutation. *New England Journal of Medicine*, *387*(2), 120–131. https://doi.org/10.1056/nejmoa2204619

Jaumot, M. & Hancock, J. F. (2001). Protein phosphatases 1 and 2A promote Raf-1 activation by regulating 14-3-3 interactions. *Oncogene*, *20*(30), 3949–3958. https://doi.org/10.1038/sj.onc.1204526

Jeong, H.-H., Kim, S. Y., Rousseaux, M. W. C., Zoghbi, H. Y. & Liu, Z. (2017). CRISPRcloud: a secure cloud-based pipeline for CRISPR pooled screen deconvolution. *Bioinformatics*, *33*(18), 2963–2965. https://doi.org/10.1093/bioinformatics/btx335

Ji, L., Xu, S., Luo, H. & Zeng, F. (2022). Insights from DOCK2 in cell function and pathophysiology. *Frontiers in Molecular Biosciences*, *9*, 997659. https://doi.org/10.3389/fmolb.2022.997659

Jiang, B.-C., Zhang, J., Wu, B., Jiang, M., Cao, H., Wu, H. & Gao, Y.-J. (2021). G protein–coupled receptor GPR151 is involved in trigeminal neuropathic pain through the induction of Gβγ/extracellular signal-regulated kinase-mediated neuroinflammation in the trigeminal ganglion. *PAIN*, *162*(5), 1434–1448. https://doi.org/10.1097/j.pain.0000000000002156

Jochems, F., Thijssen, B., Conti, G. D., Jansen, R., Pogacar, Z., Groot, K., Wang, L., Schepers, A., Wang, C., Jin, H., Beijersbergen, R. L., Oliveira, R. L. de, Wessels, L. F. A. & Bernards, R. (2021). The Cancer SENESCopedia: A delineation of cancer cell senescence. *Cell Reports*, *36*(4), 109441. https://doi.org/10.1016/j.celrep.2021.109441

John, J., Sohmen, R., Feuerstein, J., Linke, R., Wittinghofer, A. & Goody, R. S. (1990). Kinetics of interaction of nucleotides with nucleotide-free H-ras p21. *Biochemistry*, *29*(25), 6058–6065. https://doi.org/10.1021/bi00477a025

Johnson, L., Greenbaum, D., Cichowski, K., Mercer, K., Murphy, E., Schmitt, E., Bronson, R. T., Umanoff, H., Edelmann, W., Kucherlapati, R. & Jacks, T. (1997). K-ras is an essential gene in the mouse with partial functional overlap with N-ras. *Genes & Development*, *11*(19), 2468–2481. https://doi.org/10.1101/gad.11.19.2468

Johnson, L., Mercer, K., Greenbaum, D., Bronson, R. T., Crowley, D., Tuveson, D. A. & Jacks, T. (2001). Somatic activation of the K-ras oncogene causes early onset lung cancer in mice. *Nature*, *410*(6832), 1111–1116. https://doi.org/10.1038/35074129

Joung, J., Konermann, S., Gootenberg, J. S., Abudayyeh, O. O., Platt, R. J., Brigham, M. D., Sanjana, N. E. & Zhang, F. (2017). Genome-scale CRISPR-Cas9 knockout and transcriptional activation screening. *Nature Protocols*, *12*(4), 828–863. https://doi.org/10.1038/nprot.2017.016

Juneja, V. R., McGuire, K. A., Manguso, R. T., LaFleur, M. W., Collins, N., Haining, W. N., Freeman, G. J. & Sharpe, A. H. (2017). PD-L1 on tumor cells is sufficient for immune evasion in immunogenic tumors and inhibits CD8 T cell cytotoxicity. *Journal of Experimental Medicine*, *214*(4), 895–904. https://doi.org/10.1084/jem.20160801

Kamada, H., Yasuhira, S., Shibazaki, M., Amano, H. & Maesawa, C. (2022). DUSP4 Inactivation Leads to Reduced Extracellular Signal–Regulated Kinase Activity through Upregulation of DUSP6 in Melanoma Cells. *Journal of Investigative Dermatology*, *142*(9), 2499-2507.e6. https://doi.org/10.1016/j.jid.2022.02.007

Kano, Y., Gebregiworgis, T., Marshall, C. B., Radulovich, N., Poon, B. P. K., St-Germain, J., Cook, J. D., Valencia-Sama, I., Grant, B. M. M., Herrera, S. G., Miao, J., Raught, B., Irwin, M. S., Lee, J. E., Yeh, J. J., Zhang, Z.-Y., Tsao, M.-S., Ikura, M. & Ohh, M. (2019). Tyrosyl

phosphorylation of KRAS stalls GTPase cycle via alteration of switch I and II conformation. *Nature Communications*, *10*(1), 224. https://doi.org/10.1038/s41467-018-08115-8

Kaplan, F. M., Shao, Y., Mayberry, M. M. & Aplin, A. E. (2011). Hyperactivation of MEK–ERK1/2 signaling and resistance to apoptosis induced by the oncogenic B-RAF inhibitor, PLX4720, in mutant N-RAS melanoma cells. *Oncogene*, *30*(3), 366–371. https://doi.org/10.1038/onc.2010.408

Karapetis-Christos, Shirin, K.-F., J., J. D., J., O. C., Dongsheng, T., C., T. N., John, S. R., Haji, C., D., S. J., Sonia, R., J., P. T., Lois, S., Heather-Jane, A., Christiane, L., J., M. M. & R., Z. J. (2008). K-ras Mutations and Benefit from Cetuximab in Advanced Colorectal Cancer. *New England Journal of Medicine*, *359*(17), 1757–1765. https://doi.org/10.1056/nejmoa0804385

Karlsson, M., Mathers, J., Dickinson, R. J., Mandl, M. & Keyse, S. M. (2004). Both Nuclear-Cytoplasmic Shuttling of the Dual Specificity Phosphatase MKP-3 and Its Ability to Anchor MAP Kinase in the Cytoplasm Are Mediated by a Conserved Nuclear Export Signal*. *Journal of Biological Chemistry*, *279*(40), 41882–41891. https://doi.org/10.1074/jbc.m406720200

Kauko, O., O'Connor, C. M., Kulesskiy, E., Sangodkar, J., Aakula, A., Izadmehr, S., Yetukuri, L., Yadav, B., Padzik, A., Laajala, T. D., Haapaniemi, P., Momeny, M., Varila, T., Ohlmeyer, M., Aittokallio, T., Wennerberg, K., Narla, G. & Westermarck, J. (2018). PP2A inhibition is a druggable MEK inhibitor resistance mechanism in KRAS-mutant lung cancer cells. *Science Translational Medicine*, *10*(450). https://doi.org/10.1126/scitranslmed.aaq1093

Kemp, S. J., Thorley, A. J., Gorelik, J., Seckl, M. J., O'Hare, M. J., Arcaro, A., Korchev, Y., Goldstraw, P. & Tetley, T. D. (2008). Immortalization of Human Alveolar Epithelial Cells to Investigate Nanoparticle Uptake. *American Journal of Respiratory Cell and Molecular Biology*, *39*(5), 591–597. https://doi.org/10.1165/rcmb.2007-0334oc

Khan, I., Koide, A., Zuberi, M., Ketavarapu, G., Denbaum, E., Teng, K. W., Rhett, J. M., Spencer-Smith, R., Hobbs, G. A., Camp, E. R., Koide, S. & O'Bryan, J. P. (2022). Identification of the nucleotide-free state as a therapeutic vulnerability for inhibition of selected oncogenic RAS mutants. *Cell Reports*, *38*(6), 110322. https://doi.org/10.1016/j.celrep.2022.110322

Khokhlatchev, A. V., Canagarajah, B., Wilsbacher, J., Robinson, M., Atkinson, M., Goldsmith, E. & Cobb, M. H. (1998). Phosphorylation of the MAP Kinase ERK2 Promotes Its Homodimerization and Nuclear Translocation. *Cell*, *93*(4), 605–615. https://doi.org/10.1016/s0092-8674(00)81189-7

Kidger, A. M., Rushworth, L. K., Stellzig, J., Davidson, J., Bryant, C. J., Bayley, C., Caddye, E., Rogers, T., Keyse, S. M. & Caunt, C. J. (2017). Dual-specificity phosphatase 5 controls the localized inhibition, propagation, and transforming potential of ERK signaling. *Proceedings of the National Academy of Sciences*, *114*(3), E317–E326. https://doi.org/10.1073/pnas.1614684114

Kim, Daehwan, Paggi, J. M., Park, C., Bennett, C. & Salzberg, S. L. (2019). Graph-based genome alignment and genotyping with HISAT2 and HISAT-genotype. *Nature Biotechnology*, *37*(8), 907–915. https://doi.org/10.1038/s41587-019-0201-4

Kim, Dongsung, Herdeis, L., Rudolph, D., Zhao, Y., Böttcher, J., Vides, A., Ayala-Santos, C. I., Pourfarjam, Y., Cuevas-Navarro, A., Xue, J. Y., Mantoulidis, A., Bröker, J., Wunberg, T., Schaaf, O., Popow, J., Wolkerstorfer, B., Kropatsch, K. G., Qu, R., Stanchina, E. de, … Lito,

P. (2023). Pan-KRAS inhibitor disables oncogenic signalling and tumour growth. *Nature*, 1–7. https://doi.org/10.1038/s41586-023-06123-3

Kim, E. S., Herbst, R. S., Wistuba, I. I., Lee, J. J., Blumenschein, G. R., Tsao, A., Stewart, D. J., Hicks, M. E., Erasmus, J., Gupta, S., Alden, C. M., Liu, S., Tang, X., Khuri, F. R., Tran, H. T., Johnson, B. E., Heymach, J. V., Mao, L., Fossella, F., … Hong, W. K. (2011). The BATTLE Trial: Personalizing Therapy for Lung Cancer. *Cancer Discovery*, *1*(1), 44–53. https://doi.org/10.1158/2159-8274.cd-10-0010

Kinahan, H. (2022). A Rare Event of Liver Dysfunction on Sotorasib and Management Strategy. *Journal of the Advanced Practitioner in Oncology*, *13*(8), 812–815. https://doi.org/10.6004/jadpro.2022.13.8.7

Kitai, H., Ebi, H., Tomida, S., Floros, K. V., Kotani, H., Adachi, Y., Oizumi, S., Nishimura, M., Faber, A. C. & Yano, S. (2016). Epithelial-to-Mesenchymal Transition Defines Feedback Activation of Receptor Tyrosine Kinase Signaling Induced by MEK Inhibition in KRAS-Mutant Lung Cancer. *Cancer Discovery*, *6*(7), 754–769. https://doi.org/10.1158/2159-8290.cd-15-1377

Kitajima, S. & Barbie, D. A. (2018). RASA1/NF1 mutant lung cancer: Racing to the clinic? *Clinical Cancer Research*, *24*(6), clincanres.3597.2017. https://doi.org/10.1158/1078-0432.ccr-17-3597

Kochańczyk, M., Kocieniewski, P., Kozłowska, E., Jaruszewicz-Błońska, J., Sparta, B., Pargett, M., Albeck, J. G., Hlavacek, W. S. & Lipniacki, T. (2017). Relaxation oscillations and hierarchy of feedbacks in MAPK signaling. *Scientific Reports*, *7*(1), 38244. https://doi.org/10.1038/srep38244

Kolde, R., Laur, S., Adler, P. & Vilo, J. (2012). Robust rank aggregation for gene list integration and meta-analysis. *Bioinformatics*, *28*(4), 573–580. https://doi.org/10.1093/bioinformatics/btr709

Kosaka, T., Yatabe, Y., Endoh, H., Kuwano, H., Takahashi, T. & Mitsudomi, T. (2004). Mutations of the Epidermal Growth Factor Receptor Gene in Lung Cancer Biological and Clinical Implications. *Cancer Research*, *64*(24), 8919–8923. https://doi.org/10.1158/0008-5472.can-04-2818

Kotsantis, P., Petermann, E. & Boulton, S. J. (2018). Mechanisms of Oncogene-Induced Replication Stress: Jigsaw Falling into Place. *Cancer Discovery*, *8*(5), 537–555. https://doi.org/10.1158/2159-8290.cd-17-1461

Kuo, L. J. & Yang, L.-X. (2008). Gamma-H2AX - a novel biomarker for DNA double-strand breaks. *In Vivo (Athens, Greece)*, *22*(3), 305–309.

Kwan, D. H. T., Yung, L. Y., Ye, R. D. & Wong, Y. H. (2012). Activation of ras-dependent signaling pathways by G14-coupled receptors requires the adaptor protein TPR1. *Journal of Cellular Biochemistry*, *113*(11), 3486–3497. https://doi.org/10.1002/jcb.24225

Labun, K., Montague, T. G., Krause, M., Cleuren, Y. N. T., Tjeldnes, H. & Valen, E. (2019). CHOPCHOP v3: expanding the CRISPR web toolbox beyond genome editing. *Nucleic Acids Research*, *47*(W1), W171–W174. https://doi.org/10.1093/nar/gkz365

Lake, D., Correa, S. A. L. & Ller, • Jü Rgen M̈u. (2016). Negative feedback regulation of the ERK1/2 MAPK pathway. *Cellular and Molecular Life Sciences*, *73*(23), 4397–4413. https://doi.org/10.1007/s00018-016-2297-8

Land, H., Parada, L. F. & Weinberg, R. A. (1983). Tumorigenic conversion of primary embryo fibroblasts requires at least two cooperating oncogenes. *Nature*, *304*(5927), 596–602. https://doi.org/10.1038/304596a0

Lang, R. & Raffi, F. A. M. (2019). Dual-Specificity Phosphatases in Immunity and Infection: An Update. *International Journal of Molecular Sciences*, *20*(11), 2710. https://doi.org/10.3390/ijms20112710

Langen, A. J. de, Johnson, M. L., Mazieres, J., Dingemans, A.-M. C., Mountzios, G., Pless, M., Wolf, J., Schuler, M., Lena, H., Skoulidis, F., Yoneshima, Y., Kim, S.-W., Linardou, H., Novello, S., Wekken, A. J. van der, Chen, Y., Peters, S., Felip, E., Solomon, B. J., … Investigators, C. 200. (2023). Sotorasib versus docetaxel for previously treated non-small-cell lung cancer with KRAS G12C mutation: a randomised, open-label, phase 3 trial. *The Lancet*, *401*(10378), 733–746. https://doi.org/10.1016/s0140-6736(23)00221-0

Lawan, A., Al-Harthi, S., Cadalbert, L., McCluskey, A. G., Shweash, M., Grassia, G., Grant, A., Boyd, M., Currie, S. & Plevin, R. (2011). Deletion of the Dual Specific Phosphatase-4 (DUSP-4) Gene Reveals an Essential Non-redundant Role for MAP Kinase Phosphatase-2 (MKP-2) in Proliferation and Cell Survival*. *Journal of Biological Chemistry*, *286*(15), 12933–12943. https://doi.org/10.1074/jbc.m110.181370

Leach, D. R., Krummel, M. F. & Allison, J. P. (1996). Enhancement of Antitumor Immunity by CTLA-4 Blockade. *Science*, *271*(5256), 1734–1736. https://doi.org/10.1126/science.271.5256.1734

Leung, G. P., Feng, T., Sigoillot, F. D., Geyer, F. C., Shirley, M. D., Ruddy, D. A., Rakiec, D. P., Freeman, A. K., Engelman, J. A., Jaskelioff, M. & Stuart, D. D. (2019). Hyperactivation of MAPK Signaling Is Deleterious to RAS/RAF-mutant Melanoma. *Molecular Cancer Research*, *17*(1), 199–211. https://doi.org/10.1158/1541-7786.mcr-18-0327

Li, B. & Dewey, C. N. (2011). RSEM: accurate transcript quantification from RNA-Seq data with or without a reference genome. *BMC Bioinformatics*, *12*(1), 323. https://doi.org/10.1186/1471-2105-12-323

Li, L., Fan, Y., Huang, X., Luo, J., Zhong, L., Shu, X., Lu, L., Xiang, T., Chan, A. T. C., Yeo, W., Chen, C., Chan, W. Y., Huganir, R. L. & Tao, Q. (2019). Tumor Suppression of Ras GTPase-Activating Protein RASA5 through Antagonizing Ras Signaling Perturbation in Carcinomas. *IScience*, *21*, 1–18. https://doi.org/10.1016/j.isci.2019.10.007

Li, N., Batzer, A., Daly, R., Yajnik, V., Skolnik, E., Chardin, P., Bar-Sagi, D., Margolis, B. & Schlessinger, J. (1993). Guanine-nucleotide-releasing factor hSos1 binds to Grb2 and links receptor tyrosine kinases to Ras signalling. *Nature*, *363*(6424), 85–88. https://doi.org/10.1038/363085a0

Li, S., Balmain, A. & Counter, C. M. (2018). A model for RAS mutation patterns in cancers: finding the sweet spot. *Nature Reviews Cancer*, *18*(12), 767–777. https://doi.org/10.1038/s41568-018-0076-6

Li, W., Xu, H., Xiao, T., Cong, L., Love, M. I., Zhang, F., Irizarry, R. A., Liu, J. S., Brown, M. & Liu, X. S. (2014). MAGeCK enables robust identification of essential genes from genome-scale CRISPR/Cas9 knockout screens. *Genome Biology*, *15*(12), 554. https://doi.org/10.1186/s13059-014-0554-4

Li, X., Zhao, X., Fang, Y., Jiang, X., Duong, T., Fan, C., Huang, C.-C. & Kain, S. R. (1998). Generation of Destabilized Green Fluorescent Protein as a Transcription Reporter*. *Journal of Biological Chemistry*, *273*(52), 34970–34975. https://doi.org/10.1074/jbc.273.52.34970

Li, Y., Gao, Z. & Qu, X. (2015). The Adverse Effects of Sorafenib in Patients with Advanced Cancers. *Basic & Clinical Pharmacology & Toxicology*, *116*(3), 216–221. https://doi.org/10.1111/bcpt.12365

Liao, Q., Guo, J., Kleeff, J., Zimmermann, A., Büchler, M. W., Korc, M. & Friess, H. (2003). Down-regulation of the dual-specificity phosphatase MKP-1 suppresses tumorigenicity of pancreatic cancer cells. *Molecular and Cellular Biology*, *124*(7), 1830–1845. https://doi.org/10.1016/s0016-5085(03)00398-6

Liberzon, A., Subramanian, A., Pinchback, R., Thorvaldsdóttir, H., Tamayo, P. & Mesirov, J. P. (2011). Molecular signatures database (MSigDB) 3.0. *Bioinformatics*, *27*(12), 1739–1740. https://doi.org/10.1093/bioinformatics/btr260

Lièvre, A., Bachet, J.-B., Corre, D. L., Boige, V., Landi, B., Emile, J.-F., Côté, J.-F., Tomasic, G., Penna, C., Ducreux, M., Rougier, P., Penault-Llorca, F. & Laurent-Puig, P. (2006). KRAS Mutation Status Is Predictive of Response to Cetuximab Therapy in Colorectal Cancer. *Cancer Research*, *66*(8), 3992–3995. https://doi.org/10.1158/0008-5472.can-06-0191

Lim, S., Khoo, R., Juang, Y.-C., Gopal, P., Zhang, H., Yeo, C., Peh, K. M., Teo, J., Ng, S., Henry, B. & Partridge, A. W. (2021). Exquisitely Specific anti-KRAS Biodegraders Inform on the Cellular Prevalence of Nucleotide-Loaded States. *ACS Central Science*, *7*(2), 274–291. https://doi.org/10.1021/acscentsci.0c01337

Lim, S. M., Choi, J. W., Hong, M. H., Jung, D., Lee, C. Y., Park, S. Y., Shim, H. S., Sheen, S., Kwak, K. I., Kang, D. R., Cho, B. C. & Kim, H. R. (2019). Indoor radon exposure increases tumor mutation burden in never-smoker patients with lung adenocarcinoma. *Lung Cancer*, *131*, 139–146. https://doi.org/10.1016/j.lungcan.2019.04.002

Liotti, F., Kumar, N., Prevete, N., Marotta, M., Sorriento, D., Ieranò, C., Ronchi, A., Marino, F. Z., Moretti, S., Colella, R., Puxeddu, E., Paladino, S., Kano, Y., Ohh, M., Scala, S. & Melillo, R. M. (2021). PD-1 blockade delays tumor growth by inhibiting an intrinsic SHP2/Ras/MAPK signalling in thyroid cancer cells. *Journal of Experimental & Clinical Cancer Research*, *40*(1), 22. https://doi.org/10.1186/s13046-020-01818-1

Lito, P., Saborowski, A., Yue, J., Solomon, M., Joseph, E., Gadal, S., Saborowski, M., Kastenhuber, E., Fellmann, C., Ohara, K., Morikami, K., Miura, T., Lukacs, C., Ishii, N., Lowe, S. & Rosen, N. (2014). Disruption of CRAF-Mediated MEK Activation Is Required for Effective MEK Inhibition in KRAS Mutant Tumors. *Cancer Cell*, *25*(5), 697–710. https://doi.org/10.1016/j.ccr.2014.03.011

Lito, P., Solomon, M., Li, L.-S., Hansen, R. & Rosen, N. (2016). Allele-specific inhibitors inactivate mutant KRAS G12C by a trapping mechanism. *Science*, *351*(6273), 604–608. https://doi.org/10.1126/science.aad6204

Liu, A. M. F., Lo, R. K. H., Lee, M. M. K., Wang, Y., Yeung, W. W. S., Ho, M. K. C., Su, Y., Ye, R. D. & Wong, Y. H. (2010). Gα16 activates Ras by forming a complex with tetratricopeptide repeat 1 (TPR1) and Son of Sevenless (SOS). *Cellular Signalling*, *22*(10), 1448–1458. https://doi.org/10.1016/j.cellsig.2010.05.013

Liu, C., Lu, H., Wang, H., Loo, A., Zhang, X., Yang, G., Kowal, C., Delach, S., Wang, Y., Goldoni, S., Hastings, W. D., Wong, K., Gao, H., Meyer, M. J., Moody, S. E., LaMarche, M. J., Engelman, J. A., Williams, J. A., Hammerman, P. S., … Hao, H.-X. (2021). Combinations with Allosteric SHP2 Inhibitor TNO155 to Block Receptor Tyrosine Kinase Signaling. *Clinical Cancer Research*, *27*(1), 342–354. https://doi.org/10.1158/1078-0432.ccr-20-2718

Liu, L., Cao, Y., Chen, C., Zhang, X., McNabola, A., Wilkie, D., Wilhelm, S., Lynch, M. & Carter, C. (2006). Sorafenib Blocks the RAF/MEK/ERK Pathway, Inhibits Tumor Angiogenesis, and Induces Tumor Cell Apoptosis in Hepatocellular Carcinoma Model PLC/PRF/5. *Cancer Research*, *66*(24), 11851–11858. https://doi.org/10.1158/0008-5472.can-06-1377

Loboda, A., Nebozhyn, M., Klinghoffer, R., Frazier, J., Chastain, M., Arthur, W., Roberts, B., Zhang, T., Chenard, M., Haines, B., Andersen, J., Nagashima, K., Paweletz, C., Lynch, B., Feldman, I., Dai, H., Huang, P. & Watters, J. (2010). A gene expression signature of RAS pathway dependence predicts response to PI3K and RAS pathway inhibitors and expands the population of RAS pathway activated tumors. *BMC Medical Genomics*, *3*(1), 26. https://doi.org/10.1186/1755-8794-3-26

Long, G. V., Axel, H., Mario, S., Victoria, A., Mario, M., Vanna, C.-S., James, L., Marta, N., Caroline, D., Andrew, H., Caroline, R., Laurent, M., Jacob, S., Dirk, S., Thierry, L., Ruth, P., Ran, J., Pingkuan, Z., Bijoyesh, M., … M., K. J. (2017). Adjuvant Dabrafenib plus Trametinib in Stage III BRAF-Mutated Melanoma. *New England Journal of Medicine*, *377*(19), 1813–1823. https://doi.org/10.1056/nejmoa1708539

Lopez-Bigas, N. & Gonzalez-Perez, A. (2020). Are carcinogens direct mutagens? *Nature Genetics*, *52*(11), 1137–1138. https://doi.org/10.1038/s41588-020-00730-w

Lou, K., Steri, V., Ge, A. Y., Hwang, Y. C., Yogodzinski, C. H., Shkedi, A. R., Choi, A. L. M., Mitchell, D. C., Swaney, D. L., Hann, B., Gordan, J. D., Shokat, K. M. & Gilbert, L. A. (2019). KRASG12C inhibition produces a driver-limited state revealing collateral dependencies. *Science Signaling*, *12*(583). https://doi.org/10.1126/scisignal.aaw9450

Love, M. I., Huber, W. & Anders, S. (2014). Moderated estimation of fold change and dispersion for RNA-seq data with DESeq2. *Genome Biology*, *15*(12), 550. https://doi.org/10.1186/s13059-014-0550-8

Lowenstein, E. J., Daly, R. J., Batzer, A. G., Li, W., Margolis, B., Lammers, R., Ullrich, A., Skolnik, E. Y., Bar-Sagi, D. & Schlessinger, J. (1992). The SH2 and SH3 domain-containing protein GRB2 links receptor tyrosine kinases to ras signaling. *Cell*, *70*(3), 431–442. https://doi.org/10.1016/0092-8674(92)90167-b

Lu, D., Liu, L., Ji, X., Gao, Y., Chen, X., Liu, Y., Liu, Y., Zhao, X., Li, Y., Li, Y., Jin, Y., Zhang, Y., McNutt, M. A. & Yin, Y. (2015). The phosphatase DUSP2 controls the activity of the transcription activator STAT3 and regulates TH17 differentiation. *Nature Immunology*, *16*(12), 1263–1273. https://doi.org/10.1038/ni.3278

Luo, H., Lin, Y., Liu, T., Lai, F.-L., Zhang, C.-T., Gao, F. & Zhang, R. (2020). DEG 15, an update of the Database of Essential Genes that includes built-in analysis tools. *Nucleic Acids Research*, *49*(D1), gkaa917-. https://doi.org/10.1093/nar/gkaa917

Maehama, T. & Dixon, J. E. (1998). The Tumor Suppressor, PTEN/MMAC1, Dephosphorylates the Lipid Second Messenger, Phosphatidylinositol 3,4,5-Trisphosphate*. *Journal of Biological Chemistry*, *273*(22), 13375–13378. https://doi.org/10.1074/jbc.273.22.13375

Malumbres, M. & Barbacid, M. (2003). RAS oncogenes: the first 30 years. *Nature Reviews Cancer*, *3*(6), 459–465. https://doi.org/10.1038/nrc1097

Mamoor, S. (2023). *Differential expression of DUSP4 in cancer of the skin: malignant melanoma.* https://doi.org/10.31219/osf.io/f928g

Marais, R., Light, Y., Paterson, H. F. & Marshall, C. J. (1995). Ras recruits Raf-1 to the plasma membrane for activation by tyrosine phosphorylation. *The EMBO Journal*, *14*(13), 3136–3145. https://doi.org/10.1002/j.1460-2075.1995.tb07316.x

Martinez-Garcia, M., Banerji, U., Albanell, J., Bahleda, R., Dolly, S., Kraeber-Bodéré, F., Rojo, F., Routier, E., Guarin, E., Xu, Z.-X., Rueger, R., Tessier, J. J. L., Shochat, E., Blotner, S., Naegelen, V. M. & Soria, J.-C. (2012). First-in-Human, Phase I Dose-Escalation Study of the Safety, Pharmacokinetics, and Pharmacodynamics of RO5126766, a First-in-Class Dual MEK/RAF Inhibitor in Patients with Solid Tumors. *Clinical Cancer Research*, *18*(17), 4806–4819. https://doi.org/10.1158/1078-0432.ccr-12-0742

Martínez-Jiménez, F., Muiños, F., Sentís, I., Deu-Pons, J., Reyes-Salazar, I., Arnedo-Pac, C., Mularoni, L., Pich, O., Bonet, J., Kranas, H., Gonzalez-Perez, A. & Lopez-Bigas, N. (2020). A compendium of mutational cancer driver genes. *Nature Reviews Cancer*, *20*(10), 555–572. https://doi.org/10.1038/s41568-020-0290-x

Mendoza, M. C., Er, E. E. & Blenis, J. (2011). The Ras-ERK and PI3K-mTOR pathways: cross-talk and compensation. *Trends in Biochemical Sciences*, *36*(6), 320–328. https://doi.org/10.1016/j.tibs.2011.03.006

Mermel, C. H., Schumacher, S. E., Hill, B., Meyerson, M. L., Beroukhim, R. & Getz, G. (2011). GISTIC2.0 facilitates sensitive and confident localization of the targets of focal somatic copy-number alteration in human cancers. *Genome Biology*, *12*(4), R41. https://doi.org/10.1186/gb-2011-12-4-r41

Messina, S., Frati, L., Leonetti, C., Zuchegna, C., Zazzo, E. D., Calogero, A. & Porcellini, A. (2011). Dual-specificity phosphatase DUSP6 has tumor-promoting properties in human glioblastomas. *Oncogene*, *30*(35), 3813–3820. https://doi.org/10.1038/onc.2011.99

Milburn, M. V., Tong, L., deVos, A. M., Brünger, A., Yamaizumi, Z., Nishimura, S. & Kim, S.-H. (1990). Molecular Switch for Signal Transduction: Structural Differences Between Active and Inactive Forms of Protooncogenic ras Proteins. *Science*, *247*(4945), 939–945. https://doi.org/10.1126/science.2406906

Moffat, J., Grueneberg, D. A., Yang, X., Kim, S. Y., Kloepfer, A. M., Hinkle, G., Piqani, B., Eisenhaure, T. M., Luo, B., Grenier, J. K., Carpenter, A. E., Foo, S. Y., Stewart, S. A., Stockwell, B. R., Hacohen, N., Hahn, W. C., Lander, E. S., Sabatini, D. M. & Root, D. E. (2006). A Lentiviral RNAi Library for Human and Mouse Genes Applied to an Arrayed Viral High-Content Screen. *Cell*, *124*(6), 1283–1298. https://doi.org/10.1016/j.cell.2006.01.040

Molina-Arcas, M., Moore, C., Rana, S., Maldegem, F. van, Mugarza, E., Romero-Clavijo, P., Herbert, E., Horswell, S., Li, L.-S., Janes, M. R., Hancock, D. C. & Downward, J. (2019). Development of combination therapies to maximize the impact of KRAS-G12C inhibitors in lung cancer. *Science Translational Medicine*, *11*(510). https://doi.org/10.1126/scitranslmed.aaw7999

Moncho-Amor, V., Pintado-Berninches, L., Cáceres, I. I. de, Martín-Villar, E., Quintanilla, M., Chakravarty, P., Cortes-Sempere, M., Fernández-Varas, B., Rodriguez-Antolín, C., Castro, J. de, Sastre, L. & Perona, R. (2019). Role of Dusp6 Phosphatase as a Tumor Suppressor in Non-Small Cell Lung Cancer. *International Journal of Molecular Sciences*, *20*(8), 2036. https://doi.org/10.3390/ijms20082036

Monticone, M., Biollo, E., Maffei, M., Donadini, A., Romeo, F., Storlazzi, C. T., Giaretti, W. & Castagnola, P. (2008). Gene expression deregulation by KRAS G12D and G12V in a BRAF V600E context. *Molecular Cancer*, *7*(1), 92. https://doi.org/10.1186/1476-4598-7-92

Moodie, S. A., Willumsen, B. M., Weber, M. J. & Wolfman, A. (1993). Complexes of Ras·GTP with Raf-1 and Mitogen-Activated Protein Kinase Kinase. *Science*, *260*(5114), 1658–1661. https://doi.org/10.1126/science.8503013

Mooz, J., Oberoi-Khanuja, T. K., Harms, G. S., Wang, W., Jaiswal, B. S., Seshagiri, S., Tikkanen, R. & Rajalingam, K. (2014). Dimerization of the kinase ARAF promotes MAPK pathway activation and cell migration. *Science Signaling*, *7*(337), ra73. https://doi.org/10.1126/scisignal.2005484

Moriceau, G., Hugo, W., Hong, A., Shi, H., Kong, X., Yu, C. C., Koya, R. C., Samatar, A. A., Khanlou, N., Braun, J., Ruchalski, K., Seifert, H., Larkin, J., Dahlman, K. B., Johnson, D. B., Algazi, A., Sosman, J. A., Ribas, A. & Lo, R. S. (2015). Tunable-Combinatorial Mechanisms of Acquired Resistance Limit the Efficacy of BRAF/MEK Cotargeting but Result in Melanoma Drug Addiction. *Cancer Cell*, *27*(2), 240–256. https://doi.org/10.1016/j.ccell.2014.11.018

Morri, M., Sanchez-Romero, I., Tichy, A.-M., Kainrath, S., Gerrard, E. J., Hirschfeld, P. P., Schwarz, J. & Janovjak, H. (2018). Optical functionalization of human Class A orphan G-protein-coupled receptors. *Nature Communications*, *9*(1), 1950. https://doi.org/10.1038/s41467-018-04342-1

Mysore, V. P., Zhou, Z.-W., Ambrogio, C., Li, L., Kapp, J. N., Lu, C., Wang, Q., Tucker, M. R., Okoro, J. J., Nagy-Davidescu, G., Bai, X., Plückthun, A., Jänne, P. A., Westover, K. D., Shan, Y. & Shaw, D. E. (2021). A structural model of a Ras–Raf signalosome. *Nature Structural & Molecular Biology*, *28*(10), 847–857. https://doi.org/10.1038/s41594-021-00667-6

Nakamura, A., Goto, Y., Kondo, Y. & Aoki, K. (2021). Shedding light on developmental ERK signaling with genetically encoded biosensors. *Development*, *148*(18). https://doi.org/10.1242/dev.199767

Nan, X., Tamgüney, T. M., Collisson, E. A., Lin, L. J., Pitt, C., Galeas, J., Lewis, S., Gray, J. W., McCormick, F. & Chu, S. (2015). Ras-GTP dimers activate the Mitogen-Activated Protein Kinase (MAPK) pathway. *Proceedings of the National Academy of Sciences of the United States of America*, *112*(26), 7996–8001. https://doi.org/10.1073/pnas.1509123112

National-Cancer-Institute & DCCPS. (2021). *Surveillance, Epidemiology, and End Results (SEER) Program SEER*Stat Database: Incidence - SEER Research Data, 18 Registries (2000-2018)*. www.seer.cancer.gov

Negrao, M. V., Araujo, H. A., Lamberti, G., Cooper, A. J., Akhave, N. S., Zhou, T., Delasos, L., Hicks, J. Kevin., Aldea, M., Minuti, G., Hines, J., Aredo, J. V., Dennis, M. J., Chakrabarti, T., Scott, S. C., Bironzo, P., Scheffler, M., Christopoulos, P., Stenzinger, A., … Skoulidis, F. (2023). Co-mutations and KRAS G12C inhibitor efficacy in advanced NSCLC. *Cancer Discovery*, *13*(7), 1556–1571. https://doi.org/10.1158/2159-8290.cd-22-1420

Neto, J. M. F., Nadal, E., Bosdriesz, E., Ooft, S. N., Farre, L., McLean, C., Klarenbeek, S., Jurgens, A., Hagen, H., Wang, L., Felip, E., Martinez-Marti, A., Vidal, A., Voest, E., Wessels, L. F. A., Tellingen, O. van, Villanueva, A. & Bernards, R. (2020). Multiple low dose therapy as an effective strategy to treat EGFR inhibitor-resistant NSCLC tumours. *Nature Communications*, *11*(1), 3157. https://doi.org/10.1038/s41467-020-16952-9

Neufert, C., Becker, C., Türeci, Ö., Waldner, M. J., Backert, I., Floh, K., Atreya, I., Leppkes, M., Jefremow, A., Vieth, M., Schneider-Stock, R., Klinger, P., Greten, F. R., Threadgill, D. W., Sahin, U. & Neurath, M. F. (2013). Tumor fibroblast–derived epiregulin promotes growth of colitis-associated neoplasms through ERK. *Journal of Clinical Investigation*, *123*(4), 1428–1443. https://doi.org/10.1172/jci63748

Nieto, P., Ambrogio, C., Esteban-Burgos, L., Gómez-Ĺopez, G., Blasco, M. T., Yao, Z., Marais, R., Rosen, N., Chiarle, R., Pisano, D. G., Barbacid, M. & Santamar\'ia, D. (2017). A Braf kinase-inactive mutant induces lung adenocarcinoma. *Nature*, *548*(7666), 239–243. https://doi.org/10.1038/nature23297

Nogueira, V. & Hay, N. (2013). Molecular Pathways: Reactive Oxygen Species Homeostasis in Cancer Cells and Implications for Cancer Therapy. *Clinical Cancer Research*, *19*(16), 4309–4314. https://doi.org/10.1158/1078-0432.ccr-12-1424

Novoplansky, O., Shnerb, A. B., Marripati, D., Jagadeeshan, S., Shareb, R. A., Conde-López, C., Zorea, J., Prasad, M., Lulu, T. B., Yegodayev, K. M., Benafsha, C., Li, Y., Kong, D., Kuo, F., Morris, L. G. T., Kurth, I., Hess, J. & Elkabets, M. (2023). Activation of the EGFR/PI3K/AKT pathway limits the efficacy of trametinib treatment in head and neck cancer. *Molecular Oncology*. https://doi.org/10.1002/1878-0261.13500

Oberst, M. D., Beberman, S. J., Zhao, L., Yin, J. J., Ward, Y. & Kelly, K. (2008). TDAG51 is an ERK signaling target that opposes ERK-mediated HME16C mammary epithelial cell transformation. *BMC Cancer*, *8*(1), 189. https://doi.org/10.1186/1471-2407-8-189

OECD & European-Union. (n.d.). *Health at a Glance: Europe 2020*. https://doi.org/10.1787/82129230-en

Okada, M. (2012). Regulation of the Src Family Kinases by Csk. *International Journal of Biological Sciences*, *8*(10), 1385–1397. https://doi.org/10.7150/ijbs.5141

Ostrem, J. M., Peters, U., Sos, M. L., Wells, J. A. & Shokat, K. M. (2013). K-Ras(G12C) inhibitors allosterically control GTP affinity and effector interactions. *Nature*, *503*(7477), 548–551. https://doi.org/10.1038/nature12796

Ozaki, K., Kadomoto, R., Asato, K., Tanimura, S., Itoh, N. & Kohno, M. (2001). ERK Pathway Positively Regulates the Expression of Sprouty Genes. *Biochemical and Biophysical Research Communications*, *285*(5), 1084–1088. https://doi.org/10.1006/bbrc.2001.5295

Pant, S., Furqan, M., Abdul-Karim, R. M., Chung, V., Devoe, C. E., Johnson, M. L., Leal, A. D., Park, H., Wainberg, Z. A., Welkowsky, E., Haqq, C. M., O'Reilly, E. M. & Weekes, C. D.

(2022). First-in-human phase 1 trial of ELI-002 immunotherapy as treatment for subjects with Kirsten rat sarcoma (KRAS)-mutated pancreatic ductal adenocarcinoma and other solid tumors. *Journal of Clinical Oncology*, *40*(16_suppl), TPS2701–TPS2701. https://doi.org/10.1200/jco.2022.40.16_suppl.tps2701

Patel, S., Xi, Z. F., Seo, E. Y., McGaughey, D. & Segre, J. A. (2006). Klf4 and corticosteroids activate an overlapping set of transcriptional targets to accelerate in utero epidermal barrier acquisition. *Proceedings of the National Academy of Sciences*, *103*(49), 18668–18673. https://doi.org/10.1073/pnas.0608658103

Patricelli, M. P., Janes, M. R., Li, L. S., Hansen, R., Peters, U., Kessler, L. V., Chen, Y., Kucharski, J. M., Feng, J., Ely, T., Chen, J. H., Firdaus, S. J., Babbar, A., Ren, P. & Liu, Y. (2016). Selective inhibition of oncogenic KRAS output with small molecules targeting the inactive state. *Cancer Discovery*, *6*(3), 316–329. https://doi.org/10.1158/2159-8290.cd-15-1105

Paulitschke, V., Eichhoff, O., Gerner, C., Paulitschke, P., Bileck, A., Mohr, T., Cheng, P. F., Leitner, A., Guenova, E., Saulite, I., Freiberger, S. N., Irmisch, A., Knapp, B., Zila, N., Chatziisaak, T., Stephan, J., Mangana, J., Kunstfeld, R., Pehamberger, H., … Levesque, M. P. (2019). Proteomic identification of a marker signature for MAPKi resistance in melanoma. *The EMBO Journal*, *38*(15), e95874. https://doi.org/10.15252/embj.201695874

Payne, D. M., Rossomando, A. J., Martino, P., Erickson, A. K., Her, J. H., Shabanowitz, J., Hunt, D. F., Weber, M. J. & Sturgill, T. W. (1991). Identification of the regulatory phosphorylation sites in pp42/mitogen-activated protein kinase (MAP kinase). *The EMBO Journal*, *10*(4), 885–892. https://doi.org/10.1002/j.1460-2075.1991.tb08021.x

Pelicci, G., Lanfrancone, L., Grignani, F., McGlade, J., Cavallo, F., Forni, G., Nicoletti, I., Grignani, F., Pawson, T. & Pelicci, P. G. (1992). A novel transforming protein (SHC) with an SH2 domain is implicated in mitogenic signal transduction. *Cell*, *70*(1), 93–104. https://doi.org/10.1016/0092-8674(92)90536-l

Petti, C., Molla, A., Vegetti, C., Ferrone, S., Anichini, A. & Sensi, M. (2006). Coexpression of NRASQ61R and BRAFV600E in Human Melanoma Cells Activates Senescence and Increases Susceptibility to Cell-Mediated Cytotoxicity. *Cancer Research*, *66*(13), 6503–6511. https://doi.org/10.1158/0008-5472.can-05-4671

Plowman, S. J., Muncke, C., Parton, R. G. & Hancock, J. F. (2005). H-ras, K-ras, and inner plasma membrane raft proteins operate in nanoclusters with differential dependence on the actin cytoskleton. *Proceedings of the National Academy of Sciences of the United States of America*, *102*(43), 15500–15505. https://doi.org/10.1073/pnas.0504114102

Poulikakos, P. I., Zhang, C., Bollag, G., Shokat, K. M. & Rosen, N. (2010). RAF inhibitors transactivate RAF dimers and ERK signalling in cells with wild-type BRAF. *Nature*, *464*(7287), 427–430. https://doi.org/10.1038/nature08902

Prabakaran, S., Everley, R. A., Landrieu, I., Wieruszeski, J., Lippens, G., Steen, H. & Gunawardena, J. (2011). Comparative analysis of Erk phosphorylation suggests a mixed strategy for measuring phospho-form distributions. *Molecular Systems Biology*, *7*(1), 482–482. https://doi.org/10.1038/msb.2011.15

Prahallad, A., Sun, C., Huang, S., Nicolantonio, F. D., Salazar, R., Zecchin, D., Beijersbergen, R. L., Bardelli, A. & Bernards, R. (2012). Unresponsiveness of colon cancer to BRAF(V600E)

inhibition through feedback activation of EGFR. *Nature*, *483*(7387), 100–103. https://doi.org/10.1038/nature10868

Pratilas, C. A., Taylor, B. S., Ye, Q., Viale, A., Sander, C., Solit, D. B. & Rosen, N. (2009). V600EBRAF is associated with disabled feedback inhibition of RAF-MEK signaling and elevated transcriptional output of the pathway. *Proceedings of the National Academy of Sciences of the United States of America*, *106*(11), 4519–4524. https://doi.org/10.1073/pnas.0900780106

Prior, I. A., Lewis, P. D. & Mattos, C. (2012). A Comprehensive Survey of Ras Mutations in Cancer. *Cancer Research*, *72*(10), 2457–2467. https://doi.org/10.1158/0008-5472.can-11-2612

Pulido, R. & Huijsduijnen, R. H. van. (2008). Protein tyrosine phosphatases: dual-specificity phosphatases in health and disease. *The FEBS Journal*, *275*(5), 848–866. https://doi.org/10.1111/j.1742-4658.2008.06250.x

Putri, G. H., Anders, S., Pyl, P. T., Pimanda, J. E. & Zanini, F. (2022). Analysing high-throughput sequencing data in Python with HTSeq 2.0. *Bioinformatics*, *38*(10), 2943–2945. https://doi.org/10.1093/bioinformatics/btac166

Rajakulendran, T., Sahmi, M., Lefrançois, M., Sicheri, F. & Therrien, M. (2009). A dimerization-dependent mechanism drives RAF catalytic activation. *Nature*, *461*(7263), 542–545. https://doi.org/10.1038/nature08314

Rao, L., Debbas, M., Sabbatini, P., Hockenbery, D., Korsmeyer, S. & White, E. (1992). The adenovirus E1A proteins induce apoptosis, which is inhibited by the E1B 19-kDa and Bcl-2 proteins. *Proceedings of the National Academy of Sciences*, *89*(16), 7742–7746. https://doi.org/10.1073/pnas.89.16.7742

Rauen, K. A. (2012). The RASopathies. *Genomics and Human Genetics*, *14*(1), 355–369. https://doi.org/10.1146/annurev-genom-091212-153523

Reissig, T. M., Sara, L., Ting, S., Reis, H., Metzenmacher, M., Eberhardt, W. E. E., Zaun, G., Herold, T., Aigner, C., Darwiche, K., Stuschke, M., Schildhaus, H.-U., Schuler, M. & Wiesweg, M. (2020). ERK phosphorylation as a marker of RAS activity and its prognostic value in non-small cell lung cancer. *Lung Cancer*, *149*, 10–16. https://doi.org/10.1016/j.lungcan.2020.09.005

Ren, Y., Ouyang, Z., Hou, Z., Yan, Y., Zhi, Z., Shi, M., Du, M., Liu, H., Wen, Y. & Shao, Y. (2020). CIC Is a Mediator of the ERK1/2-DUSP6 Negative Feedback Loop. *IScience*, *23*(11), 101635. https://doi.org/10.1016/j.isci.2020.101635

Riely, G. J., Johnson, M. L., Medina, C., Rizvi, N. A., Miller, V. A., Kris, M. G., Pietanza, M. C., Azzoli, C. G., Krug, L. M., Pao, W. & Ginsberg, M. S. (2011). A Phase II Trial of Salirasib in Patients with Lung Adenocarcinomas with KRAS Mutations. *Journal of Thoracic Oncology*, *6*(8), 1435–1437. https://doi.org/10.1097/jto.0b013e318223c099

Riva, L., Pandiri, A. R., Li, Y. R., Droop, A., Hewinson, J., Quail, M. A., Iyer, V., Shepherd, R., Herbert, R. A., Campbell, P. J., Sills, R. C., Alexandrov, L. B., Balmain, A. & Adams, D. J. (2020). The mutational signature profile of known and suspected human carcinogens in mice. *Nature Genetics*, *52*(11), 1189–1197. https://doi.org/10.1038/s41588-020-0692-4

Robinson, M. D., McCarthy, D. J. & Smyth, G. K. (2010). edgeR: a Bioconductor package for differential expression analysis of digital gene expression data. *Bioinformatics*, *26*(1), 139–140. https://doi.org/10.1093/bioinformatics/btp616

Rodriguez-Viciana, P., Warne, P. H., Dhand, R., Vanhaesebroeck, B., Gout, I., Fry, M. J., Waterfield, M. D. & Downward, J. (1994). Phosphatidylinositol-3-OH kinase direct target of Ras. *Nature*, *370*(6490), 527–532. https://doi.org/10.1038/370527a0

Rodriguez-Viciana, P., Warne, P. H., Khwaja, A., Marte, B. M., Pappin, D., Das, P., Waterfield, M. D., Ridley, A. & Downward, J. (1997). Role of Phosphoinositide 3-OH Kinase in Cell Transformation and Control of the Actin Cytoskeleton by Ras. *Cell*, *89*(3), 457–467. https://doi.org/10.1016/s0092-8674(00)80226-3

Rodriguez-Viciana, P., Warne, P. H., Vanhaesebroeck, B., Waterfield, M. D. & Downward, J. (1996). Activation of phosphoinositide 3-kinase by interaction with Ras and by point mutation. *The EMBO Journal*, *15*(10), 2442–2451. https://doi.org/10.1002/j.1460-2075.1996.tb00602.x

Rogakou, E. P., Pilch, D. R., Orr, A. H., Ivanova, V. S. & Bonner, W. M. (1998). DNA Double-stranded Breaks Induce Histone H2AX Phosphorylation on Serine 139*. *Journal of Biological Chemistry*, *273*(10), 5858–5868. https://doi.org/10.1074/jbc.273.10.5858

Rosenberg, S. A., Yang, J. C., Sherry, R. M., Kammula, U. S., Hughes, M. S., Phan, G. Q., Citrin, D. E., Restifo, N. P., Robbins, P. F., Wunderlich, J. R., Morton, K. E., Laurencot, C. M., Steinberg, S. M., White, D. E. & Dudley, M. E. (2011). Durable Complete Responses in Heavily Pretreated Patients with Metastatic Melanoma Using T-Cell Transfer Immunotherapy. *Clinical Cancer Research*, *17*(13), 4550–4557. https://doi.org/10.1158/1078-0432.ccr-11-0116

Roy, S., McPherson, R. A., Apolloni, A., Yan, J., Lane, A., Clyde-Smith, J. & Hancock, J. F. (1998). 14-3-3 Facilitates Ras-Dependent Raf-1 Activation In Vitro and In Vivo. *Molecular and Cellular Biology*, *18*(7), 3947–3955. https://doi.org/10.1128/mcb.18.7.3947

Ruley, H. E. (1983). Adenovirus early region 1A enables viral and cellular transforming genes to transform primary cells in culture. *Nature*, *304*(5927), 602–606. https://doi.org/10.1038/304602a0

Rushworth, L. K., Hindley, A. D., O'Neill, E. & Kolch, W. (2006). Regulation and Role of Raf-1/B-Raf Heterodimerization. *Molecular and Cellular Biology*, *26*(6), 2262–2272. https://doi.org/10.1128/mcb.26.6.2262-2272.2006

Ryan, M. B., Cruz, F. F. de la, Phat, S., Myers, D. T., Wong, E., Shahzade, H. A., Hong, C. B. & Corcoran, R. B. (2020). Vertical Pathway Inhibition Overcomes Adaptive Feedback Resistance to KRASG12C Inhibition. *Clinical Cancer Research*, *26*(7), 1633–1643. https://doi.org/10.1158/1078-0432.ccr-19-3523

Ryu, H., Chung, M., Dobrzyński, M., Fey, D., Blum, Y., Lee, S. S., Peter, M., Kholodenko, B. N., Jeon, N. L. & Pertz, O. (2015). Frequency modulation of ERK activation dynamics rewires cell fate. *Molecular Systems Biology*, *11*(11), 838. https://doi.org/10.15252/msb.20156458

Sabio, G. & Davis, R. J. (2014). TNF and MAP kinase signalling pathways. *Seminars in Immunology*, *26*(3), 237–245. https://doi.org/10.1016/j.smim.2014.02.009

Saigusa, S., Inoue, Y., Tanaka, K., Toiyama, Y., Okugawa, Y., Shimura, T., Hiro, J., Uchida, K., Mohri, Y. & Kusunoki, M. (2013). Decreased expression of DUSP4 is associated with liver and lung metastases in colorectal cancer. *Medical Oncology*, *30*(3), 620. https://doi.org/10.1007/s12032-013-0620-x

Samuels, Y., Wang, Z., Bardelli, A., Silliman, N., Ptak, J., Szabo, S., Yan, H., Gazdar, A., Powell, S. M., Riggins, G. J., Willson, J. K. V., Markowitz, S., Kinzler, K. W., Vogelstein, B. & Velculescu, V. E. (2004). High Frequency of Mutations of the PIK3CA Gene in Human Cancers. *Science*, *304*(5670), 554–554. https://doi.org/10.1126/science.1096502

Sanchez-Rivera, F. J., Papagiannakopoulos, T., Romero, R., Tammela, T., Bauer, M. R., Bhutkar, A., Joshi, N. S., Subbaraj, L., Bronson, R. T., Xue, W. & Jacks, T. (2014). Rapid modelling of cooperating genetic events in cancer through somatic genome editing. *Nature*, *516*(7531), 428–431. https://doi.org/10.1038/nature13906

Sanjana, N. E., Shalem, O. & Zhang, F. (2014). Improved vectors and genome-wide libraries for CRISPR screening. *Nature Methods*, *11*(8), 783–784. https://doi.org/10.1038/nmeth.3047

Sanson, K. R., Hanna, R. E., Hegde, M., Donovan, K. F., Strand, C., Sullender, M. E., Vaimberg, E. W., Goodale, A., Root, D. E., Piccioni, F. & Doench, J. G. (2018). Optimized libraries for CRISPR-Cas9 genetic screens with multiple modalities. *Nature Communications*, *9*(1), 1–15. https://doi.org/10.1038/s41467-018-07901-8

Santos, E., Martin-Zanca, D., Reddy, E. P., Pierotti, M. A., Porta, G. D. & Barbacid, M. (1984). Malignant Activation of a K-ras Oncogene in Lung Carcinoma But Not in Normal Tissue of the Same Patient. *Science*, *223*(4637), 661–664. https://doi.org/10.1126/science.6695174

Sarkar-Banerjee, S., Sayyed-Ahmad, A., Prakash, P., Cho, K.-J., Waxham, M. N., Hancock, J. F. & Gorfe, A. A. (2017). Spatiotemporal Analysis of K-Ras Plasma Membrane Interactions Reveals Multiple High Order Homo-oligomeric Complexes. *Journal of the American Chemical Society*, *139*(38), 13466–13475. https://doi.org/10.1021/jacs.7b06292

Schabath, M. B., Welsh, E. A., Fulp, W. J., Chen, L., Teer, J. K., Thompson, Z. J., Engel, B. E., Xie, M., Berglund, A. E., Creelan, B. C., Antonia, S. J., Gray, J. E., Eschrich, S. A., Chen, D.-T., Cress, W. D., Haura, E. B. & Beg, A. A. (2016). Differential association of STK11 and TP53 with KRAS mutation-associated gene expression, proliferation and immune surveillance in lung adenocarcinoma. *Oncogene*, *35*(24), 3209–3216. https://doi.org/10.1038/onc.2015.375

Scheffzek, K., Ahmadian, M. R., Kabsch, W., Wiesmüller, L., Lautwein, A., Schmitz, F. & Wittinghofer, A. (1997). The Ras-RasGAP Complex: Structural Basis for GTPase Activation and Its Loss in Oncogenic Ras Mutants. *Science*, *277*(5324), 333–339. https://doi.org/10.1126/science.277.5324.333

Schmitt, C. A., Fridman, J. S., Yang, M., Lee, S., Baranov, E., Hoffman, R. M. & Lowe, S. W. (2002). A Senescence Program Controlled by p53 and p16INK4a Contributes to the Outcome of Cancer Therapy. *Cell*, *109*(3), 335–346. https://doi.org/10.1016/s0092-8674(02)00734-1

Schubbert, S., Shannon, K. & Bollag, G. (2007). Hyperactive Ras in developmental disorders and cancer. *Nature Reviews Cancer*, *7*(4), 295–308. https://doi.org/10.1038/nrc2109

Schulze, C. J., Seamon, K. J., Zhao, Y., Yang, Y. C., Cregg, J., Kim, D., Tomlinson, A., Choy, T. J., Wang, Z., Sang, B., Pourfarjam, Y., Lucas, J., Cuevas-Navarro, A., Ayala-Santos, C., Vides, A., Li, C., Marquez, A., Zhong, M., Vemulapalli, V., … Lito, P. (2023). Chemical

remodeling of a cellular chaperone to target the active state of mutant KRAS. *Science*, *381*(6659), 794–799. https://doi.org/10.1126/science.adg9652

Scrucca, L., Santucci, A. & Aversa, F. (2007). Competing risk analysis using R: an easy guide for clinicians. *Bone Marrow Transplantation*, *40*(4), 381–387. https://doi.org/10.1038/sj.bmt.1705727

Seghers, A. C., Wilgenhof, S., Lebbé, C. & Neyns, B. (2012). Successful rechallenge in two patients with BRAF-V600-mutant melanoma who experienced previous progression during treatment with a selective BRAF inhibitor. *Melanoma Research*, *22*(6), 466–472. https://doi.org/10.1097/cmr.0b013e3283541541

Sensi, M., Nicolini, G., Petti, C., Bersani, I., Lozupone, F., Molla, A., Vegetti, C., Nonaka, D., Mortarini, R., Parmiani, G., Fais, S. & Anichini, A. (2006). Mutually exclusive NRASQ61R and BRAFV600E mutations at the single-cell level in the same human melanoma. *Oncogene*, *25*(24), 3357–3364. https://doi.org/10.1038/sj.onc.1209379

Serrano, M., Lin, A. W., McCurrach, M. E., Beach, D. & Lowe, S. W. (1997). Oncogenic ras provokes premature cell senescence associated with accumulation of p53 and p16(INK4a). *Cell*, *88*(5), 593–602. https://doi.org/10.1016/s0092-8674(00)81902-9

Seshacharyulu, P., Pandey, P., Datta, K. & Batra, S. K. (2013). Phosphatase: PP2A structural importance, regulation and its aberrant expression in cancer. *Cancer Letters*, *335*(1), 9–18. https://doi.org/10.1016/j.canlet.2013.02.036

Seth, R., Crook, S., Ibrahem, S., Fadhil, W., Jackson, D. & Ilyas, M. (2009). Concomitant mutations and splice variants in KRAS and BRAF demonstrate complex perturbation of the Ras/Raf signalling pathway in advanced colorectal cancer. *Gut*, *58*(9), 1234. https://doi.org/10.1136/gut.2008.159137

Shalom-Feuerstein, R., Plowman, S. J., Rotblat, B., Ariotti, N., Tian, T., Hancock, J. F. & Kloog, Y. (2008). K-Ras Nanoclustering Is Subverted by Overexpression of the Scaffold Protein Galectin-3. *Cancer Research*, *68*(16), 6608–6616. https://doi.org/10.1158/0008-5472.can-08-1117

Shi, Y. (2009). Serine/Threonine Phosphatases: Mechanism through Structure. *Cell*, *139*(3), 468–484. https://doi.org/10.1016/j.cell.2009.10.006

Shields, D. J., Murphy, E. A., Desgrosellier, J. S., Mielgo, A., Lau, S. K. M., Barnes, L. A., Lesperance, J., Huang, M., Schmedt, C., Tarin, D., Lowy, A. M. & Cheresh, D. A. (2011). Oncogenic Ras/Src cooperativity in pancreatic neoplasia. *Oncogene*, *30*(18), 2123–2134. https://doi.org/10.1038/onc.2010.589

Shih, T. Y., Papageorge, A. G., Stokes, P. E., Weeks, M. O. & Scolnick, E. M. (1980). Guanine nucleotide-binding and autophosphorylating activities associated with the p21src protein of Harvey murine sarcoma virus. *Nature*, *287*(5784), 686–691. https://doi.org/10.1038/287686a0

Shimizu, T., Tolcher, A. W., Papadopoulos, K. P., Beeram, M., Rasco, D. W., Smith, L. S., Gunn, S., Smetzer, L., Mays, T. A., Kaiser, B., Wick, M. J., Alvarez, C., Cavazos, A., Mangold, G. L. & Patnaik, A. (2012). The Clinical Effect of the Dual-Targeting Strategy Involving PI3K/AKT/mTOR and RAS/MEK/ERK Pathways in Patients with Advanced Cancer. *Clinical Cancer Research*, *18*(8), 2316–2325. https://doi.org/10.1158/1078-0432.ccr-11-2381

Shin, S.-Y., Rath, O., Choo, S.-M., Fee, F., McFerran, B., Kolch, W. & Cho, K.-H. (2009). Positive- and negative-feedback regulations coordinate the dynamic behavior of the Ras-Raf-MEK-ERK signal transduction pathway. *Journal of Cell Science*, *122*(3), 425–435. https://doi.org/10.1242/jcs.036319

Shirasawa, S., Furuse, M., Yokoyama, N. & Sasazuki, T. (1993). Altered Growth of Human Colon Cancer Cell Lines Disrupted at Activated Ki-ras. *Science*, *260*(5104), 85–88. https://doi.org/10.1126/science.8465203

Shojaee, S., Caeser, R., Buchner, M., Park, E., Swaminathan, S., Hurtz, C., Geng, H., Chan, L. N., Klemm, L., Hofmann, W. K., Qiu, Y. H., Zhang, N., Coombes, K. R., Paietta, E., Molkentin, J., Koeffler, H. P., Willman, C. L., Hunger, S. P., Melnick, A., … Müschen, M. (2015). Erk Negative Feedback Control Enables Pre-B Cell Transformation and Represents a Therapeutic Target in Acute Lymphoblastic Leukemia. *Cancer Cell*, *28*(1), 114–128. https://doi.org/10.1016/j.ccell.2015.05.008

Sim, J., Yi, K., Kim, H., Ahn, H., Chung, Y., Rehman, A., Jang, S. M., Lee, K. H., Jang, K. & Paik, S. S. (2015). Immunohistochemical Expression of Dual-Specificity Protein Phosphatase 4 in Patients with Colorectal Adenocarcinoma. *Gastroenterology Research and Practice*, *2015*, 283764. https://doi.org/10.1155/2015/283764

Simanshu, D. K. & Morrison, D. K. (2022). A Structure Is Worth a Thousand Words: New Insights for RAS and RAF Regulation. *Cancer Discovery*, *12*(4), 899–912. https://doi.org/10.1158/2159-8290.cd-21-1494

Simón-Carrasco, L., Graña, O., Salmón, M., Jacob, H. K. C., Gutierrez, A., Jiménez, G., Drosten, M. & Barbacid, M. (2017). Inactivation of Capicua in adult mice causes T-cell lymphoblastic lymphoma. *Genes & Development*, *31*(14), 1456–1468. https://doi.org/10.1101/gad.300244.117

Singh, A., Greninger, P., Rhodes, D., Koopman, L., Violette, S., Bardeesy, N. & Settleman, J. (2009). A Gene Expression Signature Associated with "K-Ras Addiction" Reveals Regulators of EMT and Tumor Cell Survival. *Cancer Cell*, *15*(6), 489–500. https://doi.org/10.1016/j.ccr.2009.03.022

Skoulidis, F., Li, B. T., Dy, G. K., Price, T. J., Falchook, G. S., Wolf, J., Italiano, A., Schuler, M., Borghaei, H., Barlesi, F., Kato, T., Curioni-Fontecedro, A., Sacher, A., Spira, A., Ramalingam, S. S., Takahashi, T., Besse, B., Anderson, A., Ang, A., … Govindan, R. (2021). Sotorasib for Lung Cancers with KRAS p.G12C Mutation. *New England Journal of Medicine*, *384*(25), 2371–2381. https://doi.org/10.1056/nejmoa2103695

Smida, M., Posevitz-Fejfar, A., Horejsi, V., Schraven, B. & Lindquist, J. A. (2007). A novel negative regulatory function of the phosphoprotein associated with glycosphingolipid-enriched microdomains: blocking Ras activation. *Blood*, *110*(2), 596–625. https://doi.org/10.1182/blood-2006-07-038752

Smith, M. P., Sanchez-Laorden, B., O'Brien, K., Brunton, H., Ferguson, J., Young, H., Dhomen, N., Flaherty, K. T., Frederick, D. T., Cooper, Z. A., Wargo, J. A., Marais, R. & Wellbrock, C. (2014). The Immune Microenvironment Confers Resistance to MAPK Pathway Inhibitors through Macrophage-Derived TNFα. *Cancer Discovery*, *4*(10), 1214–1229. https://doi.org/10.1158/2159-8290.cd-13-1007

Soerjomataram, I. & Bray, F. (2021). Planning for tomorrow: global cancer incidence and the role of prevention 2020–2070. *Nature Reviews Clinical Oncology*, *18*(10), 663–672. https://doi.org/10.1038/s41571-021-00514-z

Solanki, H. S., Welsh, E. A., Fang, B., Izumi, V., Darville, L., Stone, B., Franzese, R., Chavan, S., Kinose, F., Imbody, D., Koomen, J. M., Rix, U. & Haura, E. B. (2021). Cell Type–specific Adaptive Signaling Responses to KRASG12C Inhibition. *Clinical Cancer Research*, *27*(9), 2533–2548. https://doi.org/10.1158/1078-0432.ccr-20-3872

Son, Y., Cheong, Y.-K., Kim, N.-H., Chung, H.-T., Kang, D. G. & Pae, H.-O. (2011). Mitogen-Activated Protein Kinases and Reactive Oxygen Species: How Can ROS Activate MAPK Pathways? *Journal of Signal Transduction*, *2011*, 792639. https://doi.org/10.1155/2011/792639

Soria, J.-C., Fülöp, A., Maciel, C., Fischer, J. R., Girotto, G., Lago, S., Smit, E., Ostoros, G., Eberhardt, W. E. E., Lishkovska, P., Lovick, S., Mariani, G., McKeown, A., Kilgour, E., Smith, P., Bowen, K., Kohlmann, A., Carlile, D. J. & Jänne, P. A. (2017). SELECT-2: a phase II, double-blind, randomized, placebo-controlled study to assess the efficacy of selumetinib plus docetaxel as a second-line treatment of patients with advanced or metastatic non-small-cell lung cancer. *Annals of Oncology*, *28*(12), 3028–3036. https://doi.org/10.1093/annonc/mdx628

Spahn, P. N., Bath, T., Weiss, R. J., Kim, J., Esko, J. D., Lewis, N. E. & Harismendy, O. (2017). PinAPL-Py: A comprehensive web-application for the analysis of CRISPR/Cas9 screens. *Scientific Reports*, *7*(1), 15854. https://doi.org/10.1038/s41598-017-16193-9

Sriram, K., Moyung, K., Corriden, R., Carter, H. & Insel, P. A. (2019). GPCRs show widespread differential mRNA expression and frequent mutation and copy number variation in solid tumors. *PLoS Biology*, *17*(11), e3000434. https://doi.org/10.1371/journal.pbio.3000434

Stringer, B. W., Day, B. W., D'Souza, R. C. J., Jamieson, P. R., Ensbey, K. S., Bruce, Z. C., Lim, Y. C., Goasdoué, K., Offenhäuser, C., Akgül, S., Allan, S., Robertson, T., Lucas, P., Tollesson, G., Campbell, S., Winter, C., Do, H., Dobrovic, A., Inglis, P.-L., … Boyd, A. W. (2019). A reference collection of patient-derived cell line and xenograft models of proneural, classical and mesenchymal glioblastoma. *Scientific Reports*, *9*(1), 4902. https://doi.org/10.1038/s41598-019-41277-z

Su, F., Amaya, V., Carla, M., Kerstin, T., Gideon, B., Olivia, S., S., R.-F. J., Xiangju, K., C., K. R., T., F. K., B., C. P., Jung, K. M., Robert, H., Matthew, M., Hong, Y., Qiongqing, W., Holly, H., S., H. J., Johannes, N., … Richard, M. (2012). RAS Mutations in Cutaneous Squamous-Cell Carcinomas in Patients Treated with BRAF Inhibitors. *New England Journal of Medicine*, *366*(3), 207–215. https://doi.org/10.1056/nejmoa1105358

Sullivan, R. J., Infante, J. R., Janku, F., Wong, D. J. L., Sosman, J. A., Keedy, V., Patel, M. R., Shapiro, G. I., Mier, J. W., Tolcher, A. W., Wang-Gillam, A., Sznol, M., Flaherty, K., Buchbinder, E., Carvajal, R. D., Varghese, A. M., Lacouture, M. E., Ribas, A., Patel, S. P., … Li, B. T. (2017). First-in-Class ERK1/2 Inhibitor Ulixertinib (BVD-523) in Patients with MAPK Mutant Advanced Solid Tumors: Results of a Phase I Dose-Escalation and Expansion Study. *Cancer Discovery*, *8*(2), 184–195. https://doi.org/10.1158/2159-8290.cd-17-1119

Sun, P., Yoshizuka, N., New, L., Moser, B. A., Li, Y., Liao, R., Xie, C., Chen, J., Deng, Q., Yamout, M., Dong, M.-Q., Frangou, C. G., Yates, J. R., Wright, P. E. & Han, J. (2007). PRAK Is Essential for ras-Induced Senescence and Tumor Suppression. *Cell*, *128*(2), 295–308. https://doi.org/10.1016/j.cell.2006.11.050

Sun, S., Schiller, J. H. & Gazdar, A. F. (2007). Lung cancer in never smokers — a different disease. *Nature Reviews Cancer*, *7*(10), 778–790. https://doi.org/10.1038/nrc2190

Sung, H., Ferlay, J., Siegel, R. L., Laversanne, M., Soerjomataram, I., Jemal, A. & Bray, F. (2021). Global Cancer Statistics 2020: GLOBOCAN Estimates of Incidence and Mortality Worldwide for 36 Cancers in 185 Countries. *CA: A Cancer Journal for Clinicians*, *71*(3), 209–249. https://doi.org/10.3322/caac.21660

Sweet, R. W., Yokoyama, S., Kamata, T., Feramisco, J. R., Rosenberg, M. & Gross, M. (1984). The product of ras is a GTPase and the T24 oncogenic mutant is deficient in this activity. *Nature*, *311*(5983), 273–275. https://doi.org/10.1038/311273a0

Sweet-Cordero, A., Mukherjee, S., Subramanian, A., You, H., Roix, J. J., Ladd-Acosta, C., Mesirov, J., Golub, T. R. & Jacks, T. (2005). An oncogenic KRAS2 expression signature identified by cross-species gene-expression analysis. *Nature Genetics*, *37*(1), 48–55. https://doi.org/10.1038/ng1490

Szklarczyk, D., Kirsch, R., Koutrouli, M., Nastou, K., Mehryary, F., Hachilif, R., Gable, A. L., Fang, T., Doncheva, N. T., Pyysalo, S., Bork, P., Jensen, L. J. & Mering, C. von. (2022). The STRING database in 2023: protein–protein association networks and functional enrichment analyses for any sequenced genome of interest. *Nucleic Acids Research*, *51*(D1), D638–D646. https://doi.org/10.1093/nar/gkac1000

Thatikonda, V., Lu, H., Jurado, S., Kostyrko, K., Bristow, C. A., Bosch, K., Feng, N., Gao, S., Gerlach, D., Gmachl, M., Lieb, S., Jeschko, A., Machado, A. A., Marszalek, E. D., Mahendra, M., Jaeger, P. A., Sorokin, A., Strauss, S., Trapani, F., … Hofmann, M. H. (2023). Combined KRASG12C and SOS1 inhibition enhances and extends the anti-tumor response in KRASG12C-driven cancers by addressing intrinsic and acquired resistance. *BioRxiv*, 2023.01.23.525210. https://doi.org/10.1101/2023.01.23.525210

Therneau, T. (2023). *A package for survival analysis in R*.

Tian, T., Harding, A., Inder, K., Plowman, S., Parton, R. G. & Hancock, J. F. (2007). Plasma membrane nanoswitches generate high-fidelity Ras signal transduction. *Nature Cell Biology*, *9*(8), 905–914. https://doi.org/10.1038/ncb1615

Tolcher, A. W., Khan, K., Ong, M., Banerji, U., Papadimitrakopoulou, V., Gandara, D. R., Patnaik, A., Baird, R. D., Olmos, D., Garrett, C. R., Skolnik, J. M., Rubin, E. H., Smith, P. D., Huang, P., Learoyd, M., Shannon, K. A., Morosky, A., Tetteh, E., Jou, Y.-M., … Bono, J. S. de. (2015). Antitumor Activity in RAS-Driven Tumors by Blocking AKT and MEK. *Clinical Cancer Research*, *21*(4), 739–748. https://doi.org/10.1158/1078-0432.ccr-14-1901

Tran, E., F., R. P., Yong-Chen, L., D., P. T., J., G. J., Li, J., Anna, P., Zhili, Z., Satyajit, R., M., G. E., R., K. I. & A., R. S. (2016). T-Cell Transfer Therapy Targeting Mutant KRAS in Cancer. *New England Journal of Medicine*, *375*(23), 2255–2262. https://doi.org/10.1056/nejmoa1609279

Tsai, Y. S., Woodcock, M. G., Azam, S. H., Thorne, L. B., Kanchi, K. L., Parker, J. S., Vincent, B. G. & Pecot, C. V. (2022). Rapid idiosyncratic mechanisms of clinical resistance to KRAS G12C inhibition. *Journal of Clinical Investigation*, *132*(4), e155523. https://doi.org/10.1172/jci155523

Turke, A. B., Song, Y., Costa, C., Cook, R., Arteaga, C. L., Asara, J. M. & Engelman, J. A. (2012). MEK Inhibition Leads to PI3K/AKT Activation by Relieving a Negative Feedback on ERBB Receptors. *Cancer Research*, *72*(13), 3228–3237. https://doi.org/10.1158/0008-5472.can-11-3747

Tutuka, C. S. A., Andrews, M. C., Mariadason, J. M., Ioannidis, P., Hudson, C., Cebon, J. & Behren, A. (2017). PLX8394, a new generation BRAF inhibitor, selectively inhibits BRAF in colonic adenocarcinoma cells and prevents paradoxical MAPK pathway activation. *Molecular Cancer*, *16*(1), 112. https://doi.org/10.1186/s12943-017-0684-x

Ueda, K., Arakawa, H. & Nakamura, Y. (2003). Dual-specificity phosphatase 5 (DUSP5) as a direct transcriptional target of tumor suppressor p53. *Oncogene*, *22*(36), 5586–5591. https://doi.org/10.1038/sj.onc.1206845

Unni, A. M., Harbourne, B., Oh, M. H., Wild, S., Ferrarone, J. R., Lockwood, W. W. & Varmus, H. (2018). Hyperactivation of ERK by multiple mechanisms is toxic to RTK-RAS mutation-driven lung adenocarcinoma cells. *ELife*, *7*, e33718. https://doi.org/10.7554/elife.33718

Unni, A. M., Lockwood, W. W., Zejnullahu, K., Lee-Lin, S. Q. & Varmus, H. (2015). Evidence that synthetic lethality underlies the mutual exclusivity of oncogenic KRAS and EGFR mutations in lung adenocarcinoma. *ELife*, *4*(JUNE), 1–23. https://doi.org/10.7554/elife.06907

Vallejo, A., Perurena, N., Guruceaga, E., Mazur, P. K., Martinez-Canarias, S., Zandueta, C., Valencia, K., Arricibita, A., Gwinn, D., Sayles, L. C., Chuang, C.-H., Guembe, L., Bailey, P., Chang, D. K., Biankin, A., Ponz-Sarvise, M., Andersen, J. B., Khatri, P., Bozec, A., … Vicent, S. (2017). An integrative approach unveils FOSL1 as an oncogene vulnerability in KRAS-driven lung and pancreatic cancer. *Nature Communications*, *8*(1), 14294. https://doi.org/10.1038/ncomms14294

Varela, T., Conceição, N., Laizé, V. & Cancela, M. L. (2021). Transcriptional regulation of human DUSP4 gene by cancer-related transcription factors. *Journal of Cellular Biochemistry*, *122*(10), 1556–1566. https://doi.org/10.1002/jcb.30078

Varela, T., Laizé, V., Conceição, N., Caldeira, P., Marreiros, A., Guerreiro, H. & Cancela, M. L. (2020). Expression of DUSP4 transcript variants as a potential biomarker for colorectal cancer. *Biomarkers in Medicine*, *14*(8), 639–650. https://doi.org/10.2217/bmm-2019-0369

Vetter, I. R. & Wittinghofer, A. (2001). The Guanine Nucleotide-Binding Switch in Three Dimensions. *Science*, *294*(5545), 1299–1304. https://doi.org/10.1126/science.1062023

Vicent, S., López-Picazo, J. M., Toledo, G., Lozano, M. D., Torre, W., Garcia-Corchón, C., Quero, C., Soria, J.-C., Martín-Algarra, S., Manzano, R. G. & Montuenga, L. M. (2004). ERK1/2 is activated in non-small-cell lung cancer and associated with advanced tumours. *British Journal of Cancer*, *90*(5), 1047–1052. https://doi.org/10.1038/sj.bjc.6601644

Vidimar, V., Park, M., Stubbs, C. K., Ingram, N. K., Qiang, W., Zhang, S., Gursel, D., Melnyk, R. A. & Satchell, K. J. F. (2022). Proteolytic pan-RAS Cleavage Leads to Tumor Regression in Patient-derived Pancreatic Cancer Xenografts. *Molecular Cancer Therapeutics*, *21*(5), 810–820. https://doi.org/10.1158/1535-7163.mct-21-0550

Vineis, P., Alavanja, M., Buffler, P., Fontham, E., Franceschi, S., Gao, Y. T., Gupta, P. C., Hackshaw, A., Matos, E., Samet, J., Sitas, F., Smith, J., Stayner, L., Straif, K., Thun, M. J., Wichmann, H. E., Wu, A. H., Zaridze, D., Peto, R. & Doll, R. (2004). Tobacco and Cancer:

Recent Epidemiological Evidence. *JNCI: Journal of the National Cancer Institute*, *96*(2), 99–106. https://doi.org/10.1093/jnci/djh014

Vojtek, A. B., Hollenberg, S. M. & Cooper, J. A. (1993). Mammalian Ras interacts directly with the serine/threonine kinase raf. *Cell*, *74*(1), 205–214. https://doi.org/10.1016/0092-8674(93)90307-c

Vriendt, V. D., Roock, W. D., Narzo, A. F. D., Tian, S., Biesmans, B., Jacobs, B., Budinska, E., Sagaert, X., Rossi, S., D'Ario, G., Delorenzi, M., Simon, I., Vecchione, L. & Tejpar, S. (2013). DUSP 4 expression identifies a subset of colorectal cancer tumors that differ in MAPK activation, regardless of the genotype. *Biomarkers*, *18*(6), 516–524. https://doi.org/10.3109/1354750x.2013.819038

Wagle, M.-C., Kirouac, D., Klijn, C., Liu, B., Mahajan, S., Junttila, M., Moffat, J., Merchant, M., Huw, L., Wongchenko, M., Okrah, K., Srinivasan, S., Mounir, Z., Sumiyoshi, T., Haverty, P. M., Yauch, R. L., Yan, Y., Kabbarah, O., Hampton, G., … Huang, S.-M. A. (2018). A transcriptional MAPK Pathway Activity Score (MPAS) is a clinically relevant biomarker in multiple cancer types. *Npj Precision Oncology*, *2*(1), 7. https://doi.org/10.1038/s41698-018-0051-4

Wakioka, T., Sasaki, A., Kato, R., Shouda, T., Matsumoto, A., Miyoshi, K., Tsuneoka, M., Komiya, S., Baron, R. & Yoshimura, A. (2001). Spred is a Sprouty-related suppressor of Ras signalling. *Nature*, *412*(6847), 647–651. https://doi.org/10.1038/35088082

Wang, J., Liu, Q., Yuan, S., Xie, W., Liu, Y., Xiang, Y., Wu, N., Wu, L., Ma, X., Cai, T., Zhang, Y., Sun, Z. & Li, Y. (2017). Genetic predisposition to lung cancer: comprehensive literature integration, meta-analysis, and multiple evidence assessment of candidate-gene association studies. *Scientific Reports*, *7*(1), 8371. https://doi.org/10.1038/s41598-017-07737-0

Wang, L., Oliveira, R. L. de, Huijberts, S., Bosdriesz, E., Pencheva, N., Brunen, D., Bosma, A., Song, J.-Y., Zevenhoven, J., Vries, G. T. L., Horlings, H., Nuijen, B., Beijnen, J. H., Schellens, J. H. M. & Bernards, R. (2018). An Acquired Vulnerability of Drug-Resistant Melanoma with Therapeutic Potential. *Cell*, *173*(6), 1413-1425.e14. https://doi.org/10.1016/j.cell.2018.04.012

Wang, Q., Lu, R., Zhao, J. & Limbird, L. E. (2006). Arrestin Serves as a Molecular Switch, Linking Endogenous α2-Adrenergic Receptor to SRC-dependent, but Not SRC-independent, ERK Activation*. *Journal of Biological Chemistry*, *281*(36), 25948–25955. https://doi.org/10.1074/jbc.m605415200

Wang, T., Wei, J. J., Sabatini, D. M. & Lander, E. S. (2014). Genetic Screens in Human Cells Using the CRISPR-Cas9 System. *Science*, *343*(6166), 80–84. https://doi.org/10.1126/science.1246981

Wang, X., Ricciuti, B., Nguyen, T., Li, X., Rabin, M. S., Awad, M. M., Lin, X., Johnson, B. E. & Christiani, D. C. (2021). Association between Smoking History and Tumor Mutation Burden in Advanced Non–Small Cell Lung Cancer. *Cancer Research*, *81*(9), 2566–2573. https://doi.org/10.1158/0008-5472.can-20-3991

Wang, Y. & Prywes, R. (2000). Activation of the c-fos enhancer by the Erk MAP kinase pathway through two sequence elements: the c-fos AP-1 and p62TCF sites. *Oncogene*, *19*(11), 1379–1385. https://doi.org/10.1038/sj.onc.1203443

Weber, C. K., Slupsky, J. R., Kalmes, H. A. & Rapp, U. R. (2001). Active Ras induces heterodimerization of cRaf and BRaf. *Cancer Research*, *61*(9), 3595–3598.

Weissmann, S., Cloos, P. A., Sidoli, S., Jensen, O. N., Pollard, S. & Helin, K. (2018). The Tumor Suppressor CIC Directly Regulates MAPK Pathway Genes via Histone Deacetylation. *Cancer Research*, *78*(15), 4114–4125. https://doi.org/10.1158/0008-5472.can-18-0342

Wennerberg, K., Rossman, K. L. & Der, C. J. (2005). The Ras superfamily at a glance. *Journal of Cell Science*, *118*(5), 843–846. https://doi.org/10.1242/jcs.01660

Whitehurst, A. W., Wilsbacher, J. L., You, Y., Luby-Phelps, K., Moore, M. S. & Cobb, M. H. (2002). ERK2 enters the nucleus by a carrier-independent mechanism. *Proceedings of the National Academy of Sciences*, *99*(11), 7496–7501. https://doi.org/10.1073/pnas.112495999

Wilhelm, S., Carter, C., Lynch, M., Lowinger, T., Dumas, J., Smith, R. A., Schwartz, B., Simantov, R. & Kelley, S. (2006). Discovery and development of sorafenib: a multikinase inhibitor for treating cancer. *Nature Reviews Drug Discovery*, *5*(10), 835–844. https://doi.org/10.1038/nrd2130

Winter, J., Schwering, M., Pelz, O., Rauscher, B., Zhan, T., Heigwer, F. & Boutros, M. (2017). CRISPRAnalyzeR: Interactive analysis, annotation and documentation of pooled CRISPR screens. *BioRxiv*, 109967. https://doi.org/10.1101/109967

Wittig-Blaich, S., Wittig, R., Schmidt, S., Lyer, S., Bewerunge-Hudler, M., Gronert-Sum, S., Strobel-Freidekind, O., Müller, C., List, M., Jaskot, A., Christiansen, H., Hafner, M., Schadendorf, D., Block, I. & Mollenhauer, J. (2017). Systematic screening of isogenic cancer cells identifies DUSP6 as context-specific synthetic lethal target in melanoma. *Oncotarget*, *8*(14), 23760–23774. https://doi.org/10.18632/oncotarget.15863

Wood, K. C. (2023). Hyperactivation of oncogenic driver pathways as a precision therapeutic strategy. *Nature Genetics*, 1–2. https://doi.org/10.1038/s41588-023-01493-w

Wu, F., Yang, J., Liu, J., Wang, Y., Mu, J., Zeng, Q., Deng, S. & Zhou, H. (2021). Signaling pathways in cancer-associated fibroblasts and targeted therapy for cancer. *Signal Transduction and Targeted Therapy*, *6*(1), 218. https://doi.org/10.1038/s41392-021-00641-0

Wu, T., Hu, E., Xu, S., Chen, M., Guo, P., Dai, Z., Feng, T., Zhou, L., Tang, W., Zhan, L., Fu, X., Liu, S., Bo, X. & Yu, G. (2021). clusterProfiler 4.0: A universal enrichment tool for interpreting omics data. *The Innovation*, *2*(3), 100141. https://doi.org/10.1016/j.xinn.2021.100141

Xu, X., Rock, J. R., Lu, Y., Futtner, C., Schwab, B., Guinney, J., Hogan, B. L. M. & Onaitis, M. W. (2012). Evidence for type II cells as cells of origin of K-Ras–induced distal lung adenocarcinoma. *Proceedings of the National Academy of Sciences*, *109*(13), 4910–4915. https://doi.org/10.1073/pnas.1112499109

Xue, J. Y., Zhao, Y., Aronowitz, J., Mai, T. T., Vides, A., Qeriqi, B., Kim, D., Li, C., Stanchina, E. de, Mazutis, L., Risso, D. & Lito, P. (2020). Rapid non-uniform adaptation to conformation-specific KRAS(G12C) inhibition. *Nature*, *577*(7790), 421–425. https://doi.org/10.1038/s41586-019-1884-x

Yang, C., Tian, C., Spencer, S. L. & Hoffman, T. E. (2021). Melanoma subpopulations that rapidly escape rely on stress signalling. *Nature Communications*, *12*(2021), 1747. https://doi.org/10.1038/s41467-021-21549-x

Yang, X., Boehm, J. S., Yang, X., Salehi-Ashtiani, K., Hao, T., Shen, Y., Lubonja, R., Thomas, S. R., Alkan, O., Bhimdi, T., Green, T. M., Johannessen, C. M., Silver, S. J., Nguyen, C., Murray, R. R., Hieronymus, H., Balcha, D., Fan, C., Lin, C., … Root, D. E. (2011). A public genome-scale lentiviral expression library of human ORFs. *Nature Methods*, *8*(8), 659–661. https://doi.org/10.1038/nmeth.1638

Yao, Z., Dolginov, Y., Hanoch, T., Yung, Y., Ridner, G., Lando, Z., Zharhary, D. & Seger, R. (2000). Detection of partially phosphorylated forms of ERK by monoclonal antibodies reveals spatial regulation of ERK activity by phosphatases. *FEBS Letters*, *468*(1), 37–42. https://doi.org/10.1016/s0014-5793(00)01191-1

Yohe, M. E., Gryder, B. E., Shern, J. F., Song, Y. K., Chou, H.-C., Sindiri, S., Mendoza, A., Patidar, R., Zhang, X., Guha, R., Butcher, D., Isanogle, K. A., Robinson, C. M., Luo, X., Chen, J.-Q., Walton, A., Awasthi, P., Edmondson, E. F., Difilippantonio, S., … Khan, J. (2018). MEK inhibition induces MYOG and remodels super-enhancers in RAS-driven rhabdomyosarcoma. *Science Translational Medicine*, *10*(448). https://doi.org/10.1126/scitranslmed.aan4470

Yoshihara, K., Shahmoradgoli, M., Martínez, E., Vegesna, R., Kim, H., Torres-Garcia, W., Treviño, V., Shen, H., Laird, P. W., Levine, D. A., Carter, S. L., Getz, G., Stemke-Hale, K., Mills, G. B. & Verhaak, R. G. W. (2013). Inferring tumour purity and stromal and immune cell admixture from expression data. *Nature Communications*, *4*(1), 2612. https://doi.org/10.1038/ncomms3612

Yoshizumi, M., Abe, J., Haendeler, J., Huang, Q. & Berk, B. C. (2000). Src and Cas Mediate JNK Activation but Not ERK1/2 and p38 Kinases by Reactive Oxygen Species*. *Journal of Biological Chemistry*, *275*(16), 11706–11712. https://doi.org/10.1074/jbc.275.16.11706

Young, L. C., Hartig, N., Río, I. B. D., Sari, S., Ringham-Terry, B., Wainwright, J. R., Jones, G. G., McCormick, F. & Rodriguez-Viciana, P. (2018). SHOC2-MRAS-PP1 complex positively regulates RAF activity and contributes to Noonan syndrome pathogenesis. *Proceedings of the National Academy of Sciences of the United States of America*, *115*(45), E10576–E10585. https://doi.org/10.1073/pnas.1720352115

Yu, M., Li, G., Lee, W.-W., Yuan, M., Cui, D., Weyand, C. M. & Goronzy, J. J. (2012). Signal inhibition by the dual-specific phosphatase 4 impairs T cell-dependent B-cell responses with age. *Proceedings of the National Academy of Sciences*, *109*(15), E879–E888. https://doi.org/10.1073/pnas.1109797109

Zafra, M. P., Parsons, M. J., Kim, J., Alonso-Curbelo, D., Goswami, S., Schatoff, E. M., Han, T., Katti, A., Fernandez, M. T. C., Wilkinson, J. E., Piskounova, E. & Dow, L. E. (2020). An in vivo KRAS allelic series reveals distinct phenotypes of common oncogenic variants. *Cancer Discovery*, *10*(11), CD-20--0442. https://doi.org/10.1158/2159-8290.cd-20-0442

Zang, Y., Kahsai, A. W., Pakharukova, N., Huang, L. & Lefkowitz, R. J. (2021). The GPCR–β-arrestin complex allosterically activates C-Raf by binding its amino terminus. *Journal of Biological Chemistry*, *297*(6), 101369. https://doi.org/10.1016/j.jbc.2021.101369

Zhang, C., Spevak, W., Zhang, Y., Burton, E. A., Ma, Y., Habets, G., Zhang, J., Lin, J., Ewing, T., Matusow, B., Tsang, G., Marimuthu, A., Cho, H., Wu, G., Wang, W., Fong, D., Nguyen,

H., Shi, S., Womack, P., … Bollag, G. (2015). RAF inhibitors that evade paradoxical MAPK pathway activation. *Nature*, *526*(7574), 583–586. https://doi.org/10.1038/nature14982

Zhang, P., Chen, P.-L., Li, Z.-H., Zhang, A., Zhang, X.-R., Zhang, Y.-J., Liu, D. & Mao, C. (2022). Association of smoking and polygenic risk with the incidence of lung cancer: a prospective cohort study. *British Journal of Cancer*, *126*(11), 1637–1646. https://doi.org/10.1038/s41416-022-01736-3

Zhang, R.-Y., Yu, Z.-H., Chen, L., Walls, C. D., Zhang, S., Wu, L. & Zhang, Z.-Y. (2020). Mechanistic insights explain the transforming potential of the T507K substitution in the protein-tyrosine phosphatase SHP2. *Journal of Biological Chemistry*, *295*(18), 6187–6201. https://doi.org/10.1074/jbc.ra119.010274

Zhang, X., Gureasko, J., Shen, K., Cole, P. A. & Kuriyan, J. (2006). An Allosteric Mechanism for Activation of the Kinase Domain of Epidermal Growth Factor Receptor. *Cell*, *125*(6), 1137–1149. https://doi.org/10.1016/j.cell.2006.05.013

Zhang, X.-F., Settleman, J., Kyriakis, J., Takeuchi-Suzuki, E., Elledge, S. J., Marshall, M. S., Bruder, J. T., Rapp, U. R. & Avruch, J. (1993). Normal and oncogenic p21ras proteins bind to the amino-terminal regulatory domain of c-Raf-1. *Nature*, *364*(6435), 308–313. https://doi.org/10.1038/364308a0

Zhang & Yuan. (2018). *Practical statistical power analysis using Webpower and R*. https://doi.org/10.35566/power

Zhang, Z., Wang, Y., Vikis, H. G., Johnson, L., Liu, G., Li, J., Anderson, M. W., Sills, R. C., Hong, H. L., Devereux, T. R., Jacks, T., Guan, K.-L. & You, M. (2001). Wildtype Kras2 can inhibit lung carcinogenesis in mice. *Nature Genetics*, *29*(1), 25–33. https://doi.org/10.1038/ng721

Zhao, Y., Murciano-Goroff, Y. R., Xue, J. Y., Ang, A., Lucas, J., Mai, T. T., Paula, A. F. D. C., Saiki, A. Y., Mohn, D., Achanta, P., Sisk, A. E., Arora, K. S., Roy, R. S., Kim, D., Li, C., Lim, L. P., Li, M., Bahr, A., Loomis, B. R., … Lito, P. (2021). Diverse alterations associated with resistance to KRAS(G12C) inhibition. *Nature*, *599*(March), 679–683. https://doi.org/10.1038/s41586-021-04065-2

Zhao, Z., Chen, C.-C., Rillahan, C. D., Shen, R., Kitzing, T., McNerney, M. E., Diaz-Flores, E., Zuber, J., Shannon, K., Beau, M. M. L., Spector, M. S., Kogan, S. C. & Lowe, S. W. (2015). Cooperative loss of RAS feedback regulation drives myeloid leukemogenesis. *Nature Genetics*, *47*(5), 539–543. https://doi.org/10.1038/ng.3251

Zheng, C. F. & Guan, K. L. (1994). Activation of MEK family kinases requires phosphorylation of two conserved Ser/Thr residues. *The EMBO Journal*, *13*(5), 1123–1131. https://doi.org/10.1002/j.1460-2075.1994.tb06361.x

Zhou, Z.-W., Ambrogio, C., Bera, A. K., Li, Q., Li, X.-X., Li, L., Son, J., Gondi, S., Li, J., Campbell, E., Jin, H., Okoro, J. J., Xu, C.-X., Janne, P. A. & Westover, K. D. (2020). KRASQ61H preferentially signals through MAPK in a RAF dimer-dependent manner in non-small cell lung cancer. *Cancer Research*, *80*(17), canres.0448.2020. https://doi.org/10.1158/0008-5472.can-20-0448

Zimmermann, S. & Moelling, K. (1999). Phosphorylation and Regulation of Raf by Akt (Protein Kinase B). *Science*, *286*(5445), 1741–1744. https://doi.org/10.1126/science.286.5445.1741

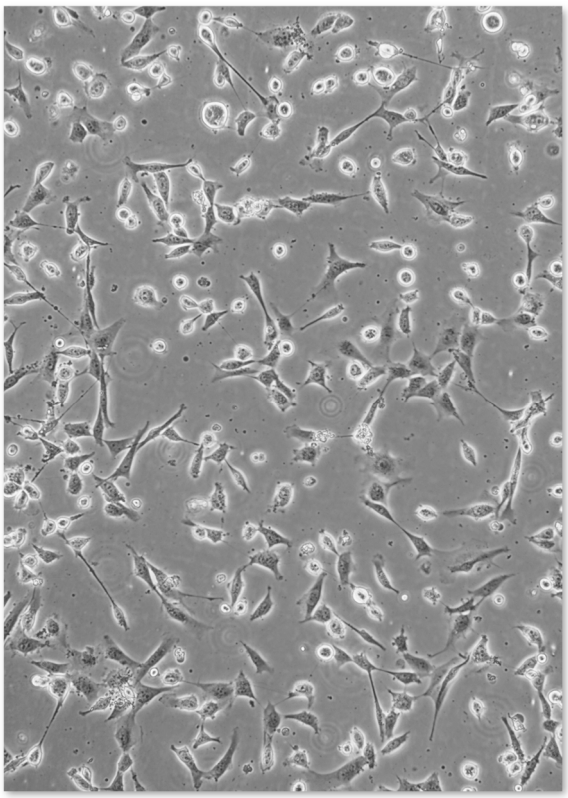

Picture VIII. ATII KRAS$^{G12V\text{-}ER}$ pCW57-BRAF^{D549A} cell line in culture, in presence of tamoxifen and doxycycline. High MAPK levels produce apoptosis and toxicity visible in this photography obtained from an inverted microscope with phase contrast illumination and a 10X magnification.

Annex

Summary in English

Objectives

Tumor progression is a complex process, requiring coordination of the tumor's abilities for a common goal. Each process and alteration of the tumor is carefully selected and dosed in order to be able to grant advantages to the malignant cells and to be able to proliferate. Regulation of the RAS-MAPK pathway is an important feature that is systematically altered in lung adenocarcinoma (LUAD). However, we now understand that signaling requires not only activating processes, but also regulatory mechanisms that maintain balance. For this reason, the ability of the tumor to modulate the MAPK pathway, and, therefore, the alterations of its regulators should determine the nature of the tumor and have clinical consequences.

For this purpose, we decided to functionally study genomic data from KRAS-mutated LUAD cases and evaluate how MAPK signaling levels affect their clinical prognosis. Based on these analyses, we want to lay the groundwork for studying how precise alterations of regulators, both known and novel, could affect tumor progression. This approach allows a direct causal relationship to be established between RAS/MAPK activity and tumor fitness in the clinic. All this information will allow a deeper understanding of the different mechanisms of regulation of the pathway, which could help determine in patients the response to treatment and possible resistances.

The overall objectives of this thesis were the following:

1. To study the MAPK component from publicly accessible clinical databases to better understand how pathway regulation affects the survival of patients with KRAS-mutated LUAD and the molecular mechanisms that might underlie its prognosis.
2. Develop models of LUAD that recapitulate the molecular context observed in the clinic to determine how excessive levels of MAPK are toxic to mutated KRAS tumors.
3. To analyze molecular changes that affect MAPK regulators, such as alterations in DUSP4 observed in patients. To understand its potential role in the specific MAPK response, try to understand how the state of DUSP4 shapes tumor fate by controlling the balance of MAPK signaling.
4. Identify and characterize novel RAS-MAPK regulators that could contribute to a better interpretation of the pathway in the molecular oncology setting.

1 SUMMARY OF THE INTRODUCTION

1.1 THE RAS PATHWAY AND MAPK IN CANCER

Cancer is a global disease with 18 million new cases diagnosed worldwide each year, and this number is forecast to rise to 40 million annually by 2070. In Europe, cancer is the second leading cause of death, claiming the lives of up to 2 million people a year. What is particularly worrying is that despite the fact that Europe is home to less than 10% of the world's population, it is responsible for a quarter of all cancer cases on the planet. This statistic highlights the growing threat that cancer poses to society in Europe and underlines the need to address this problem urgently.

Lung cancer stands as the deadliest of all cancer varieties, surpassing breast, pancreatic and prostate cancers combined in mortality. There is a lack of early detection, with most patients being diagnosed in advanced stages. The classification of non-small cell lung tumors (NSCLC) is essential for estimating survival and treatment options, with lung adenocarcinomas (LUADs) being the most common.

Smoking is a significant risk factor, smoking greatly increases the risk of developing lung cancer, and it is estimated that 80% of deaths from this disease could be prevented by smoking cessation. Despite these known factors, about 20% of lung cancer cases worldwide cannot be attributed to smoking or any other dominant factor.

In the case of the lung, the central milestone of tumor progression is the overturning of the mechanisms that regulate cell proliferation. Mutations in genes such as EGFR, TP53, and KRAS are the main drivers of the tumor. Although it is not fully understood how these mutations occur, it is suggested that they are random events that accumulate in the body over the course of a lifetime. Exposure to carcinogens or other factors, at any given time, causes selective restrictions in the tissue to change, causing alterations in the microenvironment, which promote inflammation and ultimately create conditions conducive to cancer. Cells with pre-existing mutations in proto-oncogenes have a selective advantage under these conditions, leading to clonal expansion and cancer.

When it comes to treating these tumors, the large tumor heterogeneity is a major challenge that complicates the efficacy of responses. The majority of oncogenic mutations in LUAD are related to the RAS/MAPK pathway, which has historically led to the development of therapeutic strategies focused on the main effectors of this pathway. Initially, generic inhibitors against kinases, such as sorafenib, were used, but they showed limited clinical benefit in KRAS-mutated lung cancer, necessitating the development of therapies that target tumor-specific mutations.

This is a challenge, as specifically and effectively inhibiting components of a cellular pathway is complex. It should be borne in mind that the tumor has multiple compensation mechanisms that allow the cells to adapt, resist and, eventually, progress during treatment.

The challenge of inhibiting the KRAS protein, one of the main oncogenic drivers in LUAD, was advanced with the development of specific inhibitors for the G12C mutation, with drugs such as sotorasib and adagrasib. These drugs showed promise in the clinic, but have limitations, including a short-lived response, the emergence of resistance, or incompatibility with immunotherapy, among others. A new generation of inhibitors, called pan-KRAS, inhibit all forms of KRAS, also show promise. However, more research is needed to address the challenges that these therapeutic strategies will pose in the future.

1.2 DOWNREGULATION AS AN ESSENTIAL MECHANISM FOR TUMOR DEVELOPMENT

The MAPK signaling pathway is a signaling cascade that plays a crucial role in the transmission of extracellular signals to regulate various cellular responses. This pathway is the main mechanism by which KRAS transmits its oncogenic potential.

Just as a KRAS-activating mutation has oncogenic effects, mutations in the MAPK pathway are also frequently present in LUAD tumors. However, hyperactivation of the pathway is toxic to the tumor. In order for tumor cells to maintain addiction to KRAS and/or mutations in the MAPK pathway, other alterations are necessary to deactivate cellular responses that would normally inhibit cell proliferation. It is important to maintain a balance in MAPK signaling to avoid cellular toxicity.

To regulate these responses, there are regulatory proteins such as phosphatases, especially DUSPs. These enzymes play a crucial role in deactivating ERK signaling and may have dual functions, both suppressive and tumor-promoting, depending on the specific context, due to this fine balance that must be maintained.

In order to understand how this regulation takes place in the tumor, it is crucial to be able to measure the levels of activity that each component carries and how changes in these components modify the balance. Transcriptional gene signatures may be a useful tool for assessing the activity of this pathway in cancer patients.

In this thesis, we describe the use of one of these signatures to monitor the activity of the MAPK pathway and how MAPK levels predict the survival of LUAD patients. In addition, we present an analysis that has identified a number of potential regulators of MAPK, both positive and negative. The study of these new regulators, as is the case of the DUSP4 gene, is of vital importance to better understand the RAS-MAPK signaling pathway and its regulation in various biological and pathological contexts, especially in lung cancer with KRAS mutations. This research provides a basis for advancing the field of precision oncology and improving the treatment of patients affected by this disease.

2 MAIN RESULTS

2.1 A TRANSCRIPTIONAL SIGNATURE TO DETERMINE PATIENT SURVIVAL

First, the aim of this study was to address the question of whether MAPK activity dictates the outcome of tumors with KRAS mutations. These bioinformatics results were based on data from 162 patients with KRAS mutations of lung adenocarcinoma (LUAD) in the TCGA. MAPK activity was assessed by calculating a score that considered the expression of 6 specific MAPK genes for this disease (Brant et al., 2017): DUSP4, DUSP6, ETV4, ETV5, PHLDA1, and SPRY2.

We classified patients into two groups: high and low MAPK, based on the top and bottom quartiles of the signature score. We performed a survival analysis that revealed significant differences in survival,

with lower survival in the low MAPK group. This result suggests that high levels of MAPK are detrimental in the context of KRAS-driven LUAD, and that the tumor must limit its signaling levels to ensure maximum fitness. In addition, this difference in survival was found specifically in tumors with KRAS mutations and not in other mutation drivers.

To confirm these results, a tumor purity filter was applied, resulting in a purer cohort. By performing a correlation analysis between the signature genes, we concluded that it was necessary to carry out the exclusion of the DUSP4 and PHLDA1 genes from the signature, since they were anti-correlated with the rest of the genes and, ultimately, did not contribute significantly to the predictive capacity of the signature. Survival analysis with the refined signature confirmed the difference in survival between the high- and low-MAPK groups. In addition, these results were validated in an independent microarray cohort that also recapitulated LUAD patients with mutated KRAS.

The signature was also correlated with *ontologies* associated with MAPK activation, confirming that the signature is able to reflect pathway signaling levels effectively. Analysis of the differences between the high- and low-MAPK groups revealed no associations with specific clinical features or KRAS mutations, but an association with KEAP1 mutations was found. However, the KEAP1 mutation was not associated with differences in survival.

Analysis of copy number alterations (CNVs) showed that tumors with high levels of MAPK had more genetic alterations compared to tumors with low levels of MAPK. This suggests that tumors with high levels of MAPK are more prone to genomic instability.

Additionally, we also identified that high MAPK tumors present increased levels of immune infiltration, including increased levels of CD8+ T cells.

In summary, MAPK activity has a significant impact on the survival of patients with KRAS mutations in the LUAD. The signature we have refined correlates with MAPK activation, but also with greater genomic instability, suggesting that high levels of MAPK generate greater toxicity that is determinant in the progression of these tumors.

2.2 DUSP4 IS A NEGATIVE REGULATOR THAT DETERMINES TUMOR DEVELOPMENT

In-silico *analysis* of clinical data shows significant differences in the genomic status of DUSP4, a negative regulator of MAPK, between patients with different levels of transcriptional signature. DUSP4 shows amplifications in tumors low in MAPK and genomic losses in tumors high in MAPK.

DUSP4 regulates the phosphorylation of ERK, with its loss being a pathway activating event, and its overexpression being a pathway inhibitory event. However, we identified that DUSP4 loss does not induce cell transformation on its own nor does it collaborate with other oncogenes such as RAS or PI3K, suggesting that DUSP4 is not a primary oncogenic event.

Therefore, we decided to study the impact of DUSP4 deletion on already formed mutated KRAS tumors. The results revealed that tumors without DUSP4 show an increase in genomic instability and apoptosis rate. This suggests that the loss of DUSP4 triggers cell death, likely due to an over-activation of the MAPK pathway. Although an increase in oxidative stress was observed in cells with deleted DUSP4 in a laboratory cell model, this effect was not confirmed in tumors. These findings indicate that DUSP4 plays a crucial role in the regulation of genomic stability and cell survival in the setting of KRAS-mutated tumors.

In order to study how DUSP4 contributes, in early stages, to the initiation and development of tumors, we created an in *vivo* model from a human immortalized ATII cell line, which contains a tamoxifen-activated KRAS oncogenic mutation thanks to a fusion with the estrogen receptor (KRASG12V-ER). These cells were infected with plentiCRISPR constructs targeting DUSP4 and orthotopically injected into immunodeficient mice by injection into the tail vein. Only mice that retained tamoxifen throughout the process developed a positive luciferase signal, demonstrating that this is a KRAS-dependent phenotype. Cells with DUSP4 clearance had a significantly increased luciferase signal for several weeks. However, over the past few weeks, the development of the control tumor with Z accelerated abruptly, reaching even higher luciferase levels than cells with DUSP4 clearance.

These results support the hypothesis derived from clinical data, which suggests that DUSP4 clearance events are positively selected for in the early stages of the disease, as DUSP4 loss appears to be

advantageous for initial malignant growth. However, it was observed that cells with DUSP4 clearance progressively lose the conferred advantage and are overtaken by DUSP4-competent cells, suggesting that, at later stages, the integrity of DUSP4 may be more beneficial.

To better understand the overall impact of DUSP4 on the malignant process, we sought to create a more complete model that recapitulates the entire process of tumor initiation and development of KRAS mutant cells with or without DUSP4 alterations.

For this model, the mouse strain K-ras+/lox-Stop-lox-G12V-geo was used, which allows expression of the oncogenic mutant KRASG12V-ER $^{\text{after Cre}}$ recombinase-mediated recombination. To combine KRAS activation with DUSP4 inactivation, we infected mice intranasally with lentiviral particles of the *pSECC vector*, which knocks out the DUSP4 gene using CRISPR/Cas9 technology and at the same time activates KRASG12V-ER with the expression of a recombinase CRE. In addition, this system allows the expression of a YFP reporter gene also silenced by a *lox-STOP-lox cassette*.

It was observed that the loss of DUSP4 increased the growth of early lesions in mice in the first month. Within three months, an increase in the number of positive cells was found in mice with DUSP4 removed, suggesting a synergy between DUSP4 loss and KRAS oncogenic activity in increasing tumor burden. However, at later stages (6 and 9 months), lesions were less frequent in mice with deleted DUSP4. At the last baseline, at 12 months, tumors without DUSP4 were found to be smaller in size. This could indicate that the loss of DUSP4 reduces the likelihood of developing advanced and substantial neoplasms.

In summary, this experiment suggests that, as the KRAS-driven tumor progresses, the loss of DUSP4 becomes detrimental. Initially, the absence of DUSP4 promotes tumor formation, but as the tumor progresses, DUSP4 appears to play a protective role. Further analyses are planned to understand how DUSP4 clearance affects late-stage lesions from the point of view of apoptosis, genomic toxicity, and oxidative stress.

Next, we set out to investigate how these alterations can influence the clinical response of patients, in particular, their response to MAPK inhibitors, such as MEK inhibitors and specific KRASG12C inhibitors.

Models of lung adenocarcinoma (LUAD) cells with KRAS mutations were generated and DUSP4 expression was removed or induced to evaluate how DUSP4 modulation specifically affects the response to inhibitors. DUSP4 was eliminated in these cell lines and susceptibility to MAPK inhibitors, such as trametinib, and the KRAS inhibitors adagrasib and sotorasib were evaluated. In some cell lines, removal of DUSP4 resulted in decreased sensitivity to trametinib, indicating increased resistance. This resistance to trametinib could be due to altered levels of MAPK generated by DUSP4 removal. In cell lines with KRASG12C mutations, sensitivity to KRAS inhibitors was not affected by DUSP4 deletion. On the other hand, overexpression of DUSP4 sensitized cells to MAPK inhibitors, including trametinib and KRASG12C inhibitors.

Taken together, these results suggest that DUSP4 status may be a determining factor in the efficacy of response to MAPK inhibitors, especially KRASG12C inhibitors. This could have important clinical implications, as treatment strategies could be tailored based on the status of DUSP4 in patients' tumors.

2.3 Using MAPK-Mediated Toxicity to Discover New Modulators

In this section, we seek to explore the consequences of the lack of adequate downregulation of the MAPK signaling pathway during cancer initiation and progression. To do this, we decided to perform a genome-wide screening to identify new MAPK regulators that can help understand the complex regulatory network.

To this end, we developed a model of MAPK-inducible toxicity, with a model of ATII cells immortalized with tamoxifen-activatable mutant oncogenic KRAS. In addition, we introduced the expression of the BRAFD594A mutant, which potentiates MAPK activity despite lacking kinase activity. We were able to establish precise control of BRAF activity by introducing an inducible version of BRAFD594A, allowing KRAS and BRAF activity to be dosed.

We demonstrate that the combination of KRAS activation with BRAFD594A expression in the presence of tamoxifen and doxycycline potentiates MAPK signaling. A dose-specific combination of both results in hyperactivation of MAPK, effective but controlled and dependent cell death of MAPK. We were also able to detect γH2AX phosphorylation, which indicates genomic stress, likely directly caused by MAPK hyperactivation.

These results are validated in KRAS-mutated A549 cells. The expression of BRAF D594A is capable of inducing the activation of MAPK, but at higher doses, it is toxic and limits cell growth.

In summary, these experiments demonstrate that MAPK activation is a central pathway in cell signaling and that MAPK hyperactivation can result in cellular toxicity. These findings provide the basis for exploring new regulators of the MAPK signaling pathway.

We designed a CRISPR/Cas9 screening strategy for a complete genome study. RNA guides (gRNAs) can target both positive and negative pathway regulators. When they inhibit the expression of positive regulators, toxicities stemming from excess MAPK are reduced, leading to a restoration of cell viability. In contrast, when gRNAs target negative regulators, MAPK activity and toxicities are increased. These effects will be reflected in the representation of the gRNAs in screening.

For screening, we used ATII cells modified to express the Cas9 protein and the Brunello library, which contains the genome-wide gRNAs. Three conditions were carried out in parallel: one that was not subjected to treatment (PRE), one with activation of KRAS (K), and one with activation of KRAS and BRAF (KB). Genomic DNA was extracted from all conditions and a nested PCR strategy was applied to amplify gRNAs prior to sequencing.

Analysis of the results revealed patterns of gRNA enrichment and depletion under conditions K and KB compared to PRE. Two algorithms, STARS and MAGECK, were used to analyze the data and confirm the results.

Enriched gRNAs were selected that supposedly rescued the viability of the cells by targeting mediators of the apoptotic phenotype, either directly through the control of MAPK or indirectly through other

mechanisms. On the other hand, depleted gRNAs were analyzed, suggesting that genes whose gRNAs were depleted are negative regulators of the MAPK pathway.

In this thesis, analyses were carried out to validate the effects of deletion of the TTC1 and CSK genes in ATII KB cells and in KRAS-mutated non-small cell lung adenocarcinoma (LUAD) cell lines.

With respect to TTC1, it was found that deletion of this gene did not affect the sensitivity of ATII cells to KRAS and BRAF activation, suggesting that TTC1 does not directly contribute to the MAPK signaling response. However, it was observed that TTC1 gRNAs were selected in screening, indicating a possible importance in terms of essentiality. Its role in LUAD cell lines with KRAS mutation was evaluated, where TTC1 deletion did not have a consistent effect on MAPK activation. Since TTC1 is considered an essential gene in a wide variety of human cell lines, it was concluded that it was not a suitable candidate for further study.

Regarding CSK, it was observed that deletion of this gene in ATII KB cells increased the sensitivity of the cells to KRAS and BRAF activation. This suggests that CSK acts as a negative regulator of MAPK signaling and that its loss of function compromises MAPK downregulation, leading to increased toxicity of MAPK signaling in ATII KB cells. This observation was also confirmed in KRAS-mutated LUAD cell lines, where cells lacking CSK showed increased resistance to inhibitors of the RAS-MAPK pathway. In addition, it was observed that inhibition of SRC in ATII KB cells did not significantly alter MAPK activation, suggesting that the effect of CSK on the regulation of MAPK signaling is independent of SRC. This was confirmed by evaluating the effects of SRC inhibition with the PP2 inhibitor in KRAS-mutated LUAD cell lines, where resistance to inhibitors of the RAS-MAPK pathway in cells lacking CSK was not significantly altered.

In summary, these findings suggest that CSK acts as a negative regulator of MAPK signaling and that its loss of function may increase resistance to inhibitors of the RAS-MAPK pathway.

The set of data collected in this thesis is relevant to better understand MAPK signaling in mutated LUAD KRAS tumors. It is important to understand how signals mediated by the MAPK pathway are integrated

and how a whole series of regulators allow signaling levels to be at a controlled, equilibrium level. To face the challenges of the future in precision oncology (resistance, comorbidities, etc.), they must consider how the tumor is able to restructure the pathway through alterations in these regulators, as is the case with DUSP4. Knowing and studying all these alterations, in addition to those that may occur in unknown regulators, will allow research to answer clinical questions that will provide a better future for patients affected by this disease.

Conclusions

Based on the objectives of this research, we have obtained valuable information on how the regulation of the MAPK pathway affects tumor progression, demonstrating that alterations in pathway modulators can play a fundamental role in clinical prognosis.

The overall conclusions of this work are as follows:

1. Analysis of transcriptomic data from LUAD through our firm revealed that MAPK activity determines the survival of patients with KRAS mutation, with low levels of MAPK being an indicator of poor prognosis.
2. High MAPK activity in KRAS-mutated LUAD correlates with stress phenotypes, including genomic stress, oxidative stress, and apoptosis.
3. DUSP4 is a negative regulator of MAPK that is altered differently depending on the levels of MAPK activity in the mutated LUAD KRAS. Patients with high MAPK activity have DUSP4 deletions, while patients with low MAPK activity have DUSP4 amplifications.
4. The loss of DUSP4 potentiates the activation of MAPK. Loss of DUSP4 is a selected early-stage event because it may confer a proliferative advantage to KRAS-driven neoplasms. In advanced tumors, this increased signaling correlates with toxic events suggesting that chronic loss of DUSP4 may compromise normal tumor progression.
5. Through CRISPR screening, we identified CSK as a potential regulator that could function independently of SRC by mediating the negative regulation of the pathway. Further research may be needed to complete and better understand how CSK might contribute to different stages of tumor development.

Resumen en español

Objetivos

La progresión tumoral es un proceso complejo, que requiere una coordinación de las habilidades del tumor para un objetivo común. Cada proceso y cada alteración del tumor se selecciona y dosifica cuidadosamente para poder conceder ventajas a las células malignas y poder proliferar. La regulación de la vía RAS-MAPK es una característica importante que se altera de manera sistemática en el adenocarcinoma de pulmón (LUAD, por sus siglas en inglés). Sin embargo, ahora comprendemos que la señalización no solo requiere procesos activadores, sino también mecanismos reguladores que mantienen el equilibrio. Por esta razón, la capacidad del tumor para modular la vía MAPK, y, por lo tanto, las alteraciones de sus reguladores deben determinar la naturaleza del tumor y tener consecuencias clínicas.

Con este propósito, decidimos estudiar funcionalmente datos genómicos de casos de LUAD con mutación en KRAS y evaluar cómo los niveles de señalización de MAPK afectan a su pronóstico clínico. A partir de estos análisis, queremos sentar las bases para estudiar cómo alteraciones precisas de reguladores, tanto conocidos como novedosos, podrían afectar la progresión tumoral. Este enfoque permite establecer una relación causal directa entre la actividad de RAS/MAPK y la aptitud del tumor en la clínica. Toda esta información permitirá una comprensión más profunda de los diferentes mecanismos de regulación de la vía, lo que podría ayudar a determinar en pacientes la respuesta al tratamiento y las posibles resistencias.

Los objetivos globales de esta tesis fueron los siguientes:

1. Estudiar el componente MAPK a partir de bases de datos clínicas de acceso público para comprender mejor cómo la regulación de la vía afecta la supervivencia de los pacientes con LUAD con mutación en KRAS y los mecanismos moleculares que podrían subyacer a su pronóstico.
2. Desarrollar modelos de LUAD que recapitulen el contexto molecular observado en la clínica para determinar cómo niveles excesivos de MAPK son tóxicos para tumores KRAS mutados.
3. Analizar los cambios moleculares que afectan a los reguladores de MAPK, como las alteraciones en DUSP4 observadas en pacientes. Comprender su papel potencial en la respuesta específica de MAPK, tratando de comprender cómo el estado de DUSP4 moldea el destino del tumor al controlar el equilibrio de la señalización de MAPK.
4. Identificar y caracterizar nuevos reguladores de RAS-MAPK que podrían contribuir a una mejor interpretación de la vía en el entorno de la oncología molecular.

1 RESUMEN DE LA INTRODUCCIÓN

1.1 LA RUTA DE RAS Y LAS MAPK EN CÁNCER

El cáncer es una enfermedad global de la que se diagnostican, al año, 18 millones de nuevos casos en todo el mundo, y se pronostica que esta cifra aumentará a 40 millones anuales para 2070. En Europa, el cáncer ocupa el segundo lugar como causa de muerte, cobrando la vida de hasta 2 millones de personas al año. Lo que es especialmente preocupante es que a pesar de que Europa alberga menos del 10% de la población mundial, es responsable de una cuarta parte de todos los casos de cáncer en el planeta. Esta estadística resalta la creciente amenaza que representa el cáncer para la sociedad en Europa y subraya la necesidad de abordar este problema de manera urgente.

El cáncer de pulmón se erige como el más letal entre todas las variedades de cáncer, superando en mortalidad a los cánceres de mama, páncreas y próstata combinados. Existe una falta de detección temprana, con la mayoría de los pacientes siendo diagnosticados en etapas avanzadas. La clasificación de los tumores de pulmón de células no pequeñas (NSCLC) es esencial para estimar la supervivencia y las opciones de tratamiento, siendo los adenocarcinomas pulmonares (LUAD) siendo los más comunes.

El tabaquismo es un factor de riesgo significativo, fumar aumenta considerablemente el riesgo de desarrollar cáncer de pulmón, estimándose que el 80% de las muertes por esta enfermedad podrían prevenirse mediante la cesación del tabaquismo. A pesar de estos factores conocidos, alrededor del 20% de los casos de cáncer de pulmón en todo el mundo no se pueden atribuir al tabaquismo ni a ningún otro factor dominante.

En el caso del pulmón, el hito central de la progresión tumoral es la anulación de los mecanismos que regulan la proliferación celular. Las mutaciones en genes como EGFR, TP53 y KRAS son los principales impulsores del tumor. Aunque no se comprende completamente cómo ocurren estas mutaciones, se sugiere que son eventos aleatorios que se van acumulando en el organismo a lo largo de la vida. La

exposición a carcinógenos u otros factores, en un momento dado, hacen cambiar las restricciones selectivas en el tejido, lo que provoca alteraciones en el microambiente, que promueven la inflamación y finalmente genera las condiciones propicias para el cáncer. Las células con mutaciones preexistentes en protooncogenes tienen una ventaja selectiva en estas condiciones, lo que conduce a la expansión clonal y al cáncer.

A la hora de tratar estos tumores, la gran heterogeneidad tumoral es un desafío importante que complica la eficacia de las respuestas. La mayoría de las mutaciones oncogénicas en LUAD están relacionadas con la vía RAS/MAPK, lo que ha llevado históricamente al desarrollo de estrategias terapéuticas centradas en los principales efectores de esta vía. Inicialmente, se utilizaron inhibidores genéricos contra quinasas, como el sorafenib, pero mostraron un beneficio clínico limitado en el cáncer de pulmón con mutación en KRAS, necesitando el desarrollo de terapias dirigidas a las mutaciones específicas del tumor.

Este es un desafío, ya que inhibir específicamente y de manera efectiva los componentes de una vía celular es complejo. Hay que tener cuenta que el tumor dispone de múltiples mecanismos de compensación que permiten a las células adaptarse, resistir y, eventualmente, progresar durante el tratamiento.

El desafío de inhibir la proteína KRAS, uno de los principales impulsores oncogénicos en LUAD, tuvo un avance con el desarrollo de inhibidores específicos para la mutación G12C, con fármacos como el sotorasib y el adagrasib. Estos medicamentos mostraron ser prometedores en la clínica, pero presentan limitaciones, incluida una respuesta de corta duración, la aparición de resistencia o la incompatibilidad con la inmunoterapia, entre otros. Una nueva generación de inhibidores, llamados pan-KRAS al inhibir todas las formas de KRAS, se presentan también prometedores. Sin embargo, más investigación es necesaria para poder abordar los desafíos que estas estrategias terapéuticas plantearán en el futuro.

1.2 LA REGULACIÓN NEGATIVA COMO MECANISMO ESENCIAL PARA EL DESARROLLO TUMORAL

La vía de señalización MAPK (**Figura 5**) es una cascada de señalización que desempeña un papel crucial en la transmisión de señales extracelulares para regular diversas respuestas celulares. Esta vía es el mecanismo principal por el cual KRAS transmite su potencial oncogénico.

Así como una mutación activadora de KRAS tiene efectos oncogénicos, las mutaciones en la vía MAPK se presentan también frecuentemente en tumores LUAD. Sin embargo, una hiperactivación de la vía resulta tóxica para el tumor. Para que las células tumorales mantengan la adicción a KRAS y/o a mutaciones en la vía MAPK, otras alteraciones son necesarias para desactivar las respuestas celulares que normalmente inhibirían la proliferación celular. Es importante mantener un equilibrio en la señalización MAPK para evitar la toxicidad celular.

Para regular estas respuestas, existen proteínas reguladoras como las fosfatasas, especialmente las DUSPs. Estas enzimas desempeñan un papel crucial en la desactivación de la señalización de ERK y pueden tener funciones duales, tanto supresoras como promotoras del tumor, dependiendo del contexto específico, debido a este fino equilibrio que se debe mantener.

Para poder entender cómo esta regulación se lleva a cabo en el tumor, es crucial poder medir los niveles de actividad que cada componente acarrea y cómo cambios en estos componentes modifican la balanza. Las firmas génicas transcripcionales pueden ser una herramienta útil para evaluar la actividad de esta vía en pacientes con cáncer.

En esta tesis, describimos el uso de una de estas firmas para monitorizar la actividad de la vía MAPK y cómo los niveles de la misma predicen la supervivencia de los pacientes de LUAD. Además, presentamos un análisis que ha permitido identificar una serie de posibles reguladores de MAPK, tanto positivos como negativos. El estudio de estos nuevos reguladores, como es el caso del gen DUSP4, es de vital importancia para comprender mejor la vía de señalización RAS-MAPK y su regulación en diversos contextos biológicos y patológicos, especialmente en el cáncer de pulmón con mutaciones en KRAS. Estas investigaciones presentan bases para avanzar en el campo de la oncología de precisión y mejorar el tratamiento de los pacientes afectados por esta enfermedad.

2 RESULTADOS PRINCIPALES

2.1 UNA FIRMA TRANSCRIPCIONAL PARA DETERMINAR LA SUPERVIVENCIA DE PACIENTES

En primer lugar, el objetivo de este estudio fue abordar la pregunta de si la actividad de MAPK dicta el resultado de los tumores con mutaciones en KRAS. Estos resultados bioinformáticos se basaron en datos de 162 pacientes con mutaciones en KRAS del adenocarcinoma de pulmón (LUAD) en el TCGA. Se evaluó la actividad de MAPK calculando una puntuación que consideraba la expresión de 6 genes específicos de MAPK para esta enfermedad (Brant et al., 2017): DUSP4, DUSP6, ETV4, ETV5, PHLDA1 y SPRY2 (**Figure 23**).

Clasificamos a los pacientes en dos grupos: alto y bajo nivel de MAPK, según los cuartiles superiores e inferiores de la puntuación de la firma. Realizamos un análisis de supervivencia que reveló diferencias significativas en la supervivencia, con una menor supervivencia en el grupo de bajo MAPK. Este resultado sugiere que altos niveles de MAPK son perjudiciales en el contexto de LUAD impulsado por KRAS, y que el tumor debe limitar sus niveles de señalización para asegurar su máxima aptitud. Además, esta diferencia en la supervivencia se encontró específicamente en tumores con mutaciones en KRAS y no en otros conductores de mutaciones.

Para confirmar estos resultados, se aplicó un filtro de pureza tumoral, lo que resultó en una cohorte más pura. Al realizar un análisis de correlación entre los genes de la firma, concluimos que era necesario llevar a cabo la exclusión de los genes DUSP4 y PHLDA1 de la firma, ya que anti-correlacionaban con el resto de los genes y, en definitiva, no contribuyeron significativamente a la capacidad predictiva de la firma. El análisis de supervivencia con la firma refinada confirmó la diferencia en la supervivencia entre los grupos de altos y bajos niveles de MAPK. Además, estos resultados se validaron en una cohorte independiente de microarray que recapitulaba igualmente pacientes de LUAD con KRAS mutado.

La firma también se correlacionó con *ontologies* asociadas con la activación de MAPK, lo que confirma que la firma es capaz de reflejar los niveles de señalización de la vía de manera efectiva. El análisis de las diferencias entre los grupos de alto y bajo MAPK no reveló asociaciones con características clínicas

específicas ni mutaciones en KRAS, pero se encontró una asociación con mutaciones en KEAP1. Sin embargo, la mutación de KEAP1 no se asoció con diferencias en la supervivencia.

El análisis de las alteraciones en el número de copias (CNV) demostró que los tumores con altos niveles de MAPK presentaban más alteraciones genéticas en comparación con los tumores con bajos niveles de MAPK. Esto sugiere que los tumores con altos niveles de MAPK son más propensos a la inestabilidad genómica.

En resumen, la actividad MAPK tiene un impacto significativo en la supervivencia de los pacientes con mutaciones en KRAS en el LUAD. La firma que hemos refinado se correlaciona con la activación de MAPK, pero también con una mayor inestabilidad genómica, lo que sugiere que altos niveles de MAPK generan una toxicidad mayor que es determinante en la progresión de estos tumores.

2.2 DUSP4 ES UN REGULADOR NEGATIVO QUE DETERMINA EL DESARROLLO TUMORAL

El análisis *in-silico* de los datos clínicos muestra diferencias significativas en el estado genómico de DUSP4, un regulador negativo de MAPK, entre pacientes con diferentes niveles de la firma transcripcional. DUSP4 presenta amplificaciones en tumores bajos en MAPK y pérdidas genómicas en tumores altos en MAPK.

DUSP4 regula la fosforilación de ERK, siendo su pérdida un evento activador de la vía, y su sobreexpresión un evento inhibidor de la vía. Sin embargo, identificamos que la pérdida de DUSP4 no induce la transformación celular por sí sola ni colabora con otros oncogenes como RAS o PI3K, lo que sugiere que DUSP4 no es un evento oncogénico primario.

Por ello, decidimos estudiar el impacto de la eliminación de DUSP4 en tumores KRAS mutados ya formados. Los resultados revelaron que los tumores sin DUSP4 muestran un aumento en la inestabilidad genómica y en la tasa de apoptosis. Esto sugiere que la pérdida de DUSP4 desencadena la muerte celular, probablemente por un exceso de activación de la vía MAPK. Aunque se observó un aumento en el estrés oxidativo en las células con DUSP4 eliminado en un modelo celular de laboratorio, este efecto no se

confirmó en los tumores. Estos hallazgos indican que DUSP4 juega un papel crucial en la regulación de la estabilidad genómica y la supervivencia celular en el contexto de tumores con mutación KRAS.

Para poder estudiar cómo DUSP4 contribuye, en etapas tempranas, a la iniciación y al desarrollo de los tumores, creamos un modelo *in vivo* a partir de una línea celular ATII inmortalizada humana, que contiene una mutación oncogénica KRAS activable por tamoxifeno gracias a una fusión con el receptor de estrógeno (KRASG12V-ER). Estas células se infectaron con construcciones plentiCRISPR dirigidas a DUSP4 y se inyectaron ortotópicamente en ratones inmunodeficientes por inyección en la vena de la cola. Solo los ratones que retuvieron el tamoxifeno durante todo el proceso desarrollaron una señal positiva de luciferasa, demostrando que se trata de un fenotipo dependiente de KRAS. Las células con eliminación de DUSP4 presentaron una señal de luciferasa significativamente aumentada durante varias semanas. Sin embargo, durante las últimas semanas, el desarrollo del tumor control con lacZ se aceleró abruptamente, alcanzando incluso niveles de luciferasa más altos que las células con eliminación de DUSP4.

Estos resultados respaldan la hipótesis derivada de los datos clínicos, que sugiere que los eventos de eliminación de DUSP4 son positivamente seleccionados en las etapas tempranas de la enfermedad, ya que la pérdida de DUSP4 parece ser ventajosa para el crecimiento maligno inicial. Sin embargo, se observó que las células con eliminación de DUSP4 pierden progresivamente la ventaja conferida y son superadas por las células con DUSP4 competente, lo que sugiere que, en etapas posteriores, la integridad de DUSP4 puede ser más beneficiosa.

Para comprender mejor el impacto global de DUSP4 en el proceso maligno, se buscó crear un modelo más completo que recapitulara todo el proceso de inicio y desarrollo tumoral de las células mutantes de KRAS con o sin alteraciones en DUSP4.

Para este modelo, se utilizó la cepa de ratón K-ras$^{+/lox\text{-}Stop\text{-}lox\text{-}G12V\text{-}geo}$, que permite la expresión del mutante oncogénico KRAS$^{G12V\text{-}ER}$ después de una recombinación mediada por la Cre recombinasa. Para combinar la activación de KRAS con la inactivación de DUSP4, infectamos los ratones por vía intranasal con partículas lentivirales del vector *pSECC*, que elimina el gen DUSP4 mediante la tecnología

CRISPR/Cas9 y, al mismo tiempo, activa $KRAS^{G12V-ER}$ con la expresión de una CRE recombinasa. Además, este sistema permite la expresión de un gen reportero YFP también silenciado por un casete *lox-STOP-lox*.

Se observó que la pérdida de DUSP4 aumentó el crecimiento de las lesiones tempranas en ratones en el primer mes. En tres meses, se encontró un aumento en el número de células positivas en los ratones con DUSP4 eliminado, lo que sugiere una sinergia entre la pérdida de DUSP4 y la actividad oncogénica de KRAS en el aumento de la carga tumoral. Sin embargo, en etapas posteriores (6 y 9 meses), las lesiones fueron menos frecuentes en los ratones con DUSP4 eliminado. En el último punto de referencia, a los 12 meses, se observó que los tumores sin DUSP4 eran más pequeños en tamaño. Esto podría indicar que la pérdida de DUSP4 reduce la probabilidad de generar neoplasias avanzadas y sustanciales.

En resumen, este experimento sugiere que, a medida que progresa el tumor impulsado por KRAS, la pérdida de DUSP4 se vuelve perjudicial. Inicialmente, la ausencia de DUSP4 promueve la formación de tumores, pero a medida que el tumor avanza, DUSP4 parece desempeñar un papel protector. Se planea realizar análisis adicionales para comprender cómo la eliminación de DUSP4 afecta las lesiones en etapas avanzadas desde el punto de vista de la apoptosis, la toxicidad genómica y el estrés oxidativo.

Seguidamente, nos planteamos el objetivo de investigar cómo estas alteraciones pueden influir en la respuesta clínica de los pacientes, en particular, su respuesta a inhibidores de MAPK, como los inhibidores de MEK y los inhibidores específicos de $KRAS^{G12C}$.

Se generaron modelos de células de adenocarcinoma de pulmón (LUAD) con mutaciones en KRAS y se eliminó o indujo la expresión de DUSP4 para evaluar cómo la modulación de DUSP4 afecta específicamente la respuesta a inhibidores. Se eliminó DUSP4 en estas líneas celulares y se evaluó la sensibilidad a los inhibidores de MAPK, como el trametinib y los inhibidores de KRAS adagrasib y sotorasib. En algunas líneas celulares, la eliminación de DUSP4 resultó en una disminución de la sensibilidad al trametinib, lo que indica una mayor resistencia. Esta resistencia al trametinib podría deberse a los niveles alterados de MAPK generados por la eliminación de DUSP4. En las líneas celulares con mutaciones KRASG12C, la sensibilidad a los inhibidores de KRAS no se vio afectada por la

eliminación de DUSP4. Por otro lado, la sobreexpresión de DUSP4 sensibilizó a las células a los inhibidores de MAPK, incluido el trametinib y los inhibidores de KRASG12C.

En conjunto, estos resultados sugieren que el estado de DUSP4 puede ser un factor determinante en la eficacia de la respuesta a los inhibidores de MAPK, especialmente los inhibidores de KRASG12C. Esto podría tener implicaciones clínicas importantes, ya que las estrategias de tratamiento podrían adaptarse en función del estado de DUSP4 en los tumores de pacientes.

2.3 USO DE LA TOXICIDAD MEDIADA POR MAPK PARA DESCUBRIR NUEVOS MODULADORES

En esta sección, se busca explorar las consecuencias de la falta de regulación negativa adecuada de la vía de señalización MAPK durante la iniciación y progresión del cáncer. Para ello, decidimos realizar un screening de todo el genoma para identificar nuevos reguladores de MAPK que puedan ayudar a comprender la compleja red de regulación.

Con este fin, desarrollamos un modelo de toxicidad inducible por MAPK, con un modelo de células ATII inmortalizadas con KRAS oncogénico mutante activable por tamoxifeno. Además, introdujimos la expresión del mutante $BRAF^{D594A}$, que potencia la actividad de MAPK a pesar de carecer de actividad quinasa. Pudimos establecer un control preciso de la actividad de BRAF mediante la introducción de una versión inducible de $BRAF^{D594A}$, lo que permite dosificar la actividad de KRAS y BRAF.

Demostramos que la combinación de la activación de KRAS con la expresión de $BRAF^{D594A}$ en presencia de tamoxifeno y doxiciclina potencia la señalización de MAPK. Una combinación específica de dosis de ambas resulta en una hiperactivación de MAPK, en una muerte celular efectiva pero controlada y dependiente de MAPK. También fuimos capaces de detectar la fosforilación de γH2AX, que indica estrés genómico, probablemente causado directamente por la hiperactivación de MAPK.

Estos resultados se validan en células A549 con mutación KRAS. La expresión de BRAF D594A es capaz de inducir la activación de MAPK, pero a dosis más altas, resulta tóxica y limita el crecimiento celular.

En resumen, estos experimentos demuestran que la activación de MAPK es una vía central en la señalización celular y que la hiperactivación de MAPK puede resultar en toxicidad celular. Estos hallazgos proporcionan la base para explorar nuevos reguladores de la vía de señalización MAPK.

Diseñamos una estrategia de screening CRISPR/Cas9 para un completo estudio del genoma. Los guías de ARN (gRNAs) pueden apuntar tanto a reguladores positivos y negativos de la vía. Cuando inhiben la expresión de reguladores positivos, las toxicidades derivadas del exceso de MAPK se reducen, lo que lleva a una restauración de la viabilidad celular. En contraste, cuando los gRNA se dirigen a reguladores negativos, se aumenta la actividad de MAPK y las toxicidades. Estos efectos se reflejarán en la representación de las gRNAs en el screening.

Para el screening usamos células ATII modificadas para expresar la proteína Cas9 y la biblioteca Brunello, que contiene los gRNAs dirigidas a todo el genoma. Tres condiciones se llevaron a cabo en paralelo: una que no fue sometida a tratamiento (PRE), una con activación de KRAS (K), y otra con activación de KRAS y BRAF (KB). Se extrajo el ADN genómico de todas las condiciones y se aplicó una estrategia de PCR anidada para amplificar las gRNAs antes de la secuenciación.

El análisis de los resultados reveló patrones de enriquecimiento y depleción de gRNAs en las condiciones K y KB en comparación con PRE. Se utilizaron dos algoritmos, STARS y MAGECK, para analizar los datos y confirmar los resultados.

Se seleccionaron gRNAs enriquecidas que, supuestamente, rescataron la viabilidad de las células al dirigirse a mediadores del fenotipo apoptótico, ya sea directamente a través del control de MAPK o indirectamente a través de otros mecanismos. Por otro lado, se analizaron las gRNAs agotadas, lo que sugiere que los genes cuyas gRNAs se agotaron son reguladores negativos de la vía MAPK.

En esta tesis, se llevaron a cabo análisis para validar los efectos de la eliminación de los genes TTC1 y CSK en células ATII KB y en líneas celulares de adenocarcinoma de pulmón de células no pequeñas (LUAD) con mutación KRAS.

Con respecto a TTC1, se descubrió que la eliminación de este gen no afectó la sensibilidad de las células ATII a la activación de KRAS y BRAF, lo que sugiere que TTC1 no contribuye directamente a la respuesta de señalización de MAPK. Sin embargo, se observó que las gRNAs de TTC1 se seleccionaron en el screening, lo que indica una posible importancia en términos de esencialidad. Se evaluó su papel en las líneas celulares de LUAD con mutación KRAS, donde la eliminación de TTC1 no tuvo un efecto coherente en la activación de MAPK. Dado que TTC1 se considera un gen esencial en una amplia variedad de líneas celulares humanas, se concluyó que no era un candidato adecuado para un estudio más detallado.

En cuanto a CSK, se observó que la eliminación de este gen en las células ATII KB aumentó la sensibilidad de las células a la activación de KRAS y BRAF. Esto sugiere que CSK actúa como un regulador negativo de la señalización de MAPK y que su pérdida de función compromete la regulación negativa de MAPK, lo que lleva a una mayor toxicidad de la señalización de MAPK en células ATII KB. Esta observación también se confirmó en las líneas celulares de LUAD con mutación KRAS, donde las células que carecían de CSK mostraron una mayor resistencia a los inhibidores de la vía RAS-MAPK. Además, se observó que la inhibición de SRC en las células ATII KB no alteró significativamente la activación de MAPK, lo que sugiere que el efecto de CSK en la regulación de la señalización de MAPK es independiente de SRC. Esto se confirmó al evaluar los efectos de la inhibición de SRC con el inhibidor PP2 en las líneas celulares de LUAD con mutación KRAS, donde la resistencia a los inhibidores de la vía RAS-MAPK en las células que carecían de CSK no se vio significativamente alterada.

En resumen, estos hallazgos sugieren que CSK actúa como un regulador negativo de la señalización de MAPK y que su pérdida de función puede aumentar la resistencia a los inhibidores de la vía RAS-MAPK.

El conjunto de los datos recabados en esta tesis es relevante para comprender mejor la señalización de MAPK en tumores LUAD KRAS mutados. Es importante entender cómo se integran las señales mediadas por la vía MAPK y cómo toda una serie de reguladores permiten que los niveles de señalización se sitúen en un nivel controlado, en equilibrio. Para afrontar los desafíos del futuro en

oncología de precisión (resistencias, comorbilidades, etc.) deberán tener en cuenta cómo el tumor es capaz de reestructurar la vía a través de alteraciones en estos reguladores, como es el caso de DUSP4. Conocer y estudiar todas estas alteraciones, además de las que puedan ocurrir en reguladores desconocidos, permitirá a la investigación responder a preguntas clínicas que brindarán un mejor futuro a los pacientes afectados por esta enfermedad.

Conclusiones

Basándonos en los objetivos de esta investigación, hemos obtenido información valiosa sobre cómo la regulación de la vía MAPK afecta la progresión tumoral, demostrando que las alteraciones en los moduladores de la vía pueden desempeñar un papel fundamental en el pronóstico clínico.

Las conclusiones globales de este trabajo son las siguientes:

1. El análisis de datos transcriptómicos de LUAD a través de nuestra firma reveló que la actividad de MAPK determina la supervivencia de los pacientes con mutación en KRAS, siendo bajos niveles de MAPK un indicador de mal pronóstico.
2. La alta actividad de MAPK en el LUAD con mutación en KRAS se correlaciona con fenotipos de estrés, incluyendo estrés genómico, oxidativo y apoptosis.
3. DUSP4 es un regulador negativo de MAPK que se altera de manera diferente según los niveles de actividad de MAPK en el LUAD KRAS mutado. Los pacientes con alta actividad de MAPK presentan deleciones de DUSP4, mientras que los pacientes con baja actividad de MAPK presentan amplificaciones de DUSP4.
4. La pérdida de DUSP4 potencia la activación de MAPK. La pérdida de DUSP4 es un evento seleccionado en etapas tempranas porque puede otorgar una ventaja proliferativa a las neoplasias impulsadas por KRAS. En tumores avanzados, esta señalización aumentada se correlaciona con eventos tóxicos que sugieren que la pérdida crónica de DUSP4 puede comprometer la progresión normal del tumor.
5. A través del screening CRISPR, identificamos a CSK como un regulador potencial que podría funcionar de manera independiente a SRC mediando la regulación negativa de la vía. Puede ser necesario realizar investigaciones adicionales para completar y comprender mejor cómo CSK podría contribuir a las diferentes etapas del desarrollo del tumor.

Résumé en français

Objectifs

La progression tumorale est un processus complexe qui nécessite une coordination des compétences de la tumeur pour un objectif commun. Chaque processus et chaque altération de la tumeur sont sélectionnés et dosés avec soin pour conférer des avantages aux cellules malignes et favoriser leur prolifération. La régulation de la voie RAS-MAPK est une caractéristique importante qui est systématiquement altérée dans l'adénocarcinome pulmonaire (LUAD, pour « Lung Adenocarcinoma » en anglais). Cependant, nous comprenons maintenant que la signalisation nécessite non seulement des processus activateurs, mais aussi des mécanismes régulateurs maintenant l'équilibre. C'est pourquoi la capacité de la tumeur à moduler la voie MAPK et donc les altérations de ses régulateurs doivent déterminer la nature de la tumeur et entraîner des conséquences cliniques.

Dans ce but, nous avons décidé d'étudier de manière fonctionnelle les données génomiques des cas de LUAD présentant une mutation dans le gène KRAS et d'évaluer comment les niveaux de signalisation de MAPK affectent leur pronostic clinique. À partir de ces analyses, nous souhaitons étudier comment des altérations précises des régulateurs, à la fois connus et nouveaux, pourraient influencer la progression tumorale. Cette approche permet d'établir un lien de causalité direct entre l'activité de RAS/MAPK et la viabilité de la tumeur en clinique. Toutes ces informations permettront une compréhension plus approfondie des différents mécanismes de régulation de la voie, ce qui pourrait aider à déterminer la réponse au traitement et les éventuelles résistances chez les patients.

Les objectifs globaux de cette thèse étaient les suivants :

1. Étudier le composant MAPK à partir de bases de données cliniques accessibles au public pour mieux comprendre comment la régulation de la voie affecte la survie des patients atteints de LUAD avec une mutation dans KRAS et les mécanismes moléculaires qui pourraient sous-tendre leur pronostic.
2. Développer des modèles de LUAD reproduisant le contexte moléculaire observé en clinique afin de déterminer comment des niveaux excessifs de MAPK sont toxiques pour les tumeurs mutées KRAS.
3. Analyser les changements moléculaires qui affectent les régulateurs de MAPK, tels que les altérations de DUSP4 observées chez les patients. Comprendre leur rôle potentiel dans la réponse spécifique de MAPK en essayant de comprendre comment l'état de DUSP4 façonne le destin de la tumeur en contrôlant l'équilibre de la signalisation de MAPK.
4. Identifier et caractériser de nouveaux régulateurs de RAS-MAPK qui pourraient contribuer à une meilleure compréhension de la voie dans le contexte de l'oncologie moléculaire.

1 RESUME INTRODUCTOIRE

1.1 LA VOIE RAS ET MAPK DANS LE CANCER

Le cancer est une maladie mondiale avec 18 millions de nouveaux cas diagnostiqués chaque année dans le monde, et ce nombre devrait atteindre 40 millions par an d'ici 2070. En Europe, le cancer est la deuxième cause de décès, coûtant la vie à près de 2 millions de personnes par an. Ce qui est particulièrement inquiétant, c'est que malgré le fait que l'Europe abrite moins de 10% de la population mondiale, elle est responsable d'un quart de tous les cas de cancer sur la planète. Cette statistique met en évidence la menace croissante que représente le cancer pour la société en Europe et souligne la nécessité de s'attaquer de toute urgence à ce problème.

Le cancer du poumon est le plus meurtrier de toutes les variétés de cancer, dépassant les cancers du sein, du pancréas et de la prostate combinés en termes de mortalité. Il y a un manque de détection précoce, la plupart des patients étant diagnostiqués à un stade avancé. La classification des tumeurs pulmonaires non à petites cellules (NSCLC) est essentielle pour estimer la survie et les options de traitement, les adénocarcinomes pulmonaires (LUAD) étant les plus courants.

Le tabagisme est un facteur de risque important, car le tabagisme augmente considérablement le risque de développer un cancer du poumon, et on estime que 80% des décès dus à cette maladie pourraient être évités par l'arrêt du tabac. Malgré ces facteurs connus, environ 20 % des cas de cancer du poumon dans le monde ne peuvent être attribués au tabagisme ou à tout autre facteur dominant.

Dans le cas du poumon, l'étape centrale de la progression tumorale est le renversement des mécanismes qui régulent la prolifération cellulaire. Les mutations dans les gènes tels que l'EGFR, TP53 et KRAS sont les principaux moteurs de la tumeur. Bien que l'on ne comprenne pas entièrement comment ces mutations se produisent, il est suggéré qu'il s'agit d'événements aléatoires qui s'accumulent dans le corps au cours d'une vie. L'exposition à des substances cancérigènes ou à d'autres facteurs, à un moment donné,

entraîne une modification des restrictions sélectives dans les tissus, provoquant des altérations du microenvironnement, qui favorisent l'inflammation et, en fin de compte, créent des conditions propices au cancer. Les cellules présentant des mutations préexistantes dans les proto-oncogènes ont un avantage sélectif dans ces conditions, conduisant à l'expansion clonale et au cancer.

Lorsqu'il s'agit de traiter ces tumeurs, la grande hétérogénéité tumorale est un défi majeur qui complique l'efficacité des réponses. La majorité des mutations oncogéniques de LUAD sont liées à la voie RAS/MAPK, ce qui a historiquement conduit au développement de stratégies thérapeutiques centrées sur les principaux effecteurs de cette voie. Initialement, des inhibiteurs génériques contre les kinases, tels que le sorafénib, ont été utilisés, mais ils ont montré un bénéfice clinique limité dans le cancer du poumon muté KRAS, ce qui a nécessité le développement de thérapies ciblant les mutations spécifiques de la tumeur.

Il s'agit d'un défi, car l'inhibition spécifique et efficace des composants d'une voie cellulaire est complexe. Il faut garder à l'esprit que la tumeur possède de multiples mécanismes de compensation qui permettent aux cellules de s'adapter, de résister et, éventuellement, de progresser pendant le traitement.

Le défi de l'inhibition de la protéine KRAS, l'un des principaux moteurs oncogéniques du LUAD, a été avancé avec le développement d'inhibiteurs spécifiques de la mutation G12C, avec des médicaments tels que le sotorasib et l'adagrasib. Ces médicaments se sont révélés prometteurs en clinique, mais présentent des limites, notamment une réponse de courte durée, l'émergence d'une résistance ou une incompatibilité avec l'immunothérapie, entre autres. Une nouvelle génération d'inhibiteurs, appelés pan-KRAS, inhibent toutes les formes de KRAS, est également prometteuse. Cependant, des recherches supplémentaires sont nécessaires pour relever les défis que ces stratégies thérapeutiques poseront à l'avenir.

1.2 LA REGULATION NEGATIVE COMME MECANISME ESSENTIEL AU DEVELOPPEMENT TUMORAL

La voie de signalisation MAPK est une cascade de signalisation qui joue un rôle crucial dans la transmission de signaux extracellulaires pour réguler diverses réponses cellulaires. Cette voie est le principal mécanisme par lequel KRAS transmet son potentiel oncogène.

Tout comme une mutation activatrice de KRAS a des effets oncogènes, des mutations de la voie MAPK sont également fréquemment présentes dans les tumeurs LUAD. Cependant, une hyperactivation de la voie est toxique pour la tumeur. Pour que les cellules tumorales maintiennent une dépendance au KRAS et/ou des mutations dans la voie MAPK, d'autres altérations sont nécessaires pour désactiver les réponses cellulaires qui inhiberaient normalement la prolifération cellulaire. Il est important de maintenir un équilibre dans la signalisation MAPK pour éviter la toxicité cellulaire.

Pour réguler ces réponses, il existe des protéines régulatrices telles que les phosphatases, comme les DUSP. Ces enzymes jouent un rôle crucial dans la désactivation de la signalisation ERK et peuvent avoir une double fonction, à la fois suppressive et promotrice tumorale, contexte spécifique, en raison de cet équilibre délicat qui doit être maintenu.

Afin de comprendre comment cette régulation s'exerce dans la tumeur, il est crucial de pouvoir mesurer les niveaux d'activité de chaque composant et comment les changements dans ces composants modifient l'équilibre. Les signatures génétiques transcriptionnelles peuvent être un outil utile pour évaluer l'activité de cette voie chez les patients atteints de cancer.

Dans cette thèse, nous décrivons l'utilisation de l'une de ces signatures pour évaluer l'activité de la voie MAPK et comment les niveaux de MAPK pourraient prédire la survie des patients atteints de LUAD. De plus, nous présentons une analyse qui a identifié un certain nombre de régulateurs potentiels de la MAPK, à la fois positifs et négatifs. L'étude de ces nouveaux régulateurs, comme c'est le cas du gène DUSP4, est d'une importance capitale pour mieux comprendre la voie de signalisation RAS-MAPK et sa régulation dans divers contextes biologiques et pathologiques, en particulier dans les cancers du poumon porteurs de mutations KRAS. Ces recherches permettent de faire progresser le domaine de l'oncologie de précision et d'améliorer le traitement des patients atteints de cette maladie.

2 PRINCIPAUX RESULTATS

2.1 UNE SIGNATURE TRANSCRIPTIONNELLE POUR DETERMINER LA SURVIE DES PATIENTS

Tout d'abord, l'objectif de cette étude était de répondre à la question de savoir si l'activité de MAPK dicte l'issue des tumeurs présentant des mutations KRAS. Ces résultats bio-informatiques étaient basés sur les données de 162 patients présentant des mutations KRAS de l'adénocarcinome pulmonaire dans le TCGA. L'activité de MAPK a été évaluée en calculant un score qui tenait compte de l'expression de 6 gènes MAPK spécifiques pour cette maladie (Brant et al., 2017) : DUSP4, DUSP6, ETV4, ETV5, PHLDA1 et SPRY2.

Nous avons classé les patients en deux groupes : MAPK élevé et faible, en fonction des quartiles supérieur et inférieur du score de signature. Nous avons effectué une analyse qui a révélé des différences significatives de survie, avec une survie plus faible dans le groupe à faible MAPK. Ce résultat suggère que des niveaux élevés de MAPK sont préjudiciables dans le contexte d'un LUAD KRAS muté, et que la tumeur doit limiter ses niveaux de signalisation pour assurer une aptitude maximale. De plus, cette différence de survie a été trouvée spécifiquement dans les tumeurs présentant des mutations KRAS et non dans d'autres mutations driver.

Pour confirmer ces résultats, un filtre de pureté tumorale a été appliqué, ce qui a permis d'obtenir une cohorte plus pure. En effectuant une analyse de corrélation entre les gènes de signature, nous avons conclu qu'il était nécessaire d'effectuer l'exclusion des gènes DUSP4 et PHLDA1 de la signature, car ils étaient anti-corrélés avec le reste des gènes et, in fine, ne contribuaient pas significativement à la capacité prédictive de la signature. L'analyse de survie avec la signature affinée a confirmé la différence de survie entre les groupes à MAPK élevé et à faible MAPK. De plus, ces résultats ont été validés dans une cohorte indépendante de puces à ADN qui a également récapitulé les patients atteints de LUAD avec KRAS muté.

La signature a également été corrélée avec des ontologies associées à l'activation de MAPK, confirmant que la signature est capable de refléter efficacement les niveaux de signalisation des voies. L'analyse

des différences entre les groupes à MAPK élevé et à faible MAPK n'a révélé aucune association avec des caractéristiques cliniques spécifiques ou des mutations KRAS, mais une association avec des mutations KEAP1 a été trouvée. Cependant, la mutation KEAP1 ne détermine pas de différences de survie.

L'analyse des altérations du nombre de copies (CNV) a montré que les tumeurs avec des niveaux élevés de MAPK présentaient plus d'altérations génétiques que les tumeurs avec de faibles niveaux de MAPK. Cela suggère que les tumeurs avec des niveaux élevés de MAPK sont plus susceptibles à l'instabilité génomique.

En résumé, l'activité de MAPK a un impact significatif sur la survie des patients porteurs de mutations KRAS dans le LUAD. La signature que nous avons affinée est corrélée à l'activation de MAPK, mais aussi à une plus grande instabilité génomique, ce qui suggère que des niveaux élevés de MAPK génèrent une plus grande toxicité qui est déterminante dans la progression de ces tumeurs.

2.2 DUSP4 EST UN REGULATEUR NEGATIF QUI DETERMINE LE DEVELOPPEMENT DE LA TUMEUR

L'analyse *in silico* des données cliniques montre des différences significatives dans le statut génomique de DUSP4, un régulateur négatif de MAPK, entre les patients présentant différents niveaux de signature transcriptionnelle. DUSP4 montre des amplifications dans les tumeurs faibles en MAPK et des pertes génomiques dans les tumeurs élevées en MAPK.

DUSP4 régule la phosphorylation de l'ERK, sa perte étant un événement activant la voie et sa surexpression étant un événement inhibiteur de la voie. Cependant, nous avons identifié que la perte de DUSP4 n'induit pas de transformation cellulaire par elle-même et ne collabore pas avec d'autres oncogènes tels que RAS ou PI3K, ce qui suggère que DUSP4 n'est pas un événement oncogène primaire.

Par conséquent, nous avons décidé d'étudier l'impact de la délétion de DUSP4 sur les tumeurs KRAS mutées déjà formées. Les résultats ont révélé que les tumeurs sans DUSP4 présentent une augmentation de l'instabilité génomique et du taux d'apoptose. Cela suggère que la perte de DUSP4 déclenche la mort cellulaire, probablement en raison d'une suractivation de la voie MAPK. Bien qu'une augmentation du

stress oxydatif ait été observée dans les cellules avec DUSP4 supprimé dans un modèle cellulaire de laboratoire, cet effet n'a pas été confirmé dans les tumeurs. Ces résultats indiquent que DUSP4 joue un rôle crucial dans la régulation de la stabilité génomique et de la survie cellulaire dans le cadre de tumeurs mutées par KRAS.

Afin d'étudier comment DUSP4 contribue, à un stade précoce, à l'initiation et au développement des tumeurs, nous avons créé un modèle in *vivo* à partir d'une lignée cellulaire ATII immortalisée chez l'homme, qui contient une mutation oncogénique KRAS activée par le tamoxifène grâce à une fusion avec le récepteur des œstrogènes ($KRAS^{G12V\text{-}ER}$). Ces cellules ont été infectées par des constructions CRISPR ciblant DUSP4 et injectées orthotopiquement à des souris immunodéficientes par injection dans la veine caudale. Seules les souris qui ont conservé le tamoxifène tout au long du processus ont développé un signal positif de luciférase, démontrant qu'il s'agit d'un phénotype dépendant de KRAS. Les cellules avec une délétion de DUSP4 ont eu un signal de luciférase significativement augmenté pendant plusieurs semaines. Cependant, au cours des dernières semaines, le développement de la tumeur témoin s'est brusquement accéléré, atteignant des niveaux de luciférase encore plus élevés que les cellules avec un knockout de DUSP4.

Ces résultats soutiennent l'hypothèse dérivée des données cliniques, qui suggère que les événements de délétion de DUSP4 sont sélectionnés positivement dans les premiers stades de la maladie, car la perte de DUSP4 semble être avantageuse pour la croissance maligne initiale. Cependant, il a été observé que les cellules ayant une clairance de DUSP4 perdent progressivement l'avantage conféré et sont dépassées par des cellules compétentes en DUSP4, ce qui suggère qu'à des stades ultérieurs, l'intégrité de DUSP4 peut être plus bénéfique.

Pour mieux comprendre l'impact global de DUSP4 sur le processus malin, nous avons cherché à créer un modèle plus complet qui récapitule l'ensemble du processus d'initiation tumorale et de développement des cellules mutantes KRAS avec ou sans altérations de DUSP4.

Pour ce modèle, la souche de souris $K\text{-}ras^{+/lox\text{-}Stop\text{-}lox\text{-}G12V\text{-}geo}$ a été utilisée. Elle permet l'expression du mutant oncogène $KRAS^{G12V\text{-}ER}$ après recombinaison médiée par la recombinase de Cre. Pour combiner

l'activation de KRAS avec l'inactivation de DUSP4, nous avons infecté des souris par voie intranasale avec des particules lentivirales du vecteur *pSECC*, qui élimine le gène DUSP4 à l'aide de la technologie CRISPR/Cas9 et active en même temps $KRAS^{G12V-ER}$ avec l'expression d'une CRE recombinase. De plus, ce système permet l'expression d'un gène rapporteur YFP également réduit au silence par une cassette *lox-STOP-lox.*

Nous avons observé que la perte de DUSP4 augmentait la croissance des lésions précoces chez les souris au cours du premier mois. En l'espace de trois mois, une augmentation du nombre de cellules positives a été constatée chez les souris dont DUSP4 avait été retiré, ce qui suggère une synergie entre la perte de DUSP4 et l'activité oncogénique de KRAS dans l'augmentation de la charge tumorale. Cependant, à des stades plus avancés (6 et 9 mois), les lésions étaient moins fréquentes chez les souris avec DUSP4 supprimé. À 12 mois, les tumeurs sans DUSP4 se sont avérées plus petites. Cela pourrait indiquer que la perte de DUSP4 réduit la probabilité de développer des néoplasmes avancés et importants.

En résumé, cette expérience suggère que, au fur et à mesure que la tumeur induite par le KRAS progresse, la perte de DUSP4 devient préjudiciable. Initialement, l'absence de DUSP4 favorise la formation de tumeurs, mais au fur et à mesure que la tumeur progresse, DUSP4 semble jouer un rôle protecteur. D'autres analyses sont prévues pour comprendre comment l'élimination de DUSP4 affecte les lésions à un stade avancé du point de vue de l'apoptose, de la toxicité génomique et du stress oxydatif.

Ensuite, nous avons entrepris d'étudier comment ces altérations peuvent influencer la réponse clinique des patients, en particulier leur réponse aux inhibiteurs de MAPK, tels que les inhibiteurs de MEK et les inhibiteurs spécifiques de $KRAS^{G12C}$.

Des modèles de cellules d'adénocarcinome pulmonaire (LUAD) présentant des mutations de KRAS ont été générés et l'expression de DUSP4 a été retirée ou induite afin d'évaluer comment la modulation de DUSP4 affecte spécifiquement la réponse aux inhibiteurs. DUSP4 a été éliminé dans ces lignées cellulaires et la sensibilité aux inhibiteurs de MAPK, tels que le trametinib, et aux inhibiteurs de KRAS, l'adagrasib et le sotorasib, a été évaluée. Dans certaines lignées cellulaires, l'élimination de DUSP4 a entraîné une diminution de la sensibilité au trametinib, ce qui indique une résistance accrue. Cette

résistance au trametinib pourrait être due à des niveaux modifiés de MAPK générés par l'élimination de DUSP4. Dans les lignées cellulaires présentant des mutations KRASG12C, la sensibilité aux inhibiteurs de KRAS n'a pas été affectée par la délétion de DUSP4. D'autre part, la surexpression de DUSP4 sensibilise les cellules aux inhibiteurs de MAPK, y compris le trametinib et les inhibiteurs de KRASG12C.

Pris ensemble, ces résultats suggèrent que le statut DUSP4 peut être un facteur déterminant dans l'efficacité de la réponse aux inhibiteurs de MAPK, en particulier les inhibiteurs de KRASG12C. Cela pourrait avoir des implications cliniques importantes, car les stratégies de traitement pourraient être adaptées en fonction du statut de DUSP4 dans les tumeurs des patients.

2.3 UTILISATION DE LA TOXICITE MEDIEE PAR MAPK POUR DECOUVRIR DE NOUVEAUX MODULATEURS

Dans cette section, nous cherchons à explorer les conséquences de l'absence d'une régulation négative adéquate de la voie de signalisation MAPK au cours de l'initiation et de la progression du cancer. Pour ce faire, nous avons décidé d'effectuer un criblage à l'échelle du génome afin d'identifier de nouveaux régulateurs MAPK qui peuvent aider à comprendre le réseau de régulation complexe.

À cette fin, nous avons développé un modèle de toxicité inductible par MAPK, avec un modèle de cellules ATII immortalisées avec du KRAS oncogène mutant activable par le tamoxifène. De plus, nous avons introduit l'expression du mutant $BRAF^{D594A}$, qui potentialise l'activité de MAPK malgré l'absence d'activité kinase. Nous avons pu établir un contrôle précis de l'activité de BRAF en introduisant une version inductible de $BRAF^{D594A}$, permettant de doser l'activité de KRAS et de BRAF.

Nous démontrons que la combinaison de l'activation de KRAS avec l'expression de $BRAF^{D594A}$ en présence de tamoxifène et de doxycycline potentialise la signalisation MAPK. Une combinaison dose-spécifique des deux entraîne une hyperactivation de la MAPK, une mort cellulaire efficace mais contrôlée et dépendante de la voie. Nous avons également pu détecter la phosphorylation de γH2AX, ce qui indique un stress génomique, probablement directement causé par l'hyperactivation de MAPK.

Ces résultats sont validés dans des cellules A549 mutées par KRAS. L'expression de BRAF D594A est capable d'induire l'activation de MAPK, mais à des doses plus élevées, elle est toxique et limite la croissance cellulaire.

En résumé, ces expériences démontrent que l'activation de MAPK est une voie centrale dans la signalisation cellulaire et que l'hyperactivation de MAPK peut entraîner une toxicité cellulaire. Ces résultats constituent la base de l'exploration de nouveaux régulateurs de la voie de signalisation MAPK.

Nous avons conçu une stratégie de criblage CRISPR/Cas9 pour une étude complète du génome. Les guides d'ARN (gRNA) peuvent cibler à la fois les régulateurs de voies positives et négatives. Lorsqu'ils inhibent l'expression des régulateurs positifs, les toxicités résultant d'un excès de MAPK sont réduites, ce qui conduit à une restauration de la viabilité cellulaire. En revanche, lorsque les gRNA ciblent des régulateurs négatifs, l'activité et la toxicité de MAPK sont augmentées. Ces effets se refléteront dans la représentation des gRNA dans le criblage.

Pour le criblage, nous avons utilisé des cellules ATII modifiées pour exprimer la protéine Cas9 et la banque Brunello, qui contient les gRNA à l'échelle du génome. Trois conditions ont été réalisées en parallèle : une qui n'a pas été soumise à un traitement (PRE), une avec activation de KRAS (K) et une avec activation de KRAS et BRAF (KB). L'ADN génomique a été extrait de toutes les conditions et une stratégie de PCR imbriqué a été appliquée pour amplifier les gRNA avant le séquençage.

L'analyse des résultats a révélé des modèles d'enrichissement et d'épuisement des gRNA dans les conditions K et KB par rapport à la PRE. Deux algorithmes, STARS et MAGECK, ont été utilisés pour analyser les données et confirmer les résultats.

Des gRNA enrichis ont été sélectionnés qui sont censés sauver la viabilité des cellules en ciblant des médiateurs du phénotype apoptotique, soit directement par le contrôle de MAPK, soit indirectement par d'autres mécanismes. D'autre part, les gRNA appauvris ont été analysés, ce qui suggère que les gènes dont les gRNA ont été appauvris sont des régulateurs négatifs de la voie MAPK.

Dans cette thèse, des analyses ont été effectuées pour valider les effets de la délétion des gènes TTC1 et CSK dans les cellules ATII KB et dans les lignées cellulaires humaines de LUAD KRAS muté.

En ce qui concerne TTC1, il a été constaté que la délétion de ce gène n'affectait pas la sensibilité des cellules ATII à l'activation de KRAS et BRAF, ce qui suggère que TTC1 ne contribue pas directement à la réponse de signalisation MAPK. Cependant, il a été observé que les gRNA TTC1 ont été sélectionnés lors du criblage, ce qui indique une importance possible en termes d'essentialité. Son rôle dans les lignées cellulaires LUAD porteuses de la mutation KRAS a été évalué, où la délétion de TTC1 n'a pas eu d'effet constant sur l'activation de MAPK. Étant donné que TTC1 est considéré comme un gène essentiel dans une grande variété de lignées cellulaires humaines, il a été conclu qu'il ne s'agissait pas d'un candidat approprié pour une étude plus approfondie.

En ce qui concerne CSK, il a été observé que la délétion de ce gène dans les cellules ATII KB augmentait la sensibilité des cellules à l'activation de KRAS et BRAF. Cela suggère que CSK agit comme un régulateur négatif de la signalisation MAPK et que sa perte de fonction compromet la régulation négative de MAPK, conduisant à une toxicité accrue de la signalisation MAPK dans les cellules ATII KB. Cette observation a également été confirmée dans les lignées cellulaires LUAD mutées par KRAS, où les cellules dépourvues de CSK ont montré une résistance accrue aux inhibiteurs de la voie RAS-MAPK. De plus, il a été observé que l'inhibition de SRC dans les cellules ATII KB n'a pas modifié de manière significative l'activation de la MAPK, ce qui suggère que l'effet de CSK sur la régulation de la signalisation de la MAPK est indépendant de SRC. Ceci a été confirmé en évaluant les effets de l'inhibition de la SRC avec l'inhibiteur de PP2 dans des lignées cellulaires LUAD mutées par KRAS, où la résistance aux inhibiteurs de la voie RAS-MAPK dans les cellules dépourvues de CSK n'a pas été modifiée de manière significative.

En résumé, ces résultats suggèrent que CSK agit comme un régulateur négatif de la signalisation MAPK et que sa perte de fonction peut augmenter la résistance aux inhibiteurs de la voie RAS-MAPK.

L'ensemble des données recueillies dans cette thèse est pertinent pour mieux comprendre la signalisation MAPK dans les tumeurs LUAD KRAS mutées. Il est important de comprendre comment les signaux médiés par la voie MAPK sont intégrés et comment toute une série de régulateurs permettent aux niveaux de signalisation d'être à un niveau d'équilibre contrôlé. Pour faire face aux défis de l'avenir en oncologie de précision (résistance, comorbidités, etc.), les efforts de recherche doivent prendre en

compte la manière dont la tumeur est capable de restructurer la voie par des altérations de ces régulateurs, comme c'est le cas avec DUSP4. La connaissance et l'étude de toutes ces altérations, en plus de celles qui peuvent survenir chez des régulateurs inconnus, permettront à la recherche de répondre à des questions cliniques qui offriront un avenir meilleur aux patients touchés par cette maladie.

Conclusions

A partir des objectifs de ces travaux de recherche, nous avons obtenu des informations précieuses sur la façon dont la régulation de la voie MAPK affecte la progression tumorale, démontrant que les altérations des modulateurs de la voie peuvent jouer un rôle fondamental dans le pronostic clinique.

Les conclusions générales de ce travail sont les suivantes :

1. L'analyse des données transcriptomiques de LUAD par l'intermédiaire de notre signature a révélé que l'activité de MAPK détermine la survie des patients porteurs de la mutation KRAS, de faibles niveaux de MAPK étant un indicateur de mauvais pronostic.
2. L'activité élevée de MAPK dans le LUAD KRAS muté est corrélée avec les phénotypes de stress, y compris le stress génomique, le stress oxydatif et l'apoptose.
3. DUSP4 est un régulateur négatif de MAPK qui est modifié différemment en fonction des niveaux d'activité de MAPK dans le LUAD KRAS muté. Les patients ayant une activité MAPK élevée ont des délétions de DUSP4, tandis que les patients ayant une faible activité de MAPK ont des amplifications de DUSP4.
4. La perte de DUSP4 potentialise l'activation de MAPK. La perte de DUSP4 est un événement sélectionné à un stade précoce car il peut conférer un avantage prolifératif aux néoplasmes induits par KRAS. Dans les tumeurs avancées, cette augmentation de la signalisation est corrélée à des événements toxiques, ce qui suggère qu'une perte chronique de DUSP4 peut compromettre la progression tumorale normale.
5. Grâce au criblage CRISPR, nous avons identifié CSK comme un régulateur potentiel qui pourrait fonctionner indépendamment de SRC en médiant la régulation négative de la voie. D'autres recherches peuvent être nécessaires pour compléter et mieux comprendre comment CSK pourrait contribuer à différents stades du développement de la tumeur.